DISSERTATION

QUANTIFICATION AND PREDICTION OF LATERAL CHANNEL ADJUSTMENTS DOWNSTREAM FROM COCHITI DAM, RIO GRANDE, NM

Submitted by

Gigi A. Richard

Department of Civil Engineering

In partial fulfillment of the requirements

For the Degree of Doctor of Philosophy

Colorado State University

Fort Collins, Colorado

Spring 2001

COLORADO STATE UNIVERSITY

December 14, 2000

WE HEREBY RECOMMEND THAT THE DISSERTATION PREPARED UNDER OUR SUPERVISION BY GIGI A. RICHARD ENTITLED QUANTIFICATION AND PREDICTION OF LATERAL CHANNEL ADJUSTMENTS DOWNSTREAM FROM COCHITI DAM, RIO GRANDE, NM BE ACCEPTED AS FULFILLING IN PART REQUIREMENTS FOR THE DEGREE OF DOCTOR OF PHILOSOPHY.

Committee on Graduate Work

_____

_____

_____

_____

Advisor

_____

Department Head/Director

ABSTRACT OF DISSERTATION

QUANTIFICATION AND PREDICTION OF
LATERAL CHANNEL ADJUSTMENTS DOWNSTREAM FROM COCHITI
DAM, RIO GRANDE, NM

Located downstream from Cochiti Dam in north-central New Mexico, the Cochiti reach of the middle Rio Grande spans 45 kilometers from the dam to the Highway 44 bridge in Bernalillo, NM. During the early and mid-1900's the U.S. Army Corps of Engineers and the U.S. Bureau of Reclamation constructed dams and performed channelization in an attempt to reverse the historic aggradational trend of the channel bed and to minimize flood hazards on the middle Rio Grande. Cochiti Dam, completed in 1973, was designed for sediment detention and flood control and traps virtually all of the sediment entering the Cochiti reach. Few large alluvial rivers in the southwestern U.S. have been studied and documented as well as this section of the Rio Grande. Hydraulic, topographic, photogrammetric and sediment data collection efforts conducted by numerous federal and state agencies have tracked changes in the river since 1895.

Utilizing this extensive database, the Cochiti reach of the middle Rio Grande was thoroughly characterized through analysis of flow regime, sediment transport, cross-sectional form, bed material, longitudinal profile, planform, and lateral movement rates. The response of the river to altered hydrologic regimes was studied through application of hydraulic geometry equations, sediment budget analysis, and examination of lateral migration rates. The rates of lateral movement and level of lateral stability of the river were quantified using digitized aerial photos of the active channel over 74 years (1918-1992). Four indices of lateral movement and two indicators of lateral stability were measured from the digitized active channel delineation.

Results of the historic geomorphic analysis and the quantification of lateral mobility and stability show that the channel moved toward a more stable state as the peak discharges decreased prior to and following construction of the dam. During the entire time period studied (pre and post dam), the channel narrowed and moved toward an equilibrium width as predicted by hydraulic geometry equations. Lateral movement rates have declined since 1918 and the channel has shifted from a multi-thread to a more single-thread pattern. The lateral changes that began prior to construction of Cochiti Dam appear to be the result of changes in the hydrologic regime rather than the sediment regime. The dam withholds 99% of the sediment entering the reach.

Since construction of the dam, the bed has coarsened from sand to gravel size sediment and degraded up to 2 meters. The sinuosity also increased up to 9% between 1972 and 1992.

Three models were developed to estimate the lateral migration and width change rates of the Cochiti reach from 1918 to 1985. The 1985 to 1992 data were reserved for validation of the models. The first model was a simple estimation of the movement rates as a percentage of channel width and produced rough estimates of migration and width change rates. The second model was based on the assumption that as the river moved closer to an equilibrium state, the rate of change decrease. Fitting an exponential equation based on deviation from equilibrium produced r-square values as high as 0.98 in modeling the 1918-1985 width changes of the Cochiti reach. Similar models of migration rate produced r-square values up to 0.89 for the same time period.

The third model utilized multiple regression analysis with stepwise selection techniques to identify significant associations between lateral movement rates and measures of flow energy, sediment supply, bed material and planform. The resulting equations showed that flow energy (water discharge and/or channel slope) and planform explained the highest percentage ($R^2 = 0.65$) of variance in migration rate. Width change rates were best described by an equation including unit stream power ($S(Q)^{0.5}$) combined with active channel width ($R^2 = 0.50$). More important than the predictive capabilities of this model were significant associations between lateral movement rates and flow and planform parameters. Migration rates increased with increasing flow energy, sinuosity and total channel width (width of channel including vegetated bars). Width change rate was significantly associated with active channel width only.

Validation of the models with the 1985 to 1992 Cochiti reach data showed that the regression results best estimated the migration rate. The equations combining discharge and width ratio or just mobility index produced the smallest average error (25% to 38%). The 1992 active channel width was estimated equally well (12% average error) by the simple model of width change rate as percentage of width and the regression equation using unit stream power and active channel width.

Gigi A. Richard
Department of Civil Engineering
Colorado State University
Fort Collins, CO 80523
Spring 2001

ACKNOWLEDGEMENTS

I am very thankful for the support and guidance of my graduate advisor Dr. Pierre Julien and for the patience, understanding and direction provided by my committee members, Drs. Robert Ward, Ellen Wohl, and Pete Lagasse. I especially want to thank Dr. Robert Ward, whose ideas and cheerfulness boosted my confidence on many occasions. My undergraduate advisor, Dr. Ole Madsen introduced me to the fields of sediment transport and fluid mechanics. I am grateful to have been exposed to his enthusiasm for the subject, which eventually led to my undertaking this intellectual adventure.

My deepest thanks extends to Claudia Leon for her support in creation of the database and her understanding and friendship. I could not have asked for a better office-mate or partner in undertaking the task of unraveling the mysteries of the Rio Grande. My other friends and fellow graduate students listened to me, read my drafts, babysat my daughter, exercised with me and reminded me that I would not die of stress. Thank you Rosalia Rojas, Greg Stewart, Kris Metzger, Robert Edgerton, Jonathan Root, Debbie Lew, Sara Rathburn, Dot Dickerson and Brian Bledsoe. Kristina Cash provided loving support at home, reminding me repeatedly to have patience with unanswered questions.

Funding from the U.S. Bureau of Reclamation made my studies and research possible. Thank you to Drew Baird of the U.S. Bureau of Reclamation, Albuquerque, NM who provided the incentive and the means that made this study possible. Travis Bauer did a great deal of work compiling the database used in this study. Jan Oliver and Paula Makar immensely increased my understanding of the Rio Grande and GIS.

I would also like to thank Mary Casey, Bernie Shepard, Elizabeth McCoy, Laurie Howard and Jenifer Davis for their patience in answering my many questions about the logistics of working my way through the maze of the university system.

I truly appreciate the emotional, financial and spiritual support of my family, including Gary, my dad and Mindy. My mom provided invaluable assistance with my daughter. Thank you mom. And, my grandmothers, Alice and Louise provided much-needed reminders to keep my chin up. Most importantly, my daughter and source of joy and love in my life, Josephine. Thank you Josie for your patience and smiles while “Mom writes her dissertation”. Yes, I’m finally done.

TABLE OF CONTENTS

LIST OF TABLES

LIST OF FIGURES

LIST OF SYMBOLS

b	=	Average number of channels
C	=	Suspended sediment concentration (mg/L)
d	=	Mean channel depth (m)
D_{50}	=	Median bed material size (mm)
Δl	=	Left bankline movement (m)
Δr	=	Right bankline movement (m)
Δt	=	Length of time period (years) = t_2 - t_1
ΔW	=	Total change in width (m)
dW_{act}	=	Rate of change of active channel width (m/year)
dW_{tot}	=	Rate of change of total channel width (m/year)
E	=	Total bankline change (m/year)
h	=	Bank height (m)
k_1, k_2	=	Empirical rate constants
M	=	Lateral migration rate (m/year)
M_{avg}	=	$M/2$ = Average migration rate (m/year)
MI	=	Mobility Index
M_{obs}	=	Observed or measured migration rate (m/year)
M_{pred}	=	Predicted migration rate (m/year)
N	=	Normalize lateral movement (% width/year)
P	=	Sinuosity
P_{tot}	=	Total sinuosity
Q	=	Water discharge (m^3/s)
$Q_{2\text{-}year}$	=	2-year frequency discharge (m^3/s)
Q_{eff}	=	Effective discharge (m^3/s)
Q_{sb}	=	Bed material discharge (tons/day)
R_c	=	Radius of curvature (m)
S	=	Channel slope
t_1	=	Beginning of time period (year)
t_2	=	End of time period (year)
W	=	Channel width (m)
W_1	=	Width at beginning of time period, t_1 (m)
W_2	=	Width at end of time period, t_2 (m)
W_{act}	=	Active channel width (m)
W_{act1}	=	Active channel width at beginning of time period, t_1 (m)
W_{act2}	=	Active channel width at end of time period, t_2 (m)
W_e	=	Equilibrium channel width (m)
W_o	=	Active channel width at onset of narrowing (m)
W_r	=	Width ratio
W_t	=	Active channel width at time, t (m)
W_{tot}	=	Total channel width (m)
W_{tot1}	=	Total channel width at beginning of time period, t_1 (m)
W_{tot2}	=	Total channel width at end of time period, t_2 (m)
Ω	=	Total stream power
ω	=	Specific stream power

CHAPTER 1

INTRODUCTION

In their natural state, rivers are inherently dynamic, responding to the variability in water and sediment inputs imposed upon them. Alteration to those inputs either natural or human-made can result in adjustments of the river's shape and form. The water and sediment flowing in a river create the shape and form of the channel that carries them (Leopold 1994; Schumm 1969). A river will adjust to accommodate alterations in the incoming water and sediment load by adjusting its width, depth, slope and planform (Knighton 1998). If the flow energy (water discharge and channel slope) and the sediment supply are considered to be the driving variables or inputs in the balance of stability of the reach (Nanson and Hickin 1986), the cycle of channel adjustment can be illustrated by Figure 1-1. The resisting forces or the bed material, bank stability and material, and the channel geometry define the river system. If the system is not in equilibrium, then the channel will adjust to accommodate the inputs by moving laterally or vertically.

For centuries, humans have attempted to understand and control rivers. They have attempted to harness the power of rivers and create more manageable and stable systems. Historically, human intervention in river processes has been aimed at creating less mobile, less dynamic and less variable rivers that are more easily controlled and pose decreased risk to surrounding communities. For instance, dams and levees are constructed to control flood flows, and channelization is performed to force rivers to maintain a certain course. Human-induced and natural alterations to the inputs to a river system do not always produce the expected or intended result in the shape and form of the channel. In many cases, the exertion of control is successful, resulting in simple stable channels devoid of the ecological diversity and physical dynamism of a natural river system. Thresholds and complex response can also confound predictions of channel response (Xu 1997a; Schumm 1973; Brewer and Lewin 1998).

A more controlled or stable condition is not necessarily ideal for ecologically sustainable riparian and riverine environments. Biotic communities in these environments are adapted to the natural variability and dynamics of the system (Busch and Smith 1995). Controlling the natural

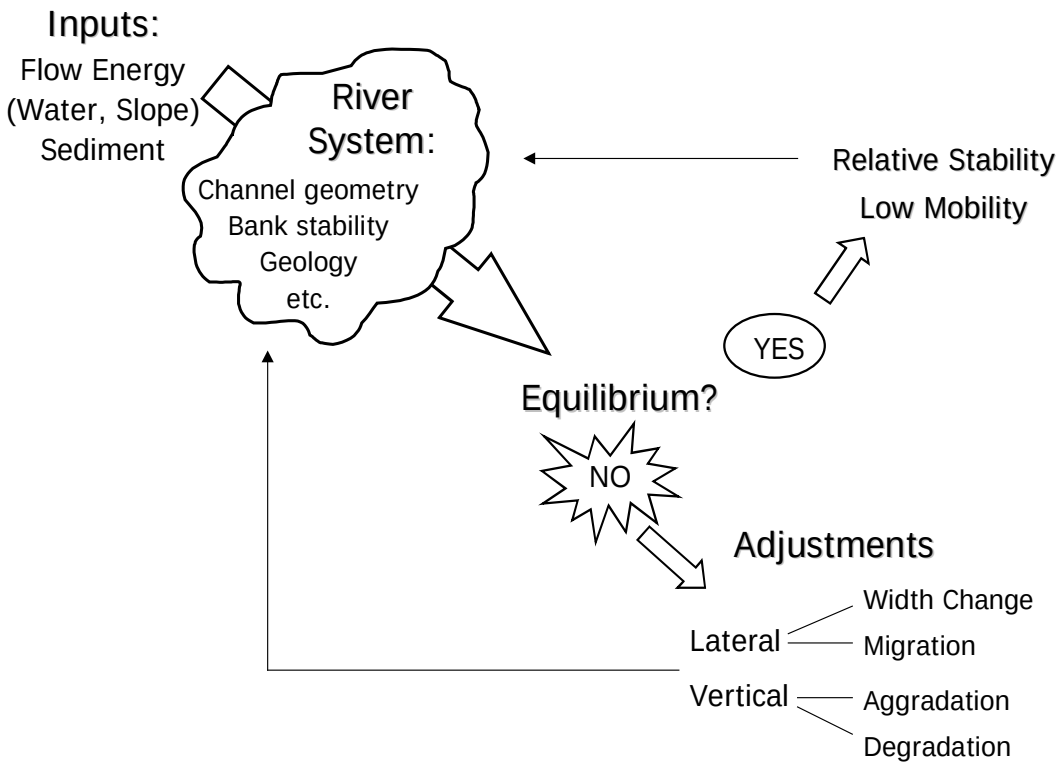

Figure 1-1 - Cycle of channel adjustment

variability of river systems and the resulting (often unexpected) response in the shape and form of the river to those controls can have adverse impacts on the native biotic communities. A more stable or less mobile channel is not necessarily a more desirable state from an ecological point of view (Poff et al. 1997; Gilvear 1993; Winterbottom 2000; Marston, et al. 1995; Bravard et al. 1997).

Sustainable management of rivers and their associated ecosystems requires greater understanding of the response of rivers to altered inputs and to controls on the natural variability and mobility of the system. Many rivers throughout the world are highly managed. Although an ideal solution to restoring a river to its natural, dynamic state might be to cease management and remove structures, this is not economical or socially realistic in many cases. Instead, better understanding of historic "natural" conditions can enhance management strategies imposed on the system (Brookes 1992). For instance, understanding that the timing of flood downstream from a dam is more important for certain species than the magnitude of the flood can allow dam operators to adjust their management plans for greater benefit to those species.

Greater understanding of historic changes both in input and response of river systems can enhance predictive capabilities, which create the best possible scenarios for management of river systems. Understanding the natural processes and forms of river systems can be used, not to

control the rivers, rather to restore some of the inherent variability and associated ecological integrity and diversity of the systems. It is in the context of promoting successful and sustainable ecological restoration that this study is undertaken.

One tool that both geomorphologists and engineers use to better understand, quantify and predict the shape and form of river channels is to consider the river in relation to an assumed equilibrium or stable condition. Rivers may exist in relatively stable states to which they will return following perturbations in environmental variables such as sediment input or water discharge. There are many different ways to consider and quantify the stability or equilibrium state of a river. Stability can refer to the lateral direction, i.e., movement of the river within its floodplain, and it can refer to the vertical movement of the channel or changes in the cross-sectional shape of the channel. Additionally, a river in equilibrium is often defined as neither aggrading, nor degrading, or non-silting, non-scouring, i.e., where the sediment inflow equals sediment outflow. The complexity of the inputs to a river system and the river's response to those inputs results in numerous definitions, descriptions, and methods of quantification of the degree of stability or level of equilibrium of a river.

For the purposes of this dissertation, a channel is considered to be in equilibrium or stable when it exhibits consistent mean behavior of a system over a given period of time (Schumm 1969). Changes in the processes or inputs acting on the system can result in a period of adjustment toward a new equilibrium state. During the ensuing adjustment period, the system is unstable or in a state of disequilibrium (Renwick 1992). A multitude of factors influences the level of stability or equilibrium state of a river, including discharge, sediment load, climate, geology, surrounding land use, vegetation, and valley slope. Changes in any of these variables, either drastically or gradually, can serve to push a river closer to or further from an equilibrium state. A river will adjust its cross-sectional geometry and channel slope to accommodate fluctuations in these variables. Climatic fluctuations can be gradual, whereas anthropogenic influences may be more sudden. The result is varying temporal and spatial scales in the river's response (Knighton 1998).

Lateral movement and stability of rivers are of particular interest, from geomorphic, engineering and ecological points of view. As described above, lateral movements may pose threats to human-made structures, while those same movements enhance the diversity that is integral to healthy riverine habitat. Conflicts exist on rivers throughout the world between the need (in populated areas) to have more stable and therefore safer rivers versus the desire to restore and maintain rivers in their natural, dynamic and often unstable state.

1.1 Cochiti reach, Rio Grande, NM

The research described in this dissertation is a contribution toward increased understanding of an alluvial river's response to varying water and sediment inputs. The focus is on lateral movement and deviation from an equilibrium state. This dissertation thoroughly documents the changing inputs to a river system before and after construction of a sediment detention and flood control dam, and then quantifies the response of the river to those changing inputs.

The Cochiti reach of the Rio Grande, located in north central New Mexico, extends about 45 kilometers downstream from Cochiti Dam (Figure 1-1). The dam was completed in November 1973 for the purposes of flood control and sediment detention (U.S. Army Corps of Engineers 1978). The wealth of data available on the Cochiti reach of the Rio Grande in New Mexico as well as stability issues related to critical habitat preservation and lateral migration rates make this reach a fascinating case study in fluvial stability.

Figure 1-2 - Location of study reach.

The active adjustment of the Cochiti reach resulting from changes in climate, land use, and water and sediment discharge combined with the documentation of these changes over the last 70 years by state and federal agencies provide an excellent opportunity to explore the relationships between changes in channel processes and the resulting channel form. Identification of portions of the reach that are more or less stable will aid in future analysis of the river in relation to the presence of endangered species in the Cochiti reach (the silvery minnow and the Southwestern willow flycatcher), the preservation of the riparian forest habitat (bosque), and the lateral migration of the channel. Conflict exists on the Cochiti reach between the desire to stabilize the river and the desire to restore it. Questions are being presented by managers, such as "Is it possible to restore natural dynamics while maintaining a safe river?" (Paul Tashjian, U.S. Fish and Wildlife Service, 1998 pers. comm.).

Cochiti Dam and Reservoir provide the largest flood control storage volume on the main stem of the Rio Grande. Located 65 kilometers upstream of the City of Albuquerque, Cochiti Dam began operation in November 1973 and controls an entire drainage area of about 37,800 km^2 (14,600 mi^2) (Bullard and Lane 1993). The dam traps virtually the entire sediment load from upstream as well as controlling the water discharge (Dewey et al. 1979). Construction of the dam has resulted in significant impacts on the channel downstream (Leon 1998; Bauer 1999; Lagasse 1980).

Documentation of changes in the Cochiti reach includes topographic and bathymetric surveys, aerial photos, sediment measurements, and discharge measurements. This abundance of information makes it possible to track the changing level of stability of the river. Prior to construction of Cochiti Dam the average active channel width was about 275 m (900 feet) and the Cochiti reach exhibited characteristics of braiding with up to four channels at some cross sections (Sanchez and Baird 1997; Lagasse 1980).

Since construction of Cochiti Dam (November 1973), the active channel width averages about 90 m (300 feet) and a majority of the river flows in a single thread channel. Degradation following closure of the dam has been documented as far as 200 km (125 miles) downstream from the dam (Sanchez and Baird 1997). Visual inspection of planform maps of the reach show that lateral migration has slowed. The bed of the river in the first few miles downstream of the dam has armored to a gravel/cobble bed (Leon 1998). Bed degradation and lateral migration still occur in some portions of the river, but the general trend of the reach appears to be toward a more stable state.

1.2 Research Premise and Objectives

The underlying premise of this study is that quantification and understanding of historic inputs and responses of the Cochiti reach can be helpful in estimation of future channel adjustments to varying water and sediment regimes. In particular, a greater understanding of the impacts of a flood control and sediment detention dam can provide guidance toward improved management strategies for the dam and possibly other dams on similar rivers. The focus of the study is on the lateral adjustments of the channel. Exploration of the research premise results in the following objectives, which are achieved using data collected on the Cochiti reach of the middle Rio Grande between 1918 and 1992:

1) To identify spatial and temporal trends in the inputs to the reach and the corresponding response of the channel both pre and post dam. Identification of trends can show if the pre and post-dam hydrologic and sediment regimes resulted in different responses of the channel downstream from the dam. The mechanisms for and rates of lateral movement of the channel varied between the pre and post dam periods, and understanding these differences can help managers create management plans that allow for enhanced mimicry of the "natural", pre-dam state of the river. The first goal is accomplished via a historic geomorphic analysis of the Cochiti reach. This includes identification of historic trends in water discharge, suspended sediment supply and channel slope. The response of the channel is measured by changes in bed material, bed elevation, channel width, and planform adjustments.

2) To evaluate the changes in channel form for evidence of an equilibrium state and compare results with existing methods of estimating equilibrium channel width. Other studies (Crawford et al. 1993; Lagasse 1994) suggest that the decreased variability in the water and sediment inputs to the reach since construction of Cochiti Dam has resulted in a more stable/less mobile channel that is approaching a state of dynamic equilibrium. Identification of an equilibrium state is accomplished by observing the rate of change of lateral movement using the definition of equilibrium as being consistent measurable behavior over a given period of time. Also, hydraulic geometry equations are used to estimate the equilibrium width of the channel using the input conditions quantified in the historic geomorphic analysis.

3) To measure spatial variability in lateral channel response by development and measurement of indices to describe the degree of lateral stability and mobility of the reach. Four measures of lateral movement are measured and analyzed. Two indices of

lateral stability are also computed. Spatial variability is measured by breaking the channel into reaches (5-10 km) and subreaches (~1 km). Lateral movement rates are measured at individual range lines along the entire Cochiti reach and then reach or subreach averaged. Measurement of lateral response of the channel at the subreach scale (~ 1 km) can provide insights into why some sections of the channel are more or less mobile than others.

4) To model and predict changes in lateral movement of the channel using statistical analyses to identify significant associations with other variables and to model lateral movement rates in relation to an equilibrium condition and to identify which measures of flow energy and planform provide the most significant association with lateral movement rates. Lateral movements of the channel are measured as rate of change of active channel width and as channel migration rate. Three methods of modeling lateral channel movement are employed and the resulting models are calibrated using the 1918 to 1985 Cochiti reach data. The first model is a simple estimation of lateral movement rates based on channel width. The second is a theoretical model of lateral adjustment based on deviation from an equilibrium state. The third uses multiple regression analysis with stepwise selection techniques to estimate width change and migration rates using the following independent variables: flow energy, sediment supply, bed material and planform. The resulting models are all validated using the 1985-1992 data from the Rio Grande.

Chapter 2 presents a review of the literature related to lateral channel adjustment, application of the equilibrium concept to rivers, prediction of lateral movement rates, and the impacts of dams on lateral migration rates. Chapter 3 describes the Rio Grande database used in the study and the subdivision of the Cochiti reach into reaches and subreaches. The historic geomorphic analysis of the Cochiti reach is presented in Chapter 4. This chapter describes the historic trends in the inputs (discharge, slope and sediment supply) and the vertical and lateral response of the channel (bed elevation change, planform adjustment and width). Chapter 5 continues with a more detailed analysis of the lateral adjustment of the Cochiti reach. Development of the indices of lateral mobility and stability is described as well as the spatial and temporal variability of these indices on the Cochiti reach. Three models to describe lateral movement are presented in Chapter 6. Chapter 7 discusses the results of Chapters 4, 5 and 6, compiles a complete picture of the channel adjustments, and presents the results in the context of other studies. Chapter 7 also

describes validation of the models from Chapter 6 with 1985-92 data from the Cochiti reach and application of the models to different rivers. Finally, Chapter 8 summarizes the conclusions and provides recommendations for further study.

CHAPTER 2

LITERATURE REVIEW

As described in the introduction, the form of a river channel is both a conduit to convey water and sediment and also a result of that conveyance (Knighton 1998). Throughout the study of river systems, scientists and engineers have endeavored to describe, quantify and classify rivers and their responding shape and form. One scheme of quantifying a river system that is used in both geomorphology and engineering is to consider the river's form relative to an equilibrium state. Figure 2-1 illustrates how the driving variables of discharge and sediment supply act on the channel bed and bank to form the channel characteristics of cross-section geometry, longitudinal profile and planform shape (Brookes 1992).

This dissertation utilizes the concept of channel adjustment toward an equilibrium state in response to variations in inputs to describe and understand the Cochiti reach of the Rio Grande. As a result, the following literature review begins by exploring definitions of equilibrium or stability with regard to alluvial channels. Then other studies of historic channel adjustment are explored followed by description of methods of predicting channel form. The next three sections focus on lateral adjustments beginning with channel pattern classification and transition, then lateral movement and finally prediction of lateral movement rates. The final two sections discuss impacts of dams on downstream channel movement and the environmental and ecological implications of the study of channel adjustment.

2.1 Equilibrium

A great deal of literature is devoted to application of equilibrium theory to the study of river channel form in an attempt to better understand and quantify how and why rivers move and change. The basic concept is that the river will adjust its cross-sectional form, bed configuration, planform and bed slope to accommodate the water and sediment entering the channel (Figure 2-1). Often slope is grouped with discharge as an input because it is a combination of water discharge and slope that provide the flow energy to erode the bed and banks (Knighton 1998).

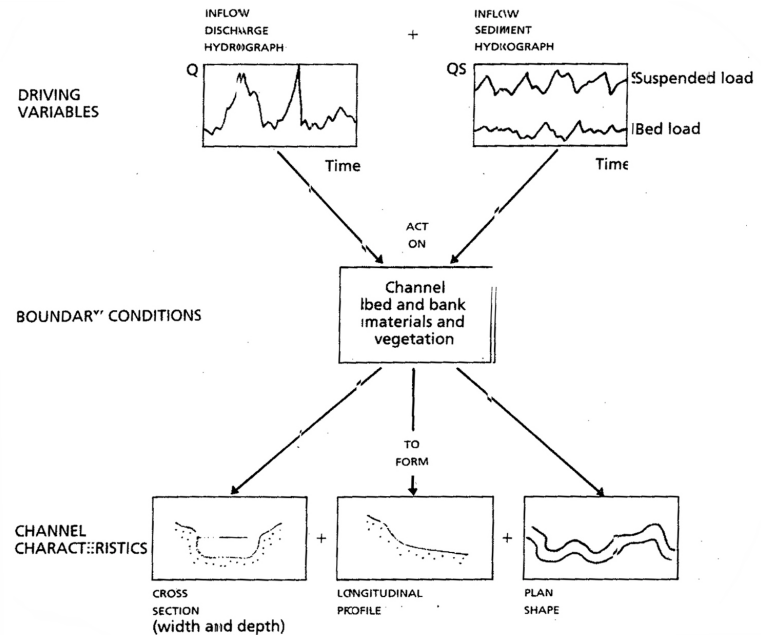

Figure 2-1 - Equilibrium concept for erodible channels (after Brookes 1992)

The study of equilibrium or stable states of rivers and the dynamics of the adjustment process began in the early 1900's with engineering studies that were focused on "regime theory" of stable canal design. Regime theory resulted from the efforts of British engineers to design stable irrigation canals in India and Egypt (Wargadalam 1993). Early geomorphologic work in the mid-1900's was primarily qualitative and looked at natural rivers in a longer time scale. Many of these earlier studies focused on adjustments in the channel slope to attain an equilibrium state. Gradually, focus shifted from slope adjustments to changes in cross-sectional form and channel pattern. Through the later 1900's, progressively more quantitative work and application to natural river systems have resulted in the modern hydraulic geometry and extremal hypotheses theories described later in this chapter (Knighton 1998). Engineers and geomorphologists both utilize the concept of equilibrium or stability, though perhaps with different terminology, intent, and time scales.

From an engineer's point of view stability and equilibrium are not necessarily the same things (Brice 1982). A river could achieve equilibrium in cross-section and longitudinal profile, but migrate laterally, and therefore not be considered stable to an engineer. Or, it could aggrade and degrade in a state of dynamic equilibrium, and as a result require special design of a bridge pier to accommodate this "instability" (Brice 1982). Parker (1979) proposed the concept that a stable channel width is incompatible with an active bed and called this conundrum the 'stable channel paradox'. Based on just these two examples, it is clear that the definitions of both stability and

equilibrium with respect to river systems are debatable. Despite the vast amount of engineering and geomorphologic literature devoted to this subject, "there is as yet no universally accepted set of criteria for determining whether all or part of a river system is in equilibrium" (Knighton 1998, p. 161).

Working through what Knighton (1998, p. 161) describes as a "terminological minefield", the following paragraphs present numerous definitions of equilibrium or stability as applied to alluvial rivers. The different definitions look at varying directions of adjustment of the channel in differing temporal and spatial scales.

Some of the earliest definitions consider slope adjustment as a criterion for equilibrium. Kennedy, who pioneered regime theory in 1895, defined a regime channel as "…a non silting and non scouring channel" (Wargadalam 1993). In 1902, Davis (Richards 1982, p. 86) defined the term 'grade' as a "balance between erosion and deposition attained by mature rivers". Mackin (1948, p. 471) defined a graded stream as one

> …in which, over a period of years, slope is delicately adjusted to provide, with available discharge and prevailing channel characteristics, just the velocity required for the transportation of the load supplied from the drainage basin.

Lane's equation (Biedenharn et al. 2000) summarizes the concept of channel adjustment toward an equilibrium state:

$$QS \propto Q_{sb} D_{50} \quad \text{.....(2-1)}$$

where: Q = water discharge;

S = channel slope;

Q_{sb} = bed material load; and

D_{50} = median bed material size.

Equation 2-1 can be used as a basis from which to study channel adjustments. Often referred to as Lane's balance, Equation 2-1 is consistent with Mackin's (1948) definition of equilibrium state which suggests a river adjusts its slope to transport the imposed water and sediment regime. Lane's balance suggests that any change in Q, Q_S or D_{50} can result in disequilibrium taking the form of aggradation or degradation to change the slope and therefore restore the balance (Biedenharn et al. 2000). Additionally, changes in slope to restore the balance can take different forms. Increased meandering or sinuosity results in decreased slope, therefore slope adjustments are not always manifested as vertical adjustments of the bed.

Another definition of equilibrium considers consistent behavior of the channel to be the criterion, rather than vertical adjustment. In 1961 Vanoni, Brooks and Kennedy described an equilibrium channel as "…if its mean measurable behavior during a given time period does not differ significantly from its mean measurable behavior during similar time periods before and after the given time period" (Wargadalam 1993). Similarly, Schumm (1969) defined a stable alluvial river as one that has shown no progressive channel adjustment during the last 10 years of record. He further postulates that the quantity of water and the quantity and type of sediment moved through the channel should control the dimensions, shape, gradient and pattern of a river.

In Richards' (1982) discussion of equilibrium, he noted that stable is not the same as static when referring to rivers. He listed the following terms as all describing this state of dynamic stability: dynamic(al) equilibrium, quasi-equilibrium, grade, regime, and steady state. Stability is a dynamic state because the stream or river is continually adjusting to maintain equilibrium with its environment. Changes in environmental variables can result in a transition to a new average equilibrium state.

Richards (1982) further broke down the definition of the equilibrium state of a river into the equilibrium of channel form and the equilibrium of channel process. The equilibrium of channel form refers to the temporal variation of the channel form or morphology. The equilibrium of channel process relates to the continuity of sediment transport, both temporally and spatially. Richards (1982) also stated that a lack of correlation between form and process is not necessarily an indication of disequilibrium. Rather, the channel could be in transition from one average steady state to another or fluctuations could reflect scatter about an average steady state.

The differences between equilibrium and disequilibrium are illustrated in Figure 2-2. Renwick (1992) differentiated between equilibrium and disequilibrium with the following definitions:

> Equilibrium – not a static state but form displays relatively stable characteristics to which it will return after disturbance;
>
> Disequilibrium – adjustment is towards equilibrium but, because response times are relatively long, there has not been sufficient time to reach such a state;
>
> Non-equilibrium – there is no net tendency toward equilibrium and therefore no possibility of identifying an average or characteristic condition.

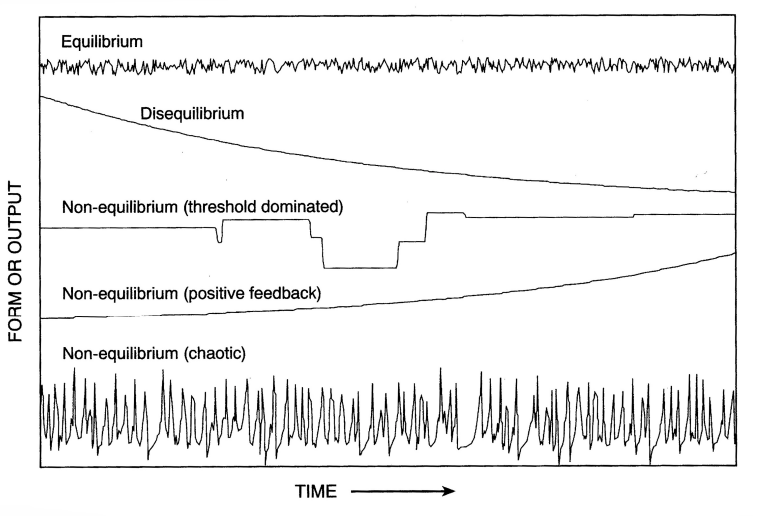

Figure 2-2 - Examples of equilibrium, disequilibrium and non-equilibrium behavior (after Renwick 1992)

Rosgen (1996) defined active or dynamic stability as a stream that laterally migrates, but maintains its bankfull width and width-depth ratio. Additionally, stable streams are consistently able to transport their sediment load, both size and type. He characterizes instability by excess scour or deposition.

Knighton (1998, p. 159) described the concept of equilibrium:

> True stability never exists in natural rivers, which frequently change their position and which must continue to pass a range of discharges and sediment loads. However, they can become relatively stable in the sense that, if disturbed, they will tend to return approximately to their previous state and the perturbation is damped down. Provided the controlling variables remain relatively constant in the mean, a natural river may develop characteristics or equilibrium forms, recognizable as statistical averages and associated with single-valued relationships to the control variables.

And on p. 162

> Rivers can at best attain an approximate equilibrium, manifest at some timescale intermediate between short-tem fluctuations and long-term evolutionary tendencies in a regularity of channel geometry adjusted to external controls.

As seen in Figure 2-3 the time period of adjustment for different components of channel form may vary from one component to another (Knighton 1998; Lewin et al. 1988).

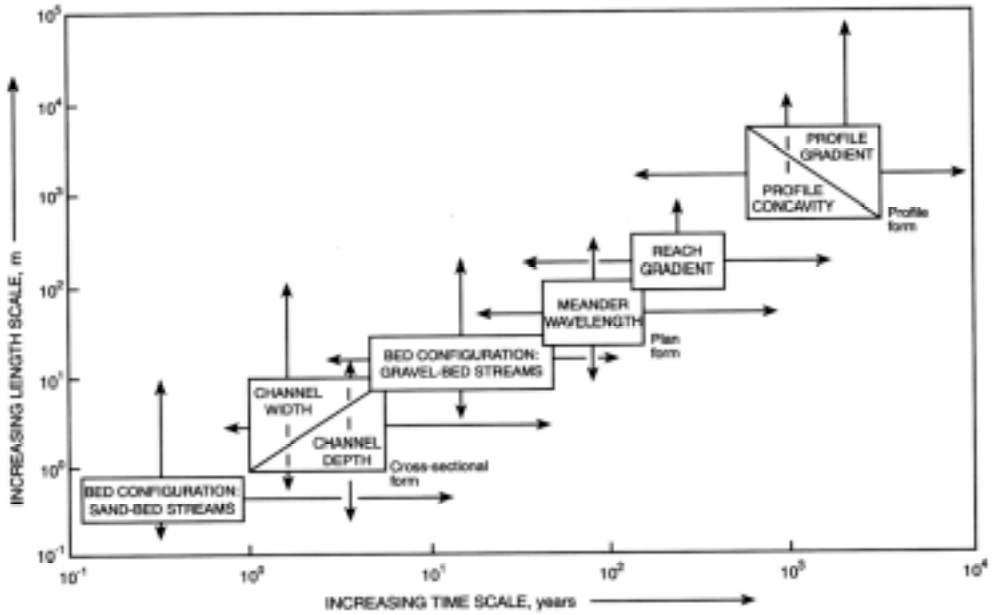

Figure 2-3 - Time-scales of adjustment (after Knighton 1998)

Winterbottom (2000) differentiates between true channel change and dynamic equilibrium. She paraphrases from Lewin et al. (1988): "…channel is adjusted to its discharge regime and although the processes of erosion and deposition continue, the overall form is preserved to produce a dynamically stable pattern."

To synthesize the concepts presented above for use in this dissertation: The terms dynamic equilibrium and relative stability are considered to be equivalent. This state is not static and accommodates lateral migration with maintenance of planform. A sediment flow balance also characterizes dynamic equilibrium. Equilibrium of channel process will lead to equilibrium of form given enough time for adjustment. Disequilibrium or instability is a period of adjustment from one equilibrium form to another and is synonymous with true channel change exemplified by planform shifts, width changes and consistent trends of aggradation or degradation. The terms equilibrium and stability will be used interchangeably in this dissertation to describe a state of dynamic equilibrium or relative stability.

2.2 Historic geomorphic analysis - Understanding channel adjustment

The abundance of studies of channel change present in the literature illustrates the importance of the study of channel adjustments (e.g., Winterbottom 2000; Nanson and Hickin 1986; Hooke and Redmond 1992; Gurnell et al. 1994; Gurnell and Petts 1995; Pizzuto 1994; Mosley 1975). Studies of channel change can be undertaken for a variety of reasons. Often the study of channel

adjustment is related to environmental implications and restoration efforts (e.g., Van Steeter and Pitlick 1998; Winterbottom 2000) or to determine the impacts of anthropogenic factors such as urbanization on channel adjustment (e.g., Mosley 1975; Bledsoe 1999). Other reasons for study of channel adjustment include navigation purposes (e.g., Abam and Omuso 2000) or loss of farmland (e.g., Hooke 1977). Historical geomorphic analyses of braided rivers reveal information that is useful in understanding the dynamics of braiding (e.g., Warburton et al. 1993; Thorne et al. 1993) and for siting structures such as bridges on braided rivers (e.g., Klaassen and Vermeer 1988). Numerous studies have attempted to quantify and understand the variability of river movement and adjustment. For instance, Komura and Simons (1967) modeled vertical changes in the river bed downstream from a dam, Brice (1982) studied lateral movement of rivers particularly related to highway structures, and Johnson et al. (1976) looked at lateral river adjustments related to cottonwoods.

As described above, channel adjustment can occur in different directions, either vertical or lateral, with as many as four (Knighton 1998) to nine degrees of freedom (Hey 1988). It is possible to study channel movement in any one of these directions, but the adjustments should not be thought of as independent from one another (Knighton 1998). Studies of channel adjustment can take the form of analysis of fluctuations in channel bed elevation (e.g., Rinaldi and Simon 1998), channel geometry including both bed elevation and width (e.g., Abam and Omuso 2000), and channel planform or lateral adjustments (e.g., Winterbottom 2000).

Studies of channel adjustment also occur at different temporal and spatial scales. Brookes (1992) highlights the importance of and need for studies of channel adjustment on the order of 100 to 500 years, which is characterized as a period of intensifying human impact. As time goes on and discharge records lengthen and the technology available, e.g., Geographic Information Systems (GIS), to analyze historic records of channel change improves, studies of this magnitude are becoming more abundant. Winterbottom's (2000) study of changes in the Rivers Tay and Tummel in Scotland addresses this need by encompassing the period from 25 to 250 years ago in addition to a short-term field study over the last 25 years. Other studies in the US and Europe including Biedenharn et al. (2000), Rinaldi and Simon (1998), Hooke (1977), Brewer and Lewin (1998) study channel adjustments within the last 200 years. Historic data and maps are more plentiful in Europe and as a result more extensive studies are possible, such as Gilvear (1993) and Gilvear and Winterbottom (1992), which utilize maps from 1700's in Scotland, and Klimek and Trafas' (1972) study in Poland. However, in the western US, studies on this time scale are not as abundant, as data prior to the 1930's are not readily available on most rivers. Some of the more

extensive historic studies in the western U.S. include Van Steeter and Pitlick's (1998) documentation of changes in the Colorado River between 1937 and 1993.

The time scales necessary to observe different adjustments vary. Dade and Friend (1998) suggest that adjustment in alluvial channels occur on the order of 10^3 to 10^5 years. At another extreme, measurements of a sediment wave progressing through a pro-glacial gravel-bed river were made over a 5-week period and highlighted the importance of diurnal discharge fluctuations in determining resulting channel morphology (Lane et al. 1996). The interaction of vegetal growth with channel narrowing can prolong periods of adjustment, whereas widening may achieve an equilibrium state more rapidly (Church 1995). Brookes (1992) extends the concept of time scale of response beyond just the physical system and includes the biota associated with rivers, with discussion of the hierarchies of channel change.

Many of the studies described above document progressive adjustments in response to controlling variables. Often, however, channel response is not a simple progression towards an equilibrium state. Channel adjustment can become more complex and include adjustment over thresholds (Brookes 1992; Schumm 1973; Brewer and Lewin 1998). Brewer and Lewin (1998) document complex response to environmental change including the importance of sequence of flows. They propose the concept of 'historic priming' which suggests that channel form can be the result of the sequence of changes in input variables. Another example of complex response is the Hanjiang River in China which initially narrowed following dam closure then later widened (Xu 1996a, 1997a).

Specific use of equilibrium concepts to describe the state of a channel relative to a defined equilibrium state is employed by Biedenharn et al. (2000), Church (1995), and Winterbottom (2000). Biedenharn et al. (2000) and Winterbottom (2000) look at both spatial and temporal deviations from equilibrium, identifying unstable and stable reaches throughout the time periods studied.

2.3 Predicting channel adjustment

Successful prediction of channel adjustment requires prediction of four elements: direction of response, magnitude of response, rate of response and extent of response (Knighton 1998). Early attempts, beginning in the 1950's, at predicting channel adjustment were qualitative and described the anticipated direction of response, not the magnitude. At the time of authorization of Cochiti Dam, 1960, the general direction of the response of the river was anticipated. More detailed

discussion of the prediction of channel adjustment downstream from Cochiti Dam is presented in Chapter 3.

Schumm's (1969) river metamorphosis concept is a qualitative attempt at predicting the response of a channel to changing inputs. He proposed relationships based on empirical equations using data from the U.S. and southeastern Australia with the assumption that the percentage of silt and clay in the bed and banks can be used as a measure of quantity of bed load. The substitution of bed material size for bed load transport creates an indirect inclusion of a sediment load factor. The resulting relationships are summarized by the following equations (after Knighton 1998), where a + or – denotes increase or decrease in the corresponding variable:

$$Q^{+} \rightarrow W^{+}, d^{+}, (W/d)^{+}, \lambda^{+}, S^{-} \quad \text{.....(2-2)}$$

$$Q^{-} \rightarrow W^{-}, d^{-}, (W/d)^{-}, \lambda^{-}, S^{+} \quad \text{.....(2-3)}$$

$$Q_{sb}{}^{+} \rightarrow W^{+}, d^{-}, (W/d)^{+}, \lambda^{+}, P^{-}, S^{+} \quad \text{.....(2-4)}$$

$$Q_{sb}{}^{-} \rightarrow W^{-}, d^{+}, (W/d)^{-}, \lambda^{-}, P^{+}, S^{-} \quad \text{.....(2-5)}$$

$$Q^{+}, Q_{sb}^{+} \rightarrow W^{+}, d^{\pm}, (W/d)^{+}, \lambda^{+}, P^{-}, S^{\pm} \quad \text{.....(2-6)}$$

$$Q^{-}, Q_{sb}^{-} \rightarrow W^{-}, d^{\pm}, (W/d)^{-}, \lambda^{-}, P^{+}, S^{\pm} \quad \text{.....(2-7)}$$

$$Q^{+}, Q_{sb}^{-} \rightarrow W^{\pm}, d^{+}, (W/d)^{\pm}, \lambda^{\pm}, P^{+}, S^{-} \quad \text{.....(2-8)}$$

$$Q^{-}, Q_{sb}^{+} \rightarrow W^{\pm}, d^{-}, (W/d)^{\pm}, \lambda^{\pm}, P^{-}, S^{+} \quad \text{.....(2-9)}$$

where: Q = water discharge;

Q_{sb} = bed-material load;

W = channel width;

d = mean channel depth;

λ = meander wavelength;

P = channel sinuosity; and

S = channel slope.

Schumm's (1969) concept is expanded upon by Brookes (1992) to provide a means of anticipating channel response to anthropogenic changes. These responses are summarized in Table 2-1.

Table 2-1 - Expansion of Schumm's river metamorphosis relationships (after Brookes 1992, Table 4.3)

Equations		Examples of change
$Qs^{+}, Qw^{++} \approx S^{-}, d_{50}{}^{+}, D^{+}, W^{+}$	(1)	Long-term effect of urbanization. Increased frequency and magnitude of discharge. Channel erosion (increasing width and depth)
$Qs^{0}, Qw^{+} \approx S^{-}, d_{50}{}^{+}, D^{+}, W^{+}$	(2)	
$Qs^{-}, Qw^{+} \approx S^{-}, d_{50}{}^{+}, D^{+}, W^{-}$	(3)	Intensification of vegetation cover through afforestation and improved land management reduces sediment loads
$Qs^{--}, Qw^{-} \approx S^{-}, d_{50}{}^{+}, D^{+}, W^{\pm}$	(4)	
$Qs^{-}, Qw^{+} \approx S^{-}, d_{50}{}^{+}, D^{+}, W^{\pm}$	(5)	Diversion of water to a river
$Qs^{+}, Qw^{+} \approx S^{\pm}, d_{50}{}^{\pm}, D^{\pm}, W^{+}$	(6)	Commensurate changes of water and sediment discharge with unpredictable changes of slope, flow depth and bed material
$Qs^{-}, Qw^{-} \approx S^{\pm}, d_{50}{}^{\pm}, D^{\pm}, W^{-}$	(7)	
$Qs^{++}, Qw^{+} \approx S^{+}, d_{50}{}^{-}, D^{-}, W^{+}$	(8)	Land use change from forest to crop production. Sediment discharge increasing more rapidly than water discharge. Bed changes from gravel to sand, wider shallower channels
$Qs^{+}, Qw^{0} \approx S^{+}, d_{50}{}^{-}, D^{-}, W^{+}$	(9)	
$Qs^{0}, Qw^{-} \approx S^{+}, d_{50}{}^{-}, D^{-}, W^{-}$	(10)	Extraction of water from river resulting in narrower stream
$Qs^{-}, Qw^{--} \approx S^{+}, d_{50}{}^{-}, D^{-}, W^{-}$	(11)	
$Qs^{+}, Qw^{-} \approx S^{+}, d_{50}{}^{-}, D^{-}, W^{\pm}$	(12)	Increased water and sediment discharge

D = flow depth; d_{50} = median particle size of bedmaterial; Qs = bedload (expressed as a percentage of total load); Qw = water discharge (e.g. mean annual discharge); S = channel slope; W = flow width.
0 indicates no change; +/− indicates increase or decrease respectively; ++/−− indicates a change of considerable magnitude.

Different attempts have been made at quantitatively predicting the magnitude and rate of channel adjustment to variations in inputs. Methods of modeling channel adjustment include regime theory or hydraulic geometry, rational methods that include theory, and mathematical models. Regime theory or hydraulic geometry equations are empirical methods that utilize the concept of equilibrium as the endpoint toward which channels are moving. Rational methods involve simultaneous solution of the equations that describe the interaction between form and process, and mathematical models apply numerical solution techniques to the rational equations (Hey 1988).

Different studies propose alternative definitions of the controlling or independent variables and the response or dependent variables in the scheme of channel adjustment. For instance, Hey (1988) proposed that rivers possess nine degrees of freedom: average channel width, average channel depth, maximum depth, height and wavelength of bedforms, slope, velocity, sinuosity and meander arc length. These response variables are determined by the inputs or controlling

variables of water discharge, sediment discharge, bed material, bank material, bank vegetation and valley slope.

Historically, a single measure of discharge was used as the defining variable for determining channel form. Recent studies are beginning to recognize the importance of combining water and sediment inputs (as seen in Schumm's relationships described above) when analyzing the response of channels (Lane et al. 1996; Van Steeter and Pitlick 1998).

The energy of the flow can be quantified by water discharge alone, or the water discharge combined with the channel slope. Studies have shown that a measure of stream power or a product of slope and discharge to be significant with respect to lateral mobility. Leopold and Wolman (1957) first introduced the concept of a relationship between slope and discharge in determining channel pattern. It follows then that total stream power

$$\Omega = \gamma Q S \quad \text{..... (2-10)}$$

where: Ω = total stream power;

γ = specific weight of water;

Q = water discharge; and

S = channel or valley slope

could be associated with the channel pattern sequence of straight-meandering-braided (Chang 1979). Nanson and Hickin (1983) also proposed that total stream power could be a factor influencing lateral migration rates.

Specific stream power (ω), or the rate at which the potential energy of water flowing downhill is expended per unit area of stream bed, has also been associated with changes in channel planform (Nanson and Croke 1992; Ferguson 1987; Carson 1984) and lateral migration (Nanson and Hickin 1986). Specific stream power is defined as

$$\omega = \frac{\gamma QS}{W} \quad \text{.....(2-11)}$$

where: W = channel width.

The well-documented relationship between channel width and the square root of dominant discharge (Knighton 1998, Ferguson 1987):

$$W = \alpha Q^{0.5} \quad \text{.....(2-12)}$$

can be substituted into the definition of specific stream power and yields an approximation of specific stream power of the form (Bledsoe 1999):

$$\omega \approx \frac{\gamma}{\alpha}\sqrt{Q} \cdot S \quad \text{.....(2-13)}$$

where α is an empirically derived constant.

Another measure of flow energy combines driving (water discharge and channel slope) and resisting (bed material size) forces. Bledsoe (1999), in his analysis of stream power and channel stability, proposed a "mobility index", (*MI*), to describe the potential of a river to move toward its equilibrium state. The mobility index is defined as:

$$MI = S\sqrt{\frac{Q}{D_{50}}} \quad \text{.....(2-14)}$$

where: D_{50} = median bed material size.

The mobility index could also be thought of as a ratio of flow energy or unit stream power to the resisting force of the channel bed represented by the bed material grain size. Thus it becomes an index of the erosive power of the flow or mobility capacity of the channel. Bledsoe (1999) found that the mobility index is a "…robust predictor of channel planform and stability".

2.4 Planform transition

One way a river channel can adjust to changing inputs is by altering its planform or channel pattern. Channel planform is one of the most rapidly changing features of a river channel. It is therefore an important means of quantifying and understanding adjustments of a channel to various disturbances and impulses in the system (Hooke 1995).

In order to study channel pattern transitions, it is necessary to first classify or quantify channel pattern. Since Leopold and Wolman's (1957) first definition of meandering, braided and straight channel patterns, numerous other classification schemes and indices have emerged in the literature. As explained clearly by Bledsoe (1999), channel pattern classifications are now viewed as a continuum rather than discrete types (Ferguson 1987; Knighton and Nanson 1993). However, others suggest that thresholds, albeit "fuzzy ones", do exist (Begin 1981, p. 318).

For the purposes of this review the broad and admittedly general classes of meandering and braiding are used. This simple classification is illustrated in Figure 2-4. The transition of the

Cochiti reach of the Rio Grande from a braided to a single-thread, meandering pattern (Lagasse 1994) makes the understanding of the causes of planform transition and the relevance of planform transition to lateral stability particularly pertinent to this dissertation.

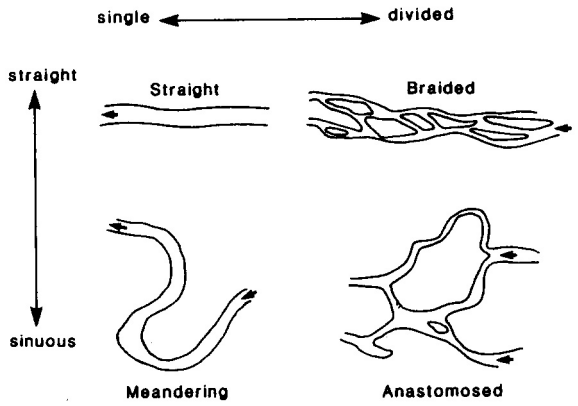

Figure 2-4 - Endpoints of planform continuum (after Ferguson 1987)

There are two kinds of pattern change that can be distinguished (Lewin 1977). Autogenic changes are those that are inherent in the river regime and include channel migration, cutoffs and avulsion. Allogenic changes occur in response to external changes such as climatic fluctuations or altered water and sediment regimes resulting from human impacts. To explain these changes in the context of the previous discussion of channel adjustment toward equilibrium, autogenic changes could be considered to be the kind of movement exhibited by a channel in dynamic equilibrium. When experiencing autogenic changes, a channel would maintain a consistent channel pattern, either meandering or braided. Allogenic changes could be thought of as the adjustments that a channel makes as it moves to a new equilibrium state. Channel planform transition would be an allogenic change.

As a result, the occurrence of channel pattern alteration can be used as a discriminator between reaches in dynamic equilibrium (stable) and those experiencing 'true channel change' (unstable). Alteration of channel pattern can be quantified by change in sinuosity, braiding index, width and pattern classification (i.e., braided vs. meandering) (Winterbottom 2000; Hooke 1977). Mosley's (1975) study of channel changes on the River Bollin, United Kingdom is a good example of these concepts. He identified two time periods during which the processes and rates of channel changed differed significantly. During the period from 1872 to 1935 minor channel migration occurred that was associated with point-bar deposition and bank erosion in bends (autogenic changes = dynamic equilibrium). More rapid channel movements and cutoffs characterized the period from 1935 to 1972. The sinuosity declined, slope steepened and channel

widened (allogenic changes = adjustment to a new equilibrium state). Channel processes changed as a result of human activity, and the form of the channel underwent alteration to adjust to the new hydrologic regime.

Others have shown that the transition to a braided planform is a manifestation of instability resulting from excess stream power (Bledsoe 1999; Alekseevskii and Berkovich 1992). Carson (1984) recognized the importance of stream power in planform transition, but suggested that bedload supply is the critical factor that governs the transition to a braided planform. High stream power alone cannot sustain braiding without high loads of bed-calibre material (Carson 1984; Osterkamp 1978; Alekseevskii and Berkovich 1992). Others suggest that both braiding and meandering can be manifestations of instability if bar development is present and that both patterns can exist in quasi-equilibrium if sediment transport is balanced (Callander 1969; Parker 1976).

Brice (1982) tied different planform classifications or stream types (Figure 2-5) to lateral movement rates. He showed that wide-bend meandering streams and braided streams with point-bars exhibited the highest rates of lateral movement (most unstable) relative to channel width and that equiwidth meandering and straight braided streams were the most stable.

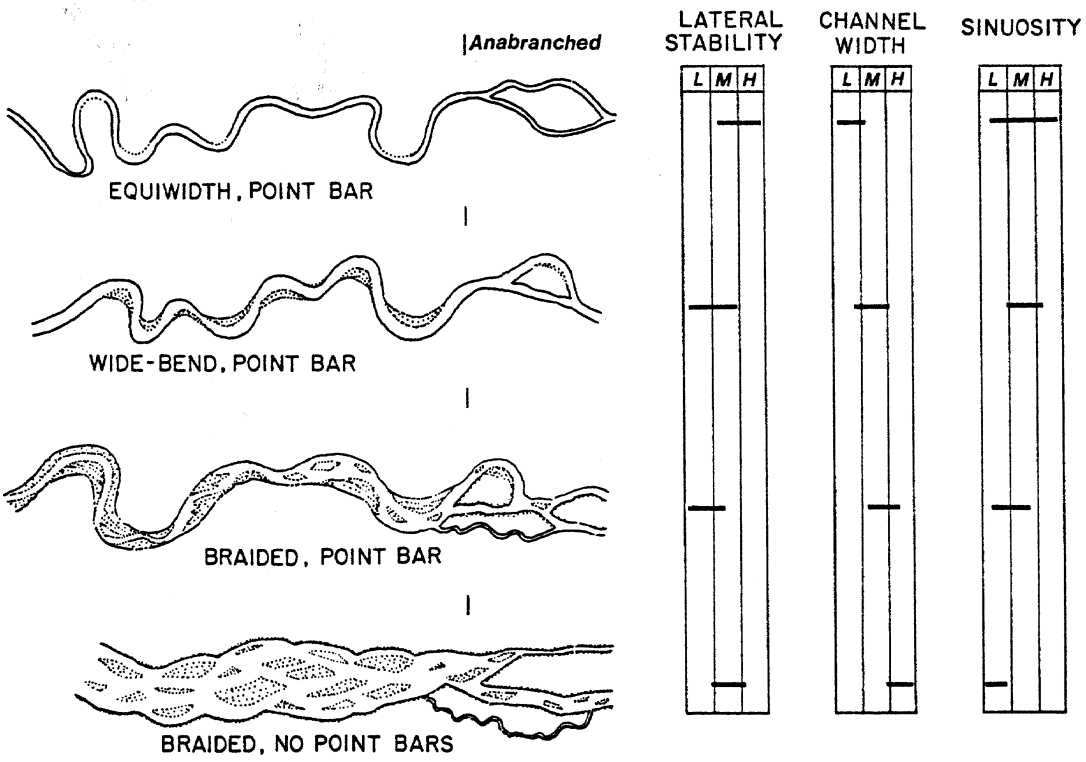

Figure 2-5 - Alluvial stream types (after Brice 1982)

Understanding the channel pattern and whether it is undergoing transition is important in the analysis of lateral (and vertical) channel adjustments. Both the flow energy (water discharge and channel slope) and the sediment supply play important roles in determining the planform conditions of a channel.

2.5 Lateral Movement - Mechanisms, rates and methods of measurement

Lateral movement of a channel, whether in a state of dynamic equilibrium or in an unstable state adjusting from one equilibrium condition to another, can be generalized as a response to the flow strength (water discharge and channel slope) and the sediment supplied to the system. Depending on the input conditions, lateral movement can take different forms. Some possibilities include: narrowing, widening, meander migration, avulsion and cutoffs. The varying form of the response depends upon the input conditions and the existing pattern and geometry of the channel (Friedman et al. 1998). Rivers exhibiting different planform types have been shown to move at different rates and to result from different causes or mechanisms (Brice 1982; Friedman et al. 1998). This section explores existing studies of the mechanisms by which channels move laterally, the rates of movement, and methods used to measure lateral movement.

Lateral movements occur at different rates and are caused by different processes. Mechanisms of movement also vary with planform. Meander movement has been studied thoroughly (e.g., Hooke 1977) and can be broken down into several different types of movement as shown in Figure 2-6. Meanders can migrate consistently across their floodplain by eroding the concave bank and accreting on the convex bank (extension) or they can migrate down valley (translation). Braided rivers can move laterally by avulsion, cutoffs, migration and width change as shown in Figure 2-7.

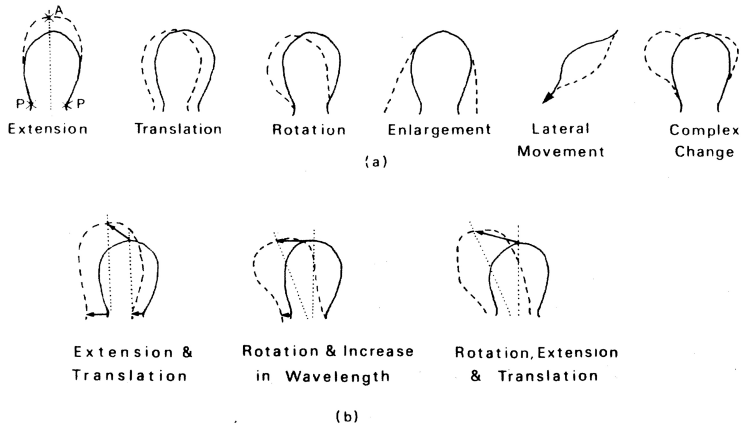

Figure 2-6 - Types of meander movement (a) primary elements and (b) combinations (after Hooke 1977)

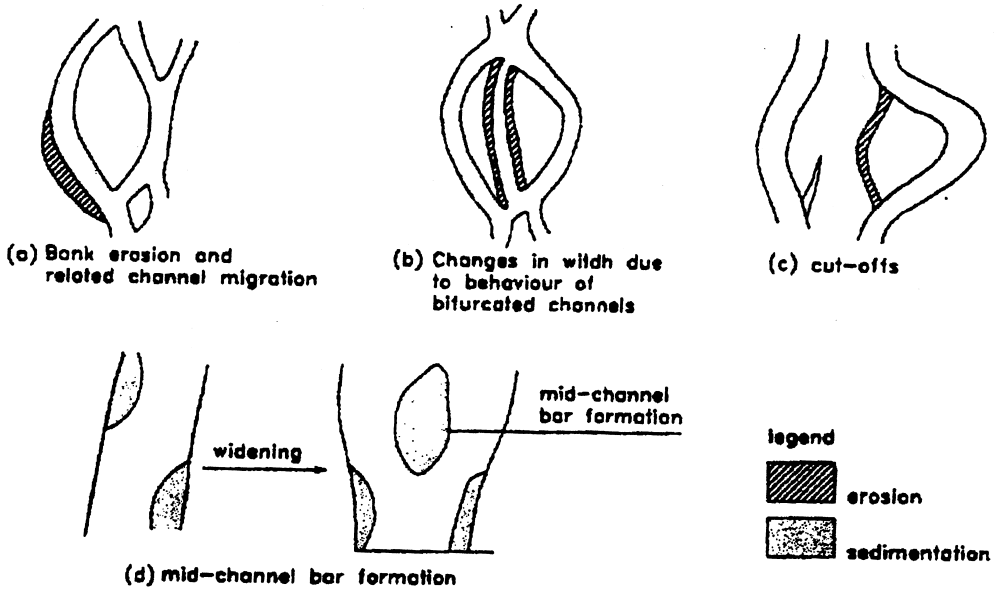

Figure 2-7 - Aggregated mechanisms of planform change in a braided river (after Mosselman 1995)

A majority of the literature on lateral channel movement focuses on migration of meanders and bank erosion of the concave bank of meander bends (e.g., Hooke 1980; Nanson and Hickin 1986; Lawler 1993; Thorne 1991). Literature regarding measurement of lateral movement of braiding rivers is primarily focused on the movements of the Brahmaputra/Jamuna river (e.g., Coleman 1969; Klaassen and Masselink 1992), although studies of other braided rivers do exist (e.g., Warburton et al. 1993). Few studies include both meandering and braided channels (e.g., Brice 1982).

2.5.1 Mechanisms

The mechanisms of meandering formation and migration are the subject of entire conferences and books (e.g., Parker and Ikeda 1989; Elliott 1984). As such, a complete discussion is far beyond the scope of this review, though it is useful to understand the basic processes by which bank erosion occurs as well as the spatial and temporal variability in other variables that may influence lateral movement rates (Lawler 1992). This review focuses on studies that explore empirical relationships between lateral movement rates and other channel process and form parameters as summarized in Table 2-2.

Table 2-2 - Summarization of studies that explored empirical relationships between lateral movement rates and channel process and form variables.

Study	Channel Process Variables
Lawler 1992	Freeze/thaw, Downstream changes
Lawler et al. 1999	Downstream changes (stream power, bank material and seasonal factors)
Hooke 1979	Discharge and rainfall magnitude, timing and frequency, Soil moisture
Nanson and Hickin 1986	Stream power/Discharge-Slope-Bed Material

Study	Channel Form Variables
Hooke 1980	Drainage area, Bank material
Brice 1982	Planform, Width
Nanson and Hickin 1983	R_c/W
Hooke 1987	R_c/W, Sinuosity, Type of meander movement
Biedenharn et al. 1989 Thorne 1991	R_c/W

Note: R_c = Radius of curvature, W = channel width

Some of the more in-depth discussions and empirical analyses of the relationships between lateral movement and channel processes and form are provided by studies performed by Hickin (1974), Nanson and Hickin (1983, 1986) and Hickin and Nanson (1975, 1984). Nanson and Hickin (1983) proposed that lateral migration can be expressed by the following general function: M = F ($\Omega, \tau_b, h, Q_s, p$), where the variables, as listed, are total stream power ($\Omega = \gamma QS$, Equation 2-10), erosional resistance of concave bank, bank height, sediment supply rate and planform. From their analysis of rivers in Canada, they determined that channel width is a reasonable linear scaling factor to account for variations in stream power. As such, lateral movement reduces to a function of R_c/W (R_c = radius of curvature, W = channel width), with all the other parameters accounted for in a coefficient of proportionality. Hickin and Nanson (1984) revised their earlier proposal and suggested that lateral movement can be described by the following general function: M = f ($\omega, \tau_b, h, R_c, W$). They eliminated sediment transport as a significant variable because data are hard to find and because for meandering rivers, suspended load is from bank erosion, rather than vice versa.

Using dimensional analysis and the results from Nanson and Hickin (1983) ($M = f(R_c/W)$), Nanson and Hickin (1986) suggested the following relationship:

$$Mh/W = K\omega/\tau_b \quad \text{.....(2-15)}$$

where: K = constant of proportionality.

which shows that the rate of migration expressed as sediment volume per unit channel width and length is proportional to the ratio of driving to resisting forces in a bend, given a consistent radius of curvature. They assume that bank strength is determined primarily by the size of the basal sediment at the outer bank. Bank strength declines as grain size declines from cobbles to fine sand, with fine sand representing the minimum bank strength. Bank strength increases again with cohesion.

Based on the results described above, Nanson and Hickin (1986) continued to show that τ_b is largely a function of the size of sediment at the base of the channel (D_{50}). As a result, they proposed a new relationship (Nanson and Hickin 1986): $M = f(\omega, W, D_{50}, h, R_c)$. Again, they recognized the importance of the relationship between channel migration rate and sediment load. However, they eliminated sediment load from their analysis because of lack of data.

Other studies identify different channel features and parameters that influence channel migration rates. For instance, vegetation has been shown to play an important role in lateral channel changes (Hey and Thorne 1986; Abernathy and Rutherfurd 1998; Friedman et al. 1998; Gray and MacDonald 1989; Huang and Nanson 1997; Johnson 1998; Marston et al. 1995; Millar 2000). Additionally, bank material and stability have been identified as important (Thorne and Osman 1988; Osman and Thorne 1988a, 1988b; Huang and Nanson 1998; Thorne and Tovey 1981).

2.5.2 Methods of measurement

Three main sources of data used in studies of lateral movement rates include field measurements (e.g., Hooke 1980; Lawler et al. 1999), maps and aerial photos (e.g., Shields et al. 2000; Nanson and Hickin 1986; Hooke 1977) and dateable sedimentary and biological evidence (e.g., Everitt 1968; Hickin and Nanson 1975). The different methods are appropriate and often applied to differing timespans: 1 to 10 years for field measurement, 10 to 200 years for maps and aerial photos, and 30 to 500 years for deposits and biological evidence (Hooke 1980; Hooke and Redmond 1989). Different methods of measurement can give rise to differences in measured rates.

Field measurements are typically taken using erosion pins (Hooke 1979, 1980; Lawler et al. 1999; Lawler 1992, 1993). Other methods such as terrestrial photogrammetry and repeat surveys can be employed (Lawler 1993). As they are typically taken over short time frames, field measurements may be higher than rates measured over longer time periods. Hooke (1980) suggests that averaging rates over a longer time period, such as when using sequential maps or aerial photos, can result in lower rates that are smoothed out over the longer time period. Other differences could result from differences in magnitude and frequency of discharge events and whether a large event occurs during the period studied. This review focuses on literature related to the use of aerial photos, as that is the method of measurement employed in this study.

Use of historical aerial photos can be helpful in determining trends in movements and planform behavior of rivers. Aerial photos are used in many studies to measure changes in channel width (Beschta 1998; Winterbottom 2000; Xu 1997a), lateral movement rates (Hooke 1977; Brice 1982; Xu 1997a; MacDonald 1991; Mosley 1975; Hickin 1974), channel planform (Beschta 1998; Warburton et al. 1993; Klaassen and Vermeer 1988; Winterbottom 2000; Van Steeter and Pitlick 1998; Marston et al. 1995; Brice 1982), bank and flood plain vegetation (Beschta 1998, Marston et al 1995), chute cutoffs and avulsions (Beschta 1998), bar development (Macklin et al. 1998) and qualitative impressions of how a river changes with time (Winterbottom 2000; Macklin et al. 1998; Marston et al 1995; Van Steeter and Pitlick 1998). Satellite imagery can be useful on larger rivers: for instance, Klaassen and Masselink (1992) used LANDSAT images on the Jamuna River to measure lateral movement rates.

Combining older cartographic surveys (pre-1930's) with more recent aerial photos can extend the record of channel change even further into the past (see Macklin et al. 1998; Winterbottom 2000). Klimek and Trafas (1972) combine use of recent aerial photos and historic topographic surveys from 1787 to quantify changes in the Dunajec River in Poland, producing one of the longest records of lateral channel change available. Obviously, extensive records are more readily available in Europe where human records of rivers extend further into the past. However, paleohydrologic evidence, dendrochronlogy and other paleo-methods (e.g., Everitt 1968) have been used in the western U.S. where human records are more limited. Everitt (1968, p. 417), who studied channel migration of the Little Missouri River in North Dakota over the last 300 years, concluded that "…the forest is a living record of recent migration of the channel", with recent being defined in the context of geologic time.

With recent improvements in computer mapping capabilities or Geographic Information Systems (GIS), combining various photogrammetric and cartographic sources into a single

database has become easier. It also becomes easier to more thoroughly quantify channel changes (Winterbottom 2000; Van Steeter and Pitlick 1998; Gurnell 1997), automating what Brice (1982) and others did with projectors before GIS. Winterbottom (2000) notes that GIS has not been used much to look at channel changes in wandering gravel-bed rivers and concludes that GIS is an effective and accurate tool for quantifying channel change along the study reach.

Once aerial photos or maps are compiled into a consistent database, lateral movement rates must somehow be measured or estimated. One such means of measurement is to compare successive channel centerlines (Shields et al. 2000; Hooke 1977; MacDonald 1991). The method of measurement of centerline movement used by Shields et al. (2000) is shown in Figure 2-8.

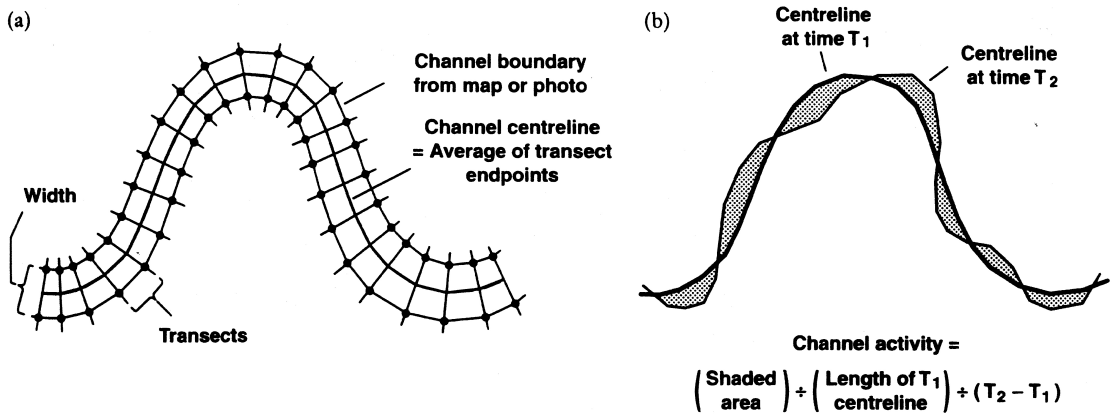

Figure 2-8 - Methods for measuring channel geometry and activity (a) Determination of channel centerline location and channel width, (b) Determination of channel activity (after Shields et al. 2000)

2.5.3 Rates

Lateral movement rates found in other published studies range from 0.1 m/year on small meandering streams (Hooke 1980; MacDonald 1991; Brice 1982) to 150 m/year on the Mississippi River (Kolb 1963) and 500 m/year on the Brahmaputra River (Klaassen and Masselink 1992). Some rates found in published literature are summarized in Table 2-3. Methods of measurement and time periods of study vary between the different studies. Lawler (1993) presents a comprehensive listing of published rates between 1863 and 1988.

Table 2-3 - Lateral movement rates from published studies.

River	Width (m)	Average Movement (m/year)	Mvmt/ Width, (%-width /year)	Planform	Source
Brahmaputra		0-500		Braided	Klaassen and Masselink 1992
Dunajec R., Poland - straight		< 0.1		Straight	Klimek and Trafas 1972
Dunajec R., Poland - winding		0.4-1		Meandering	Klimek and Trafas 1972
Average Max rates		0.24-0.64	3%	Meandering	Hooke 1987
Big Fork	55	0.72	1.3%	Meandering	MacDonald 1991
Buff.Cr.	17	0.63	3.6%	Meandering	MacDonald 1991
Cott.R.	24	0.32	1.3%	Meandering	MacDonald 1991
Hawk Cr.	23	0.35	1.5%	Meandering	MacDonald 1991
Kan. Cr.	8	0.41	5.4%	Meandering	MacDonald 1991
Minn.R. A	43	0.61	1.4%	Meandering	MacDonald 1991
Minn.R. B	88	0.89	1.0%	Meandering	MacDonald 1991
Miss. R. A	56	0.28	0.5%	Meandering	MacDonald 1991
Miss.R. B	67	0.31	0.5%	Meandering	MacDonald 1991
Nemadji R.	34	0.15	0.4%	Meandering	MacDonald 1991
Rice Cr.	13	0.10	0.8%	Meandering	MacDonald 1991
Root R.	34	2.21	6.6%	Meandering	MacDonald 1991
Rum R.	26	0.36	1.4%	Meandering	MacDonald 1991
Wild R.	27	0.34	1.2%	Meandering	MacDonald 1991
Yel. Med. R.	21	0.34	1.6%	Meandering	MacDonald 1991
Zumbro R.	49	0.62	1.3%	Meandering	MacDonald 1991
Missouri R. pre-dam	384	6.6	1.7%		Shields et al. 2000
Missouri R. post-dam	308	1.8	0.6%		Shields et al. 2000
Little Smokey	37	0.57	1.5%	Meandering	Nanson & Hickin 1986
Milk River	48	1.68	3.5%	Meandering	Nanson & Hickin 1986
Belly River	40	1.18	3.0%	Meandering	Nanson & Hickin 1986
West Prairie	30	0.86	2.9%	Meandering	Nanson & Hickin 1986
Beaver	52	1.41	2.7%	Meandering	Nanson & Hickin 1986
Waterton	70	3.93	5.6%	Meandering	Nanson & Hickin 1986
Eagle (Upper)	49	1.34	2.7%	Meandering	Nanson & Hickin 1986
Eagle (Lower)	50	0.71	1.4%	Meandering	Nanson & Hickin 1986
Swan	46	1.52	3.3%	Meandering	Nanson & Hickin 1986
Shuswap (Upper)	63	1.73	2.7%	Meandering	Nanson & Hickin 1986
Pembina	79	2.60	3.3%	Meandering	Nanson & Hickin 1986
Muskwa	49	2.65	5.4%	Meandering	Nanson & Hickin 1986
Oldman	93	7.26	7.8%	Meandering	Nanson & Hickin 1986
Shuswap (Lower)	92	1.89	2.1%	Meandering	Nanson & Hickin 1986
Chinchaga	90	1.03	1.1%	Meandering	Nanson & Hickin 1986
Prophet	140	2.34	1.7%	Meandering	Nanson & Hickin 1986
Sikanni Chief	127	2.92	2.3%	Meandering	Nanson & Hickin 1986
Fort Nelson	278	4.44	1.6%	Meandering	Nanson & Hickin 1986
Exe A	25	1.13	4.5%	Meandering	Hooke 1980
Exe C	26	0.41	1.6%	Meandering	Hooke 1980

River	Width (m)	Average Movement (m/year)	Mvmt/ Width, (%-width /year)	Planform	Source
Exe D	21	0.60	2.9%	Meandering	Hooke 1980
Exe E	30	0.92	3.1%	Meandering	Hooke 1980
Creedy	16	0.06	0.4%	Meandering	Hooke 1980
Culm-Lower	17	0.56	3.2%	Meandering	Hooke 1980
Culm-Upper	13	0.42	3.3%	Meandering	Hooke 1980
Axe 1	38	0.34	0.9%	Meandering	Hooke 1980
Axe 3	16	0.22	1.4%	Meandering	Hooke 1980
Axe 4	38	0.31	0.8%	Meandering	Hooke 1980
Axe 5	20	0.32	1.6%	Meandering	Hooke 1980
Yarty Upper Bend	8	0.67	8.5%	Meandering	Hooke 1980
Coly	42	0.33	0.8%	Meandering	Hooke 1980
R. Endrick, Scotland	25	0.50	2.0%		Data from Hooke 1980
R. Brahmaputra	6000	140.50	2.3%	Braided	Coleman 1969
R. Pembina, Alberta	64	3.35	5.2%		Data from Hooke 1980
Little Missouri R., SD	91.5	4.35	4.8%		Everitt 1968
R. Beatton, BC	370	0.48	0.1%	Meandering	Data from Hooke 1980
R. Cound, Shropshire	17	0.64	3.8%		Data from Hooke 1980
R. Mississippi	1200	152.81	12.7%	Meandering	Kolb 1963
Dunajec R., Poland	75	0.70	0.9%	Braided	Klimek and Trafas 1972
R. Hernad, Czechosloviakia	55	7.50	13.6%		Laczay 1977
R. Bollin-Dean, Cheshire	13	0.16	1.2%		Mosley 1975
R. Klaralven, Sweden	120	1.60	1.3%		Data from Hooke 1980
Apalachicola R., FL	180	1.6	0.9%	Equiwidth	Brice 1982
Apalachicola R., FL	180	1.16	0.6%	Equiwidth	Brice 1982
Apalachicola R., FL	220	1.16	0.5%	Equiwidth	Brice 1982
Big Raccoon Creek, IN	25	0.49	2.0%	Equiwidth	Brice 1982
Bigorn R., WY	55	0.9	1.6%	Wide bend, locally braided	Brice 1982
Bigorn R., WY	75	1.1	1.5%	Wide bend, locally braided	Brice 1982
Black R., AR	80	0.6	0.8%	Equiwidth	Brice 1982
Black R., AR	80	0.47	0.6%	Equiwidth	Brice 1982
Brazos R. TX	150	2.3	1.5%	Wide bend	Brice 1982
Brouilletts Crk., IN	20	0.48	2.4%	Wide bend	Brice 1982
Cache Crk, CA	80	2.3	2.9%	Braided point bar	Brice 1982
Choctawhatchee R,, FL	95	0.5	0.5%	Equiwidth, locally anabranched	Brice 1982
Choctawhatchee R,, FL	95	0.64	0.7%	Equiwidth, anabranched	Brice 1982
Congaree R., SC	90	0.83	0.9%	Wide bend, trans. To equiwidth	Brice 1982
Frenchman Crk, NE	10	0.29	2.9%	wide bend	Brice 1982
Greybull R., WY	90	1.7	1.9%	Braided point bar	Brice 1982

River	Width (m)	Average Movement (m/year)	Mvmt/ Width, (%-width /year)	Planform	Source
Iowa R., IA	75	0.8	1.1%	Wide bend	Brice 1982
Middle Crk., NE	10	0.26	2.6%	Equiwidth, incised	Brice 1982
Middle Loup R., NE	200	0.48	0.2%	Braided no point bars	Brice 1982
Niobrara R., NE	350	0.96	0.3%	Braided no point bars	Brice 1982
N Canadian R., OK	70	4.5	6.4%	Braided point bar, anabranched	Brice 1982
Sacramento R., CA	330	5.1	1.5%	Wide bend, locally braided	Brice 1982
Sacramento R. CA	255	3.1	1.2%	Wide bend	Brice 1982
Snake R., ID	60	0.7	1.2%	Braided point bar, anabranched	Brice 1982
Stevens Crk, IL	8	0.15	1.9%	Equiwidth	Brice 1982
Sugar Crk, IN	23	0.12	0.5%	Equiwidth	Brice 1982
Tallahala Crk, MS	37		0.4%	Wide bend	Brice 1982
White R., AR	160	0.72	0.5%	Equiwidth	Brice 1982
White R., AR	160	0.75	0.5%	Equiwidth	Brice 1982
White R., AR	160	1.8	1.1%	Equiwidth	Brice 1982
White R., East Fork, IN	60	1.9	3.2%	Wide bend	Brice 1982
White R., West Fork, IN	85	1.7	2.0%	Wide bend	Brice 1982
Williamette R., OR	90	0.82	0.9%	Wide bend, anabranched	Brice 1982
Wisconsin R., WI	360	0.36	0.1%	Braided, no point bars	Brice 1982
Yellowstone R., MT	250	5.3	2.1%	Wide bend, anabranched and braided	Brice 1982
Yellowstone R., MT	325	4.1	1.3%	Wide bend, anabranched and braided	Brice 1982
Missouri R., SD-NE	600	9	1.5%	Braided point bar	Brice 1982

2.6 Prediction of lateral migration rates

In order to model lateral movement, many assumptions are necessary. As a result, empirical data are useful in improving prediction of lateral migration rates (Hooke 1977). The theory of meandering movement and formation, as well as the mechanisms of braiding (e.g., bar formation, convergent/divergent flow), are beyond the scope of this study. The following review focuses on studies primarily utilizing empirical means of prediction and modeling. Hasegawa (1989)

provided a summary of more analytical efforts to predict meander migration (e.g., Parker 1984) or other methods including stream power minimization (e.g., Chang 1984).

Hooke (1977, 1979, 1980, 1995) performed extensive studies of lateral movement on meandering streams in the United Kingdom (UK). Hooke (1979) used stepwise multiple regression to correlate hydrologic and climatic conditions with field-measured bank erosion rates. The emphasis was on mechanisms of bank failure, so she looked at antecedent precipitation index, time since last peak, rainfall intensity, and rainfall duration. Hooke (1980) found a slight correlation between size of stream (measured by drainage area) and rate of erosion (m/year). Hooke (1987) found a complex relationship between maximum rate of movement and sinuosity and attributed the variability in the magnitude of the relationship to variations in resistance contributed by the composition of the bank material and the vegetation.

Nanson and Hickin (1983) studied 16 bends on the Beatton River in Western Canada, measured mean radius of curvature and produced a relationship between migration rate and radius of curvature/width. They concluded that measuring erosion rates at a single bend from aerial photos 20-30 years apart is not accurate because of the discontinuous nature of bank erosion. However, a reach-averaged rate may be more indicative of the erosion to be expected given the flow regime of the time period. Hickin and Nanson (1984) expanded the study to include 189 bends on 21 rivers in Western Canada.

Other studies have successfully related lateral movement rates with the ratio of radius of curvature to width. These studies were primarily focused specifically on meander migration (Hickin 1974; Thorne 1992). However, Klaassen and Masselink (1992) were somewhat successful in using the radius of curvature of individual branches of the braided Brahmaputra River. Ligeng and Schiara (1992) provided a theoretical basis for the relationship between meander bend expansion and radius of curvature. Begin (1981) also derived a theoretical relationship between meander migration and the radius of curvature based on the momentum equation of flow. Most recently, Gilvear et al. (2000) combined use of a GIS with an empirically derived relationship between migration rate and channel curvature to predict erosion rates along the course of the meandering Luangwa River in Zambia.

Little work has been performed on predicting migration rates of braided rivers. Klaassen and Masselink (1992) wanted to develop a deterministic method of prediction, but were not successful. They state that “No predictive models are available for braided river systems…" (Klaassen and Masselink 1992, p. 459). As mentioned above, they did correlate bank erosion to a radius of curvature of individual channels. They applied the function: $E = f(W, R_c/W, C, B)$

where, E = bank erosion, W = width, R_c = radius of curvature, C = Chezy coefficient, B = bank resistance. They assume that C and B were consistent along the reach of channel under consideration, so W and R_c/W must determine bank erosion rates.

Building on previous studies, Nanson and Hickin (1986) used data from 18 single-thread, meandering, gravel-bed and sand-bed river reaches with sequential aerial photos that show channel shifting over periods of 21-33 years. They performed multiple regressions on migration rates with discharge, Q, slope, S, and bed material, D_{50}. The best result was:

$$M^* h = f(Q, S, D_{50}), \quad r^2 = 69.1$$

where, M^*h represents the volume of migration. The conclusion is that river size is the most important contributor to channel migration. They used either Q or W to represent river size.

Nanson and Hickin (1986) also scaled migration rate to the size of the river (width) and found that this did not increase the success of the regression, but it did reveal the importance of the size of basal sediments. When the migration rate was scaled by the river's size (using width), the D_{50} of the basal sediment was more important than the stream power (similar to result shown by Hooke 1980 where she used % silt-clay in the bank material). They argued that erosion at the toe of the slope and therefore the bed material is more important in bank erosion rates. Undermining of the bank by basal erosion can cause bank erosion even if the upper sediments are well vegetated. This is in the case of meandering rivers that are relatively deep.

Nanson and Hickin (1986) went on to postulate that bank erosion and channel migration are probably largely determined by bed-material transport. They also suggested that this determination supported their theory that "…a simple relationship involving stream power and basal sediment size provides such an effective means of expressing the driving and resisting forces in this predictive model of channel migration" (Nanson and Hickin 1986, p. 504). They also argued that their model did not support Begin's (1981) momentum/bank shear theory; rather, it supported Bagnold's (1980) bedload transport process. The conclusion that bed-material transport may play a large role in lateral migration suggests that dam construction may have a large impact on downstream lateral channel movement.

Others have attempted similar regressions as a means to estimate migration rates. MacDonald (1991) analyzed 16 meandering streams in Minnesota using photos and maps on a 20-year time interval. The stream centerline and valley centerline were digitized and a program (MEANDER) computed the direction and magnitude of movement of meanders. He then performed regressions with meander migration and channel width, depth, sinuosity, slope and

discharge. Mostly he did not find very good fits in his regressions. The normal average movement of meanders correlated best with discharge and depth.

Shields et al. (2000) also performed regressions with lateral movement rates measured from the Missouri River downstream from Fort Peck Dam. Pre-dam channel activity was slightly correlated with meandering length. Post-dam activity was positively correlated with width. Distance downstream from the dam also produced significant correlation. Significant correlations emerged between channel activity and reach-averaged radius of curvature.

One of the more comprehensive studies of lateral movement rates was performed by Brice (1982) to provide a means of estimating the rate and magnitude of lateral migration for streams of different types, particularly for use by bridge and highway engineers. He based his analysis on data for 200 stream reaches in the US. Brice (1982) shows that bank erosion rates are directly proportional to increases in stream size (W) and to the square root of the drainage area. He also described a qualitative means of measuring stability from aerial photos. Looking at a photo taken during "normal" stage, or the level at which water reaches the permanent vegetation line, he infers stability from the nature of the point bars and the presence or absence of cut banks, and the variability of stream width. He proposed a progression of channel type (Figure 2-5) that varies from equiwidth (uniform width and narrow point bars), wide bend (wide at bends and wide point bars - point bar can be vegetated, but inundated at high flow), braided with point bars, and braided without point bars. Generally he found the wide bend and braided with point bars to be the least stable of the classes (Figure 2-9). As shown in Figure 2-10, the highest values of erosion index occur for sinuosities between 1.2 and 2 (wide-bend and braided point-bar). Sinuosities higher than 2 were generally more stable, and straight segments remained very stable.

Others have used similar planform classifications to subdivide meandering rivers based on point-bar configuration. Ikeda (1989) and Kinoshita (1961, as described by Hasegawa 1989, p. 215) use different terminology but both conclude that different meander patterns correlate to more or less active lateral migration.

Brice (1982) also pointed out the importance of flood duration on erosion rates. He suggested that erosion associated with a major flood might depend more on duration than on magnitude. Median erosion rates tended to increase with stream size (width); however, width, drainage area and discharge are not good indicators of stream size in arid and semiarid regions as opposed to humid regions (Brice 1982).

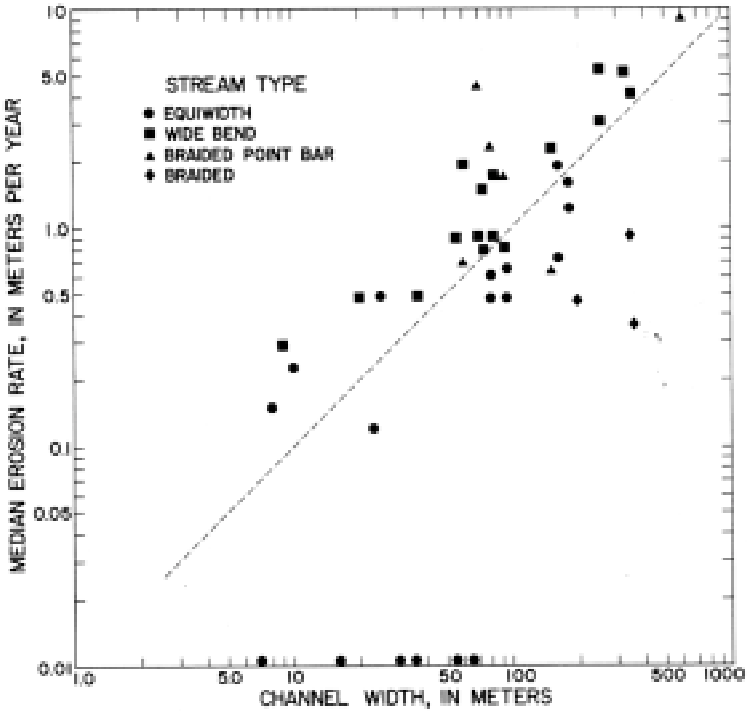

Figure 2-9 - Relationship between lateral channel movement and channel width (after Brice 1982)

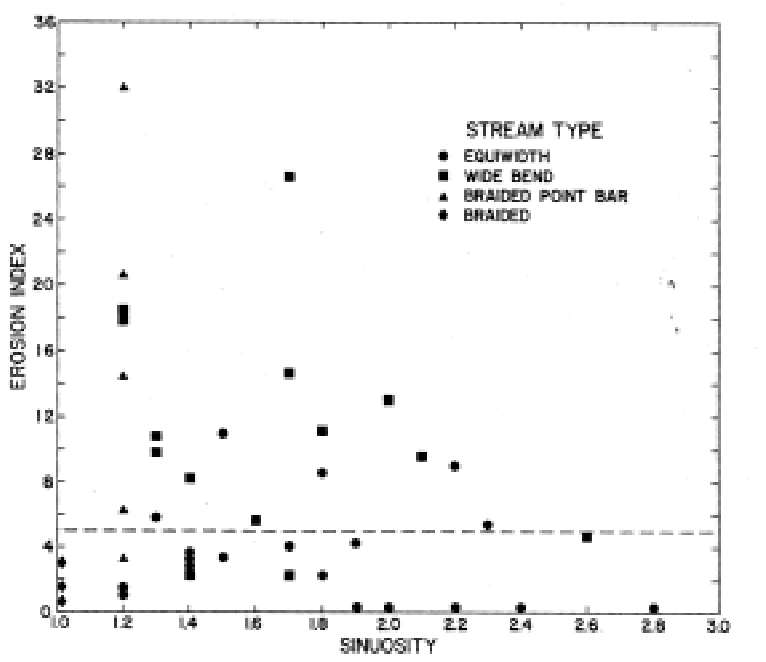

Figure 2-10 - Relationship between erosion index and channel planform (after Brice 1982)

2.7 Impacts of dam construction on lateral mobility and channel planform

Numerous studies document the impacts of dam construction on downstream river channels (e.g., Komura and Simons 1967; Pemberton 1976; Williams and Wolman 1984). Early studies were conducted on the Rio Grande downstream from Elephant Butte Reservoir (Fiock 1931; Ainsworth 1932; International Boundary Commission 1933). These early studies summarize changes in the channel width, slope and elevation as a result of the sediment detention and flow reduction caused by Elephant Butte Dam. Initial degradation of the channel resulting from clear water release was followed by aggradation from sediment deposited by tributaries that the main channel flow no longer had the competence to mobilize (Ainsworth 1932). The general gradient of the channel decreased by as much as 50% further reducing the sediment transport capabilities of the channel. Additionally, the channel narrowed, but no major changes in the course of the river channel by erosion or avulsion were observed (Fiock 1931; International Boundary Commission 1933). Decreased erosion rates were attributed to the encroachment of vegetation on the banks that the reduced flood peaks were not competent to disturb (Fiock 1931). Other studies have been conducted to understand the impacts of Cochiti Dam on the Rio Grande (Lagasse 1981, 1981, 1994; Leon 1998) and are discussed in Chapter 3.

The impact of dam construction on downstream channel pattern and width is documented by numerous studies including Surian (1999), Williams and Wolman (1984), Kellerhals and Church (1989), Shields et al. (2000), Brookes (1992) and Xu (1996a, 1996b, 1996c, 1997a, 1997b), to name a few. Most often the change in channel pattern resulting from an upstream dam involves simplification of the channel, often from a multi-thread channel to single-thread (Brookes 1992). Channel shrinkage is documented on the Platte River following diversion and regulation from 1940 to 1995 (Johnson 1998). Varying response of meandering vs. braided rivers to dam construction has also been documented (Johnson 1998; Friedman et al. 1998).

The impact of dams on channel width is variable (Williams and Wolman 1984). Examples of both widening (e.g., Nicholas et al. 1999) and narrowing (e.g., Bradley and Smith 1984) can be found in the literature. The Hanjiang River in China initially narrowed, then later widened (Xu 1997a). Friedman et al. (1998) provided an overview based on a literature review of impacts of dams on large rivers. They suggested that the effects vary with the pre-existing planform of the river. Braided rivers narrow, whereas meandering rivers do not.

Studies of the impacts of dams on lateral migration rates are not abundant, though most studies report decreased lateral movement following dam construction (Bradley and Smith 1984; Shields et al. 2000; Johnson 1992, 1998; Friedman et al. 1998). Shields et al. (2000) studied the

impacts of Fort Peck dam on lateral migration and channel pattern of the Missouri River. Friedman et al. (1998) found that the rates of lateral migration on already meandering rivers decreased following construction of dam. Other studies document declining migration rates in meandering rivers where peak flows were reduced by dam construction (Johnson 1998; Scott et al. 1997).

Xu (1997a) studied changes in lateral migration rates on the Hanjiang River in China. Pre-dam measured bank erosion rates were 20-25 m/year and post dam they were about 7 m/year right after the dam and about 35 m/year 25 years later. He showed a positive relationship between braiding and number of bars per unit length of channel with bank erosion rate.

2.8 Applications and environmental ramifications

Hydrologic and geomorphic changes resulting from river regulation and stabilization influence both the riparian environment and the aquatic environment (Brookes 1992). Numerous studies document both physical and biological response to river regulation and subsequent adjustment. Shields et al. (2000) concluded that changes in the Missouri River resulting from regulation decreased aquatic habitat quantity, habitat diversity and quality, commercial fish harvest, sport fishing, and fish species composition. They suggested that these effects are part of a global trend of habitat degradation and loss of biodiversity in major rivers. Gilvear (1993) shows the importance of braided reaches of river in Scotland as habitat.

Floodplain and river ecosystems are complex and diverse (Ward et al. 1999). Channel adjustments followed by biotic adjustments can be equally complex and diverse. For example, it has been shown that rivers with different planforms prior to regulation will respond differently to river regulation. As a result, the response of the riparian species can vary (Friedman et al. 1998; Johnson 1998). Johnson (1998) documented the varying responses of riparian cottonwoods to regulation on the Platte and Missouri Rivers. Impacts on cottonwoods can in turn impact other species such as the bald eagles that nest in them. Studies such as Johnson (1992, 1998), Johnson et al. (1976) and Shields et al. (2000) have shown that increased understanding of physical adjustments in river systems can greatly increase our understanding of the subsequent biological and ecological responses.

CHAPTER 3

COCHITI REACH: SITE BACKGROUND AND DATABASE

This chapter provides background information about the Cochiti reach. The first section presents a brief history of the study site including the tributaries and the major anthropogenic impacts. A description of the data collection efforts on the Rio Grande and the database utilized in this dissertation follows. In order to perform the historic geomorphic analysis and measurement of lateral mobility and stability indices in Chapter 4 and 5, the study reach had to be broken down into smaller reaches and subreaches. This definition is described at the end of this chapter.

3.1 Site Background

The middle Rio Grande has a long history of regulation, diversion and other impacts by humans beginning with the Pueblo Indians diverting water from the Rio Grande centuries ago. Major regulation of the river began in the 1920's with the commencement of construction of numerous diversion structures, dams, levees, and channelization works (Scurlock 1998). The dams, built for flood control and sediment detention, were intended to reverse the channel aggradation trend that commenced as much as 11,000 years ago (Sanchez and Baird 1997). The construction of levees to prevent avulsions into surrounding agricultural lands along the river exacerbated the aggradation by confining sediment deposition to a smaller area (Scurlock 1998; Sanchez and Baird 1997).

Woodson and Martin (1962) report that based on a sediment transport analysis, the US Bureau of Reclamation (USBR) predicted that the aggradational trend in the channel downstream from Cochiti Dam would be reversed and that the channel could degrade more than a meter. The degradation was predicted to extend downstream to at least the Rio Puerco. The study suggested that more degradation could occur in certain locations, but it did not specify which locations those would be. The study described by Woodson and Martin (1962) also provided speculation regarding coarsening of the channel bed that would inhibit further degradation. Woodson and

Martin suggested that shifts in planform would impact sediment transport capacity and therefore inhibit degradation.

The middle Rio Grande was described in 1944 by Rittenhouse (p.150) at low-stages as a…"winding, elongated sand flat, averaging about 200-300 yards in width. One or more small low-water channels meander over the sand flat, re-working the deposits in it. At high stages the entire sand flat, as well as the adjacent floodway area beyond the low banks, is under water. Between large floods the width of the sand flat is decreased by growth of cottonwoods and salt cedars. These may be removed or the entire channel shifted during high flows". Rittenhouse also noted that the floodway was nearly a kilometer wide.

The Cochiti reach of the Rio Grande extends from Cochiti dam 45 kilometers downstream to the Highway 44 Bridge in Bernalillo. Several tributaries enter the Rio Grande in this reach, contributing both water and sediment (Figure 3-2). Most are ephemeral arroyos. The two major tributaries, Galisteo Creek and the Jemez River, were also dammed in 1970 and 1953, respectively.

Historically, the Rio Grande at Cochiti was perennial, but became intermittent further downstream at Bernalillo and Albuquerque as a result of irrigation diversions and natural losses downstream from Cochiti. Additionally, releases from El Vado Reservoir on the Rio Chama historically could result in several months of sustained winter flow (Nordin and Beverage 1965). Peak flows resulting from thunderstorm runoff often were as high or higher than the spring snowmelt peak, but usually the duration was only a few hours to a few days (Nordin and Beverage 1965).

Since construction of Cochiti dam, several studies have explored the changing morphology of the reach. Lagasse (1980, 1981 and 1994) presented the results of a qualitative study in terms of trends to assess the response of the Rio Grande to the construction of Cochiti Dam. He compared cross sections, planform and profile data for 1970 – 1980 and attempted to correlate this information with the hydrologic record, hydraulic and sediment data, and the history of engineering activity in the reach. He concluded that sediment inflow from tributaries and arroyos downstream from Cochiti dam has dominated the response of the river to the closure of the dam in planform, base level, and channel cross section. He suggested that the reach between the dam and the Jemez River approached a stable condition more rapidly than the river downstream of the Jemez confluence, and that the reach between the dam and Galisteo Creek may already have completed adjustment to the closure of the dam. He also noted that by 1979 evidence of armoring had progressed to locations as far downstream as Albuquerque.

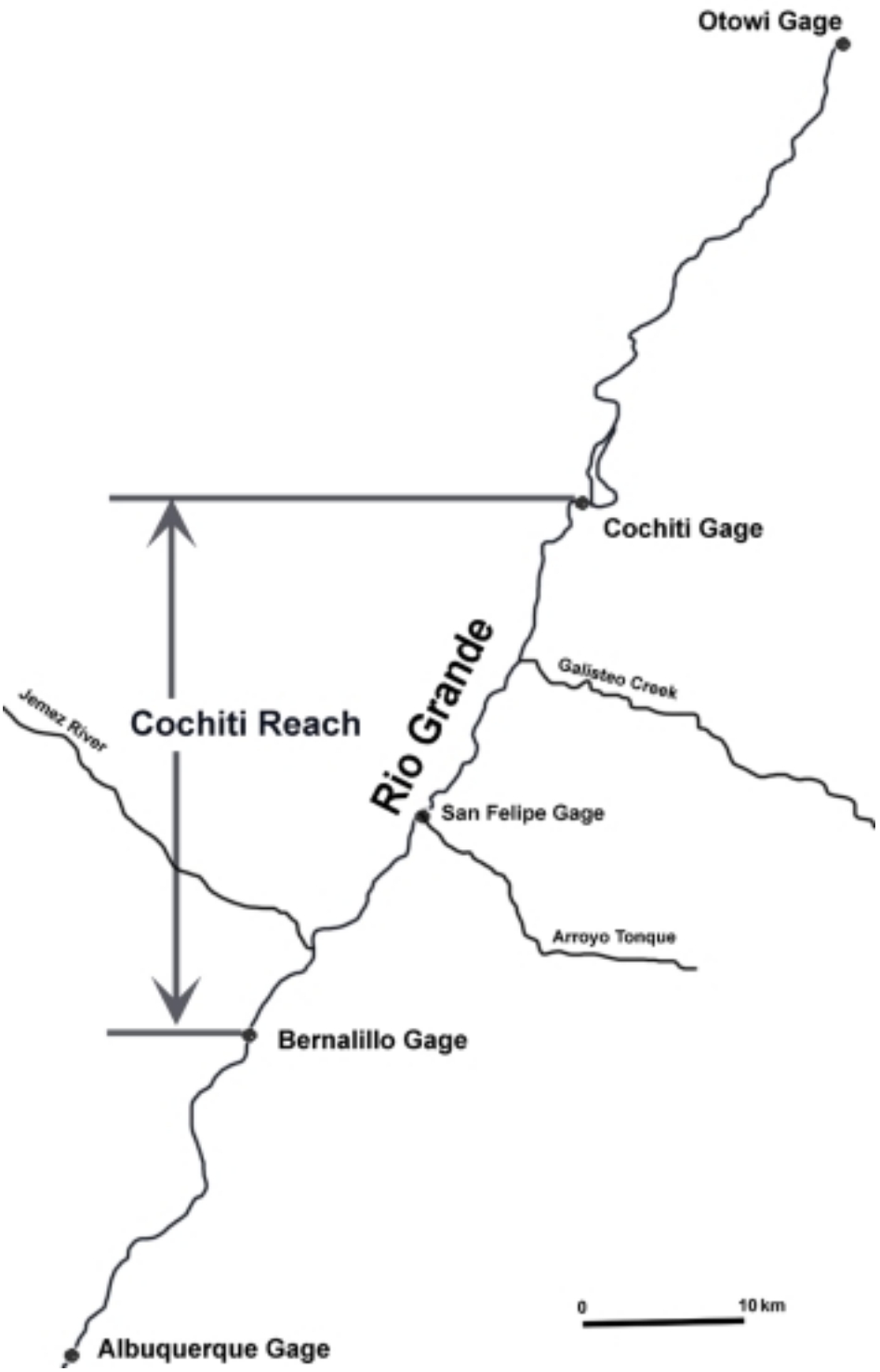

Figure 3-1 - Cochiti Study Reach, Rio Grande, NM showing locations of USGS gaging stations.

Sanchez and Baird (1997) documented changes in the channel of the Cochiti reach since 1918. They noted that a trend toward a narrower channel has been consistent during that time period and has not accelerated since closure of Cochiti Dam. They also showed that the sinuosity increased since construction of the dam, but has not reached the peak level of 1949.

Mosley and Boelman (1998, Draft) studied the geomorphology of the Santa Ana Reach, from Angostura Diversion to the Highway 44 Bridge in Bernalillo. They concluded that the reach moved from a braided to a meandering channel pattern with a high width/depth ratio, and gravel-dominated, riffle/pool channel. Since construction of the dam, the width/depth ratio has decreased.

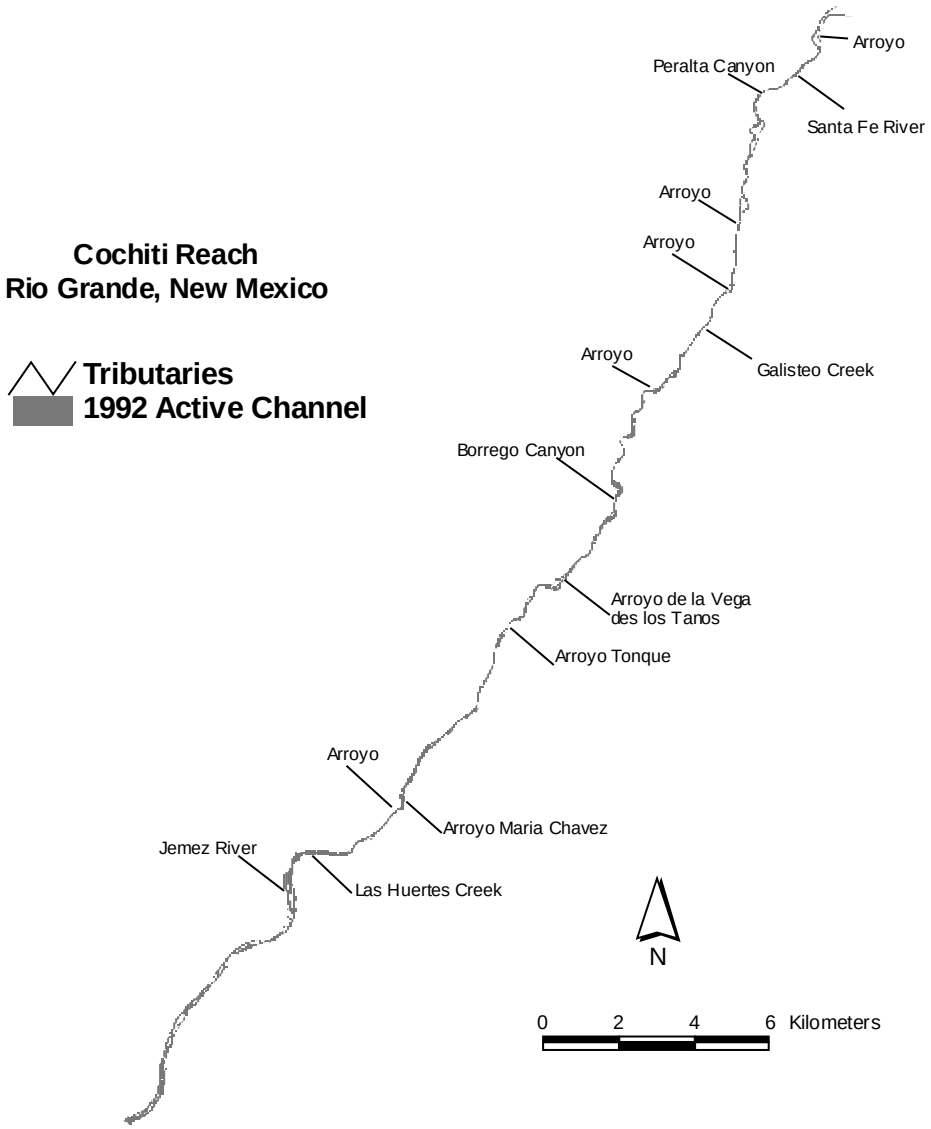

Figure 3-2 - Map of study reach with locations of tributaries.

3.2 Database Development

Data collection began on the Rio Grande in 1889 with the establishment of the first gaging station in the United States at Embudo by the U.S. Geological Survey (USGS). In 1895, the Otowi station was established and provides the longest record of discharge and suspended sediment data used in this study. The locations of these stations and others on the middle Rio Grande are indicated in Figure 3-1.

The combination of severe flooding and sedimentation along with irrigation needs in the middle Rio Grande valley in the early 1900's prompted state and federal agencies including the U.S. Army Corps of Engineers (the Corps), the U.S. Bureau of Reclamation (USBR), the USGS and the Soil Conservation Service (SCS, now the Natural Resources Conservation Service, or NRCS) to begin more intensive surveys of the river. Cross section surveys were collected beginning in 1918, bed material sampling began in the 1930's, suspended sediment measurements were initiated in the 1940's, and aerial photography or topographic surveys are available from 1918 to 1992. The net result of these data collection efforts is a comprehensive, although somewhat confusing documentation of the Cochiti reach for almost 100 years.

Compilation of the Cochiti reach data into a consistent database began in 1997 by the author and others at Colorado State University (CSU) under contract with the USBR Albuquerque office. The end-result of the compilation efforts was a computer database (on CD-ROM, Leon et al. 1999h) and seven volume report (Leon et al. 1999a, 1999b, 1999c, 1999d, 1999e, 1999f, 1999g). The database consists of Microsoft-Excel spreadsheets containing cross-section geometry data and plots, water discharge plots, suspended sediment discharge, concentration and grain size data, and bed material grain size data. Conversion of the historic data, particularly the pre-1970 data, into consistent useable formats proved to be a challenging task. Data collection methods, frequencies and locations were not necessarily consistent between the different agencies. Notes are included in the database indicating the sources, quality and editing required for each data set.

Other studies have looked at the same data and their results are compared with those found in this dissertation in later chapters. Lagasse (1980) utilized the USGS (Dewey et al. 1979) data from 1970 to 1979 in his analysis of downstream channel changes following construction of Cochiti Dam. Leon (1998) performed a comprehensive compilation and summarization of the CSU database described above (Leon et al. 1999h) from 1970 to present.

Expanding on previous studies, this dissertation utilizes the data collected between 1918 and 1992. Some discussion of water and sediment data gathered after 1992 is included. Additionally,

pre-1918 discharge records were used to increase understanding of channel processes before 1918. The CSU database (Leon et al. 1999h) was supplemented by data from historic studies such as Rittenhouse (1944), Nordin and Culbertson (1961) and Nordin and Beverage (1964). The data used are described in detail in the sections below and Appendix A.

Aerial Photos

In addition to surveys and measurements, the middle Rio Grande has been photographed occasionally from the air. Beginning with a topographic survey from 1918, aerial photos of the river are available for 1935, 1949, 1962, 1972, 1985 and 1992. In 1997 USBR, Remote Sensing and Geographic Information Group in Denver, CO digitized the aerial photos, identifying the location of active channel, floodplain, and vegetated islands, as well as numerous other important features. Appendix A, Table A-1 lists the aerial photos that were digitized by USBR and used in the analyses presented herein.

The non-vegetated active channel was used as the delineation of the channel throughout this study. The size of vegetation that begins to show up on the aerial photos is woody bushes that give texture to the area (Jan Oliver, USBR, Remote Sensing and Geographic Information Group, Denver, CO, 1998 pers. comm.). Winterbottom (2000) also used the "non-vegetated" channel for channel boundary delineation. She suggested that it provided consistency between photos with different water levels. The non-vegetated channel was more representative of the channel that is formed by the dominant or channel-forming discharge.

Discharge records

Stream gage data along the Cochiti reach were available from 1895 to 1997 at various USGS gaging stations (Leon et al. 1999c, 1999h). The water-discharge data were collected by the USGS and recorded as daily mean discharge measurements. Dates of available data are summarized in Appendix A, Table A-2. Locations of the gaging stations are indicated in Figure 3-1. The longest record pertinent to this reach is from the Otowi gage (1895-present). This gage, located upstream from Cochiti reservoir, is used as a non-regulated reference discharge for the post-dam period. No major tributaries enter the Rio Grande between the Otowi gage and Cochiti reservoir. The Cochiti gage is located just downstream from Cochiti dam and began operation in 1927. Further downstream are the San Felipe gage, the Bernalillo gage and the Albuquerque gage. The two largest tributaries, Galisteo Creek and the Jemez River, are also gauged. The San Felipe gage, on the main stem, is downstream from Galisteo Creek. The Bernalillo and Albuquerque gages are located downstream from the confluence with the Jemez River.

Cross Section Surveys

Three major sets of cross-section or range lines were established on the middle Rio Grande beginning in 1936. The relative locations of the three different sets of range lines and their locations within the reach are listed in a table in Appendix A, Table A-3. Since 1980, the USBR established several sets of range lines targeting areas of special interest. The locations of these lines are also listed in Appendix A, Table A-3, but are not used in the primary analyses in this study. The cross-section survey data were included in the CSU database (Leon et al. 1999a, 1999b, 1999h) and were reviewed and revised by the USBR Albuquerque office.

In 1936 and 1937, a series of range lines was established by the Soil Conservation Service (SCS) on the Cochiti reach that averaged 5 to 6 kilometers (3 to 4 miles) apart. Additional range lines were added by the Corps in 1944 that reduced the spacing to about 1.5 kilometers (~1 mile) apart. These lines are referred to as the SCS lines and are numbered from 860.4 to 885 and were field surveyed at irregular intervals from 1936 to 1952 by the SCS and the Corps. The USBR, Remote Sensing and Geographic Information Group, Denver, CO digitized the SCS range line surveys. The dates of the available data are summarized in Appendix A, Table A-4.

From the aerial surveys beginning in 1962, a series of lines (cross sections) called the aggradation/degradation (agg/deg) lines was established (Figure 3-3). The agg/deg lines are located approximately 150 meters (500 feet) apart throughout the entire middle Rio Grande from Velarde to Elephant Butte Reservoir, NM. The lengths of the agg/deg lines were determined by the width of the river in 1962 when the cross sections were established. Agg/deg line number 17 is located just downstream from Cochiti dam and establishes the beginning of the Cochiti reach analyzed in this study. Line 298 represents the conclusion of the Cochiti reach. The elevation of the floodplain and non-inundated channel was estimated from the aerial photos by the USBR. The mean channel bed elevation was also estimated by the USBR assuming a trapezoidal channel, using the discharge at the time of the photo, water surface elevation and HEC-RAS hydraulic modeling. Cross section plots were created from topographic data obtained from the aerial photos. Agg/deg line surveys are available for 1962, 1972, and 1992.

A new set of range lines, called the Cochiti range lines or CO-lines (Figure 3-4), was established by the USGS and first surveyed in 1970. Beginning in 1970, the USGS and later the USBR surveyed these lines at irregular time intervals. There was an intensive flurry of surveys between 1970 and 1975, just prior to and after construction of Cochiti dam (November 1973). Surveying of the CO-lines by the USBR and their contractors has continued to the present, with the most recent survey conducted for the USBR during the summer of 1998. The locations of

these lines are indicated in Figure 3-4 and the dates of available cross-section survey data are summarized in Appendix A, Table A-5. A digital version of these data was compiled by Leon (1998) and was reviewed and revised by the USBR in 1999.

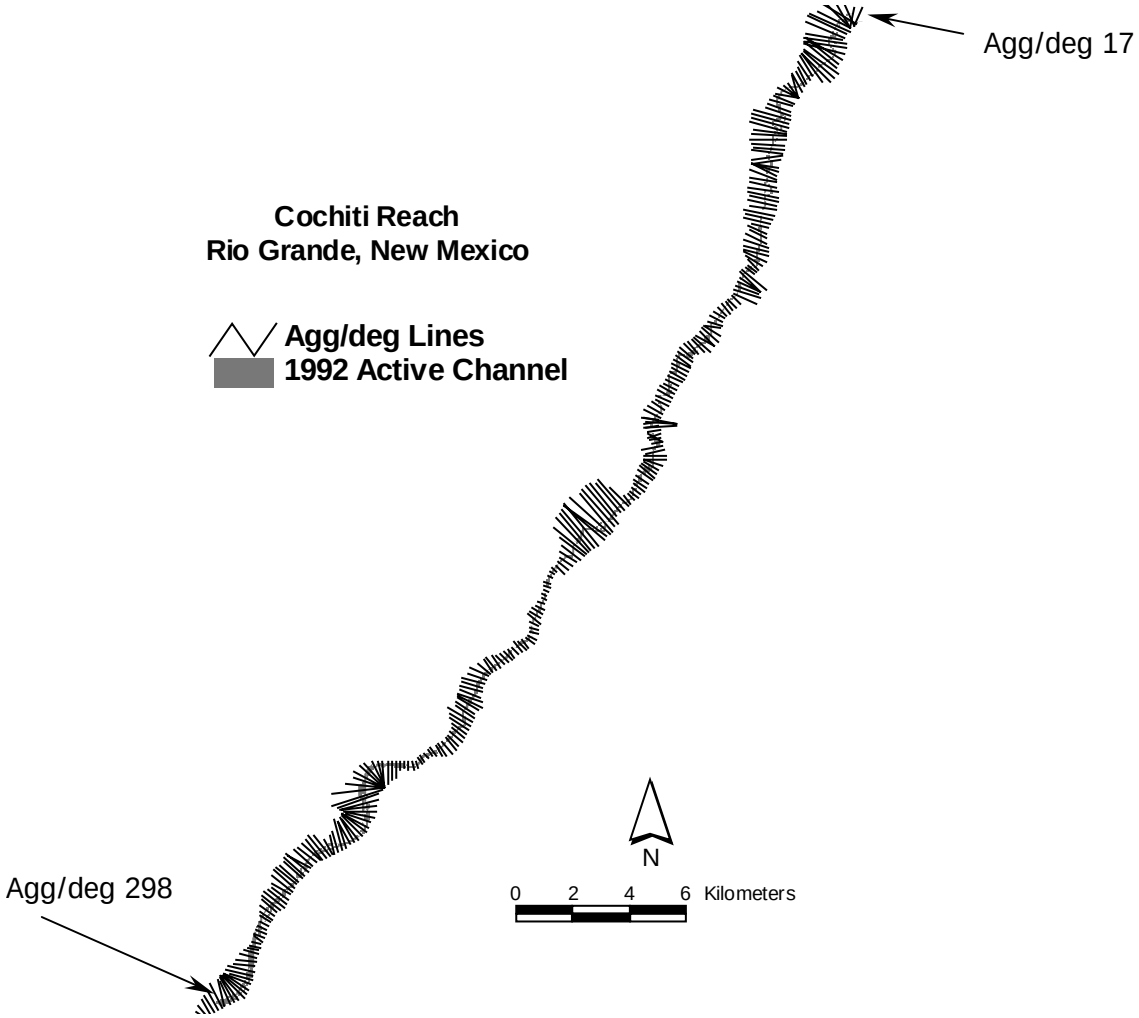

Figure 3-3 - Locations of agg/deg range lines.

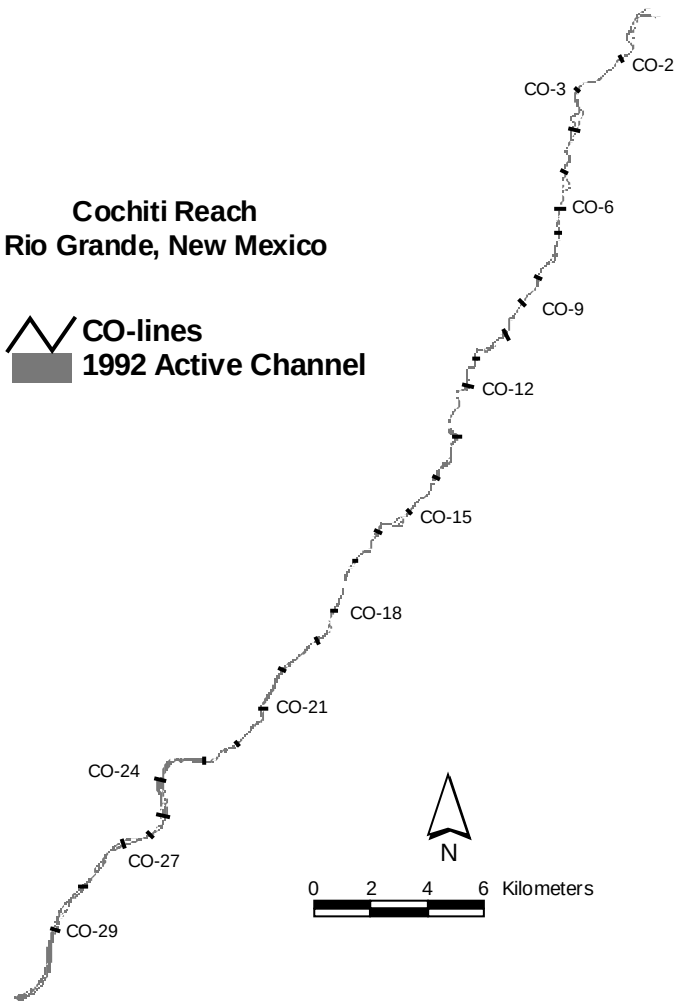

Figure 3-4 - Locations of CO-lines.

Sediment Sampling

Bed material samples were collected during several of the cross-section surveys described in the preceding section between 1970 and 1998 by the USGS, the USBR and their contractors (Leon et al. 1999d, 1999h). The dates of the available bed material data are summarized in Appendix A, Table A-6. The available information includes median bed material size and particle size distributions. Additionally, bed material samples were taken at the USGS gaging stations at irregular intervals between 1960 and 1992 (Leon et al. 1999d, 1999h). The locations and dates of these samples are also shown in Table A-6. Data from Rittenhouse (1944), Nordin

and Culbertson (1961) and Nordin and Beverage (1964) were also used when necessary to supplement the CSU database.

Sampling of suspended sediment at the Otowi gaging station commenced in 1947. Suspended sediment has been measured on the Rio Grande by the USGS at numerous gaging stations for differing periods of time since 1947. Prior to 1947, the only continuous data available are at the San Marcial gage located downstream from this study reach. Additional sporadic suspended sediment data were collected by the USGS and retrieved from EPA's STORET database. The periods of continuous record and dates for the sporadic data for the Cochiti reach are shown in Appendix A, Table A-7 (Leon et al. 1999e, 1999f, 1999g, 1999h).

The 1950's and 60's was a period of intensive data collection and study of the sediment transport characteristics of the middle Rio Grande. Pemberton (1964) described the cooperative study efforts by the USBR and the Corps. In addition, the USGS was active in analyzing and studying the characteristics of the reach. A test reach was established at Bernalillo and results of surveys, including cross section geometry, bed material and suspended sediment data, at numerous cross sections were analyzed by Pemberton (1964), Nordin (1964), Nordin and Beverage (1964 and 1965), Nordin and Culbertson (1961), and Culbertson and Dawdy (1964). The suspended sediment data from these studies are used where possible to fill in the gaps in the gaging record.

3.3 Definition of reaches and subreaches

In order to facilitate analysis of the Cochiti reach, the reach was divided into four smaller reaches and 26 subreaches based on channel characteristics and the existence of natural or manmade controls (Figure 3-5). The reach definitions and lengths are described in Table 3-1.

Table 3-1 - Reach definition and lengths

Reach #	Description	CO Line #'s	Agg/deg line #'s	Valley Length (km)	Average Thalweg Length (km)
1	Cochiti Dam – Galisteo Creek	2-8	17 – 98	11.9	13.2
2	Galisteo Creek – Arroyo Tonque (San Felipe)	9-16	98 – 174	11.3	13.1
3	Arroyo Tonque – Angostura Diversion Dam	17-23	174 – 236	9.4	9.9
4	Angostura Diversion Dam – Bernalillo (Hwy 44 Bridge)	24-30	236 – 313	9.7	10.6

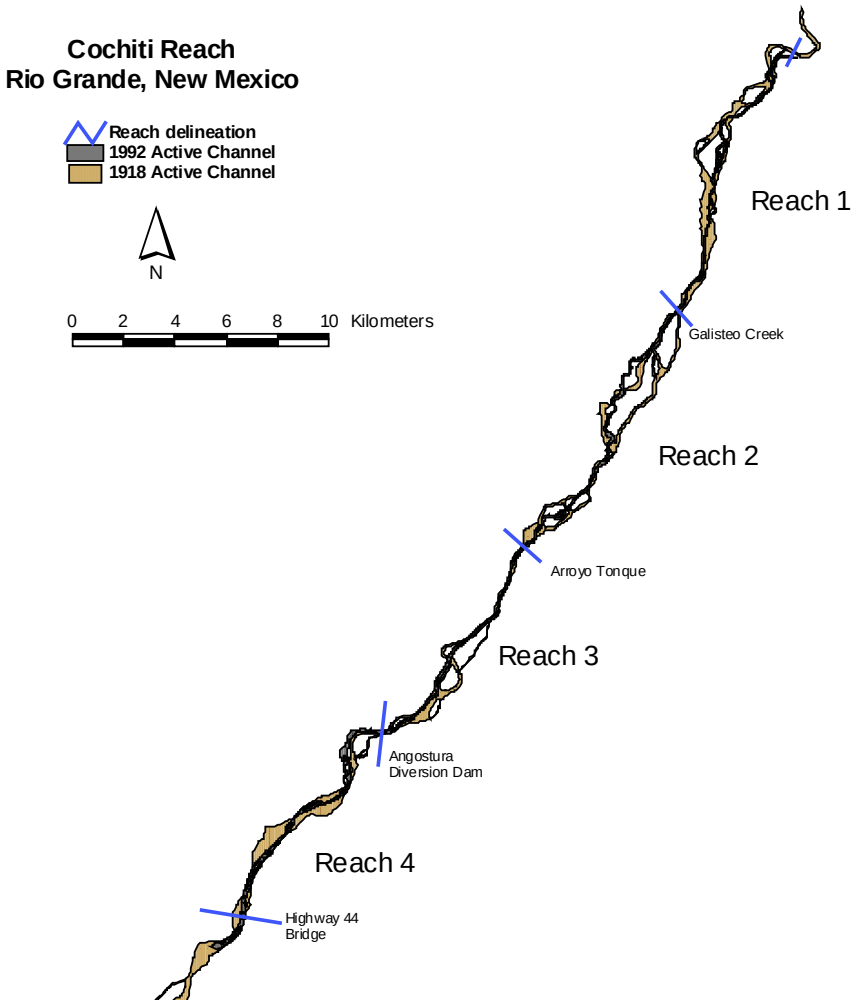

Figure 3-5 - Reach definition.

To better describe the spatial variability of the Cochiti section, reaches 1, 2, 3 and 4 were further subdivided into subreaches. The subreaches were identified using the GIS coverages of the historic active channel, the 1992 aerial photos and the 1997 (1" = 2000') aerial photos. Criteria used were degree of braiding vs. meandering, width (magnitude and spatial and temporal variation), confinement, tributaries, other manmade controls (e.g., Angostura diversion dam), and appearance of floodplain. For instance, a reach that had very variable width and multiple channels in previous years would be separated from a section of consistent width that meanders in 1992. The final result was a total of 26 subreaches as shown in Table 3-2. They vary in length from 0.9 to 3.7 km. The dividing line is the beginning of the next downstream subreach.

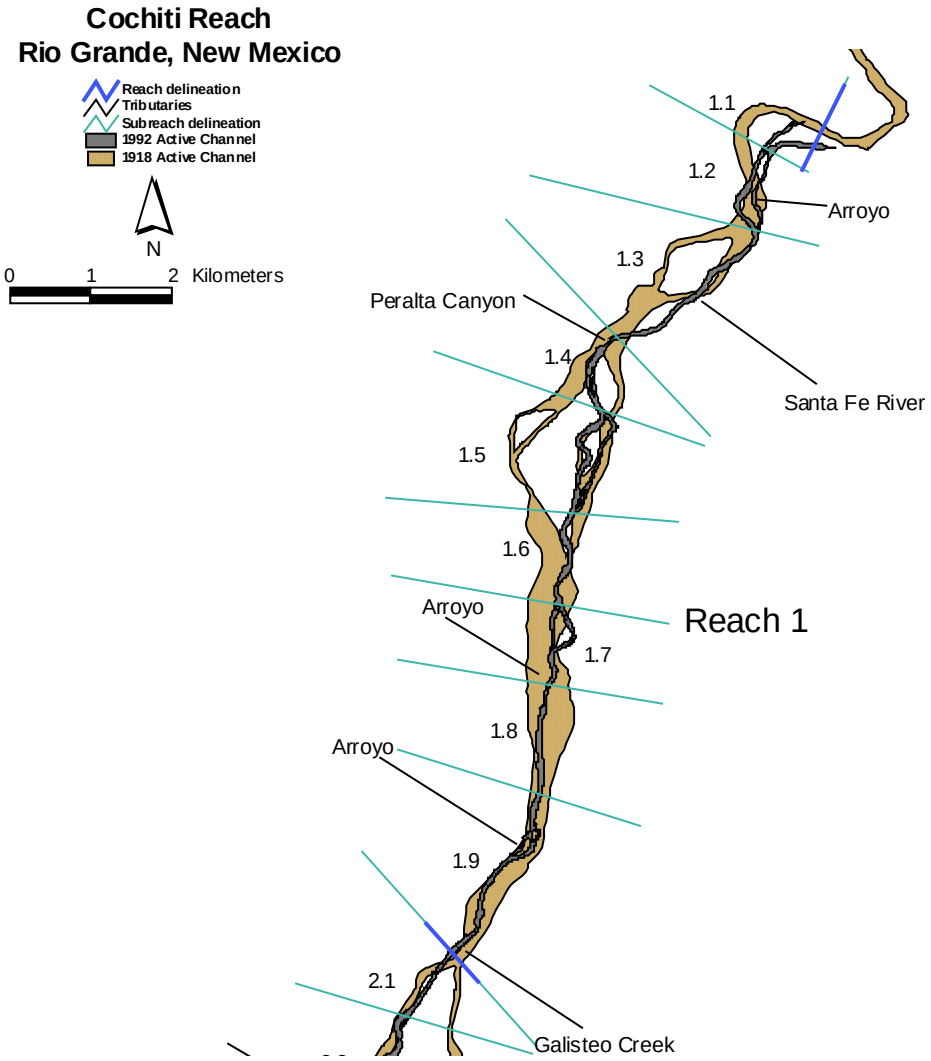

Figure 3-6 - Reach 1 - subreach delineation

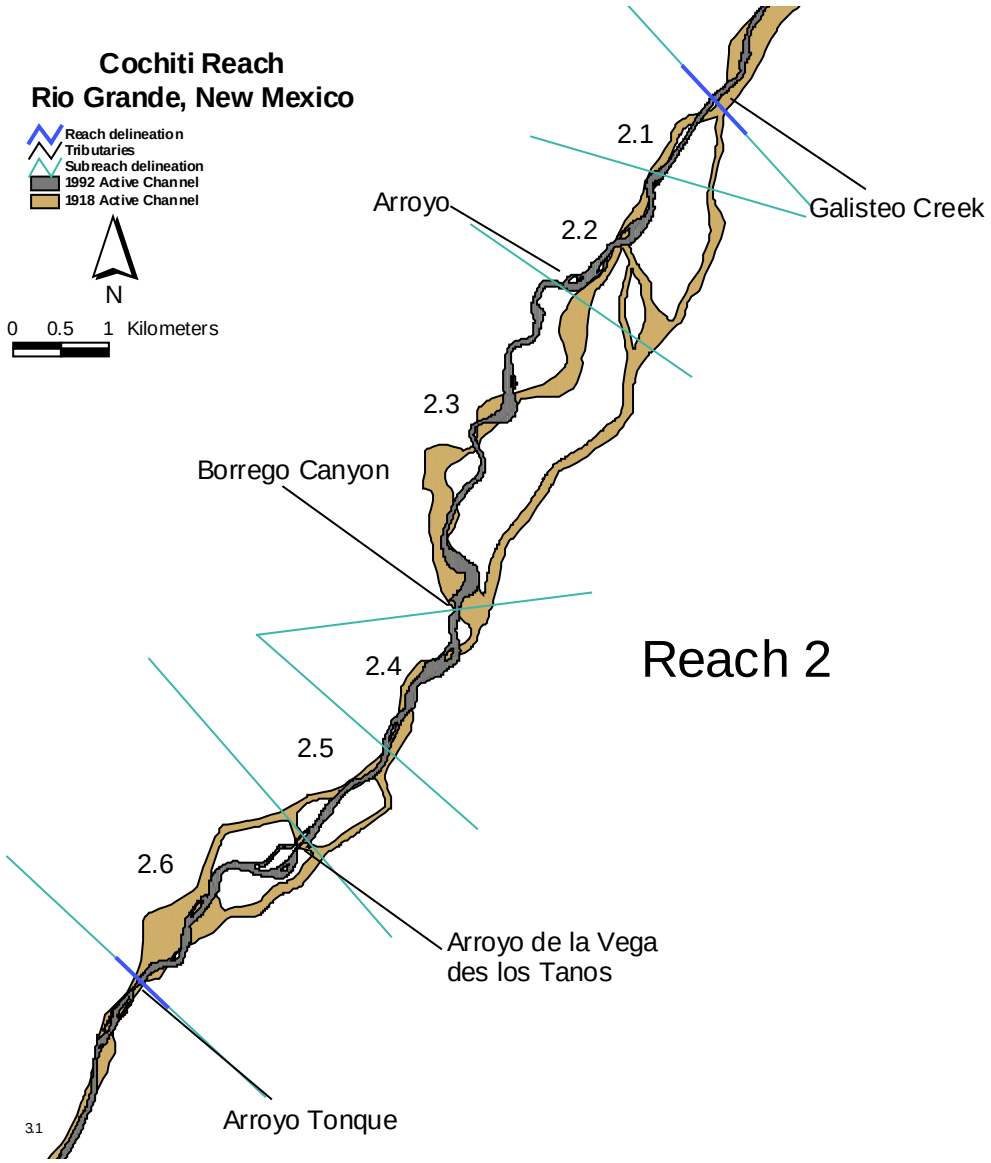

Figure 3-7 - Reach 2 - subreach delineation

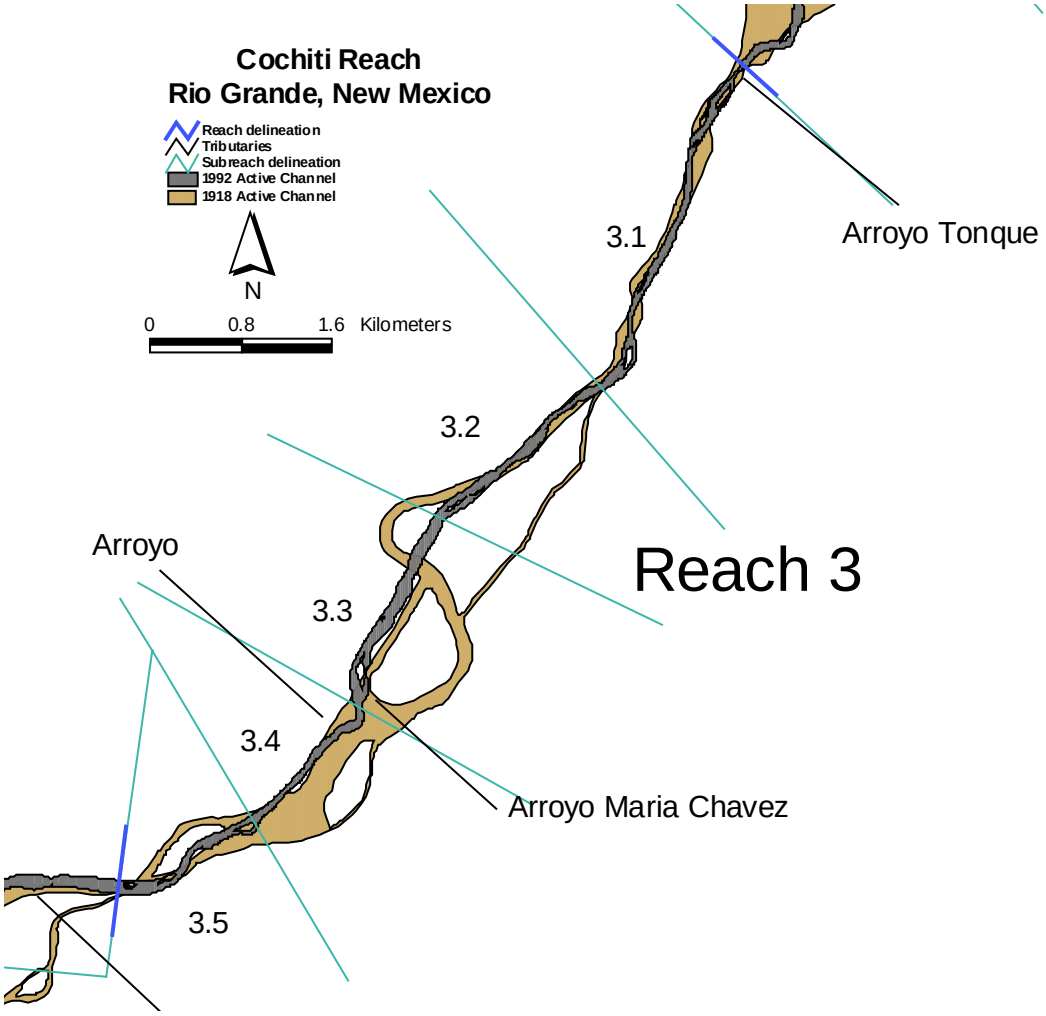

Figure 3-8 - Reach 3 - subreach delineation

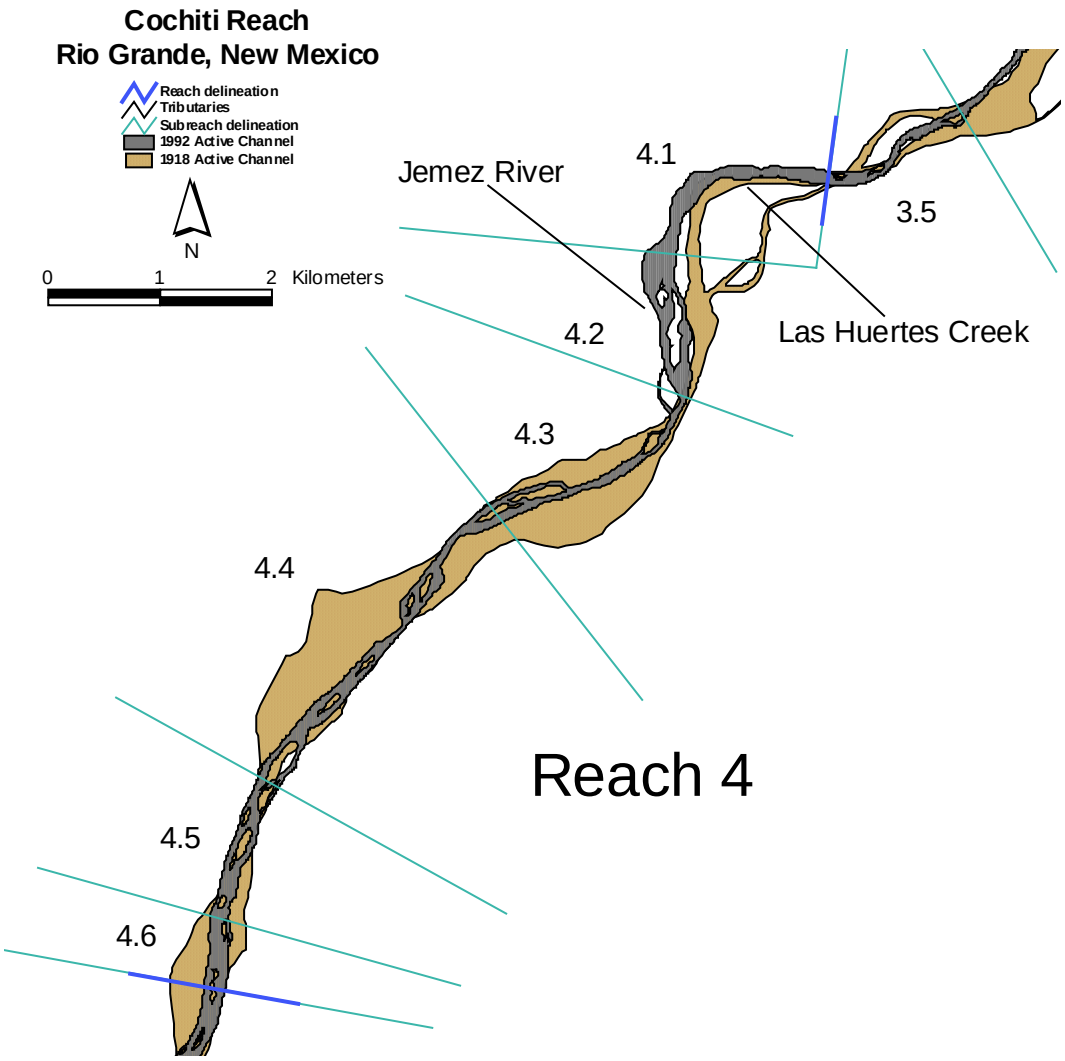

Figure 3-9 - Reach 4 - subreach delineation.

Table 3-2 - Subreach division by agg/deg line. The centerline lengths shown are measured from the approximate center of one agg/deg line to the center of the next line.

Reach #	Subreach #	Start Line	End Line	Centerline Subreach Length (km)
1	1.1	17	22	0.9
	1.2	23	29	1.1
	1.3	30	44	2.0
	1.4	45	50	0.9
	1.5	51	59	1.4
	1.6	60	67	1.1
	1.7	68	73	1.0
	1.8	74	81	1.3
	1.9	82	97	2.4
				12.1
2	2.1	98	103	0.9
	2.2	104	114	1.6
	2.3	115	139	3.7
	2.4	140	151	1.8
	2.5	152	159	1.3
	2.6	160	173	2.4
				11.8
3	3.1	174	193	3.2
	3.2	194	205	1.9
	3.3	206	217	1.8
	3.4	218	226	1.5
	3.5	227	235	1.4
				9.7
4	4.1	236	247	1.5
	4.2	248	255	1.3
	4.3	256	268	1.9
	4.4	269	289	3.1
	4.5	290	298	1.3
	4.6	299	303	0.8
				9.9

3.4 Summary

An extensive database was developed, including water discharge, suspended sediment supply, channel slope, bed material size, cross section surveys, and digitized GIS coverages of the active channel from maps and aerial photos. The data were measured by different government agencies (USGS, SCS, Corps, USBR) beginning in 1895 and continuing through 1998 (for this study). The exact dates and source of all the data are presented in Appendix A.

Additionally, to aid in the study of the spatial variability of response of the study reach, the Cochiti reach was subdivided into 4 reaches and 26 subreaches to facilitate quantification of parameters and analysis of changes in these parameters.

The geomorphic analyses in this dissertation are based on channel changes between digitized coverages of the active channel. Digitized coverages of the active channel are available for 1918, 1935, 1949, 1962, 1972, 1985 and 1992. As a result, the following time periods were analyzed: 1918-35, 1935-49, 1949-62, 1962-72, 1972-85 and 1985-92. Those analyses are presented in the following chapters.

CHAPTER 4

HISTORIC GEOMORPHIC ANALYSIS

COCHITI REACH - RIO GRANDE, NM

River channels respond to the inputs of flow energy (water and slope) and sediment supply, as shown in Figure 2-1. The concept of input and response is utilized for the characterization presented in the following chapter. The processes that shape the river system as well as the resulting shape and form of the channel (see Figure 2-1) of the Cochiti reach, Rio Grande, NM are quantified. The characterization is performed to understand changes that have occurred spatially and temporally in the study reach, as well as to determine reach-averaged variables for use in the stability analyses. The inputs to the channel in the form of water discharge, suspended sediment concentration and channel slope were quantified. The vertical response of the channel was measured by changes in the bed material and the bed elevation. Then, lateral changes in the study reach are described by measurements of width and changes in channel pattern. Chapter 5 continues with more detailed quantification of changes in lateral mobility and stability.

The input and response variables were measured during the 1918 to 1992 time period. Measurements were made to estimate historic trends in the input and response variables and to identify representative values for use in the lateral stability analyses in Chapter 6. Representative values were obtained for the years corresponding to the digitized aerial surveys: 1918, 1935, 1949, 1962, 1972, 1985 and 1992. Each of the variables were also averaged over the reaches and subreaches identified in Chapter 3.

4.1 Inputs

4.1.1 Water Discharge

Along with the sediment supply and the channel slope, the water discharge determines the character and adjustments in the form of the river (See Figure 2-1). In addition to natural variations in water discharge regimes, dams can have varying effects on the discharge regime in

the river downstream from the dam. Some dams pass the natural hydrograph, only reducing the peak discharges. Other dams may completely alter the natural flow regime for hydropower generation (Williams and Wolman 1984). Understanding the changes that occurred in the discharge regime of the Cochiti reach between 1918 and 1992 is necessary for a complete understanding of natural changes in the hydraulic regime as well as the impacts of Cochiti Dam on the downstream channel. Additionally, it is essential to summarize the historic discharge data in order to estimate the channel-forming discharge acting on the channel during each time period studied.

The study of the historic discharge record of the Cochiti reach is broken down into three main goals:

1) Identification of temporal trends in historic mean daily discharge data,
2) Identification of the impacts of Cochiti dam on annual water discharge regime, if any, and
3) Determination of channel-forming discharge for each time period analyzed.

The methods and results for each of these tasks are presented in the following sections.

Methods

Historic Analysis - Trends and Dam Impacts

Detection of trends in the discharge regime during the study period enhances our understanding of the changes in the geomorphology of the Cochiti reach. The time periods analyzed and representative gaging stations are shown in Table 4-1. The locations of the gages are indicated in Figure 3-1.

Table 4-1 - Water discharge data used in historic trend analysis

Gaging Station	Representation	Period of Record
Otowi	Unregulated inflow	1896-1997
Otowi (1896-1926) Cochiti (1927-1984)	Regulated inflow to study reach	1896-1996
Albuquerque	Regulated outflow of study reach	1943-1997

The Otowi gage data were used to represent the unregulated conditions for the inflow to the study reach. Data at the Cochiti gage were only available for the period 1927-1996, so the pre-1927 Otowi data were combined with post-1927 Cochiti data to represent the regulated flow regime at the inlet to the study reach. To justify the use of the Otowi gage data for the pre-1927 time period, the Cochiti gage data were plotted against the Otowi gage data for 1930-1970 and a regression line was fit (Figure 4-1). All of the data were within 10% on average of a 1:1 line representing perfect agreement. The least square fit line has a slope of 0.99 with an r-squared of 0.99. The higher values (>15,000 cfs or 425 m^3/sec) at Cochiti are consistently underestimated by the Otowi data, however the difference is less than 10%. Based on the results of this analysis the Otowi discharge data were used to represent the Cochiti discharge for the pre-1927 time period.

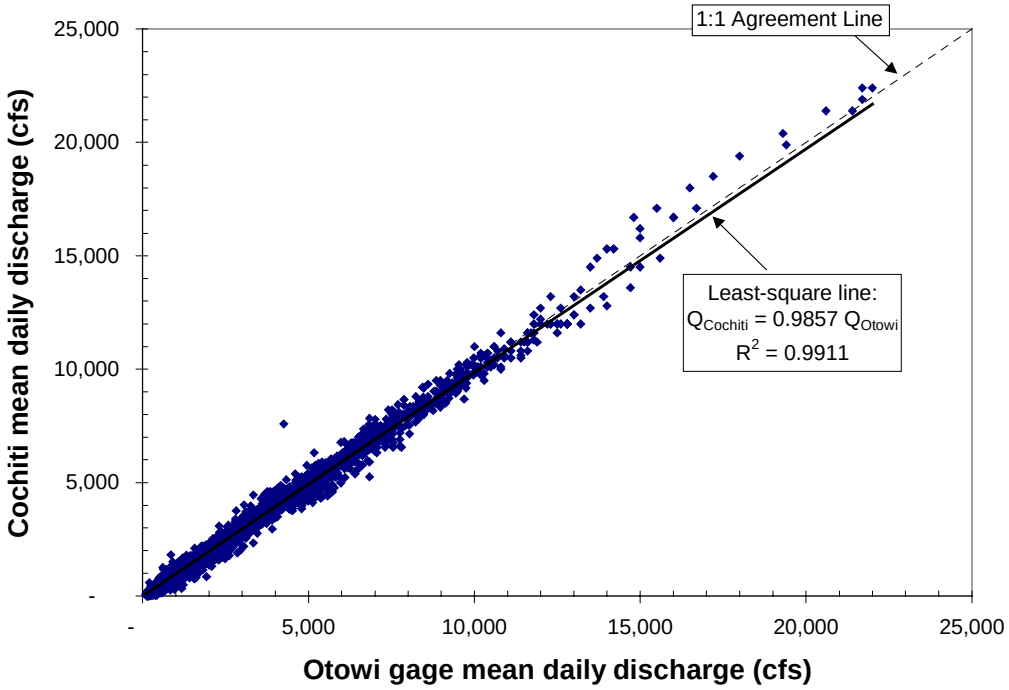

Figure 4-1 - Comparison of daily mean discharge measured at the Otowi and Cochiti gages (1927 to 1996).

The Albuquerque gage is located about 30 km downstream from the Bernalillo bridge. The Bernalillo gage is closer to the outlet of the study reach, but the period of record at Bernalillo is shorter. A comparison between the available Bernalillo gage record (1943-69) and the Albuquerque record revealed little difference in daily mean discharge between these two gages. No major tributaries enter the Rio Grande between the end of the study reach and the Albuquerque gage. As a result, the Albuquerque gage data were substituted for the years where Bernalillo data were unavailable.

Five analyses were performed to identify temporal variations in the historic discharge record and to quantify the impacts of the dam on the discharge regime:

1) Plots of daily mean discharge and peak annual discharge were created for the Otowi, Cochiti, and Bernalillo/Albuquerque gages (Leon et al. 1999c). Qualitative conclusions regarding the seasonal pattern of the water discharge regime and changes in the peak flows were drawn based on visual inspection of the plots.

2) Using USGS gaging station data from the Otowi, Cochiti and Albuquerque gages the following statistics were measured: average monthly flows, annual minimum, annual maximum, duration of high pulse, average rate of rise and fall of high pulse. Least square lines were fit to a plot of each statistic with time and an F-test was performed to determine if the slope of the line was significantly ($\alpha = 0.05$) different from zero (Richter et al. 1996; The Nature Conservancy 1997). This analysis was performed with the data arranged by water year (October 1 through September 30) and utilized the Indicators of Hydrologic Alteration (IHA) methodology (Richter et al. 1996; The Nature Conservancy 1997).

3) Single mass curves of total annual water yield were developed for the Otowi, Cochiti and Albuquerque gages using the annual discharge measured in acre-feet per year. Break points in the curves were identified and the average slopes were computed for the intervening time periods. Additionally, single mass curves were developed for the peak discharge to determine where significant shifts in annual peak flows occurred. Based on preliminary qualitative analyses of time series plots of annual peak discharges using the combined Otowi and Cochiti gage records, peak discharges began to decline during the early part of the 1900's prior to construction of Cochiti dam. The single mass curves were used to identify more specifically when this shift in discharge regime occurred.

4) The Indicators of Hydrologic Alteration (IHA) methods, as proposed by Richter et al (1996), were employed to quantify the impacts of Cochiti Dam on the discharge regime of the study reach. The IHA methods, which included computation of 32 parameters of both the pre and post-dam flow regime, were applied to the Otowi, Otowi/Cochiti combined and Albuquerque gage data as shown in Table 4-1. The IHA methods were designed to evaluate changes in flow regime using pre-impact and post-impact daily average flows. The resulting 32 parameters statistically characterize monthly water conditions, magnitude and duration of annual extreme water conditions, timing of annual extremes, frequency and duration of high and low pulses, and rate and frequency of water

condition changes. The parameters that are of interest from geomorphic and ecological perspectives for the Cochiti reach are the monthly flow conditions, the annual minimum and maximum discharge, the rates of rise and fall, and the duration of the flood peak. The difference between the pre and post-dam means and coefficients of deviation of those parameters were calculated. Differences of greater than 50% were considered to be significant.

5) The mean annual flood (MAF) was computed for the pre-dam (1895-1973) and post-dam (1974-1996) time periods using the combined Otowi/Cochiti gage records. Additionally, based on study of the time series plots and the single-mass curves described above, the MAF's were computed for the pre-1942 and post-1942 time periods and also compared. The MAF's and the medians of the annual flood data for the different time periods were compared using parametric and non-parametric statistical tests to accommodate for potential non-normality in the data. T-tests were performed to test the null hypothesis that the means were the same. A significant result ($p<0.05$) suggests that the null hypothesis can be rejected and that the means are significantly different. The non-parametric tests do not presume that the underlying distributions are normal. The non-parametric tests applied were the Wilcoxon Signed Rank test for confidence intervals on the median of the samples for each time period, and the Mann-Whitney test.

Channel-forming Discharge

Although channel form and response of the channel are likely the result of a range of flows and the temporal sequence of flow events (Bledsoe 1999), representation the "channel-forming" flow regime by a single discharge is helpful (Knighton 1998). In order to determine a correlation between the stability of the Rio Grande and the discharge, estimating a single channel-forming discharge is useful. Methods of estimation include using the bankfull discharge (Williams 1978; Knighton 1998; Andrews 1980), the 2-year frequency flow (Dubler 1997), mean annual flood (Schumm 1969), and the effective discharge, defined as the frequency discharge that carries the most sediment (Wolman and Miller 1960; Andrews 1980; Nash 1994). Thorne et al. (1993) showed that for the braided Brahmaputra River, the dominant discharge was actually less than bankfull, but that inundation of the channel bars is necessary. Similar results have been shown for the Lower Mississippi River (Knighton 1998).

Estimating the channel-forming discharge for the Cochiti reach is not a clear and easy task. Often, the two-year discharge is considered to be equivalent to bankfull, and is used as the channel-forming discharge. The bankfull discharge of the Rio Grande, Cochiti reach has changed

since construction of the dam. At many locations along this reach, the river has incised so that releases from the dam no longer reach the tops of the banks. The potential difference between 2-year frequency discharge, bankfull flow, and effective discharge suggests that more than one method be employed to estimate the channel-forming discharge for the Cochiti reach for the study periods.

The stability analyses presented in Chapters 5 and 6 require a single discharge as an input parameter. As a result, an estimate of channel-forming discharge for each reach and each study period is required. Three different methods of estimating the dominant discharge were compared in this study:

1) 2-year frequency discharge - The 2-year discharge or the annual peak flow with a probability of occurrence of 0.5 was estimated from empirical cumulative distribution functions (CDF's) and from Log Pearson III and Log Normal III distributions. The distributions were developed for the combined Otowi/Cochiti discharge record. The 2-year discharge was also estimated based on empirical distributions for the pre-dam (1895-1973) and post-dam (1974-1997) periods separately. Additionally, 1942 was used as an estimate of the date of the shift in the discharge regime. The 2-year flow was estimated for 1895-1942, 1943-1972, and 1973-1997 separately.

2) Effective discharge - The effective discharge or discharge that moves the most sediment was also computed using a total sediment load rating curve and the frequency distribution of daily mean discharge data (Wolman and Miller 1960; Andrews 1980; Nash 1994). A probability distribution function of the post-dam discharge was created empirically using the USGS bin method (Dubler 1997) from mean daily discharges at the Cochiti gage (1974 to 1997). A sediment rating curve was computed using total sediment load estimates from the Bernalillo Island range lines (1992-1996) (Leon et al. 1999h). The product of the total sediment load and the frequency of occurrence is called the transport effectiveness (Nash 1994) and was computed for incremental discharges. The peak of the transport effectiveness curve corresponds to the effective discharge, which over time will transport the most sediment or do the most work in the channel.

3) Peak flow for each study period or 5-year period prior to survey date - Knighton (1998) suggested that it is the high magnitude, low frequency floods that may control the channel form in arid-zone rivers where the flow regime is very variable. With this as a guideline, the peak mean daily discharge for each time period was selected for use in the

lateral movement studies. For the hydraulic geometry equations, the peak discharge from the 5 years prior to the survey was used.

Results

Historic Analysis - Trends and Dam Impacts

Visual inspection of the time series plots of mean daily discharge (Leon et al. 1999c) revealed that the seasonal variation of the hydrograph characterized by an annual spring snowmelt peak and late-summer thunderstorm peaks has remained consistent since 1895. Spring snowmelt peaks are evident for most years with smaller peaks occurring during the late summer from monsoonal thunderstorms. However, the magnitude of the peaks declined with time since 1895. The time series of annual peak flows at the Otowi and Cochiti gages combined are presented in Figure 4-2. After 1942, the peak discharge does not exceed 340 m^3/s (12,000 cfs). The minimum values of peak flows also decrease with time. Prior to 1934, there was no peak flow less than 126 m^3/s (4,440 cfs), but between 1934 and 1996 there are ten years in which the peak flow was less than 57 m^3/s (2,000 cfs).

El Vado Dam on the Rio Chama was completed in 1935 and served to reduce flood peaks and increase duration of lower flows on the Rio Grande (Crawford et al. 1993, p. 18). Between the mid-1920's and 1950, water diversion in the middle valley and upstream in the Rio Grande basin increased. The combination of decreased flows and confinement by levees exacerbated aggradation by confining aggradation to a smaller area (Crawford et al. 1993, p. 21).

An F-test was employed to test if the slope of the least-square regression line was different ($\alpha = 0.05$) from zero. Trend analysis of the different gaging station data revealed significant decreases in annual maximum discharge for the combined Otowi-Cochiti data set (1895-1997, $p<0.001$) and the Otowi data (1895-1997, $p<0.02$). There was no significant trend ($p>0.05$, suggesting that the slope was not significantly different from zero) in the Albuquerque gage data (1942-1997) for annual maximum flow. The duration of the annual high flows increased significantly ($p<0.005$) for all gages. The number of low flows and the length of low flow periods both decreased for all gages. The magnitude of low flows increased. The trends in monthly average flows varied between the gages highlighting the spatial variability in the reach resulting from localized storms, tributary inputs and diversions.

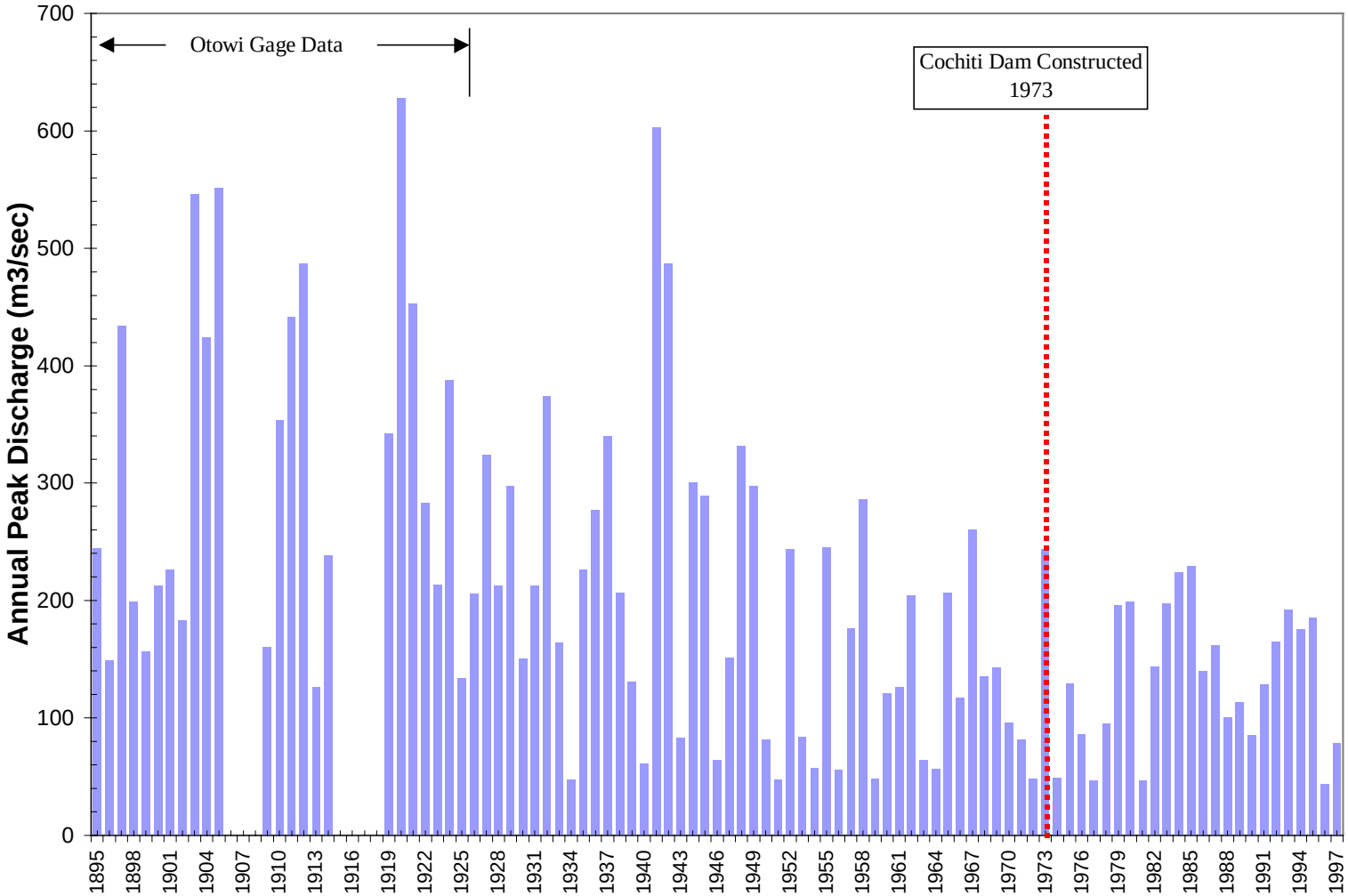

Figure 4-2 – Annual peak discharge at the Cochiti gage (Otowi gage data are substituted for 1895 to 1926).

The cumulative discharge plot (Figure 4-3) of the Cochiti gage shows a drier period from about 1942 through about 1978. The high flow years of 1941-42 and 1979 are evident on the plot. On average, the total discharge has been higher since 1979 than it was prior to 1942. The San Juan-Chama project was completed in 1971 and imports up to 85 million cubic meters (69,100 ac-ft) of San Juan River water from the Colorado River Basin to the middle Rio Grande. This additional water has increased daily mean flows (Crawford et al. 1993). The cumulative discharge plot for the Otowi gage is presented in Figure 4-4 and illustrates the shift in the discharge regime in 1942 mentioned above.

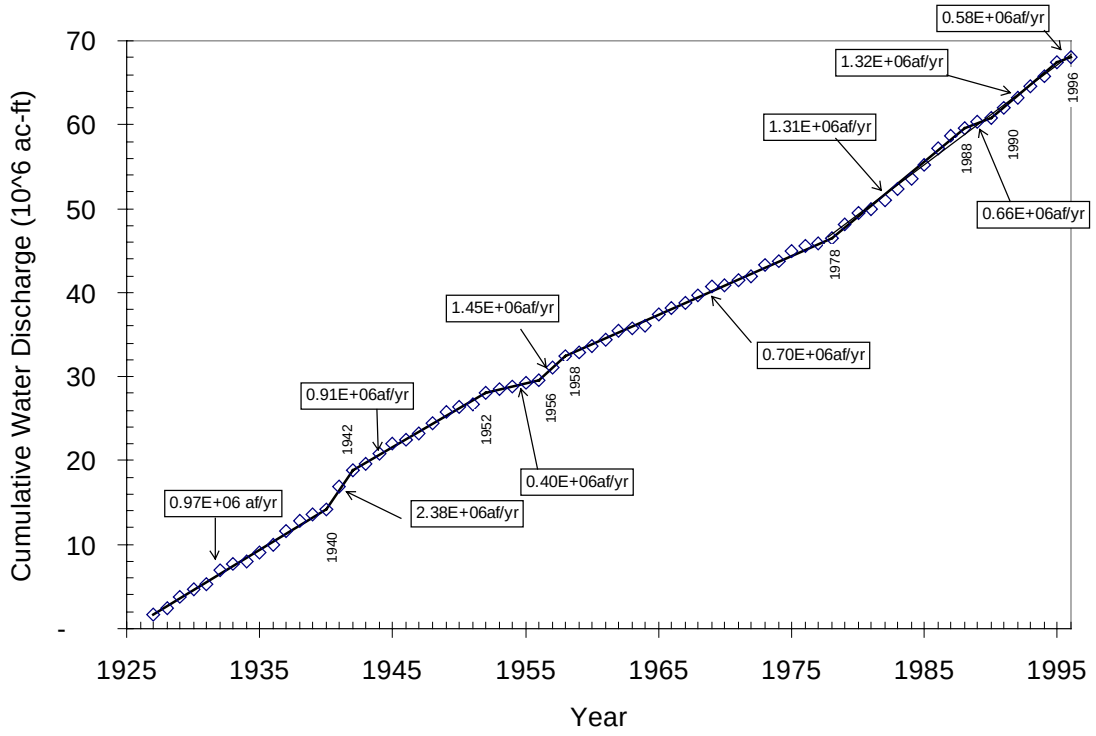

Figure 4-3 - Cumulative discharge for Cochiti Gage (1927-1996) (1ac-ft = 1,233 m^3)

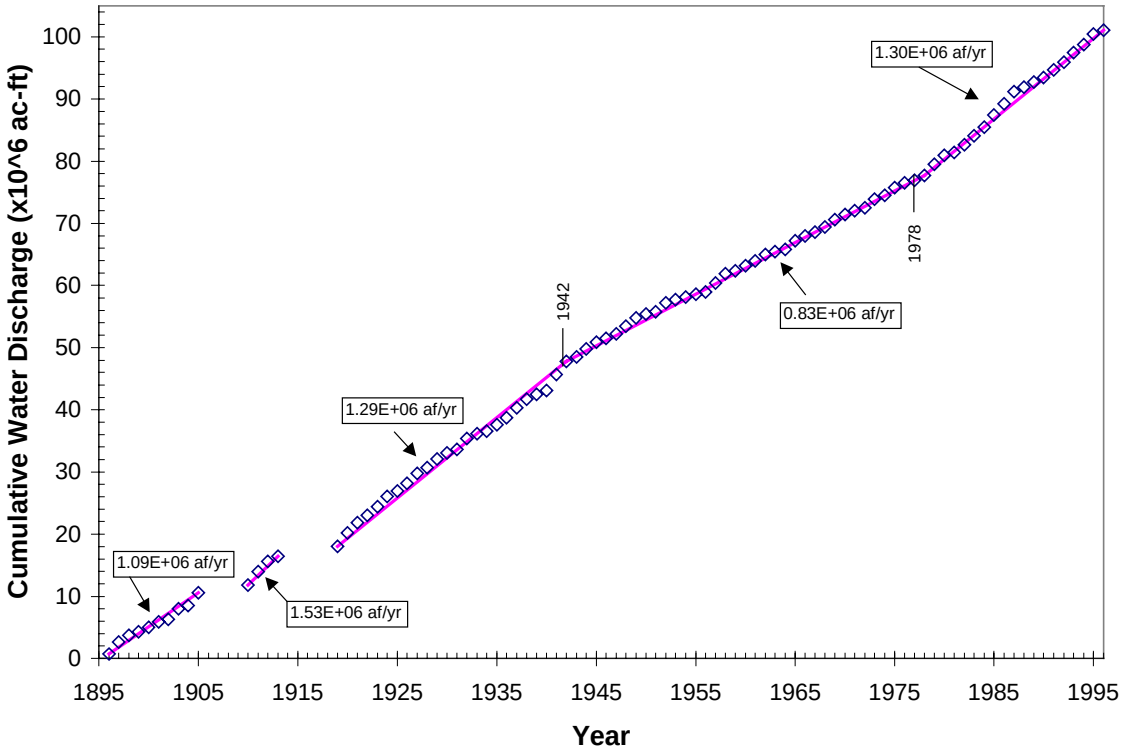

Figure 4-4 - Cumulative discharge for Otowi gage (1895-1996). (1ac-ft = 1,233 m^3)

The results of application of the IHA methodology (Richter et al. 1996) to the Cochiti Reach gage data are presented in Appendix B, Tables B-3, B-4 and B-5. The most significant results (highest % deviation between pre and post-dam periods) are presented in Table 4-2. The one-day maximum (annual flood) decreased at all of the gages, with the greatest decrease being just downstream of the dam at the Cochiti gage. The duration of the high pulse increased at all gages as well as the mean annual flow.

Mean annual flood (MAF) data for the different time periods are presented in Table 4-3. The MAF for the period of 1895-1942 is statistically different from the subsequent period, 1943-1996, ($p=0.000033$ for a two-tailed t-test) at a 99% confidence level. However, the mean annual flood for the 1943-1973 time period is not statistically different ($p>0.05$) from that of 1974-1996 at a 95% confidence level using a two-tailed t-test.

Table 4-2 - Impacts of Cochiti dam on the water discharge regime of the Cochiti reach.

Gaging Station	Average % Change between pre-dam (pre-1973) and post-dam (post-1973) periods			Mean Annual Flow (m^3/sec)	
	1-day Maximum	Mean Annual Flow	High Pulse duration	Pre-dam	Post-dam
Otowi (non-impacted) (1895 - 1996)	-15%	16%	124%	41	48
Otowi/Cochiti (1895 - 1996)	-38%	3%	60%	41	42
Albuquerque (1943 To 1997)	-4%	51%	131%	28	42

Table 4-3 - Mean annual flood data for different time periods. Data from 1895 through 1926 are from the Otowi gaging station. Data from 1927 though 1996 are from the Cochiti gaging station.

Time Period	Description of Time Period	Mean Annual Flood (m^3/s)	Two-year Discharge (m^3/s)
1895 – 1996	Entire Period of Record	202	177
1895 – 1942	Early Higher Flow Period	284	232
1943 – 1973	Low flow Pre-dam Period	142	118
1974 - 1996	Post-dam	136	145
1895 – 1942	Early Higher Flow Period	284	232
1943 – 1996	Post 1942 Lower Flows	139	130
1895 - 1973	Entire Pre-dam Period	223	200
1974 - 1996	Post-dam	136	145

The results of a Wilcoxon Signed Rank test for confidence intervals on the medians of the samples are presented in Table 4-4. This is a non-parametric method that does not presume that the underlying distribution is normal and tests the null hypothesis that the medians are equal. A significant result suggests that the null hypothesis can be rejected, indicating that the medians of

the two sample data sets are not equivalent. The results show that the median peak discharge from 1895 to 1942 is significantly different ($p<0.05$) from the median peak discharge from 1943 to 1996. Use of the Mann-Whitney test to determine whether the medians of the samples were different also revealed that the medians of the samples were different at a 95% confidence level.

Table 4-4 - Results of a Wilcoxon Signed Rank test for confidence intervals on the median of the Cochiti peak flow data.

	Median Peak Discharge (m^3/s)	95% Confidence Interval	
1895-1942	276	219	327
1943-1996	135	113	160

The results of the statistical tests on MAF described above show that the peak flows between 1943 and 1973 (pre-dam) are not statistically different from those between 1974 and 1996 (post-dam). Cochiti dam is operated so that the maximum released discharge is 142 to 170 m^3/s. As a result, operation of the dam only affects flood peaks in excess of 142 m^3/s. This impact can be seen in Figure 4-5, which overlays the peak flows at the Otowi and Cochiti gages from 1974 to 1996. Additionally, attenuation of the flood wave increases the duration of the annual peak as can be seen in the hydrograph for 1979, an exceptionally high flow year (Figure 4-6).

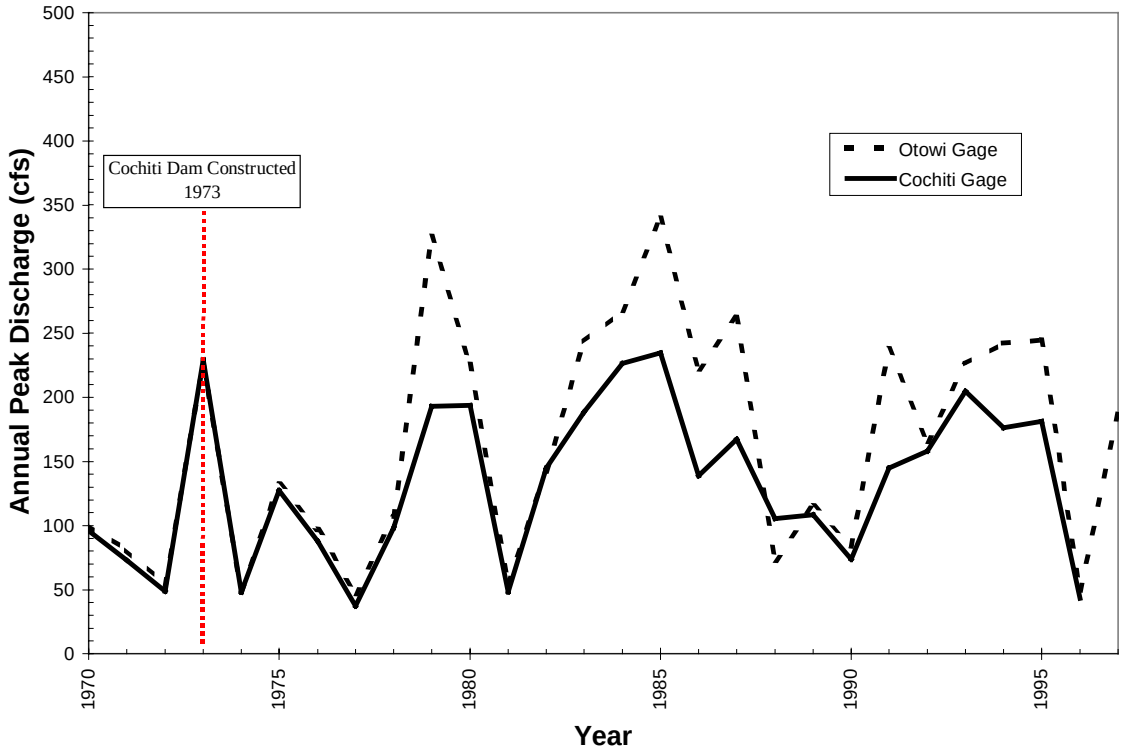

Figure 4-5 - Post-dam annual peak flows at Otowi and Cochiti gages

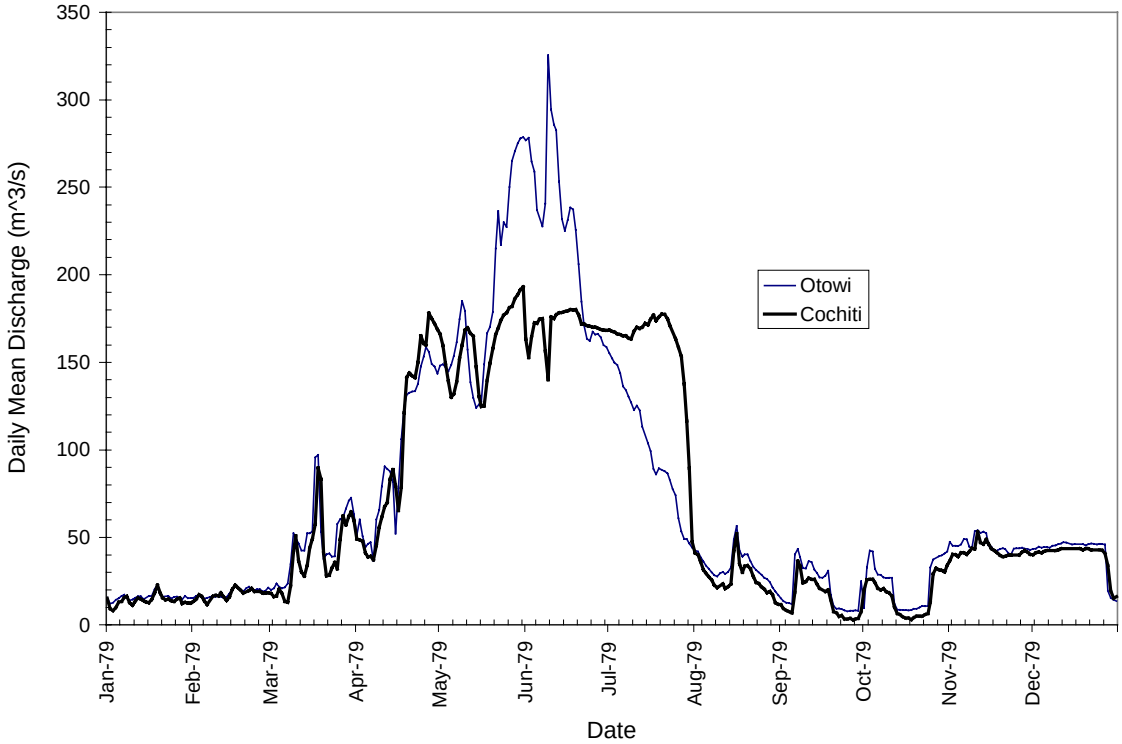

Figure 4-6 - 1979 Discharge hydrograph at Otowi and Cochiti gaging stations.

Dominant Discharge

The two-year frequency discharges resulting from the empirical CDF using Cunnane's plotting position formula (Salas et al. 1998) are presented in Table 4-5. The results are compared with those from a study performed by Bullard and Lane (1993) that estimated the regulated and unregulated 2-year discharge for the Rio Grande at various stations. Bullard and Lane (1993) calculate the unregulated flows to show what the flow would have been like if El Vado, Abiquiu and Cochiti Dams had not been constructed. As a result, their unregulated (pre-dam) 2-year discharge is higher than that computed from gaging station data for Otowi and Cochiti.

Table 4-5 - Two-year frequency discharge (m^3/sec) from empirical cumulative distribution functions fit using Cunnane's plotting position formula for Otowi-Cochiti data from 1895 to 1996.

Time Period	$Q_{2\text{-year}}$	$Q_{2\text{-year}}$ Cochiti (Bullard & Lane 1993)	$Q_{2\text{-year}}$ San Felipe (Bullard & Lane 1993)
1895 –1973	199	262	316
1974 – 1996	145	111	160
1895 – 1996	177		

The effective discharge was determined from the total sediment load rating curve and the flood frequency curve (Wolman and Miller 1960). The total sediment load rating curve developed from the Bernalillo Island total-load data from 1992 to 1996 is shown in Figure 4-7. The total sediment load was estimated by USBR using the Modified Einstein Procedure. The estimates were reported in the CSU database on the Cochiti reach (Leon et al. 1999h). The probability distribution function or frequency distribution for daily-mean discharge data from the Cochiti gage is presented in Figure 4-8.

The transport effectiveness is the product of the total sediment load and the daily discharge frequency and is plotted in Figure 4-9. The transport effectiveness reaches a maximum at an effective discharge of about 153 m^3/sec (5,400 cfs). The effective discharge is equaled or exceeded ~10% of the time according to the flow duration curve for daily data at Cochiti (1974-1997) (Figure 4-8).

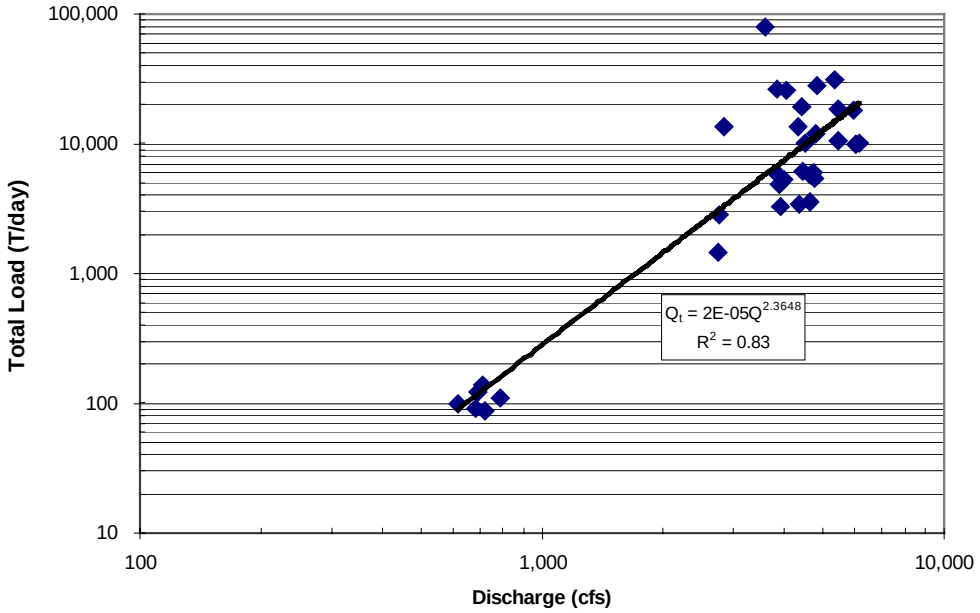

Figure 4-7 - Total sediment load rating curve developed from Bernalillo Island total sediment data (1992-1996) estimated using Modified Einstein Procedure.

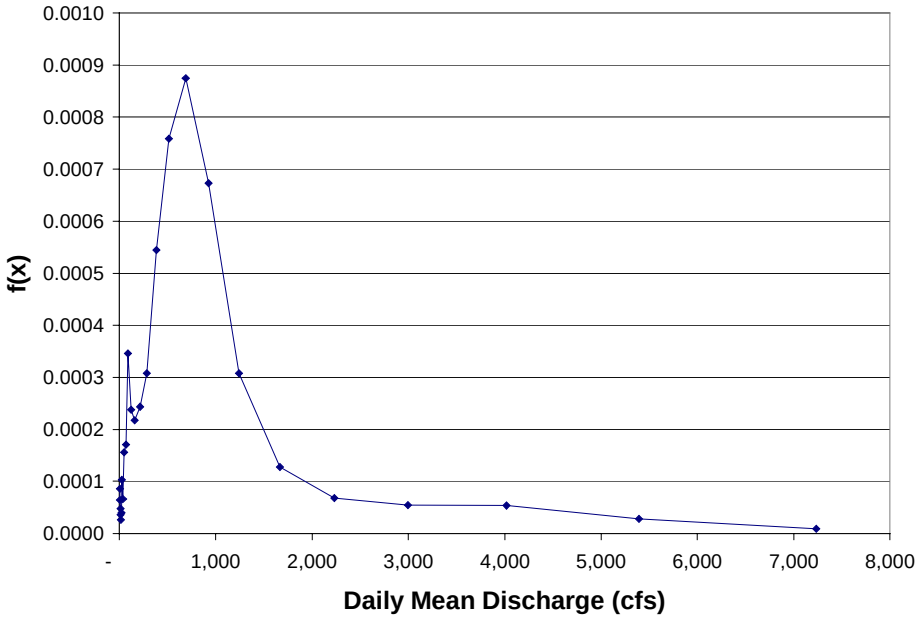

Figure 4-8 - Probability distribution function of daily mean discharge data (1 cfs = 0.0283 m^3/sec) from Rio Grande at Cochiti (1974-1997)

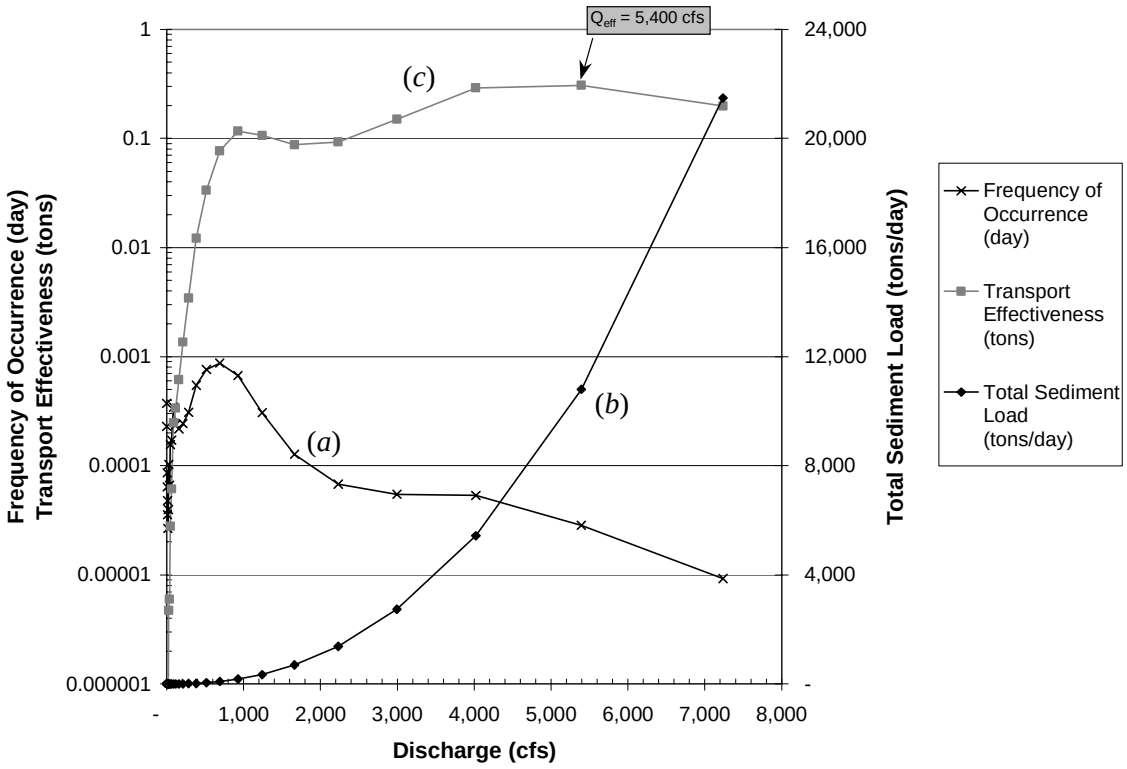

Figure 4-9 - (*a*) Daily mean discharge frequency (Rio Grande at Cochiti, 1974 - 1997), (*b*) Total sediment transport rate as a power function of discharge (Bernalillo Island total sediment load data, 1992-1996), and, (*c*) The product of *a* and *b*, transport effectiveness. The maximum of the transport effectiveness curve is the effective discharge, Q_{eff}. (1 cfs = 0.0283 m^3/sec)

Prior to construction of the dam, the river was transport limited. The bed was aggrading and there was an ample supply of sediment (Graf 1994). As a result, use of the peak discharges for the channel-forming discharge makes sense because the higher the discharge, the more sediment transported. Post-dam, the river became supply limited. Comparison of the effective discharge computed from the total load rating curve and the daily flow frequency shows that for 1992 the effective discharge is approximately equal to the 5-year peak daily mean discharge. Based on these two arguments as well as Knighton's (1998) suggestion that it is the high magnitude and low frequency events that shape the channel in arid regions, the 5-year peak daily mean discharge was selected as the representative channel-forming discharge (Table 4-6).

Table 4-6 - Summary of dominant discharge calculations.

	5-year Peak Daily Mean Discharge (m^3/sec)			
	Reach 1	**Reach 2**	**Reach 3**	**Reach 4**
1918	487	487	487	487
1935	382	382	374	374
1949	328	328	331	376
1962	300	300	286	334
1972	145	145	143	183
1985	235	235	229	245
1992	158	158	165	167

4.2 Sediment Supply

Methods

As shown in Figure 2-1, the sediment supply is one of the inputs that influences the changing response of the channel. Unfortunately, sediment supply is difficult to measure, and as a result, the available data are limited. Additionally, it is primarily the bedload that influences the adjustment of the channel, but it is usually the suspended load that is measured. Graf (1994) suggested that estimating the bedload as a ratio of the suspended load on the Rio Grande, given the amount of published research on the river, should produce an error of less than 50%. Additionally, Woodson and Martin (1962) proposed that the suspended sediment load of the Rio Grande is indicative of the total load of the river because of the high turbulence of the river. They show that the percentage of bed material (sand-sized) in suspension varies with discharge. Based on these arguments and the lack of bedload data, the suspended load measurements are used in the following analyses.

The time periods analyzed are shown in Table 4-7. The Otowi gage data were used to represent the unregulated conditions for the inflow to the study reach. Data at the Cochiti gage are only available for the post-dam period, so the pre-dam Otowi data were combined with post-dam Cochiti to represent the sediment concentration flowing into the study reach. The Bernalillo gage was moved in 1969 to a location 30 km downstream from the Highway 44 Bridge and re-named to be the Albuquerque gage. The records for these two gages are combined and represent the sediment concentration at the outlet of the Cochiti reach. No major tributaries enter the Rio Grande between the Bernalillo and Albuquerque gages.

Table 4-7 - Sediment records analyzed.

Gaging Station	Representation	Period of Record
Otowi	Unregulated condition	1956-1994
Otowi (1956-1973) Cochiti (1974-1984)	Input to reach	1956-1984
Bernalillo (1956-1969) Albuquerque (1969-1995)	Output of reach	1956-1995

The analyses of the sediment supply record have similar objectives to those of the water discharge analysis:

1) Identify historic trends - Time series plots of suspended sediment concentration and discharge were plotted for the Otowi, Cochiti, Bernalillo, and Albuquerque gaging stations (Leon et al. 1999e, 1999f). Also, the mean annual sediment concentration and annual maximum were compared for pre and post dam conditions at the Otowi, Cochiti and Bernalillo gages. A cumulative mass curve of the annual suspended sediment yield was also created for Otowi, Bernalillo and Albuquerque gages to identify changes in the sediment yield.

2) Identify dam impacts - Investigation of the impact of the dam was performed with the daily mean suspended sediment concentration data arranged by water year (October 1 through September 30) and utilized the Indicators of Hydrologic Alteration (IHA) methodology (Richter et al. 1996). Although this methodology was not developed for use on sediment data, the statistical analyses can be performed on any daily time series of data. Some of the parameters computed using the IHA methodology are not of interest when applied to sediment data, such as rate of rise or fall. However, comparison of the annual extreme values and monthly average values between the pre and post-dam periods using the IHA methodology provides quantification of the dam impacts on sediment supply.

3) Estimate the historic suspended sediment balance of the reach - The total annual sediment input and output for the Cochiti reach was estimated. The sediment load (tons/day) measured at each gaging station (Leon et al. 1999f) was summed for the entire year. The input is defined as the annual sediment yield at either Otowi (1956-1973) or Cochiti (1974-1987) combined with the Jemez River and Galisteo Creek. The output is the sediment yield at either Bernalillo (1956-69) or Albuquerque (1969-1995). Comparison

of the input and output shows the amount of sediment stored or lost in the reach, an estimate of the annual volume of aggradation/degradation in the reach, and a measure of the level of sediment transport equilibrium. Annual suspended sediment yield was calculated for each year for which continuous sediment discharge data were available. Of the three major tributaries to the Cochiti reach, only one, Galisteo Creek, has continuously recorded data for more than three years. This limited the ability to draw conclusions regarding sediment storage and losses or the sediment budget of the reach. For the pre-dam period, the input consisted of the Otowi gage plus Galisteo and Jemez data. For the post-dam period, the input consists of the Cochiti gage data plus Galisteo data. The output was represented by the Bernalillo and Albuquerque gages for the pre and post dam periods, respectively.

4) Determine representative values of suspended sediment concentration for each study period and reach - To determine representative values of sediment concentration for the survey periods, double mass curves were created by plotting the cumulative suspended sediment discharge with the cumulative water discharge for each gaging station. Changes in the slope of the double mass curves indicate changes in the sediment concentration of the flow. Breaks in the curves were identified and the slopes calculated for each segment. The slopes were then converted from units of ton/ac-ft to mg/L. This represents an average sediment concentration for the period. Where obvious break-points in the double mass curves did not fall on the years for which aerial photos are available, the suspended sediment concentration was estimated by computing the slope for each year during the time period and averaging those slopes.

The Otowi (pre-dam) and Cochiti (post-dam) gage data were used for reach 1. The Bernalillo-Albuquerque gage data were used for reach 4. Cumulative data were also calculated using Otowi and Cochiti data plus Galisteo Creek to estimate the concentration for reach 2. Combining the Galisteo at Domingo gage (1956-1970) data with Galisteo below Galisteo dam data (1970-78) created a complete record for Galisteo Creek for 1956-78. Galisteo Dam was constructed in 1970. Data from the San Felipe gage were averaged to estimate the concentration for reach 3 from 1972-92 as well as for reach 2 for 1985-92. The San Felipe concentration data were sporadic data obtained from the EPA's STORET database. The representative concentration for reach 3 for 1949-62 was obtained by averaging the concentrations from reach 2 and reach 4 for that time period. It would be expected that reach 3 would have a higher concentration than reach 2, but lower

than reach 4 because of the presence of Arroyo Tonque at the upstream end and the Jemez River at the downstream end.

The biggest gap in the data set was between 1918 and 1935. No suspended sediment records were available for this portion of the Rio Grande for that time period. The nearest records were at San Marcial, located downstream of the confluence with the Rio Puerco, a very large sediment contributor to the middle Rio Grande. As a result, rating curves were created from the Otowi and Bernalillo-Albuquerque pre-dam gage data. The annual water discharge was plotted against the annual sediment yield for the available pre-dam years. The available Otowi and the Bernalillo-Albuquerque data both spanned from 1956 to 1972. Power-law lines were fit to the data and produced r-square values of 0.8 for both data sets. The resulting equations were used to estimate the annual sediment yield for the pre-record years using the measured water discharges.

Results

The average annual sediment concentrations for Otowi, Bernalillo, Cochiti and Albuquerque are plotted in Figure 4-10 for 1956-95. Otowi and Cochiti represent the inflowing sediment concentration to the reach, and Bernalillo and Albuquerque represent the outflowing sediment concentration. The post-dam concentration at Albuquerque is up to two orders of magnitude higher than that at Cochiti, indicating that the tributaries, and/or the channel bed and banks were contributing to the sediment concentration at Albuquerque. The annual average suspended sediment concentration at Cochiti was less than 100 mg/L for 1975-83, and the concentration increased to over 500 mg/L at the Albuquerque gage.

Historically, Galisteo Creek, the largest tributary between Otowi and Belen, contributed heavy sediment loads to the Rio Grande (Nordin and Beverage 1965) prior to construction of Galisteo Dam in 1970. Since dam construction, Galisteo Creek has continued to be a source of fine sands, silts and clays. The bed material of Galisteo Creek is reddish brown, and when Galisteo Creek is flowing, the Rio Grande flows reddish brown downstream from the confluence with Galisteo (Drew Baird, USBR Albuquerque, NM, pers. comm.11/13/97).

The Jemez River was dammed in October 1953 and according to Nordin and Beverage (1965) since then did not contribute appreciably to the sediment in the reach downstream. Williams and Wolman (1984) report that channel bed of the Jemez River, 1.3 kilometers downstream from the Jemez River Dam, degraded 2.3 meters between 1953 and 1958. Therefore, some sediment in the Rio Grande during this period was from the bed of the Jemez River. Also,

2.4 kilometers downstream from Jemez River Dam, a total of 2 meters of degradation was evident 20 years after closure, although there was evidence of aggradation from 10 to 20 years after dam closure (Williams and Wolman 1984).

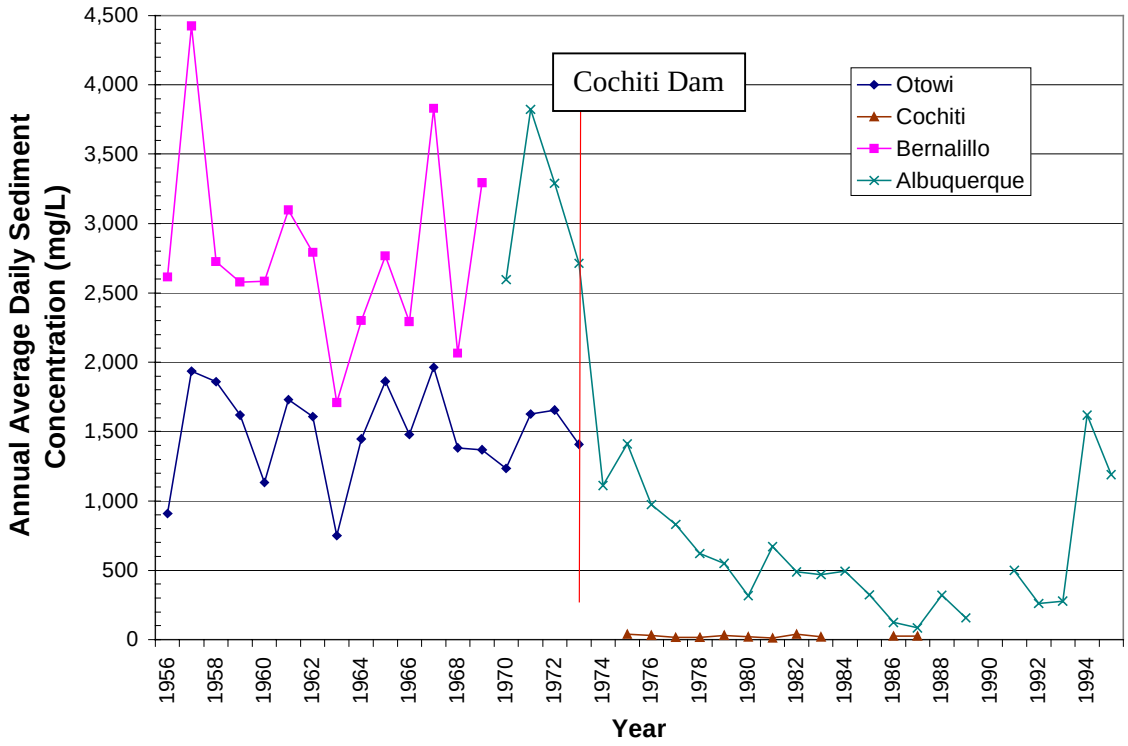

Figure 4-10 - Annual average suspended sediment concentration Rio Grande at Cochiti and Albuquerque (1975-1987).

Figure 4-11 is a plot of the cumulative annual suspended sediment yield at the Otowi, Bernalillo and Albuquerque gages. The slope of the Albuquerque line decreases following closure of Cochiti dam in 1973. Both gages show higher sediment loads from 1956 to 1958. Interestingly, there is a decline in the sediment load at the Otowi gage (upstream from Cochiti dam) around 1973. Graf (1994) and Norman (1968) also note a downward trend in the sediment supply at the Otowi gage following 1958, which was the highest year on record.

Figure 4-12 is a plot of the cumulative annual sediment and water data combined. Breakpoints were identified and the slope of the line represents the average suspended sediment concentration during ensuing time periods. The decline in sediment concentration at the Albuquerque gage following completion of Cochiti dam in 1973 is evident. A decline in the concentration at the Otowi gage, located upstream of Cochiti Dam, is also evident at the same time period. Norman (1968) also noted a decline in the sediment concentration at the Otowi and Bernalillo gages following 1958 and suggested that a change in the basin climate from a

relatively dry period to a relatively wet period was the reason for the decline in sediment concentration. He also found no significant impacts on sediment supply in the Rio Grande from the construction of Abiquiu Dam and the Jemez River Dam.

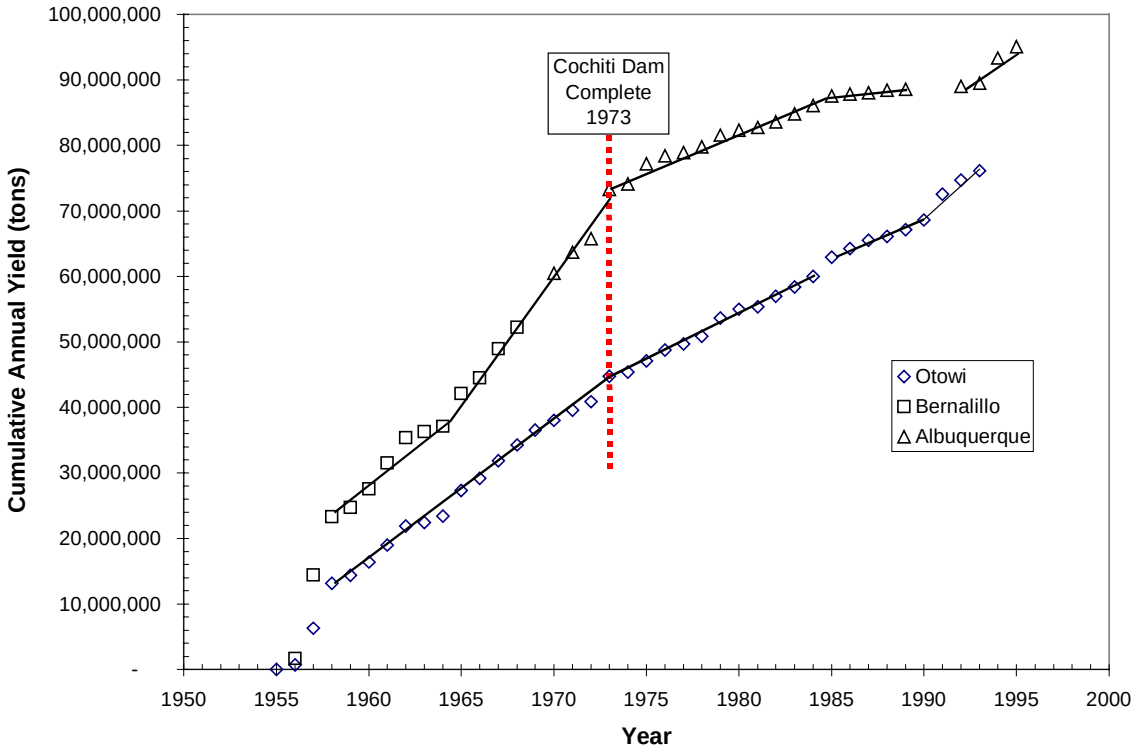

Figure 4-11 - Cumulative mass curve of annual suspended sediment yield.

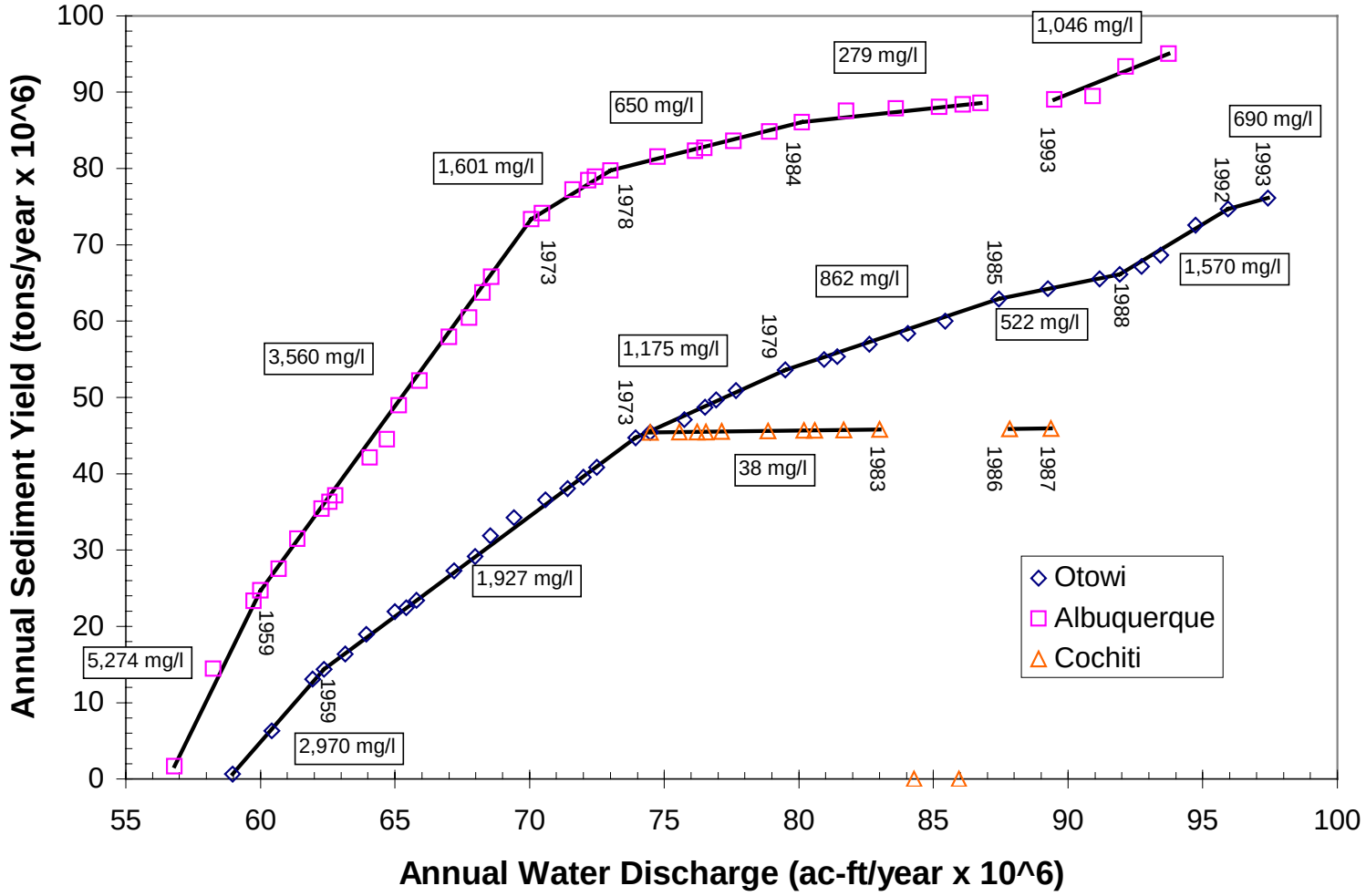

Figure 4-12 - Double-mass curve of annual water and sediment discharge at the Otowi, Cochiti and Albuquerque gages. The slope of the curve indicates the average suspended sediment concentration for the time period.

Impacts of Cochiti Dam on the suspended sediment supply to the reach are also evident based on the IHA analysis of daily average suspended sediment concentration records from the Otowi, Cochiti, Bernalillo and Albuquerque gage records. A comparison of the pre-dam (until November 1973) with post-dam (after November 1973) conditions is presented in Table 4-8. The results for each gage are presented in Appendix B, Tables B-6, B-7 and B-8. The greatest impacts of the dam are seen at the Cochiti gage located directly downstream from the dam, where the sediment concentration decreased as much as 99%. Prior to construction of the dam, the suspended sediment concentration at Bernalillo was typically about 2 times greater than the concentration at Otowi. Following construction of the dam, the average concentration at Bernalillo was less than that at Otowi. It is interesting that the annual mean suspended sediment concentration at the Otowi gage decreased by 44% from the pre to post dam period.

Table 4-8 - Impacts of Cochiti dam on the suspended sediment concentration.

Gaging Station	Average % Change		Mean Annual Sediment Concentration (mg/L)	
	1-day Maximum	Annual Mean	Pre-dam	Post-dam
Otowi	-27%	-44%	1,460	819
Otowi/Cochiti	-99%	-96%	1,455	64
Bernalillo/Albuquerque	-73%	-78%	2,823	622

Figure 4-13 is a time series of sediment yield for the available inputs and outputs of the Cochiti reach. From 1963 through 1966, there was net storage or aggradation in the Cochiti reach. For all other years, both pre and post dam, it appears that the outflow of sediment exceeded the input. For the pre-dam years, the difference is small enough that unmeasured tributary inputs could make the inputs exceed the outputs. For the post-dam period, it is unlikely that even the addition of the unmeasured tributary inputs would cause the input to exceed the output. This leads to the conclusion that the bed and banks were the source of the higher sediment yield at the Albuquerque gaging station indicating degradation and bank erosion in the Cochiti reach. The annual sediment yield at Albuquerque maintained a low value from 1986 through 1993 and then increased significantly in 1994 for unknown reasons. Graf (1994) performed a sediment budget including estimates of bedload. He found that storage dominated the system from the late 1950's through the late 1960's and again in the late 1970's. Losses dominated in the late 1940's and early 1970's.

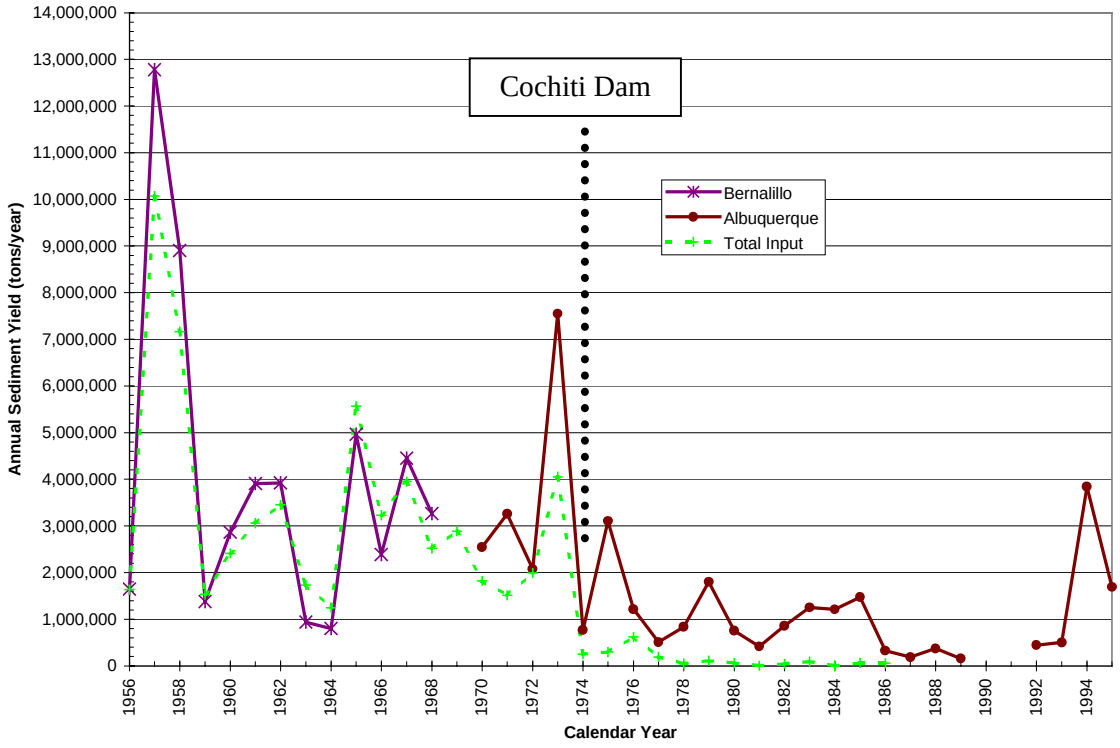

Figure 4-13 - Annual suspended sediment yield – Rio Grande, Cochiti reach

Representative values of sediment concentration for each of the study periods and reaches were obtained from the double-mass curves shown in Figure 4-12 and other double mass curves that included tributary inputs. The resulting values for the different study periods and reaches are presented in Table 4-9 as well as Appendix B, Table B-1.

Table 4-9 - Representative suspended sediment values (mg/L)

Reach #	1918-1935	1935-1949	1949-1962	1962-1972	1972-1985	1985-1992
1	2,218	2,195	2,449	1,871	33	33
2	2,218	2,195	3,010	2,640	346	182
3	3,050	3,042	3,603	3,701	504	182
4	3,882	3,888	4,196	3,701	1,229	175

4.3 Slope

Methods

Ideally the water surface slope at bankfull flow should be measured and used in the lateral stability and movement analyses (Nanson and Hickin 1986; Nanson and Hickin 1984; Schumm et al. 1984; Burnett and Schumm 1983). Often water surface elevations are not readily available and valley slope measured from topographic surveys and maps is substituted (Nanson and Hickin

1986; Nanson and Hickin 1984). The sporadic nature of the data used in this study complicates the slope measurements. To maintain consistency between the different survey years, the channel bed elevation was plotted against distance downstream measured between agg/deg lines. This distance is not quite a valley length, and it does not follow the thalweg. It is the same for every year, so it does not include changes in sinuosity. A linear regression was fit to the available data for each reach for each survey year. The slopes of the regression line were computed for each reach for each year. The survey data for the year closest to the aerial survey dates were used when the years did not match exactly (1935, 1949 and 1985). Different slopes for the subreaches were not computed.

The data used are from the 1918 topographic survey, profiles from 1918, 1936 and 1944 (USBR 1951), 1952-72 agg/deg studies and reports (USBR 1967 and 1972), and 1970-1992 CO-line surveys.

Results

The time series plots of the channel slopes measured using the bed elevation of the reaches (Figure 4-14) show that Reach 1 has consistently been the steepest of the reaches. Additionally, Reach 4 on average is the mildest. None of the reaches exhibit significant changes resulting from the completion of Cochiti dam.

Nordin and Culbertson (1961) suggested that upstream of San Felipe the Rio Grande was dominated by pool-riffle sequences that result in highly variable water surface slopes. They noted that the pool-riffle sequences are flooded out at high discharges. Downstream of a slope break that occurs approximately at San Felipe, the water surface slope became more constant as the channel became more of a sand-bed channel.

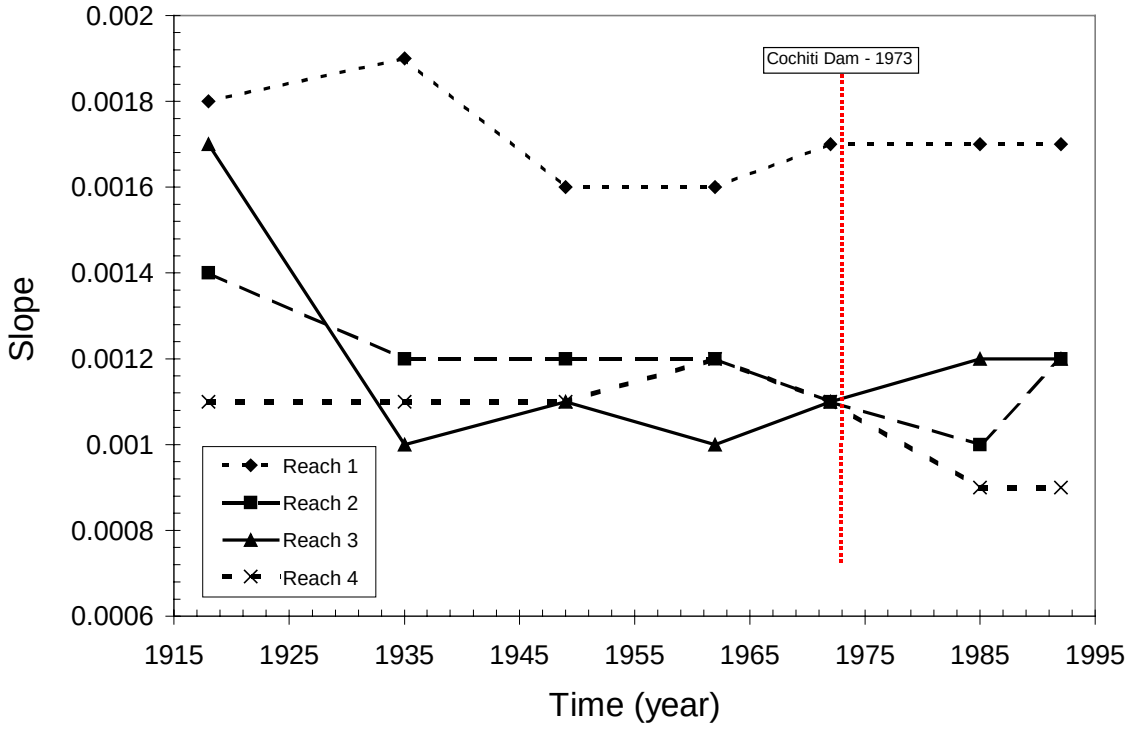

Figure 4-14 - Time series of slope for reach 1 through 4 of the Cochiti study reach.

4.4 Vertical Response

The vertical response of the study reach was measured by changes in bed material size and bed elevation. The methods and results for the vertical response are presented below.

4.4.1 Bed material

Methods

In analyzing the bed material, once again it is desired to characterize the spatial and temporal trends and to determine representative values for each subreach for each survey period. The spatial distribution of the bed material sampling is comprehensive enough to allow for variation in values between the subreaches for the more recent surveys. Bed material data prior to 1970 are more limited. As a result, the available data are used to represent the early river channel (1918 to 1949) based on the assumption that the material making up the bed did not change significantly from 1918 to the 1940's. The earliest available data were published by Rittenhouse (1944) and include samples taken in 1937. Other surveys from the 1940's through 1960's include Nordin and Beverage (1965), Nordin (1964), and Culbertson and Dawdy (1964). Fortunately, all of the samples and descriptions of the bed material prior to construction of Cochiti Dam demonstrate

that the size distribution of the material did not change with time prior to construction of the dam. The median-grain sizes were consistently find to medium sand for all data from the pre-1960's surveys.

From 1972 to 1992, the USGS and USBR sampled the channel bed more frequently. These data were compiled by Leon et al. (1999d) from the original sources. The median grain size data for all available samples (See Appendix A, Table A-6) during each time period for each subreach were averaged. A matrix showing the data applied for the different subreaches and years is shown in Table 4-10

Table 4-10 - Sources of bed material data

<table>
<tr><th>Subreach #</th><th colspan="2">1918</th><th>1935</th><th>1949</th><th>1962</th><th>1972</th><th>1985</th><th>1992</th></tr>
<tr><td>1.1</td><td colspan="2" rowspan="26">1937 Data from Rittenhouse (1944) - for Above Santa Fe, San Felipe, Above Jemez, and Bernalillo stations. Taken from particle size distribution plots.</td><td rowspan="15">Average of 1935 and 1962 data</td><td rowspan="15">1961 Cochiti gage average – from Nordin & Beverage (1965)</td><td>Average</td><td rowspan="4">1979, 1980 and 1982 CO line data (averaged where possible)</td><td rowspan="2">Average</td></tr>
<tr><td>1.2</td><td rowspan="14">1972 Values are from the mean of all samples taken during 1972 at CO-lines and assigned to subreach by CO-line.</td></tr>
<tr><td>1.3</td></tr>
<tr><td>1.4</td><td>1992 CO</td></tr>
<tr><td>1.5</td><td>Average</td></tr>
<tr><td>1.6</td><td rowspan="4">1992 CO line data</td></tr>
<tr><td>1.7</td></tr>
<tr><td>1.8</td></tr>
<tr><td>1.9</td></tr>
<tr><td>2.1</td></tr>
<tr><td>2.2</td><td rowspan="2">Nov. 1985 SD Line data</td><td rowspan="2">Feb 1992 SD line data</td></tr>
<tr><td>2.3</td></tr>
<tr><td>2.4</td></tr>
<tr><td>2.5</td><td>CO line</td><td>Average</td></tr>
<tr><td>2.6</td><td rowspan="3">1989 San Felipe line data</td><td>1992 CO</td></tr>
<tr><td>3.1</td><td rowspan="11">1952 Section A-2 and F data (Bernalillo) from Nordin (1964)</td><td rowspan="3">1961 San Felipe gage data - from Nordin & Beverage (1965)</td><td>1992 BI</td></tr>
<tr><td>3.2</td><td>Average</td></tr>
<tr><td>3.3</td><td rowspan="3">1979-82 CO line</td><td rowspan="2">1992 CO line</td></tr>
<tr><td>3.4</td></tr>
<tr><td>3.5</td><td rowspan="2">Average</td></tr>
<tr><td>4.1</td><td rowspan="8">1962 Bernalillo gage average – from Nordin & Beverage (1965)</td><td>Average</td><td rowspan="3">1990 Santa Ana (TA) line data</td></tr>
<tr><td>4.2</td><td>1972 CO line</td><td rowspan="3">1992 CO line</td></tr>
<tr><td>4.3</td></tr>
<tr><td>4.4</td><td rowspan="3">Average</td><td rowspan="3">1990 BI line data</td></tr>
<tr><td>4.5</td><td>1992 BI</td></tr>
<tr><td>4.6</td><td>Average</td></tr>
</table>

NOTE: “Average” means that either a spatial or temporal average was used to fill in missing data. BI = Bernalillo Island lines.

Results

Prior to construction of Cochiti dam, the size of the bed material did not change significantly with time. Rittenhouse (1944, p. 165), when discussing the Rio Grande from Cochiti to the mouth of the Jemez River, states: "In the upper part of the Middle Valley the Rio Grande channel deposits consist of fine to medium sands overlying a bed pavement of cobbles and pebbles. Downstream the gravel becomes less abundant and below Albuquerque seldom constitutes more than a few per cent in the upper 5 feet of the deposits." Nordin and Beverage (1961) corroborate these observations.

Rittenhouse (1944) performed an analysis to determine the source of sediment in the bed of the Rio Grande. He determined that between Albuquerque and Bernardo, about 21-39 percent have come from the Jemez River, 2-6 percent from Galisteo Creek, 0.6-2.0 percent from Santa Fe Creek, 11-37 percent from the Rio Grande above Cochiti, and the rest from smaller tributaries that were not measured. He noted that 90% of the channel deposits were sand, of which 75% was between 0.351 and 0.088 mm in diameter. The percentage of sand size sediment in the floodplain was less, only 40%. Between Cochiti and Albuquerque, the channel deposits consisted of fine to medium sands overlying a bed pavement of cobbles and pebbles. The gravel became less abundant further downstream from Cochiti. Galisteo Creek contributed notably coarser sediment than that in the main stem, and the Jemez River bed sediment was similar to that of the main stem.

Nordin and Culberston (1961) examined the bed material at eight sites between Otowi Bridge and San Marcial. They showed that the sediment size becomes finer moving downstream from Otowi. They suggested that the transition from the coarser bed in White Rock Canyon to more of a sand-bed channel occurs between San Felipe and Bernalillo. This is evidenced by a break in the bed slope of the channel. Additionally, cores of the bed material at Cochiti and San Felipe exhibited a bimodal distribution of median grain sizes with peaks in the both the gravel and fine sand grain sizes. The upstream stations exhibited greater variability in bed material sizes, whereas the bed material at downstream stations was primarily sand with little variation. In the upstream portion (from Otowi to San Felipe) of the study reach the bed material size increased with increasing discharge. From Bernalillo to San Marcial, the bed material size remained constant or decreased with increasing discharge. Nordin and Beverage (1964) showed that mid-channel and lateral bars were a source of fine sediment when resuspended after deposition during the falling limb of the spring peak hydrograph.

The reach and subreach averaged results are presented in tabular form in Appendix B, Tables B-1 and B-2, respectively. The reach-averaged results are plotted in Figure 4-15. The most significant historic change is the shift from a primarily sand-sized to a gravel-bed following construction of Cochiti dam in 1973. The small variations in grain size between 1918 and 1972 are within the variability observed in the bed of the Rio Grande between storm events and during different periods of the spring-runoff hydrograph. Reaches 1 and 2 were coarser than reaches 3 and 4 prior to dam construction as suggested by Nordin and Culbertson (1961) and Rittenhouse (1944).

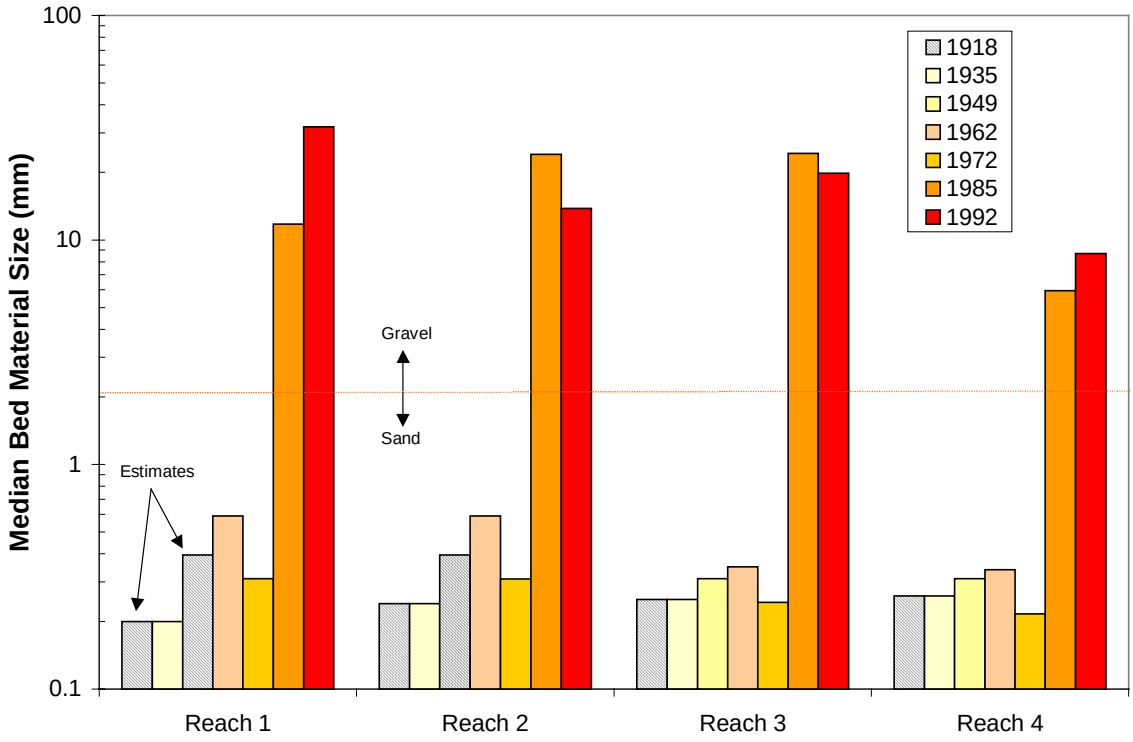

Figure 4-15 - Reach averaged median bed material size.

4.4.2 Bed elevation

Variations in both the sediment supply and available flow energy or transport capacity of the river can result in changes in the elevation of the bed. If the transport capacity exceeds the sediment supply rate and is sufficient to mobilize particles in the bed, then degradation can occur. If the sediment supply rate is higher than the available capacity of the flow to transport the sediment, it deposits and the bed aggrades. With this balance in mind, changes in the elevation of the bed can be a good barometer of the degree of stability of a section of a river. Alluvial sand and gravel-bed rivers often have dynamic beds, combining seasonal variations in sediment supply

with bedform movement. Pinning down a value for bed elevation is not an easy task. Variations of up to a meter in weeks or months are not uncommon. However, continued trends over a period of years can become evident with repeated sampling.

Construction of dams and detention of sediment supply contribute significantly to changes in bed elevation. In all 21 channels studied by Williams and Wolman (1984) downstream from dams, the channel bed degraded. In those same channels, other changes such as width variation were not as consistent. Some channels widened, others narrowed, but they all degraded following dam construction.

In order to review the historic trends in bed elevation change on the Cochiti reach, longitudinal profiles of the bed elevation were plotted using all of the available data. The distance between cross-section lines was kept consistent between years so that changes in sinuosity and meandering of the thalweg are not included in this analysis. Elevations are interpolated with a straight line fit between surveyed cross-sections. Additionally, for the recent CO-line surveys, total change in bed elevation was computed at each cross-section from just prior to closure of Cochiti Dam to the most recent survey. Changes in the bed elevation for the earlier surveys were estimated where possible. The early bed elevation data are sporadic and resurveys at the same location are not always available. Also, the time of year during which the survey was performed can have a significant influence on the bed elevation. As described above, the bed of alluvial rivers is often dynamic and can fluctuate dramatically between storms.

The profile of the channel (USBR 1951) from 1918 to 1944 was used to estimate rates of bed elevation changes for the reaches and subreaches. Rates of change from SCS lines from 1937 to 1953 as well as the change in agg/deg lines from 1962 to 1972 were also averaged for each reach. This is an attempt to quantify the pre-dam changes in bed elevation. The pre-1962 data are limited and sporadic, as well as highly variable. Mean bed elevations were available from the agg/deg surveys for 1962, 1972 and 1992. Mean-bed elevations were also computed from the CO-line surveys from the 1970's through 1990's.

The pre-dam rates of bed elevation change are plotted in Figure 4-16. The 1962 to 72 data are the most reliable. Reaches 1, 2 and 3 degraded on average from 1918 to 1936 while reach 4 aggraded. From 1936 to 1972 generally, the entire study reach aggraded more than it degraded, which is supported by observations of the channel during this time period (Graf 1994).

Table 4-11 - Pre-dam aggradation.

	1937-53		1953-62		1962-72	
Reach #	Total number of samples	% Aggraded	Total number of samples	% Aggraded	Total number of samples	% Aggraded
1	6	50%	6	83%	78	46%
2	13	54%	5	100%	75	69%
3	10	50%	3	100%	62	76%
4	19	63%	10	70%	66	97%

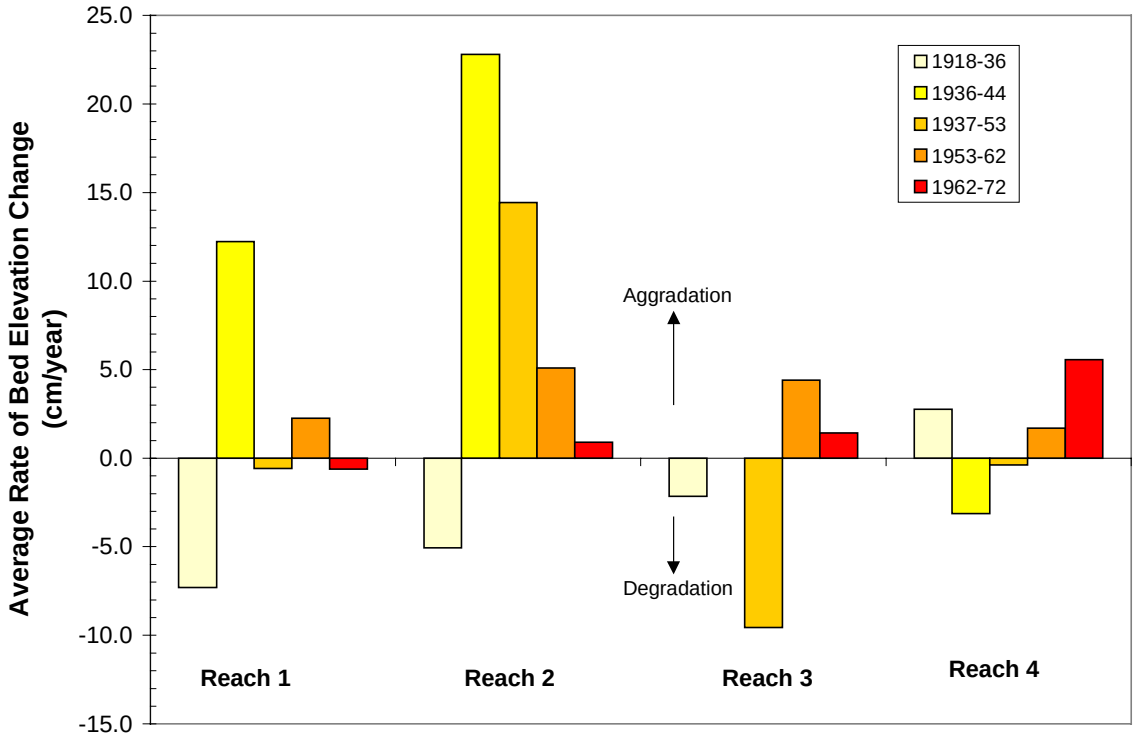

Figure 4-16 - Pre-dam average rate of bed elevation change (cm/year).

Graf (1994) developed a sediment budget for the Rio Grande from Otowi to San Acacia from annual sediment yield data. From his total sediment load budget, he estimated that storage dominated the system above Albuquerque in the late 1950's to late 1960's, and then again in the late 1970's. Losses were prominent in the late 1940's and early 1970's.

In 1967 and again later in the 1970's the USBR's Hydraulics Division produced reports summarizing the aggradation and degradation of the middle Rio Grande (USBR 1967 and USBR

1972). These reports are based on the early SCS, Corps and USBR surveys and the later 1962 and 1972 agg/deg line data. The results are total volume estimates of the net change in the channel and flood plain between each set of surveys. The results generally concur with Graf's (1994) conclusions from his total sediment budget. The USBR's estimates show primarily losses from 1937 to 1954 and storage in the 1960's from Cochiti to Angostura Diversion.

Post-dam bed elevation changes measured in this study using the thalweg elevation at the CO-lines from May 1971 to August 1998 are presented in Figure 4-17. All of the reaches degrade following construction of Cochiti dam (November 1973). Reach 4 degrades the most with almost two meters of degradation. Reaches 1 and 2 only degrade about 0.5 meters. The bed elevation of reach 3 appeared to stabilize by 1987.

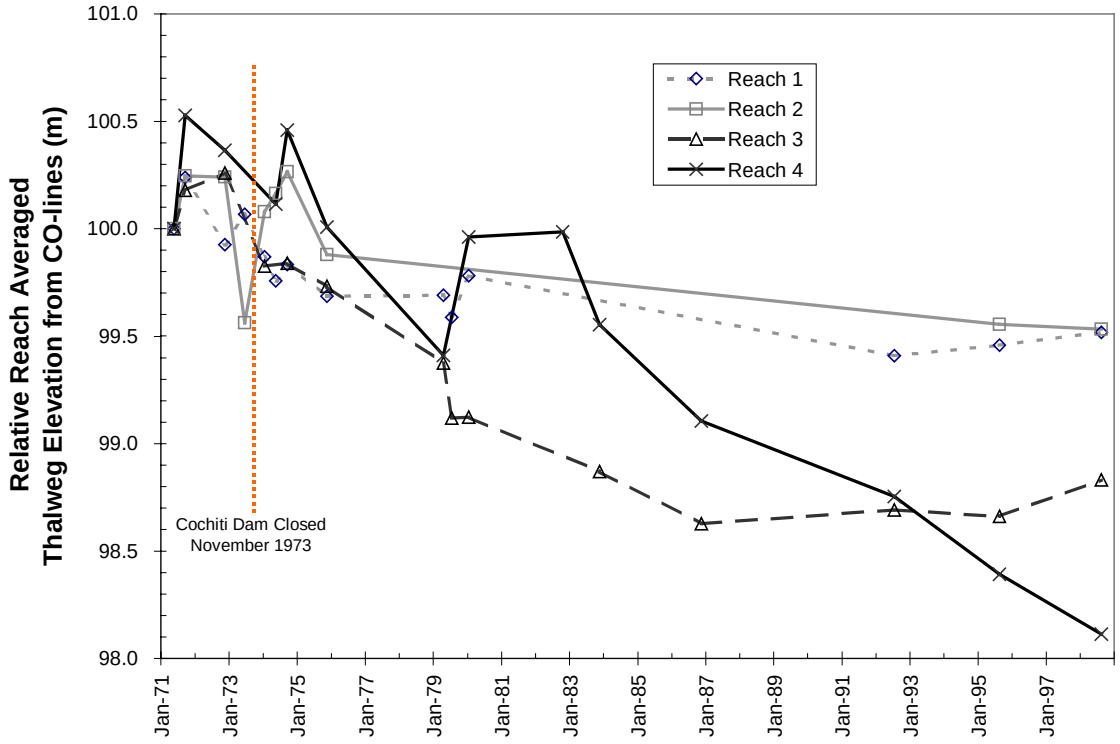

Figure 4-17 - Post-dam thalweg elevation changes using CO-line surveys from 1971 to 1998.

4.5 Lateral Response

Changes in width and channel pattern are described in the next two sections. Further quantification and discussion of lateral movement is presented in Chapter 5.

4.5.1 Width

Methods

For the analyses in this study, the “active channel width”, defined as the non-vegetated channel as delineated by the USBR's GIS and Remote Sensing Group from aerial photos and topographic surveys (USBR 1998), is used for the width. The rationalization is that the higher flows will clear away newly established vegetation. If there are no high flows for the 5 or so years prior to survey, then the vegetation will be more established, and therefore not "active channel" anymore.

The width at each agg/deg line was measured from digitized coverages of the active channel. Measurement of the active channel width was performed by clipping the agg/deg line coverage with the active channel polygon. It should be noted that many of the agg/deg lines are not perfectly perpendicular to the channel in every year. It is difficult to have the same set of range lines used over the course of this many years and have them be perpendicular in every year. Two lines (21 and 137) were deleted from the analysis because of their skewed orientation with respect to the active channel for all years. It was assumed that the skewness was not a significant factor for the rest of the lines. Additionally, for the earlier years (1918-49), there were several agg/deg lines that did not span the entire width of a channel (either the channel was wider than the line, or the channel was in a different location). For these lines, the line was extended to intersect with the active channel boundary. In a few cases in bends, when the lines were extended they intersected other agg/deg lines before reaching the active channel boundary. In these cases, the lines were redrawn in a manner to represent the original location of the lines as best as possible.

The total channel width from outer bank of non-vegetated channel to outer bank was measured. Measurement of the total channel provided a measure of the total width of the channel including any vegetated islands or area designated as "recent channel change" (USBR 1998). To compute the active channel width, the island width and "recent channel change" width were subtracted for the lines where these areas were present. The active channel width is the total width minus the width of the islands and recent change area.

The total width and active channel width were averaged over the four reaches and 26 subreaches using one-half the distance to the nearest upstream and downstream cross sections as

the weighting factor. The change in width from survey year to survey year was calculated as a percentage of the 1918 width. Also the post-dam width change was computed as a percentage of the 1972 width. This was done for each agg-deg line, and then reach and subreach averaged.

Results

Figure 4-18 illustrates the changes in active channel width with time and distance downstream. For each of the reaches, the width has decreased with time since 1918. Reach 4, the furthest downstream subreach, is the widest. Reach 1 exhibits the greatest variability in width, changing from 304 meters (998 feet) wide in 1918 to 73 meters (240 feet) wide in 1992. The changes in channel width since construction of the dam are summarized in Figure 4-19.

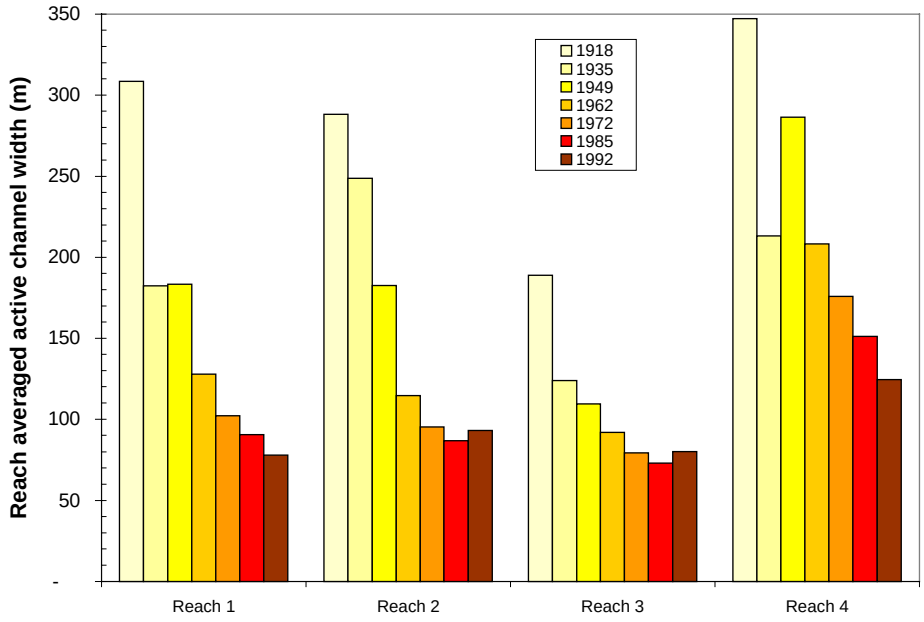

Figure 4-18 - Reach averaged active channel width.

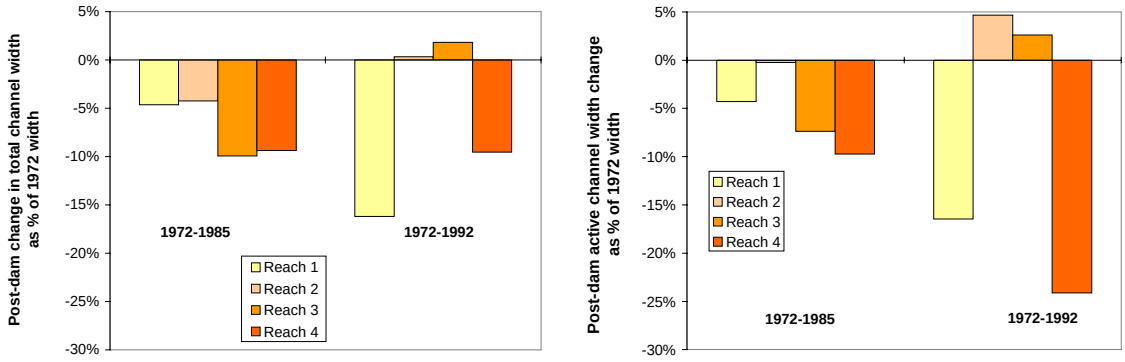

Figure 4-19 - Post-dam change in channel width as % of 1972 width.

Equilibrium Width Analysis - Existing methods

One of the stated objectives of this study is to evaluate the shape or form of the study reach in light of existing methods of predicting the equilibrium or stable configuration of the channel. Two methods are employed in this section. The first was developed by Williams and Wolman (1984) to model regular changes in channel width (either consistent widening or narrowing) following dam construction. The second method is the application of hydraulic geometry equations, from which an equilibrium channel width can be computed based on other hydraulic, sedimentary and channel form parameters. Both methods can help show whether or not the width of the study reach is approaching an equilibrium condition.

Williams and Wolman (1984) found that "regular" width change downstream from a dam could often be modeled using a hyperbolic function of the form (Figure 4-20):

$$\frac{W_t}{W_o} = \left(\frac{t}{a + bt} \right) + 1 \quad \text{.....(4-1)}$$

where,

W_t = active channel width at time, t

W_o = active channel width at onset of narrowing,

a and b = empirically determined constants.

The constants a and b are determined empirically by plotting $\frac{1}{\left[\frac{W_t}{W_o} - 1 \right]}$ vs. $\frac{1}{t}$ and fitting a least square regression line to the data. The resulting equation for the line is of the form:

$$\frac{1}{\left[\frac{W_t}{W_o} - 1 \right]} = \frac{a}{t} + b \quad \text{.....(4-2)}$$

where, a is the slope and b is the intercept of the line. This model was applied to the reach-averaged width data. The results are shown in Figure 4-21. The r-square values vary from 0.80 for Reach 4 to 0.99 for Reach 3.

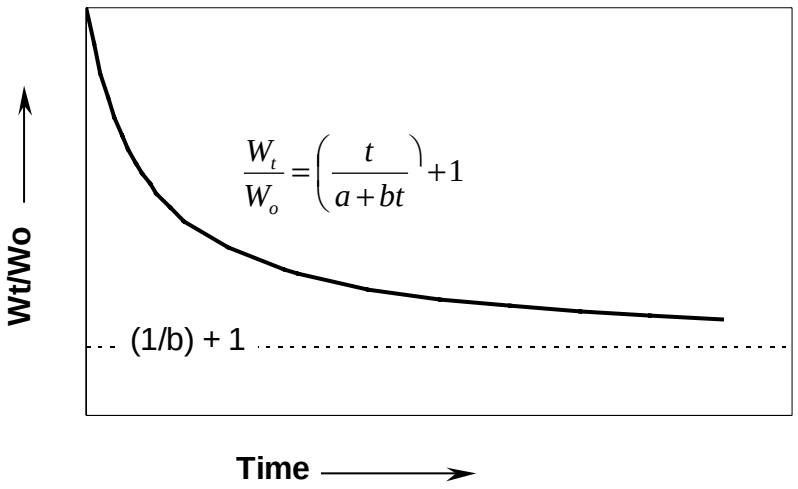

Figure 4-20 - Hyperbolic model of width change with time.

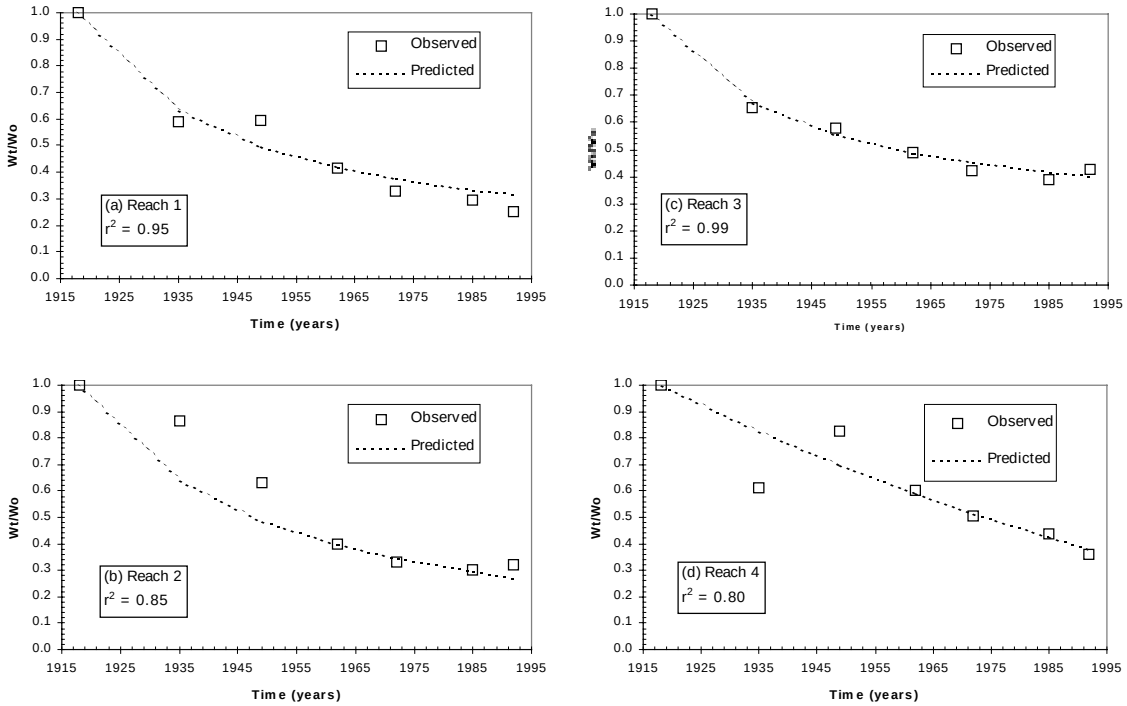

Figure 4-21 - Application of Williams and Wolman (1984) hyperbolic width change model to reaches 1-4 of the study reach.

Hydraulic geometry

Hydraulic geometry equations are intended to describe the stable channel width of a channel that has had the time to adjust itself to an imposed water and/or sediment regime. In general, hydraulic geometry equations are set up as power functions based on the premise that water and sediment discharge are the two most important factors that form channel geometry and that the channel adjusts its width, depth, velocity and slope according to changes in water and sediment discharge. Most equations are derived for a particular region or set of data. Many hydraulic geometry equations compute the channel width based only on the discharge in the form, $W = a\,Q^{b}$, where a and b are usually empirically derived constants.

During the first half of the 1900's, engineers applied this theory primarily to predict a stable form for irrigation canals. In 1953, Leopold and Maddock developed a set of empirical equations that they called hydraulic geometry equations, which apply to natural rivers and streams. Their equations related the hydraulic geometry of alluvial channels to a power function of bankfull discharge:

$$W = aQ^{b}$$

$$D = cQ^{e}$$

$$V = kQ^{m}$$

where, $ack = 1$ and $b+e+m = 1$ and b=0.50, e=0.40 and m=0.10.

Since then numerous other sets of equations have been developed to describe the equilibrium state of alluvial channels. Some more recent studies have taken more of an analytical approach than Leopold and Maddock (1953). For instance, Julien and Wargadalam's (1995) hydraulic geometry equations are "semi-theoretical" equations developed by simplifying Julien's (1988) theoretically based equations (Wargadalam 1993).

Six hydraulic geometry equations were selected for application to the study reach. Discussions of each equation are presented in Appendix C. The methods were selected based on the variability of the rivers and conditions they were developed from. There are many other similar equations (such as Kennedy, Lindley, Bose, and Chitale) that are of the form $W = a\,Q^{0.5}$. These equations were not applied because of the similarity to Lacey and Simons-Albertson (1963).

The discharge used in the hydraulic geometry calculations was the 5-year peak mean daily discharge as described in Section 4.1. The median bed material and slope are determined as

described in the preceding Sections 4.4 and 4.3, respectively. A table summarizing the data used is presented in Appendix C, Table C-1.

Figure 4-22 is a plot of the resulting predicted width from the equations against the measured active channel width from aerial photos. Three of the methods predict widths between 40 and 120 meters. As a result, the measured active channel widths before 1962 are higher than the equilibrium widths estimated by these equations. However, a group of the more recent measurements (1962-92) are closer to the width predicted by Julien and Wargadalam (1995) and Simons and Albertson (1963) for sand bed and banks. Julien and Wargadalam (1995) and Simons and Albertson (1963) produce the most accurate results for measured widths since construction of the dam. Plots of these two methods showing the temporal changes in width are presented in Figure 4-23.

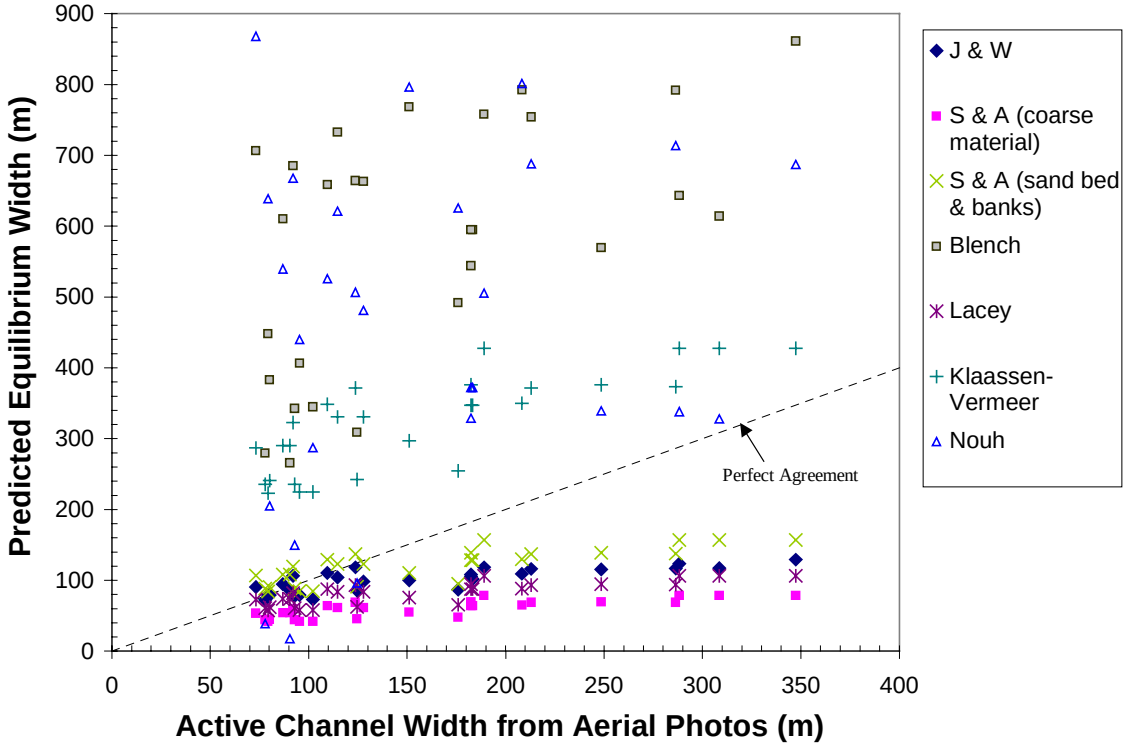

Figure 4-22 - Results of equilibrium width prediction by hydraulic geometry equations.

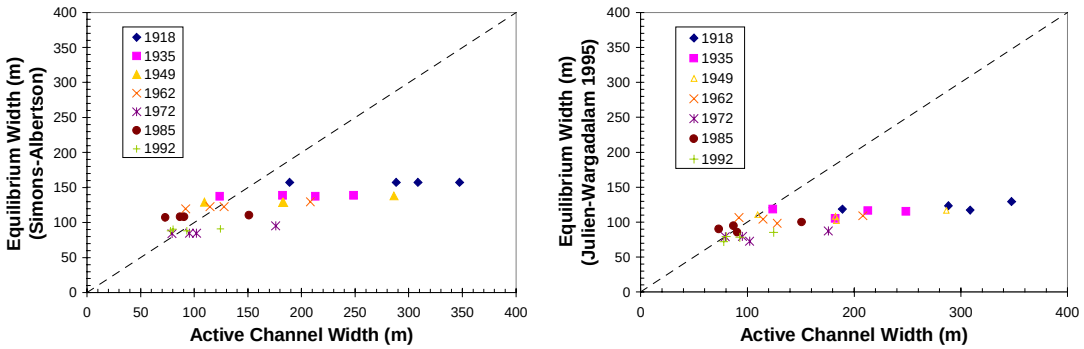

Figure 4-23 - Equilibrium width prediction using Simons and Alberston (1963) and Julien and Wargadalam (1995).

The inaccuracies at larger widths when the channel was sandy and braided may be because the channel was not in equilibrium at that time. It was an aggrading system flowing through multiple channels. If this is the case, then the hydraulic geometry equations are predicting the stable or equilibrium state towards which the river should be moving. The closer agreement between the current widths and the results of the regime equations suggests that the geometry of the river may be closer to an equilibrium or stable state now.

Blench (1957), Nouh (1988) and Klaassen-Vermeer (1988) all predict widths that are larger than those measured in the Cochiti reach. Blench's (1957) equations are sensitive to the measurement of sediment concentration used in the input. Nouh's (1988) equations were developed for channels in extremely arid regions. Klaassen-Vermeer (1988) used data from the Jamuna River, a very wide braided river with high sediment loads, for the development of their equations.

4.5.2 Channel pattern

Channel pattern is often considered to be a function of stream power, or a slope-discharge relationship combined with sediment supply (Bledsoe 1999). Given this presumption, the changes in flow energy and sediment supply documented in sections 4.1 and 4.2 should have resulted in changes in the channel pattern or planform of the Cochiti reach from 1918 to 1992. Several studies have presented theories and methods of classifying the pattern of alluvial channels (See Appendix D) and are applied to the Cochiti reach for each survey date from 1918 to 1992. The results are described in this section. Also, there are different indices that can be computed from the maps of the active channel. The following measures are computed for the reaches and subreaches of the study reach:

1) Sinuosity,

2) Reach averaged number of channels,

3) Total sinuosity, and

4) Width ratio.

Each measure reveals different characteristics of the reach and is described in greater detail below. These different measures of planform are also computed for use in the multivariate analysis of lateral movement in Chapter 6.

Planform classification

Methods

Qualitative observations were made based on visual inspection of the aerial photos, topographic surveys and digitized active channel GIS coverages (USBR 1998). Observations included notation of changes in the degree of braiding and meandering and changes in width.

Several methods of channel classification were applied to the Cochiti reach to determine spatial and temporal trends in the pattern of the reach. Brief descriptions of each of the methods are presented in Appendix D. The methods that incorporate slope-discharge relationships were Leopold and Wolman (1957), Lane (1957, from Bauer 1999, pp. 69), Henderson (1961), Ackers and Charlton (1970, from Ferguson 1987), and Schumm and Khan (1972). Rosgen's (1996) method of stream classification based on channel morphology was also applied. Additionally, several methods that utilize the concept of unit stream power were computed for the Bernardo reach: Chang (1979), Van den Berg (1995), Knighton and Nanson (1993), and Nanson and Croke (1992). Parker's (1976) method, which employs slope/Froude number and flow depth/flow width, was applied to the reaches as well as the entire Cochiti reach. Dade's (2000) method, based on Parker (1976) was also applied.

Results

Planform maps of the Cochiti reach active channel are presented in Figure 4-24. These maps show the non-vegetated active channel from 1918 through 1992. Based on qualitative observations of the planform maps, as shown in Figure 4-24, the number and size of mid-channel bars and islands decreased along with the active channel. The width of the entire Cochiti reach also decreased with time and the sinuosity of reach 2 increased.

The results of the planform classification are presented in Table 4-12 and some of the classifications support the observed variation in channel planform seen in Figure 4-24. The results of the channel classification methods estimate varying channel pattern. Leopold and Wolman (1957), Lane (1957, from Bauer 1999, pp. 69), Van den Berg (1995), Parker (1976), Change (1979) and Dade (2000) all demonstrate the shift from multi-channel toward a single-thread straight or meandering configuration.

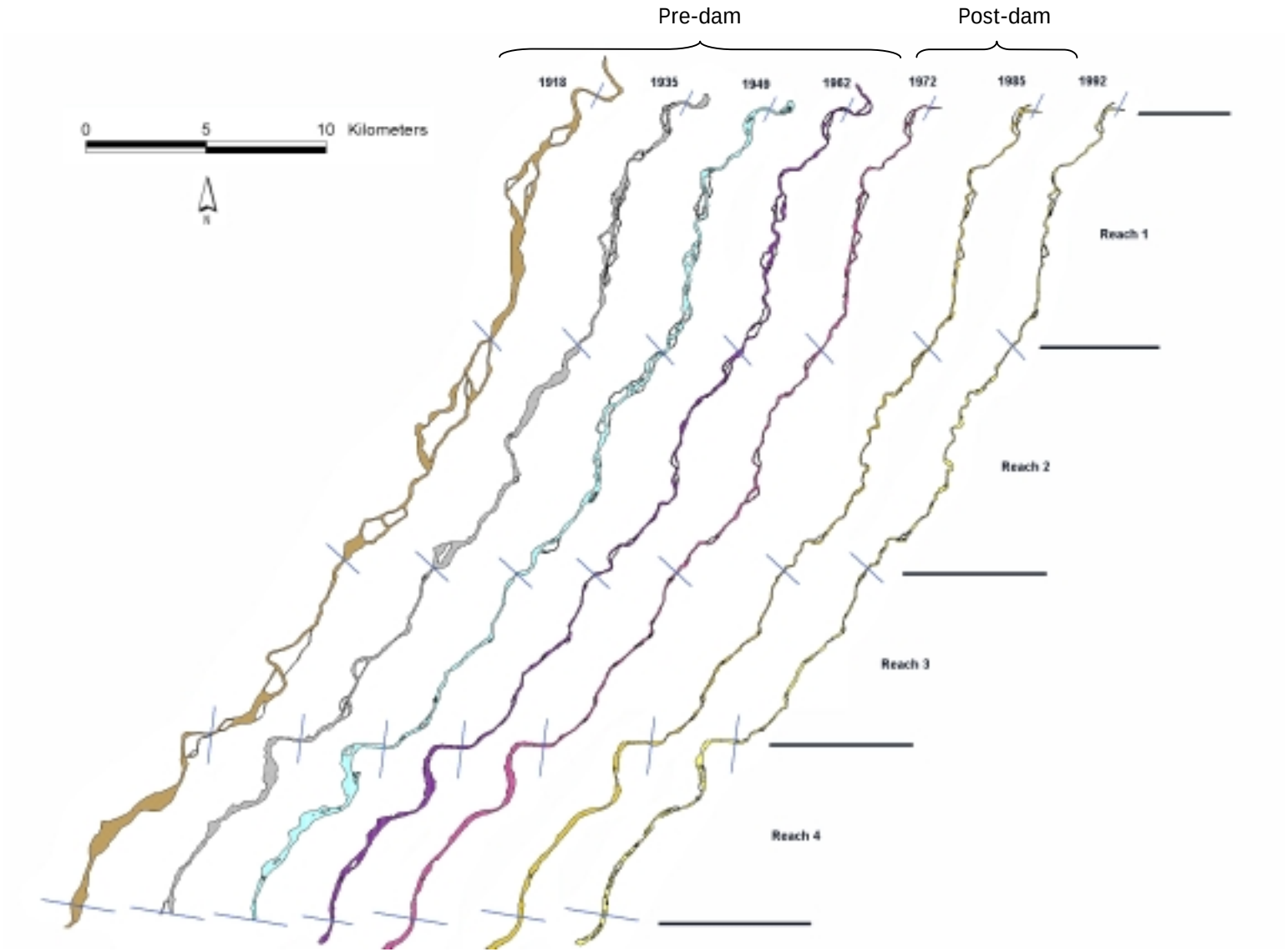

Figure 4-24 - Planform maps of the active channel of the Cochiti reach for 1918 through 1992.

Table 4-12 - Results of channel pattern classification

		Leopold and Wolman	Lane	Henderson	Ackers & Charlton	Schumm & Khan	Parker	Van den Berg	Nanson & Croke	Chang	Dade
1918	**1**	Braided	Braided	Braided	Meandering	Straight	Transition/1-2 Braids	Multi-thread	Lateral migration	Stp Braided	Braided
	2	Braided	Braided	Braided	Meandering	Straight	Transition/1-2 Braids	Multi-thread	Lateral migration	Stp Braided	Braided
	3	Braided	Braided	Braided	Meandering	Straight	Meandering	Multi-thread	Lateral migration	Stp Braided	Braided
	4	Braided	Braided	Braided	Meandering	Straight	Transition/1-2 Braids	Multi-thread	Lateral migration	Between M & B	Braided
1935	**1**	Braided	Braided	Braided	Meandering	Straight	Transition	Multi-thread	Lateral migration	Stp Braided	Braided
	2	Braided	Braided	Braided	Meandering	Straight	Transition	Multi-thread	Lateral migration	Stp Braided	Braided
	3	Braided	Braided	Braided	Meandering	Straight	Meandering	Multi-thread	Lateral migration	Between M & B	Braided
	4	Braided	Braided	Braided	Meandering	Straight	Meandering	Multi-thread	Lateral migration	Between M & B	Braided
1949	**1**	Braided	Braided	Braided	Meandering	Straight	Transition	Multi-thread	Lateral migration	Stp Braided	Braided
	2	Braided	Braided	Braided	Meandering	Straight	Meandering	Multi-thread	Lateral migration	Between M & B	Braided
	3	Braided	Braided	Braided	Meandering	Straight	Meandering	Multi-thread	Lateral migration	Between M & B	Braided
	4	Braided	Braided	Braided	Meandering	Straight	Transition	Multi-thread	Lateral migration	Between M & B	Braided
1962	**1**	Braided	Braided	Braided	Meandering	Straight	Meandering	Multi-thread	Lateral migration	Stp Braided	Braided
	2	Braided	Braided	Braided	Meandering	Straight	Meandering	Multi-thread	Lateral migration	Between M & B	Braided
	3	Straight	Braided	Braided	Meandering	Straight	Meandering	Multi-thread	Lateral migration	Between M & B	Braided
	4	Braided	Braided	Braided	Meandering	Straight	Transition	Multi-thread	Lateral migration	Between M & B	Braided
1972	**1**	Braided	Braided	Braided	Meandering	Straight	Meandering	Multi-thread	Lateral migration	Between M & B	Braided
	2	Straight	Intermediate	Braided	Meandering	Straight	Meandering	Single-thread	Lateral migration	Meandering	Braided
	3	Straight	Intermediate	Braided	Meandering	Straight	Meandering	Multi-thread	Lateral migration	Meandering	Braided
	4	Straight	Intermediate	Braided	Meandering	Straight	Transition	Multi-thread	Lateral migration	Meandering	Braided
1985	**1**	Braided	Braided	Braided	Meandering	Straight	Meandering	Single-thread	Lateral migration	Between M & B	Meandering
	2	Straight	Intermediate	Braided	Meandering	Straight	Meandering	Single-thread	Lateral migration	Meandering	Meandering
	3	Braided	Braided	Braided	Meandering	Straight	Meandering	Single-thread	Lateral migration	Between M & B	Meandering
	4	Straight	Intermediate	Braided	Meandering	Straight	Meandering	Single-thread	Lateral migration	Meandering	Meandering
1992	**1**	Braided	Braided	Braided	Meandering	Straight	Meandering	Single-thread	Lateral migration	Between M & B	Meandering
	2	Straight	Braided	Braided	Meandering	Straight	Meandering	Single-thread	Lateral migration	Meandering	Meandering
	3	Straight	Braided	Braided	Meandering	Straight	Meandering	Single-thread	Lateral migration	Meandering	Meandering
	4	Straight	Intermediate	Braided	Meandering	Straight	Meandering	Single-thread	Lateral migration	Meandering	Meandering

Sinuosity

The sinuosity for each subreach is computed from the digitized aerial photos for the years 1918, 1935, 1949, 1962, 1972, 1985 and 1992. The sinuosity was calculated by dividing the thalweg length by the valley length.

Figure 4-25 shows the sinuosity for each reach and each aerial photo. The sinuosity of each reach increased after construction of Cochiti Dam in 1973. Reach 2, from Galisteo Creek to San Felipe, was the most sinuous.

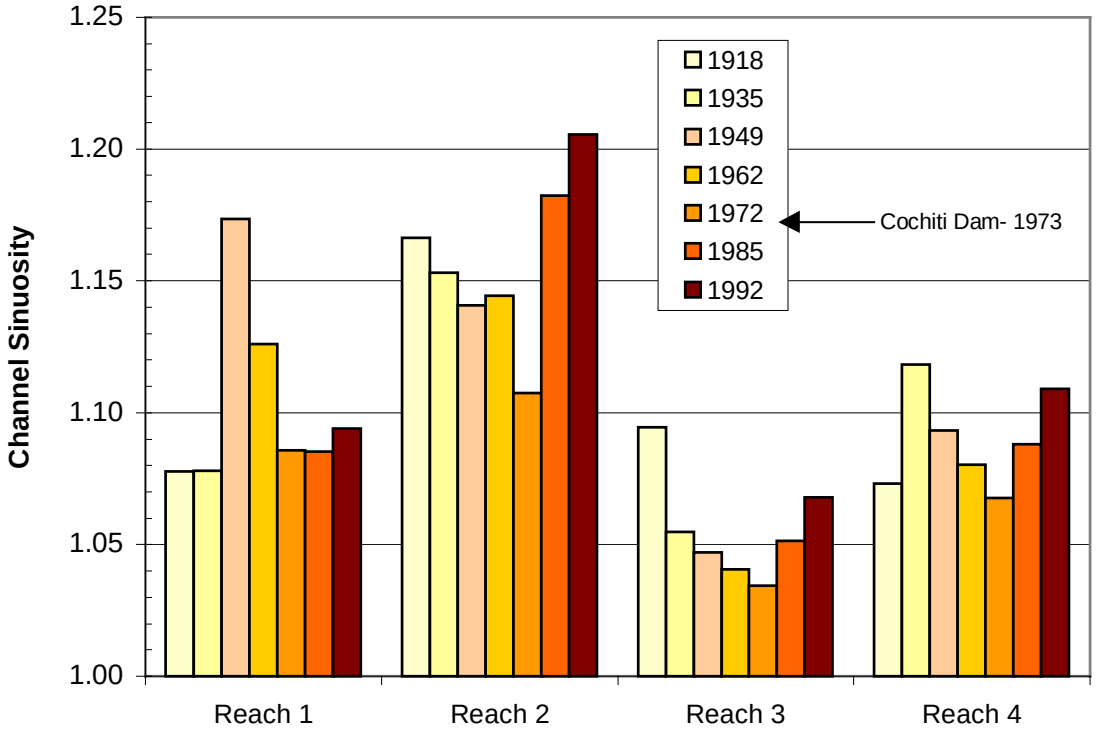

Figure 4-25 - Sinuosity of the reaches

Braiding

Numerous methods of quantifying the degree of braiding have been employed in other studies (e.g., Bridge 1993; Friend and Sinha 1993). The number of channels at each agg/deg line was measured from planform maps digitized from aerial photos by the USBR (1998). A weighted average of the number of channels per reach and subreach of the Cochiti reach was calculated. The result is a weighted-average of the number of channels per reach of river, *b*.

The time series plot of the average number of channels for the entire Cochiti reach is presented in Figure 4-26. Reaches 1 and 2 exhibit a decrease in number of channels between 1935 and 1992. Reach 4 had the fewest number of channel through 1985.

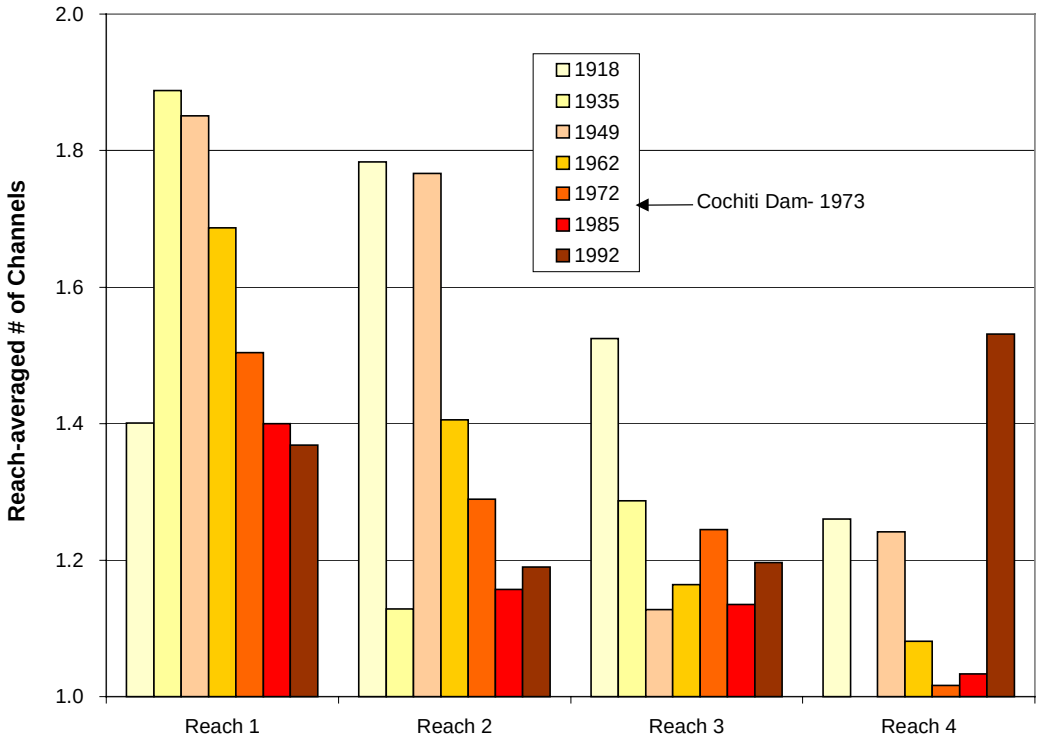

Figure 4-26 - Time Series of Average Number of Channels – Cochiti reach.

Total Sinuosity

The total sinuosity, P_{tot} (Hong and Davies 1979), of the channel was measured for the reaches and subreaches for each survey year. Total sinuosity is a measure of the degree of braiding as well as the sinuosity of the channel. It is measured by dividing the total length of all the channels in the reach by the straight-line reach length. The channel lengths were measured at the centerline of each channel, rather than the thalweg (Hong and Davies 1979; Robertson-Rintoul and Richards 1993).

The results are plotted in Figure 4-27. The increase in the total sinuosity of reach 4 between 1985 and 1992 resulted from the establishment of vegetation on previously inundated mid-channel bars. Williams and Wolman (1984) measure changes in vegetation from aerial photos. They show an example of vegetation encroachment on islands on the Republican River, similar to the changes seen in Reach 4.

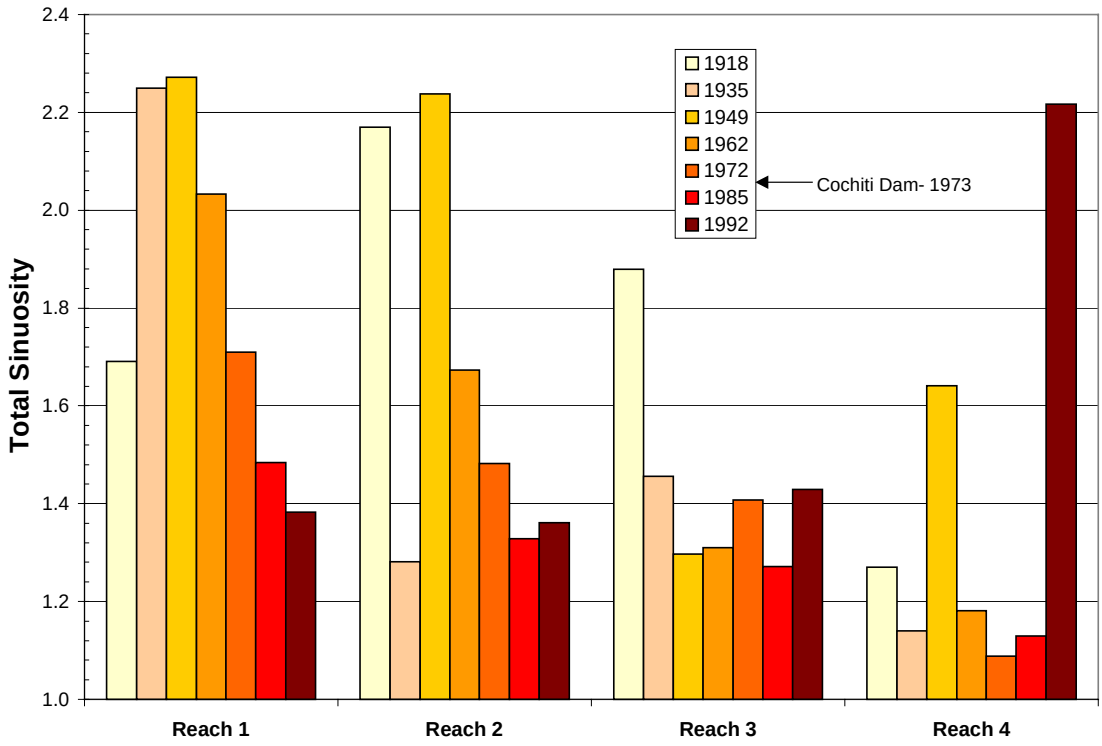

Figure 4-27 - Time series of total sinuosity.

Width Ratio

The width ratio is the ratio of the active channel width to the total channel width. The active channel width does not include vegetated mid-channel bars. The total width is the entire with of the channel from outerbank to outerbank. The width ratio approaches a value of one as the channel becomes more single thread. Values of less than one indicate the presence of islands, but a smaller value does not necessarily mean more channels, possibly bigger islands. The width ratio was measured at each agg/deg line for each aerial survey. Then the ratios were averaged over the reaches and sub-reaches using the distance between agg/deg lines as the weighting factor. The results are presented in Figure 4-28. The width ration approaches a value of one for all reaches between 1918 and 1992.

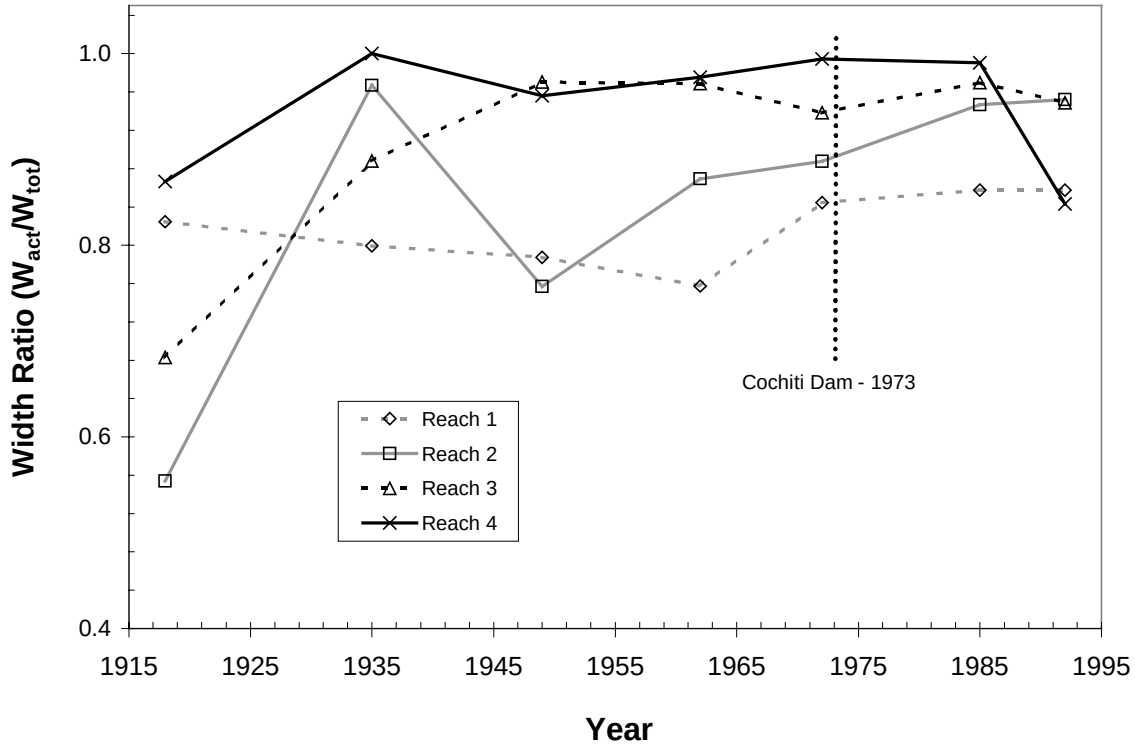

Figure 4-28 - Time series of width ratio for reaches 1 through 4

4.6 Summary

The database described in Chapter 3 was utilized to quantify the changing inputs to and responses of the study reach. The inputs of water discharge, slope and sediment supply were quantified and analyzed to identify historic trends. Also, representative values for each of these variables were identified for use in the stability analysis in later chapters.

Water discharge records since 1895 reveal a decline in annual peak flows. This decline occurred independent of Cochiti dam as evidenced by the significant ($p<0.02$) negative trend in peak flows at the Otowi gage located upstream from Cochiti dam. From single mass curves of the water discharge, a shift in the water regime was identified in 1942. Statistical comparison of mean annual flood from 1895-1942 with the mean annual flood from 1943-1996 revealed significant ($p=0.00003$) difference between the two periods at a 99% confidence level.

Other historic trends included an increase in duration of peak flows between 1918 and 1996. Also, the total water discharge decreased between 1942 and 1978. Higher water yields occurred during the pre-1942 and 1979-1996 periods.

Quantified impacts of Cochiti Dam on the annual water discharge regime included:

1) The dam attenuated peak flows greater than 142 m^3/sec (5,000 cfs). The peak flow period (duration of high pulse) increased 60 to 130% from the pre-dam to post-dam periods.

2) The mean annual flow was greater during the post-dam (1974-96) period than during the pre-dam (1895-1973) period. The increase ranged from 3% at the Cochiti gage to 51% at the Albuquerque gage.

Channel forming discharge was estimated by different methods. Given the similarities between the different estimations of dominant discharge (Table 4-13) and the assumption that it is the high magnitude, low frequency flows that form channels in arid environments (Knighton 1998), the maximum mean daily discharge (5-year peak) was selected for use as the channel-forming discharge for each study period.

Table 4-13 - Comparison of dominant discharge estimates for post-dam period.

Estimation method	Discharge value	Time period used
Effective discharge	Q_{eff} = 5,400 cfs	1992-1996
2-year frequency flow	$Q_{2\text{-}yr}$ = 5,120 cfs	1974-1996
Maximum flow	Q_{max} = 5,600 cfs	1985-1996

The trends in suspended sediment records are summarized below:

1) Decrease in sediment yield in 1958 at Otowi and Bernalillo/Albuquerque.

2) Completion of Cochiti Dam (1973) resulted in a 99% reduction in sediment concentration flowing into the study reach. The suspended sediment concentration also declined around this time at the Otowi gage located upstream from the dam. The impact from the dam is less pronounced at the Albuquerque gage indicating another source of sediment, either tributary inflow or erosion of bed and banks.

3) Sediment budget revealed that the pre-dam inflow was approximately equal to the outflow, but all of the inflows are not accounted for. As a result, there is a potential for higher inflow than outflow meaning sediment storage in the reach or aggradation. Other historic studies suggest periods of aggradation prior to dam construction (Graf 1994). Post-dam sediment budget showed that the outflow greatly exceeded the inflows, including gauged tributary inputs, indicating that the channel itself (bed and banks) was a source of sediment. It is unlikely that even the tributaries that are not accounted for could make up the difference.

The slope of reaches 2, 3 and 4 remained between 0.0009 and 0.0012 for the time period 1935 through 1992. Reach 1 was consistently the steepest (>0.0016) and reach 4 the mildest (<0.0012). Generally, prior to construction of Cochiti dam, the slope declined slightly. Following dam construction, no clear trend was evident.

Vertical and lateral responses of the study reach to the changing inputs described above were also quantified. Vertical responses included changes in bed material and bed elevation. The lateral responses measured in this chapter included active channel width at each aerial survey date, channel pattern classification and four planform indices.

The bed material of the Cochiti reach changed following construction of Cochiti Dam. Prior to dam construction, the bed was somewhat coarser in reaches 1 and 2 than the downstream reaches. The bed of the entire Cochiti reach was primarily sand. Reach 1 and 2 exhibited a bi-modal distribution with a pavement of cobbles and gravel overlain by fine and medium sand (Rittenhouse 1944; Nordin and Culbertson 1962). Following dam construction, the bed of the entire Cochiti reach coarsened to gravel/cobble size.

Comparisons of bed elevation were only made between consistent surveys (i.e., measured at same location, preferably by the same agency). The pre-dam period exhibited smaller changes in bed elevation. Changes were primarily aggradational, although data were limited. During the post-dam period, larger degradational changes occurred. Reaches 1 and 2 degraded about 0.5 meters. Reaches 3 and 4 degraded 1.2 and 1.9 meters, respectively, between 1972 and 1998.

Width changes were measured from the non-vegetated active channel digitized from historic maps and aerial photos. All reaches exhibited a decrease in width with time since 1918. Reach 1 exhibited the greatest change; almost 70% decrease between 1918 and 1992. Reach 4 was the widest reach for the entire time period. Reaches 2 and 3 both widened following dam closure.

The rate of change of width slowed with time between 1918 and 1992, suggesting that the width is approaching equilibrium form given the consistent input conditions since construction of the dam. The changes in width were studied to determine the deviation from an equilibrium state. Both the hyperbolic model (Williams and Wolman 1984) and hydraulic geometry equations (Julien and Wargadalam 1995; Simons and Albertson 1963) support this conclusion.

Numerous channel pattern classification methods were applied, and some illustrate a shift from multi-thread or braided to a meandering/single-thread pattern with time since 1918. This general trend is evidenced in the planform maps of the non-vegetated active channel, as well as conclusions drawn in other studies (Lagasse 1980; Leon 1998; Graf 1994).

Four planform indices were measured for the reaches and subreaches:

1) Sinuosity - Sinuosity of all reaches increased after the dam was constructed. Reach 3 was the least sinuous and exhibited the least variability in sinuosity.

2) Number of channels - Reach 1 was the highest. Reach 4 increased between 1985 and 1992 as the channel incised and mid-channel bars became vegetated.

3) Total sinuosity - Follows similar pattern to the number of channels. Reach 4 also increases between 1985 and 1992. This parameter is easier to measure using GIS and as a result may be better for future use than the number of channels.

4) Width Ratio - Moves toward a value of one with time for all reaches. This indicates that the number of channels and/or island widths decreased.

Overall, the planform indices illustrate that reach 3 is the least sinuous and exhibits the most stable behavior. Reach 1 is the most multi-channel and reaches 1 and 2 exhibit the greatest variability in planform.

CHAPTER 5

INDICES OF LATERAL MOBILITY AND STABILITY

There are different means by which a river can move laterally, as discussed in Chapter 2. The river can change its width, erode its banks causing migration, or avulse out of the channel. One index of lateral movement would not be sufficient to describe the complexity of the changes in the Cochiti reach. From 1918 to 1992, the Cochiti reach of the Rio Grande exhibited different planform types, changes in width, lateral migration, and avulsions. Figure 5-1 exemplifies the spatial variability in lateral movement in a small 1,500-meter reach between agg/deg lines 140 and 150 from 1918 to 1935.

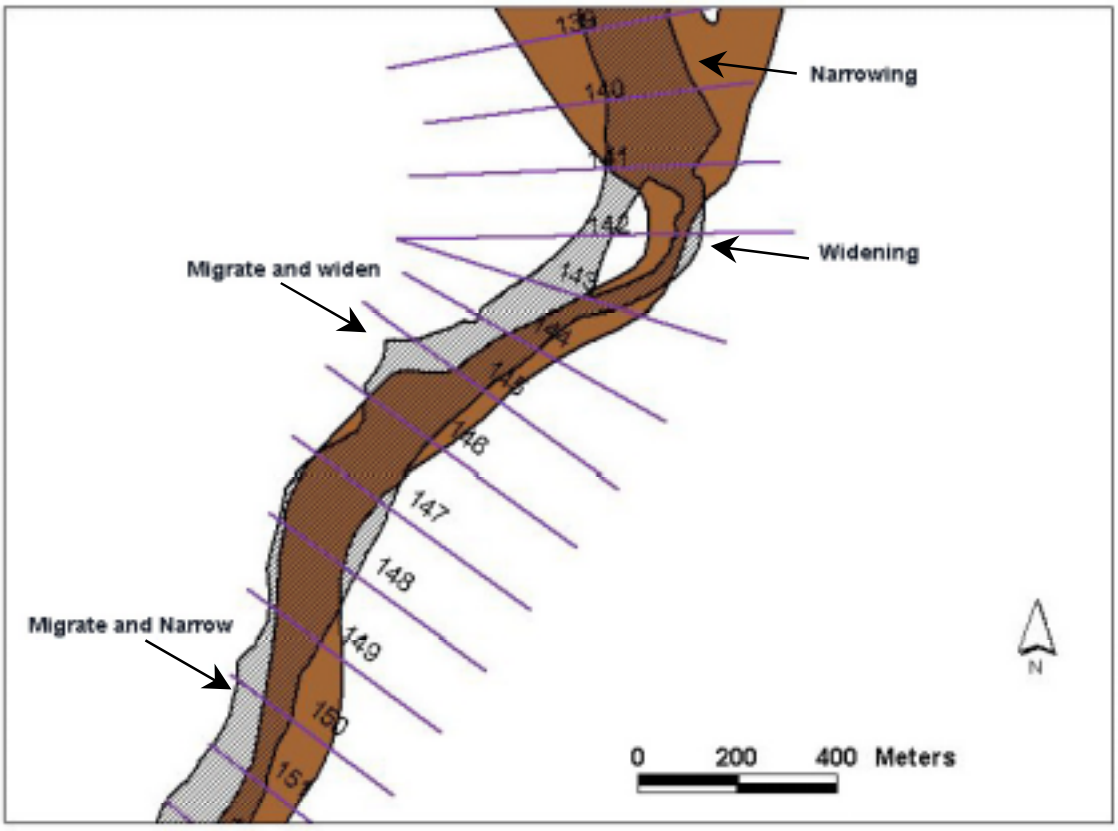

Figure 5-1 - River planform changes from 1918 to 1935, Rio Grande, NM.

Four indices of lateral movement and two indices quantifying lateral stability are measured on the Cochiti reach and discussed in this chapter. Lateral movement and lateral stability of the channel are measured by two different methods. The lateral mobility or movement of the reach was characterized by changes in the outermost bankline of the channel. The lateral stability is measured by changes in active channel area. All of the indices were quantified on a subreach and reach averaged scale for each of the digitized map/aerial surveys. Details of meander formation, direction of movement, and braid-bar formation were not studied in this analysis. The planform of the Cochiti reach varies spatially and temporally across the planform continuum from meandering to straight to braided patterns as shown in Chapter 4. The meandering pattern, however, is not strong (sinuosity < 1.5) and there is little evidence of true meander migration during the time period studied.

The four indices of lateral movement begin with a gross measurement of total bankline change, then break down the lateral movement into width change and migration. The indices are as follows:

1) Total bankline change, E (m/year)
2) Normalized lateral movement, N (% width/year)
3) Width change, dW (m/year)
4) True migration, M (m/year)

Lateral stability is measured by quantifying how much the active channel area changes with time and how much of the active channel area remains in the same place.

Bankline changes and active channel area of the Cochiti reach were measured using the GIS coverages of the active channel area from 1918 to 1992 described in Chapter 3. The measurements were performed using ARC/Info v.7 and ArcView v. 3.2.

5.1.1 Lateral Movement

Lateral movement rates were measured both by total outer bankline change and by separating width change from migration. The lateral movement rate of the channel was computed by measuring the movement of the left and right banks of the channel at each agg/deg line over the following time periods: 1918-35, 1935-49, 1949-62, 1972-85, and 1985-92. The four measures of lateral movement were listed in the preceding section and each is described in detail in the following sections.

Each measure of lateral movement provides different insights to how the channel moved. Measurements of *E* and *N* provide insights into when and where the river is most mobile without taking into account how it is moving. Normalizing the movement rate by the channel width, *N*, allows for comparison with rivers of different sizes and between the reaches and subreaches of this channel.

For each measure of lateral mobility, the spatial variability within the reach is analyzed via a plot of the movement rates at each agg/deg line. The temporal variability is analyzed using frequency distributions of the measurements at each agg/deg line for each survey period. Reach and subreach averaged rates are also computed to identify changes between reaches and for use in modeling of lateral mobility in Chapter 6.

Lateral channel movement has been measured by bankline change in other studies, such as Brice (1982), Nanson and Hickin (1986), and Hooke (1986). Others have chosen to quantify lateral movement by using the channel centerline (Shields et al. 2000) or by area of floodplain eroded (Marston et al. 1995; Lewin et al. 1977). Hooke (1986) found that maximum rates of erosion between bank lines were higher than those between centerlines, but were of the same order of magnitude. Also, she found that difficulties in distinguishing eroded from deposited areas made measurement of average lateral movement rates by quantifying areas of movement and dividing by the reach length unsatisfactory.

Measuring changes in the banklines of the Rio Grande allowed for measurement of all forms of lateral movement, including width change, and not just meander migration. The multi-channel nature of the Cochiti reach would make it necessary to determine which channel is the main channel in order to use centerlines for lateral movement measurements.

Because of the variability in mechanisms of lateral movement, some studies, such as Klaassen and Masselink (1992), exclude reaches that exhibit increases or decreases in channel width because it becomes difficult to distinguish between bank erosion and change in bank-line caused by increase or decrease in discharge. Width changes were included in this study because of their importance in the lateral channel changes in this reach. Width change is an important lateral response to changes in flow regime such as those that occurred in the Cochiti reach.

Total Bankline Change, *E*

Total movement of the channel banks, *E*, incorporates width change and lateral migration of the channel. The lateral movement of the outermost left bank and right bank (See Figure 5-2) were summed at each agg/deg line and divided by the length of the time period:

$$E = \frac{\Delta r + \Delta l}{t_2 - t_1} \quad \text{.....(5-1)}$$

where:

$\Delta r = dr$ = lateral movement of outermost right bankline (meters);

$\Delta l = dl$ = lateral movement of outermost left bankline (meters);

t_2 = year of 2nd aerial survey (end of time period); and

t_1 = year of 1st aerial survey (beginning of time period).

This is the sum of the bankline change, not the average. As a result, *E* will be two times the migration rates presented in other studies that look at the bank erosion or migration rate in meandering channels.

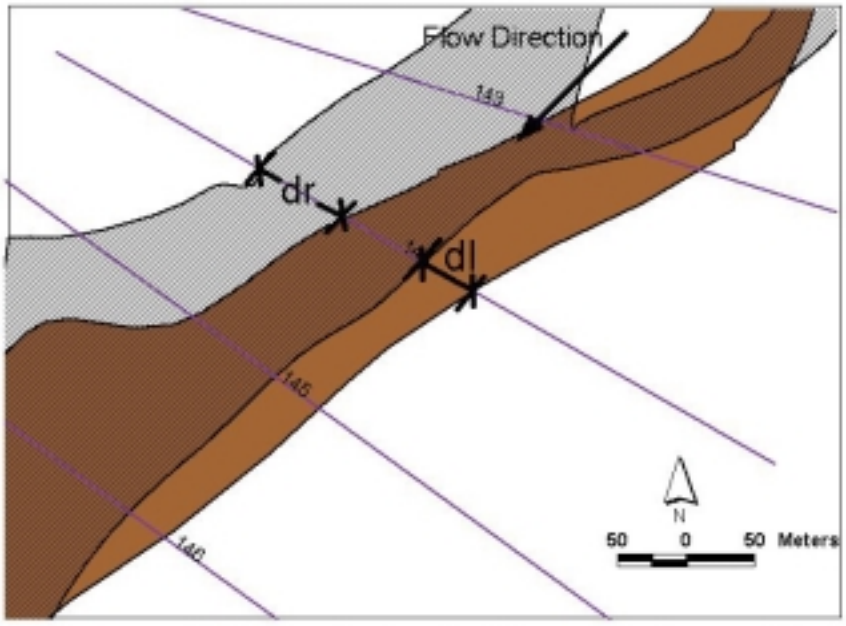

Figure 5-2 - Measurement of bankline change at agg/deg 144 between 1918 and 1935.

Spatial trends - The measured values of *E* for each agg/deg line are plotted in Figure 5-3. Subreaches 2.2 and 2.3, from about 13 km to 17 km, begin less than 1 km downstream from the confluence with Galisteo Creek. This section exhibited higher rates of movement through the time period 1918-62. From 1918 to 1962, the planform was braided with point bars. Beginning

with the 1972 photo, the planform shifted to a more single thread, wide-bend point bar configuration, and continued to exhibit this planform in 1992. Galisteo Dam was constructed in 1970 and may have had some impact on the changes in the Rio Grande downstream from its confluence between 1962 and 1972. Both subreaches 2.2 and 2.3 narrowed to less than 30% of their 1918 width by 1972, then widened an additional 10 to 25% between 1972 and 1992. Between 1918 and 1962, the average number of channels in subreaches 2.2 and 2.3 varied from 2.83 to 1 with no consistent trend, which is not unexpected for an unstable braided channel. After 1962, subreach 2.3 moved toward a single thread channel and remained one in 1985 and 1992. Subreach 2.2 continued to exhibit minor multi-threadness.

Subreaches 3.1 to 3.3, between 25 and 30 km downstream from agg/deg 17, exhibited low lateral mobility for the entire time period. This section is located downstream from the confluence with the Arroyo Tonque, an ephemeral arroyo that contributes significant amounts of coarse material when it flows (Drew Baird, USBR Albuquerque, NM, pers. comm. 1998). Additionally, this section of river is confined by mesas on the west side of the river. The planform of this section was straight and primarily single thread through the entire time period with width ratios close to one for the entire period (section 4.5.2). The width of subreaches 3.1, 3.2 and 3.3 declined from 1918 to 1972 then increased slightly by 1992. However, the total variability in the width for this section was much less than the rest of the Cochiti reach.

There is a consistent peak in the bankline change plot at about 36 km downstream from agg/deg 17 in subreach 4.2, which corresponds to a region near the confluence and just downstream of the Jemez River. Although this tributary was dammed in 1953, it appears to have continued to influence the mainstem channel through 1992. Subreach 4.2 exhibited high variability in width, number of channels and sinuosity relative to the other subreaches.

Temporal Trends - Histograms of the frequency distributions of the total bank line change for all agg/deg lines are presented for each time period in Figure 5-4. The highest rates of movement occured during the 1918-35 time period. By 1962, more than 50% of the lines moved less than 10 m/year and by 1985 70% of the lines fall into this grouping.

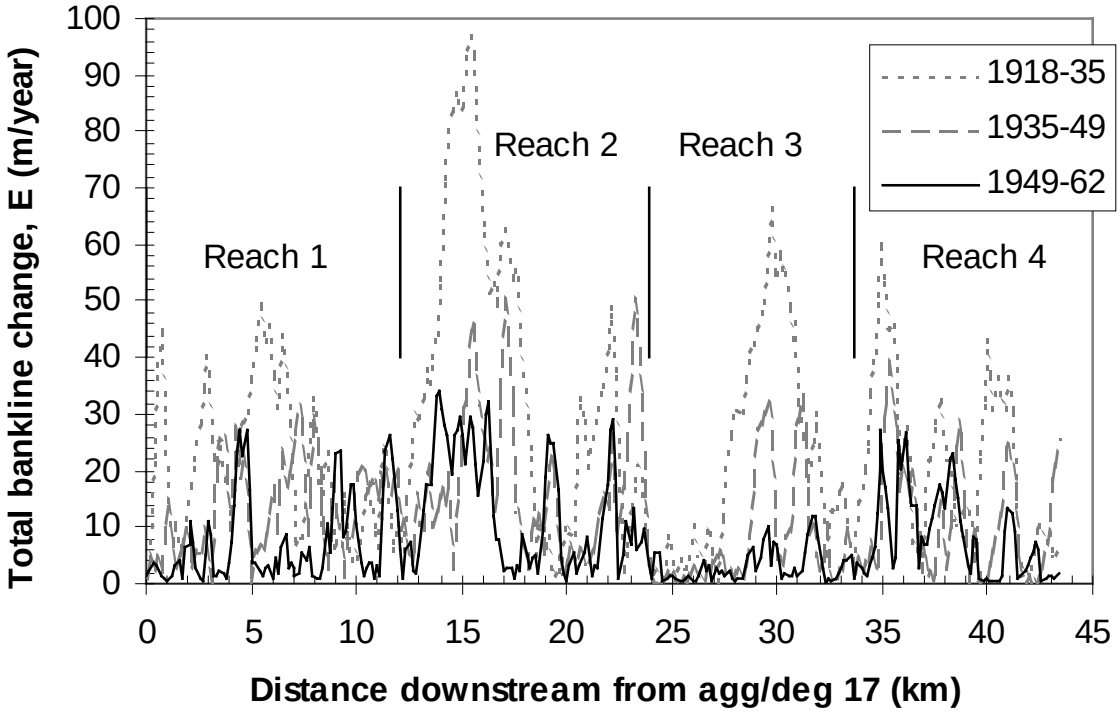

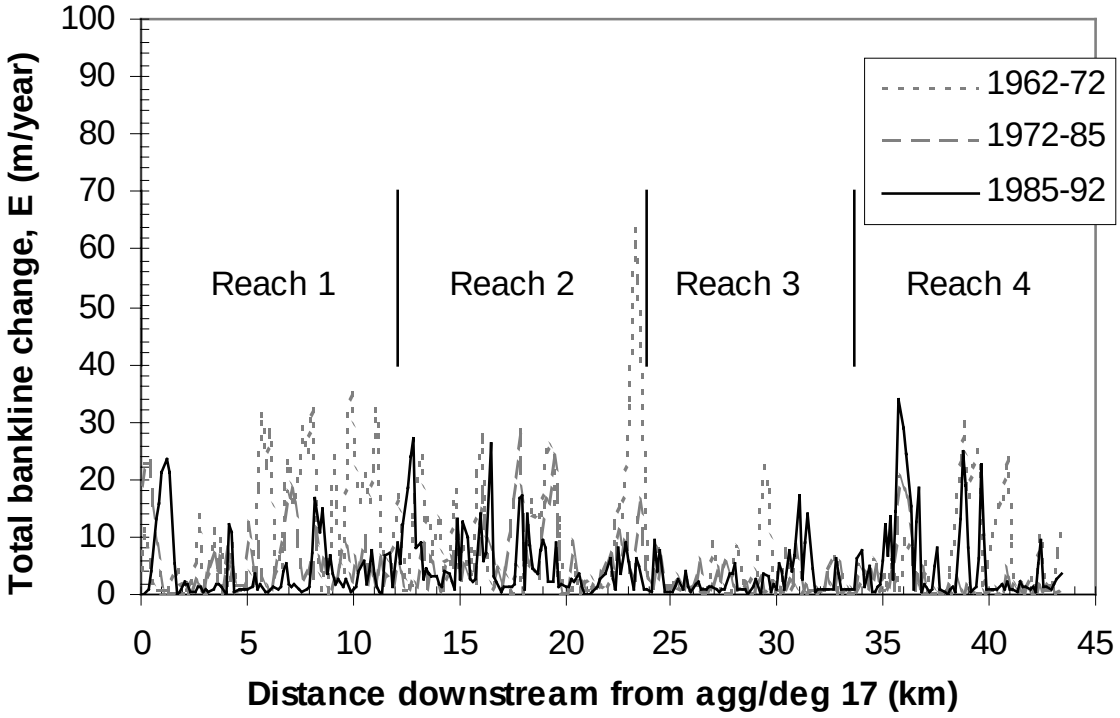

Figure 5-3 - Total bankline change, E, for each agg/deg line

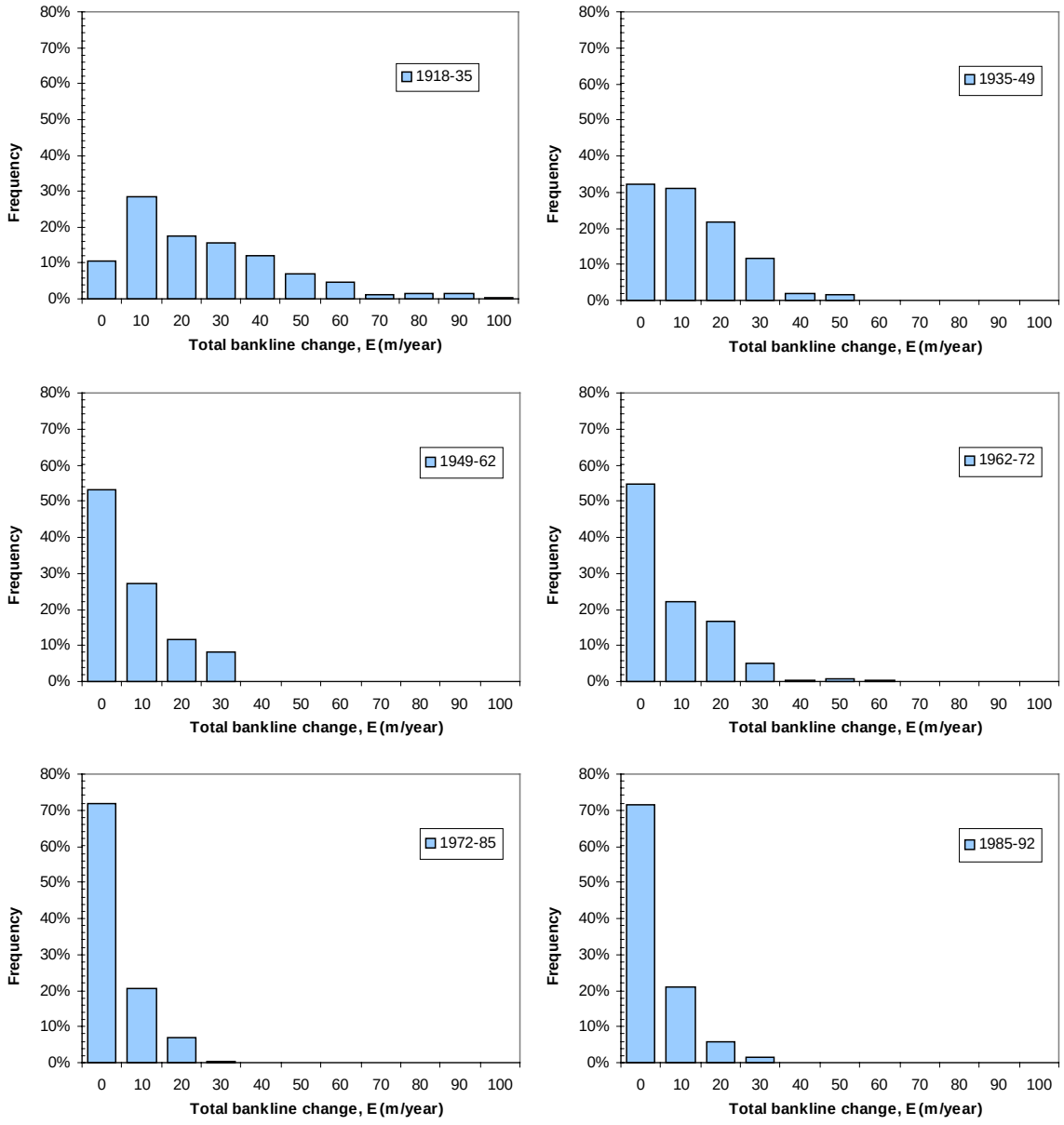

Figure 5-4 - Histograms of frequency of the total bankline change at all agg/deg lines.

Reach Averaged - The reach and subreach averaged rates provide a summary of both spatial and temporal trends. A weighted average was performed using 1/2 the distance between the adjacent upstream and downstream lines as the weighting factor. The reach-averaged results are presented in Figure 5-5. The maximum values of total bankline movement occured between 1918 and 1935 and decreased to a more constant value in the more recent time periods. Movement rates of both reaches 3 and 4 increased from 1985-92. Reach 3 is the least mobile, with rates of

movement remaining less than 3 m/year after 1949. By 1992 the rate of movement for all of the reaches was less than 6 m/year. Reach 2 was the most mobile.

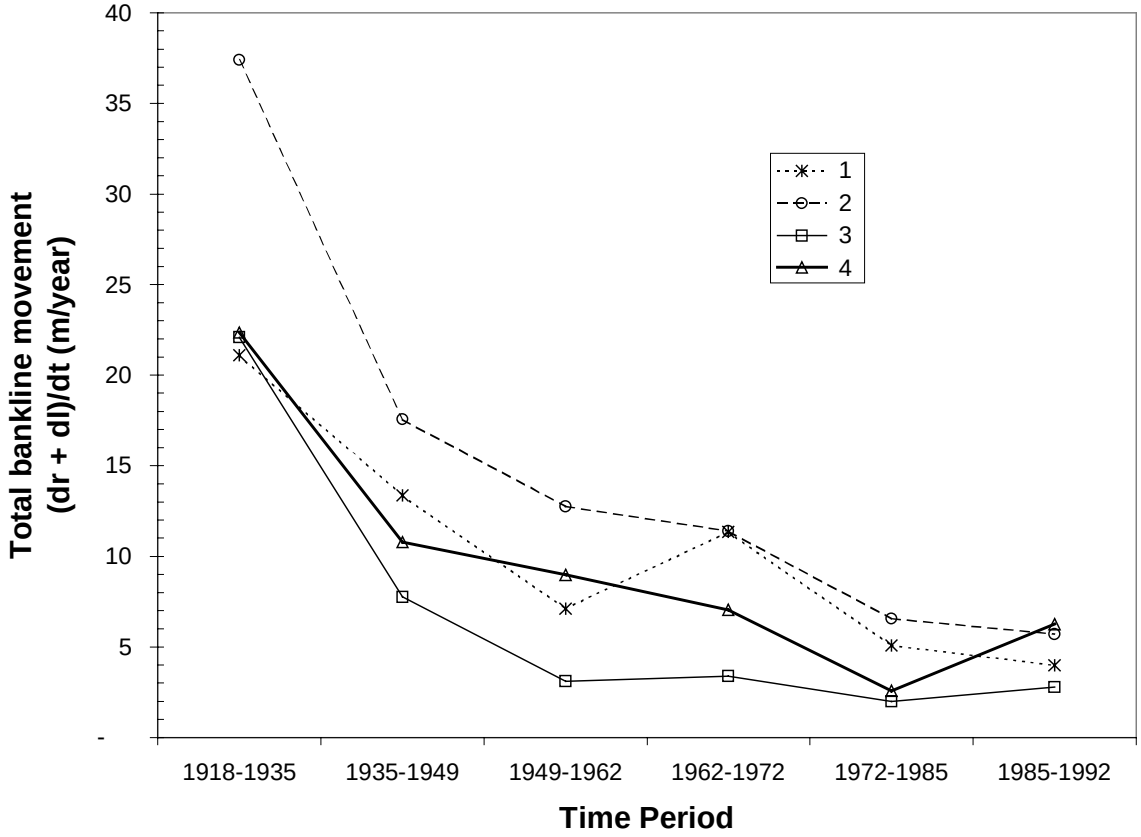

Figure 5-5 - Reach-averaged - Total bankline change per year, Erosion rate, E

Normalized Lateral Movement Rates

The normalized lateral movement rates were computed by dividing the average of the right and left bank change by the active channel width averaged over the time period. This value was then divided by the number of years in the time period to get an annual rate. The resulting value is the normalized average annual movement of the channel, N, expressed as a percentage of the average width of the channel:

$$N = \frac{\left[\frac{(\Delta r + \Delta l)/2}{(W_1 + W_2)/2}\right]}{\Delta t} = \frac{\left[\frac{\Delta r + \Delta l}{W_1 + W_2}\right]}{\Delta t} \text{, (\% width/year)}$$

where:

t_1 and t_2 = dates of compared aerial surveys (years);

$\Delta r = dr =$ movement of right bank of channel from time t_1 to t_2 (m);

$\Delta l = dl$ = movement of left bank of active channel from t_1 to t_2 (m);

W_1 = Active channel width at time t_1 (m);

W_2 = Active channel width at time t_2 (m); and

$\Delta t = t_2 - t_1$ = length of time period between aerial surveys in years.

Figure 5-6 illustrates how the bankline change and widths are measured, using agg/deg line 144 in 1918 and 1935 as an example. The normalized lateral movement rate, *N*, was computed at each agg/deg line and then averaged for each reach. The normalized lateral movement rate incorporates width change and lateral migration and normalizes for river size. It removes the potential correlation that larger rivers move more and allows for comparison with other studies. The normalizing width is the active channel width, or the nonvegetated width excluding mid-channel bar and islands. The active channel width should be more indicative of the "size" of the river as this is the channel that is formed or created by the imposed water and sediment regime. Also, the bankline change is averaged between the right and left bank to measure movement of the river across the flooplain.

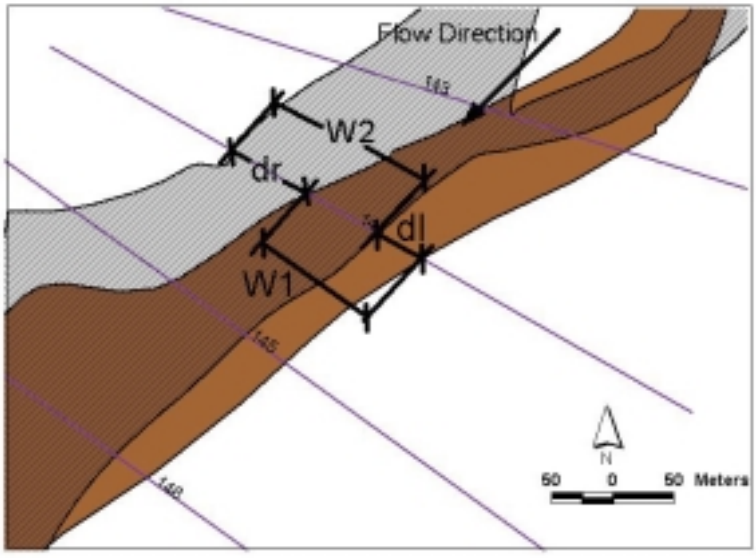

Figure 5-6 - Example of measurement of N at agg/deg 144 between 1918 and 1935.

Spatial trends - The measurements of *N* at each agg/deg line are presented in Figure 5-7. The stable reach downstream from the Arroyo Tonque is evident as discussed above. The high peaks at the ends of reaches 1 and 2 between 1962 and 1972 appear to be a result of either avulsions/abandonment of old side channels, or manmade cutoff/channelization. In both cases, the channel moved to a new location and abandons the old channel, which became vegetated by 1972. There is no evidence on the aerial photos of human intervention; however, channelization activities may have occurred during that time period. Also, the high mobility in the reach downstream from Galisteo Creek (13-17 km) between 1918 and 1962 is evident again as discussed above.

Temporal trends - Histograms of the frequency distributions of the normalized movement rates are presented in Figure 5-8. The temporal trends seen in the normalized movement rates are similar to those in the total bankline change rate, *E*. The highest movement rates were in 1918-35, with more than 20% of the reach moving by more than 10% of the channel width per year. By 1985 45% of the lines were moving at less than 2% per year. Distributions from 1949 to 1992 are highly skewed with 32 to 46% of the lines moving less than 1% of channel width per year.

Reach averaged - Figure 5-9 shows the variation in measured reach-averaged annual lateral movement rates in time and with distance downstream from Cochiti Dam. All reaches show an increase between 1962 and 1972 with bigger peaks for reach 1 and 2 resulting from the avulsions described above. The movement rates of reaches 3 and 4 also increased between 1985 and 1992, possibly as a result of channel incision, and vegetation encroachment on the active channel creating a narrower channel. When the movement rates are normalized by width, reach 4 is the least mobile and reach 2 is the most.

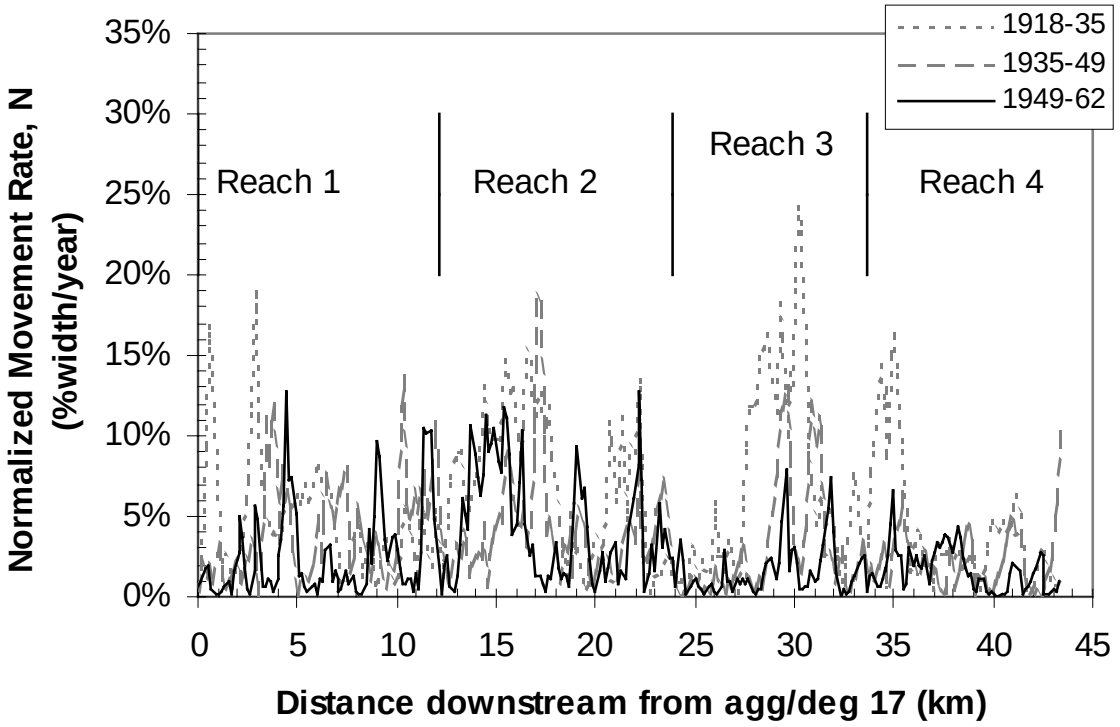

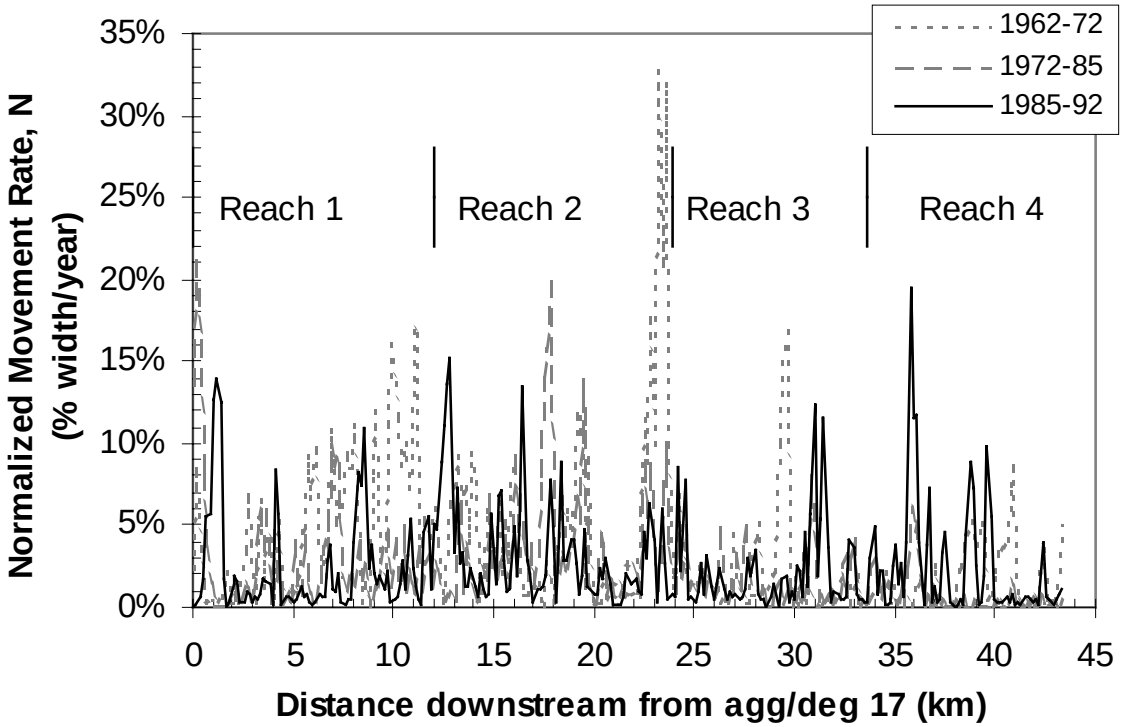

Figure 5-7 - Normalized lateral movement rates, *N*, expressed as % of width per year measured at each agg/deg line.

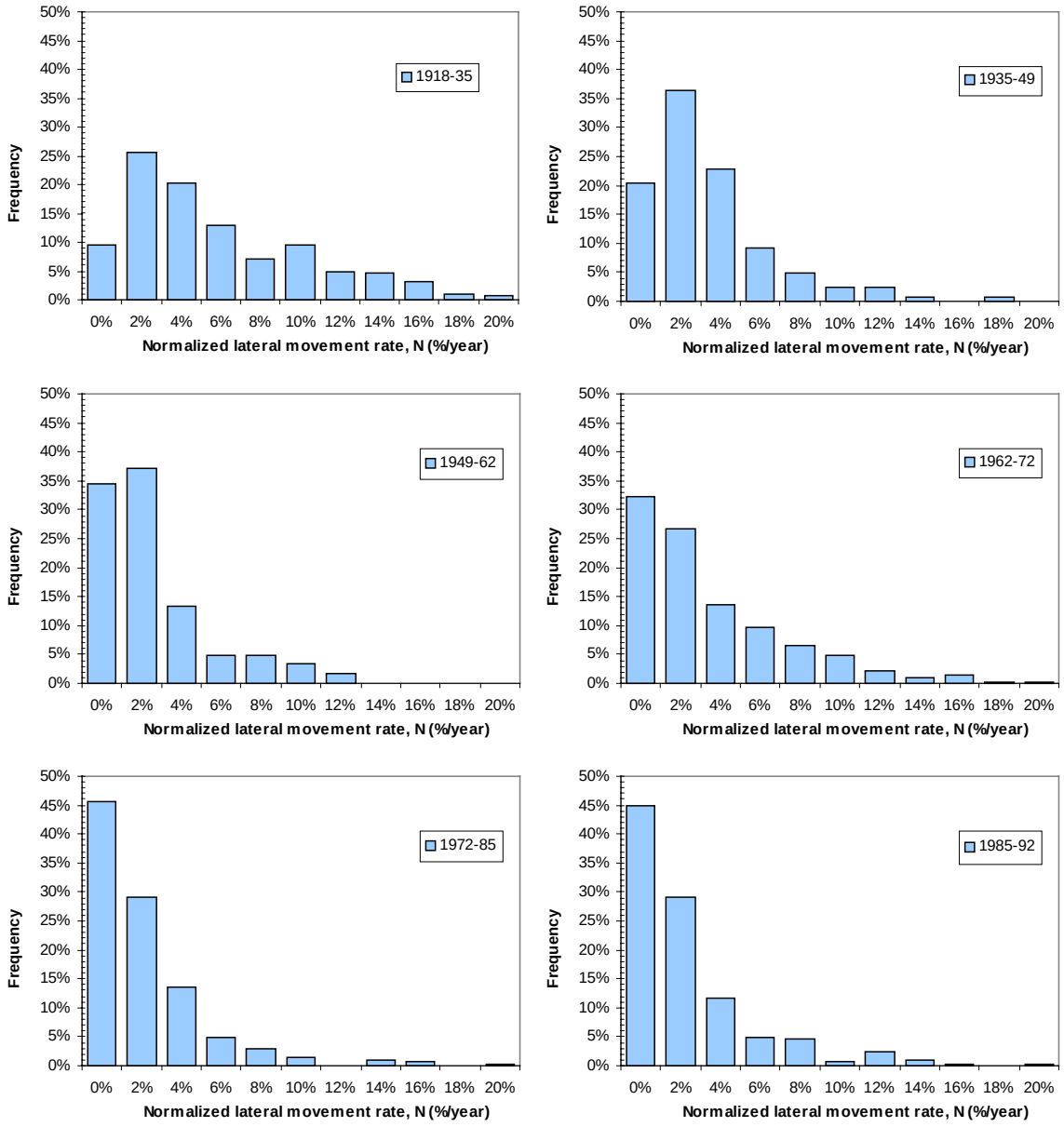

Figure 5-8 - Histograms of the frequency of the normalized lateral movement rate measured at each agg/deg line.

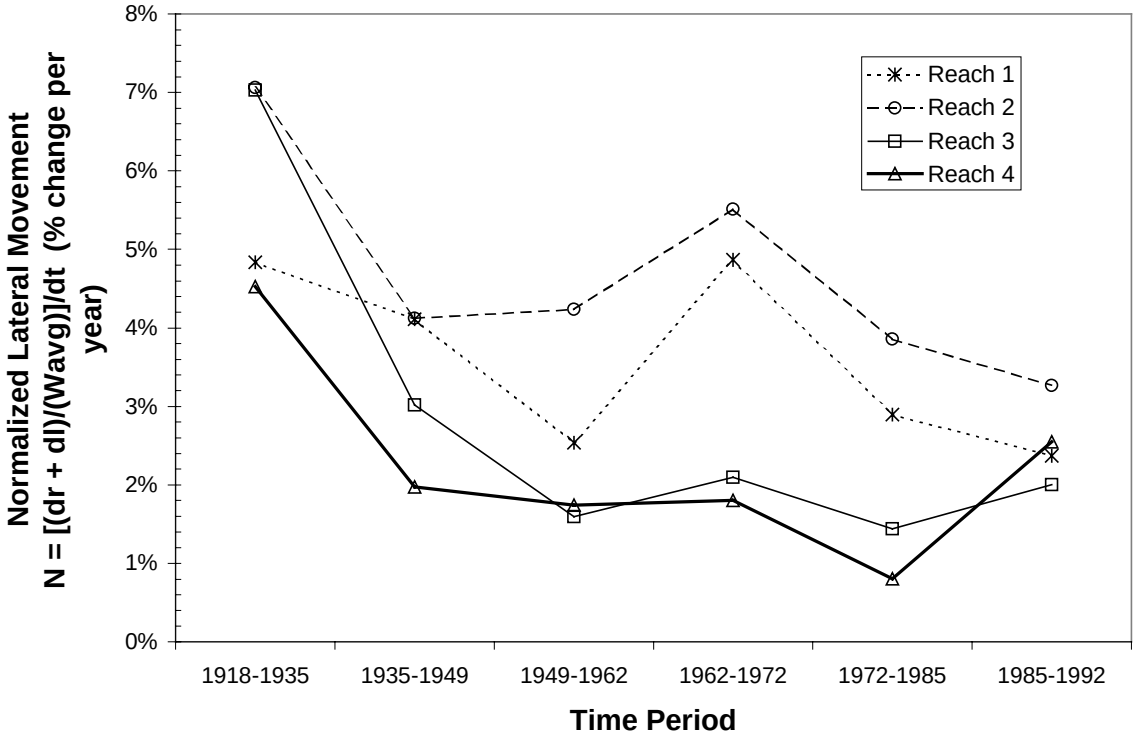

Figure 5-9 - Normalized lateral movement, *N*

Width Change

Two different measures of channel width were described in Chapter 4: the active channel width and the total channel width. The non-vegetated active channel width does not include mid-channel bars or islands and is considered to be representative of the channel formed by the prevailing water and sediment regime. The total channel width includes mid-channel bars and islands. For a single thread channel, the active channel width and the total channel width are equal. Changes in the active channel width in theory could indicate response to the driving water and sediment regime and a move toward an equilibrium width. Changes in total channel width are also in response to water and sediment regime, but they can include planform adjustments in the form of changes in size of mid-channel bars or islands. Additionally, it is the measure of total width change that is subtracted from the total movement rate to compute the migration rate because it is measured from outer bankline to outer bankline. Changes in both measures of width are analyzed here.

Change in Active Channel Width

The active channel width, defined as the non-vegetated channel, was measured from the GIS coverages. The results are presented in Chapter 4. From these measurements, the change in width at each agg/deg line over each time period was also computed by subtracting the width at the end of the time period from the width at the beginning and dividing by the length of the time period:

$$dW_{act} = \frac{\Delta W_{act}}{\Delta t} = \frac{W_{act-2} - W_{act-1}}{t_2 - t_1} \text{ , (m/year)}$$

where:

dW_{act} = rate of change in active channel width (m/year);

t_1 and t_2 = dates of compared aerial surveys (years);

ΔW_{act} = total change in active channel width between t_1 and t_2 (m);

W_{act-1} = Active channel width at time t_1 (m);

W_{act-2} = Active channel width at time t_2 (m); and

$\Delta t = t_2 - t_1$ = length of time period between aerial surveys in years.

If the value of dW_{act} is negative then the channel narrowed and if it is positive, the channel widened.

Spatial Variability - The rate of change of width at each agg/deg line is plotted in Figure 5-10. The section from 25-30 km, corresponding to subreaches 3.1 through 3.3, exhibited little change in width between 1918 and 1962. The greatest variability in active channel width occured in reach 4. Between 1985 and 1992, reaches 2 and 3 had more lines that widened than other reaches and time periods. Reach 4 exhibited higher variability in width than the other reaches.

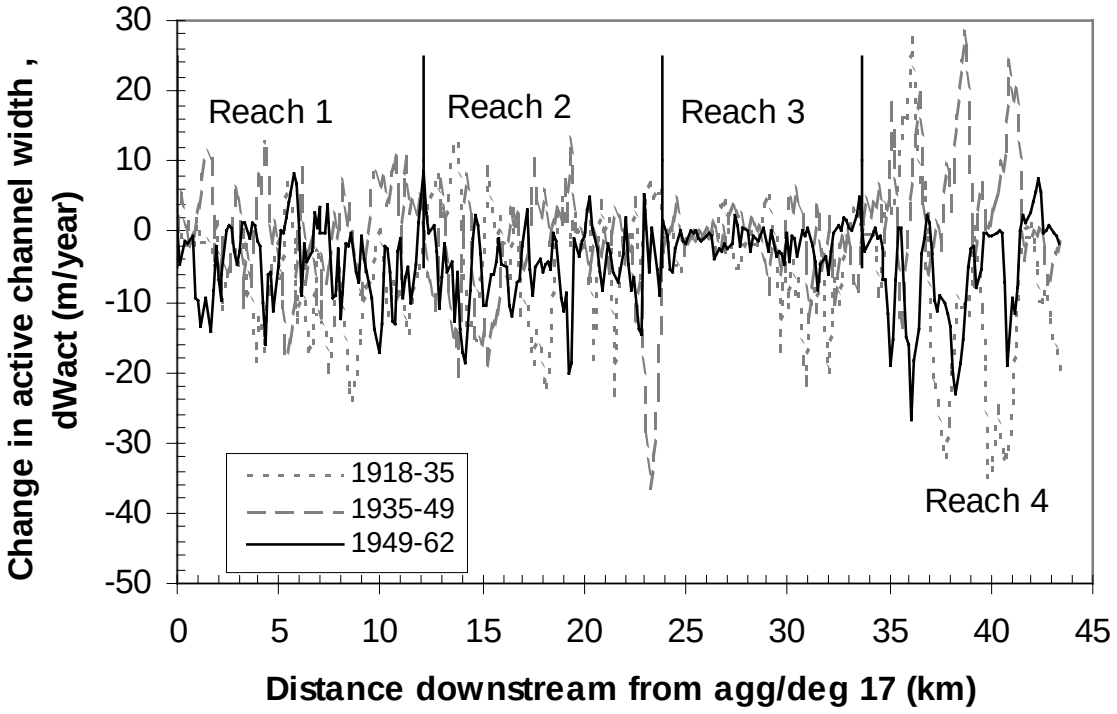

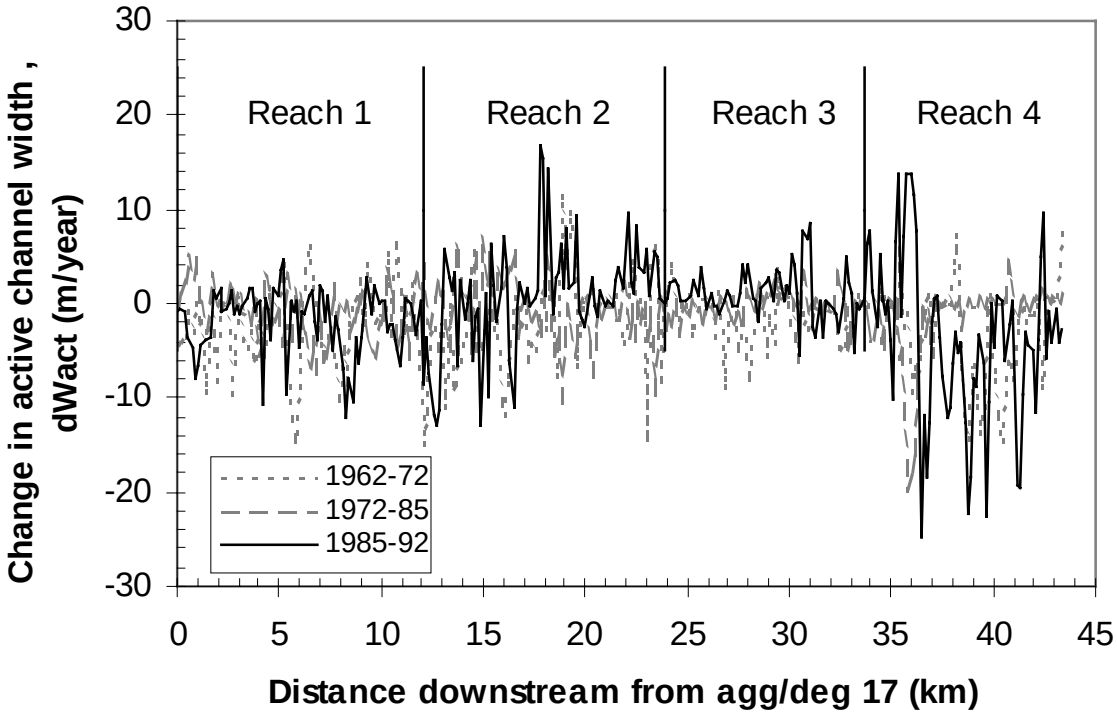

Figure 5-10 - Downstream plots of change in active channel width at the agg/deg lines for each.

Temporal variability - Histograms of the frequency distributions are presented in Figure 5-11. The distributions narrowed with time, indicating that more lines exhibited little or no change in width. Between 1985 and 1992 19% of the lines widened at a rate greater than 5 m/year.

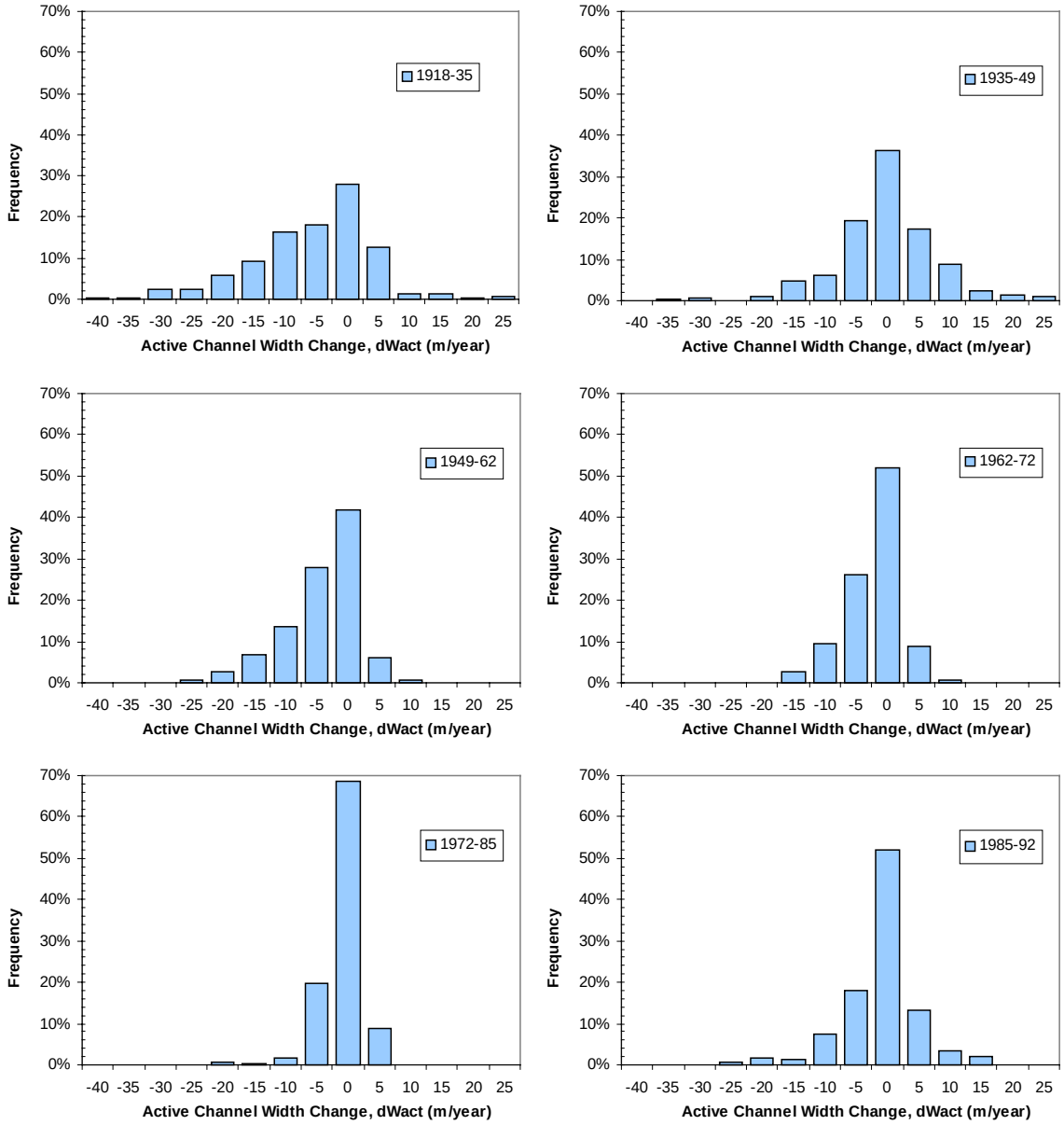

Figure 5-11 - Probability density functions of change in active channel width at agg/deg lines.

Change in Total Channel Width

The change in total channel width, which includes mid-channel bars and islands, was also measured. The rate of change was computed as the difference between the total width at the beginning of the time period and the total width at the end of the time period, divided by the length of the time period:

$$dW_{tot} = \frac{\Delta W_{tot}}{\Delta t} = \frac{W_{tot-2} - W_{tot-1}}{t_2 - t_1} \text{ , (m/year)}$$

where:

dW_{tot} = rate of change in active channel width (m/year);

t_1 and t_2 = dates of compared aerial surveys (years);

ΔW_{tot} = total change in active channel width between t_1 and t_2 (m);

W_{tot-1} = Active channel width at time t_1 (m);

W_{tot-2} = Active channel width at time t_2 (m); and

$\Delta t = t_2 - t_1$ = length of time period between aerial surveys in years.

A negative value of dW_{tot} indicates a narrowing of the total channel and a positive value indicates a widening of the total channel. Changes in total width could result from changes in active channel width and/or mid-channel bar or island width.

Spatial Variability - The rates of changes in total width at each agg/deg line are presented in Figure 5-12. There is a large negative spike at about 18 km downstream in reach 2 between 1918 and 1935 from greater than 170 meters of narrowing at agg/deg 133. This high rate of narrowing is an example of a transition from a multi-thread channel with a wide island to a narrower single thread configuration. The island was 600 meters wide and the channel in 1935 was only 95 m wide at that point, whereas the active channel in 1918 was 400 m.

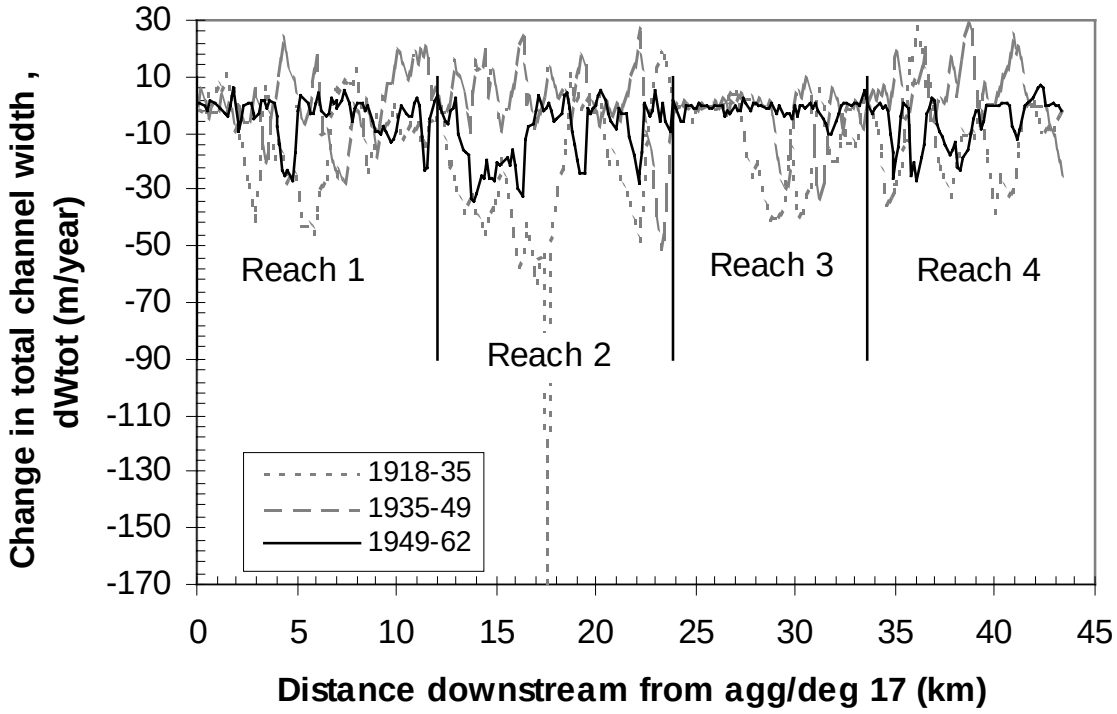

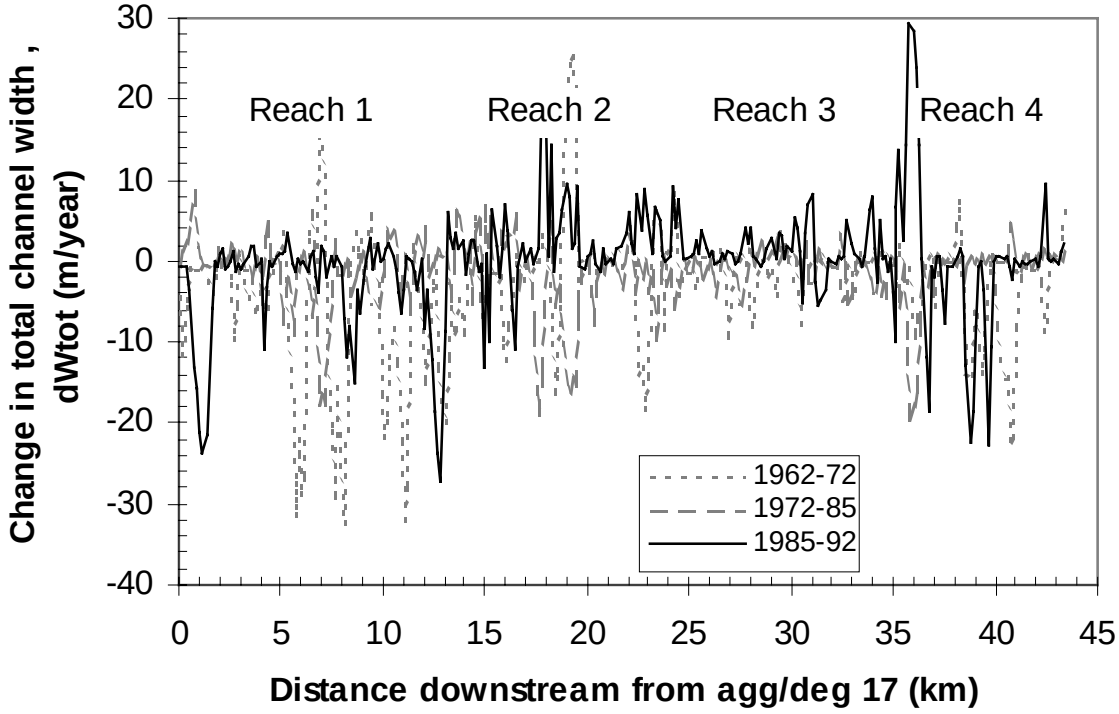

Figure 5-12 - Downstream plots of change in total channel width at each agg/deg line.

Temporal Variability - The histograms of the frequency distributions of the rate of change of total width are presented in Figure 5-13. Similar trends are seen to that for active channel width. More and more lines exhibit less than 5 m/year change in total width with time.

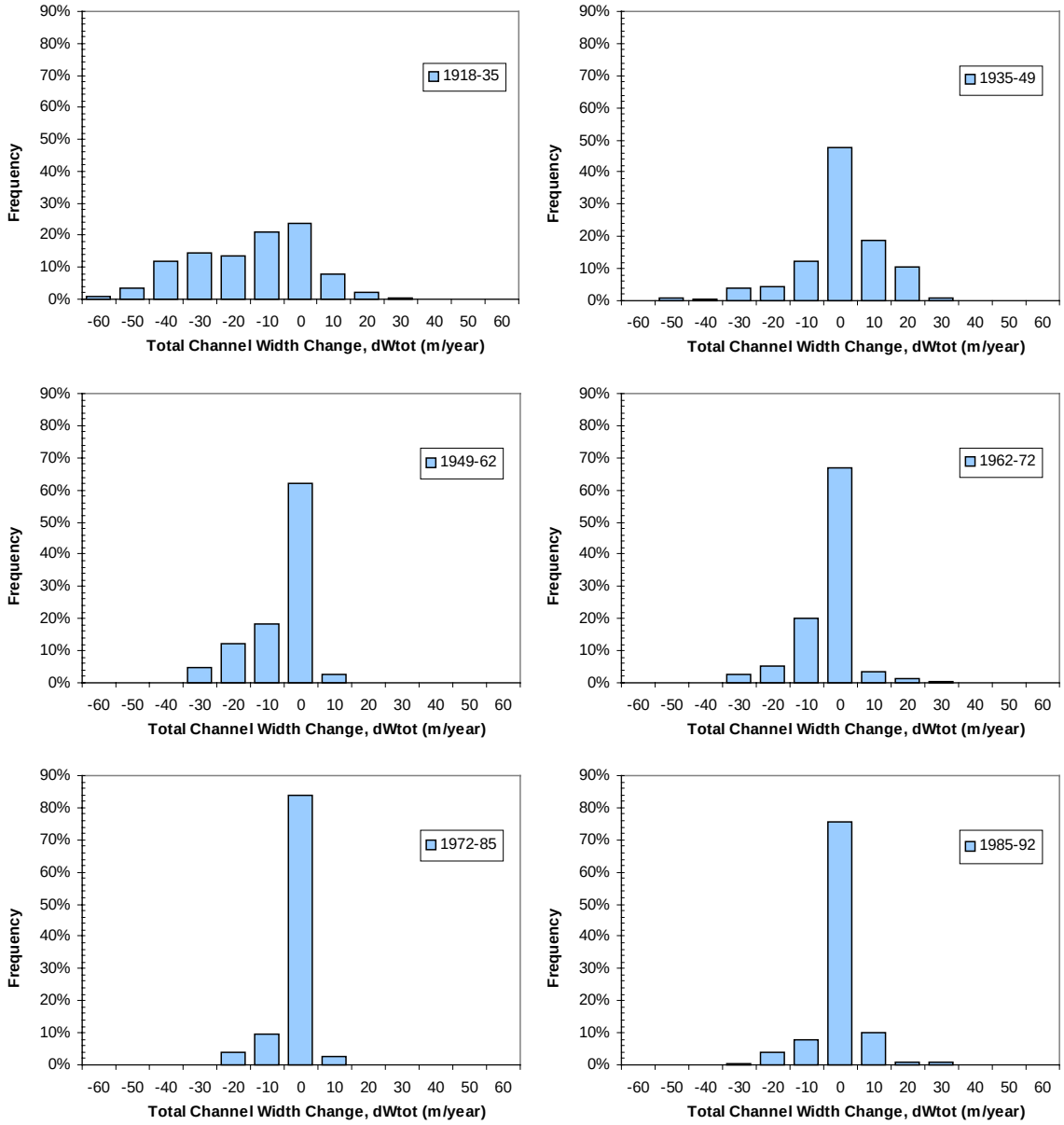

Figure 5-13 - Probability density functions of change in total channel width at agg/deg lines.

Reach averaged - The total width changes were averaged by subreach and by reach. The results of the reach-averaging are presented in Figure 5-14. Between 1985 and 1992 the total channel width of Reach 4 did not change while the active channel width decreased. This demonstrates that the outer banks of the channel did not move on average, while the active channel narrowed through vegetative growth on mid-channel bars. The same phenomenon occurred on Reach 2 between 1918 and 1935.

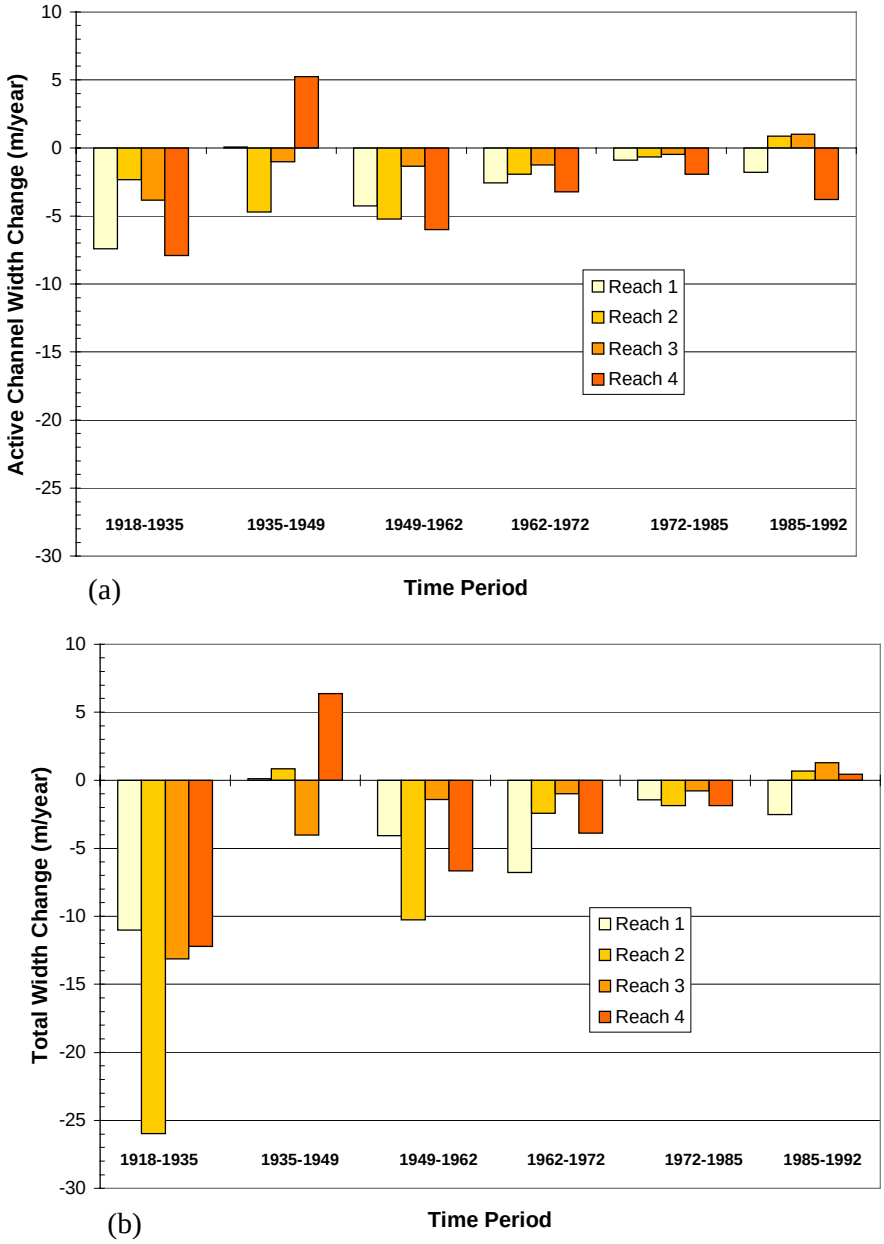

Figure 5-14 - Reach averaged change in channel width (a) change in non-vegetated active channel width, (b) change in total channel width between outer bank lines, including mid-channel bars and islands.

Lateral Migration Rates

The lateral movement rates (*E* and *N*) described above were derived from the total bankline change, which included narrowing or widening of the channel as well as migration. In the interest of comparing the migration rates of the Rio Grande with those on other rivers and for attempting to sort out relationships between the inputs to the channel and the type and rate of resulting movements, the true migration rate, *M*, was computed as follows:

$$M = \frac{\Delta r + \Delta l}{t_2 - t_1} - \frac{W_{tot-2} - W_{tot-1}}{t_2 - t_1} = E - dW_{tot} \text{ , (m/year)}$$

where:

M = Migration rate (m/year);

t_1 and t_2 = dates of compared aerial surveys (years);

W_{tot-1} = Active channel width at time t_1 (m);

W_{tot-2} = Active channel width at time t_2 (m); and

$\Delta t = t_2 - t_1$ = length of time period between aerial surveys in years.

The total width was subtracted because it is the measure of width between the outermost banks of the channel. As with the other lateral movement and width change rates, the true migration was computed at each agg/deg line from the GIS coverages of the active channel. Then, the rates at each line were subreach and reach averaged using distance between lines as weighted factors.

Spatial variability - Migration rates at agg/deg lines are plotted in Figure 5-15. The reach between 24 and 28 km downstream is stable. The rates decrease with time. Reach 4 from 1972 to 1992 exhibited low rates, therefore changes in *N* result from width changes not true migration. The peaks at the downstream ends of reaches 1 and 2 result from the avulsions described above and were therefore not due to changes in width. The rate of migration in reach 4 after 1962 was lower than the other reaches.

There is less variability and fewer peaks in the plots of M than in the other measures of lateral movement. The decreased variability demonstrates that much of the fluctuation in *E* and *N* was actually changes in width, not true migration of the channel.

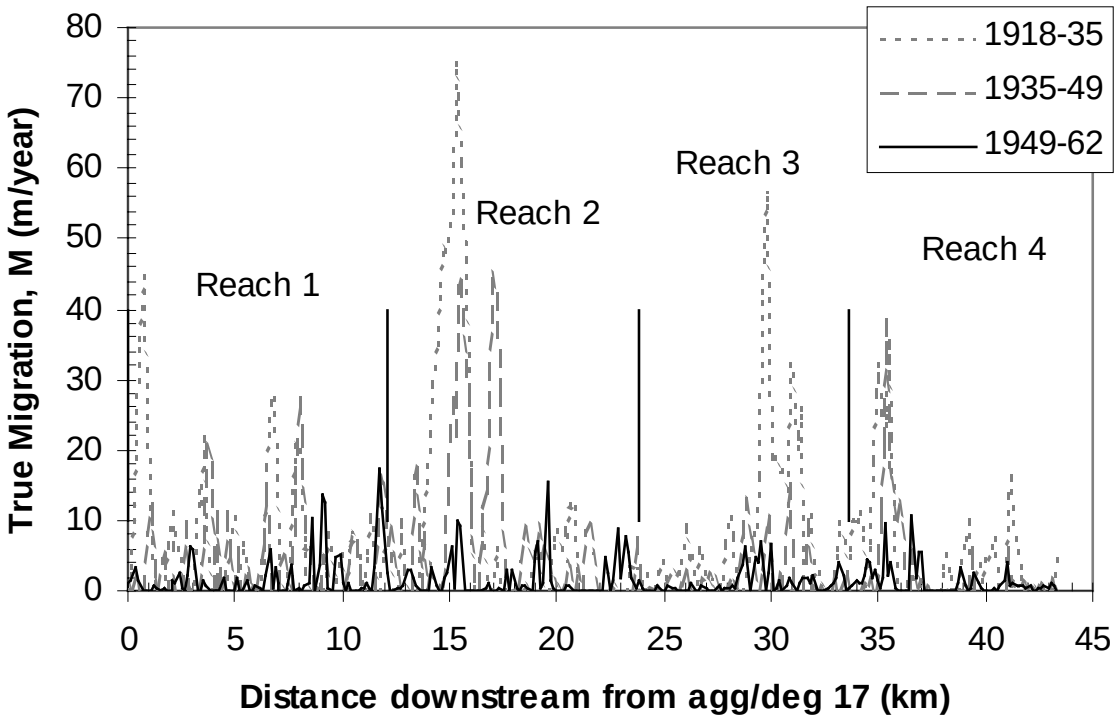

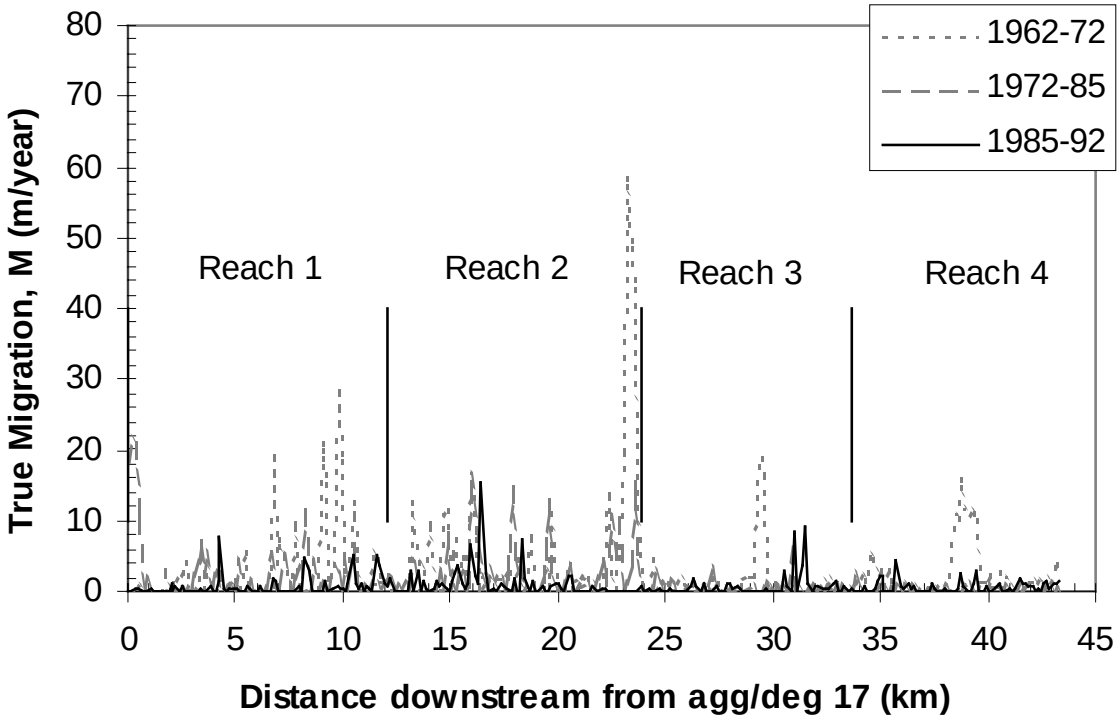

Figure 5-15 - True migration rate, M measured at each agg/deg line.

Temporal variability - Histograms of frequency distributions are plotted in Figure 5-16. The frequency distributions of *M* are skewed for all time periods. Greater proportions of the lines exhibited low migration rates through the entire study period.

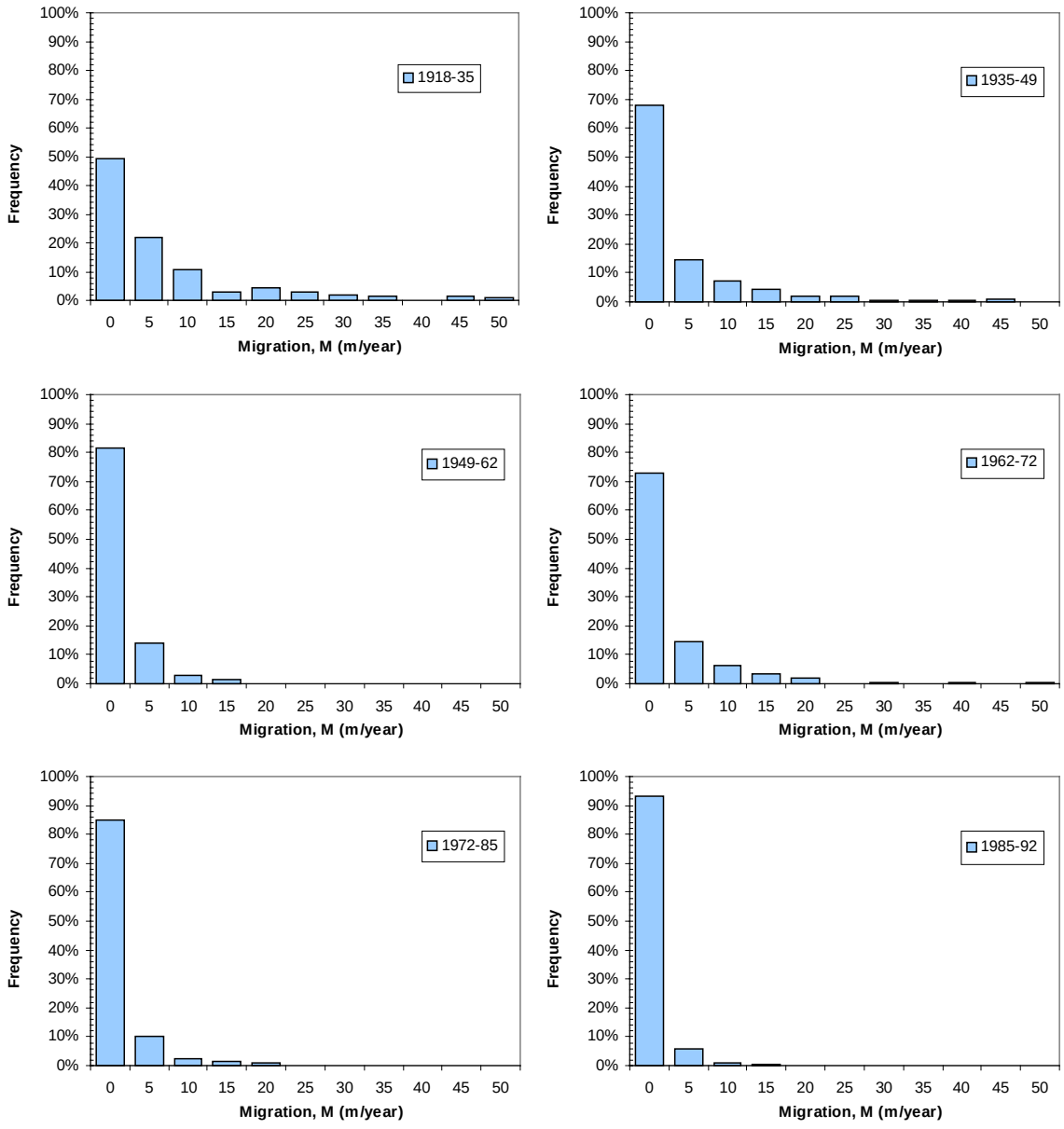

Figure 5-16 - Histograms of frequency of occurrence of migration rate at all the agg/deg lines.

Reach averaged – Reach averaged migration rates peaked during the 1962-72 period as a result of the avulsion/channel abandonment described above. Reach 2 exhibited the highest rates of true migration for the entire time period, except between 1949 and 1962. The migration rates for reaches 3 and 4 increased between 1985 and 1992. These reaches also exhibited the lowest migration rates through the whole time period. By 1992, all reaches migrated at a rate less than 2 m/year.

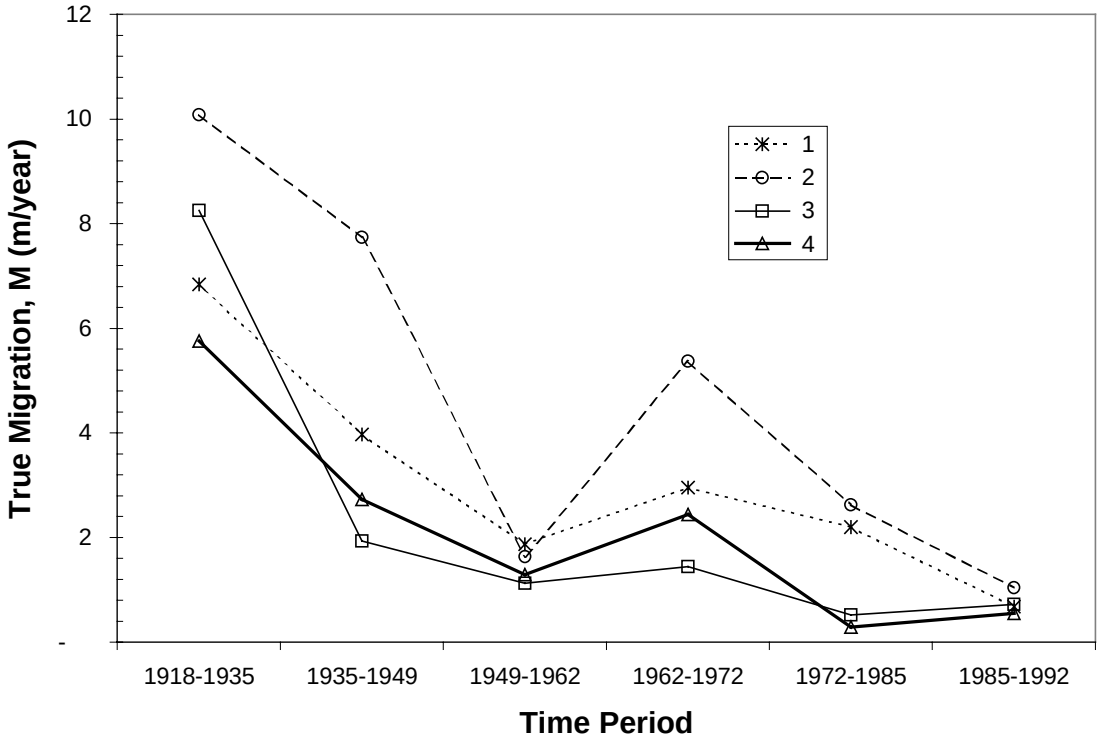

Figure 5-17 - Time series of true migration rate, *M*

5.1.2 Lateral Stability

The lateral stability of the channel was quantified by measuring the changes in the non-vegetated active channel area with time. First the total channel area was computed for the reaches and subreaches for each aerial survey. Then coverages were overlain and the area of unchanged active channel area from one survey to the next was measured. Dividing this area by the active channel area at the beginning of the time period results in the lateral stability index.

Change in Active Channel Area

The planview non-vegetated active channel area was measured from the GIS coverages. Subreach and reach areas were measured for each survey available.

Figure 5-18 is a time series of the active channel area for the reaches. As expected, the total active channel area for the entire reach declined over the study period. This is consistent with the narrowing trend seen in the time series of active channel width. Between 1935 and 1949, the areas of subreaches 1 and 4 increased. The increase may be a result of the high floods during the early 1940's that may have kept the channel area larger rather than continued the high rate of decrease prior to 1935 and after 1949. The areas of reaches 2 and 3 both increased between 1985 and 1992. The active channel widths of reaches 2 and 3 increased between 1985 and 1992.

In order to compare changes between reaches of different area, the reach area for each survey was divided by the area in 1918. These normalized channel areas are plotted in Figure 5-19. Reach 1 decreased the most, to only 24% of the original 1918 area.

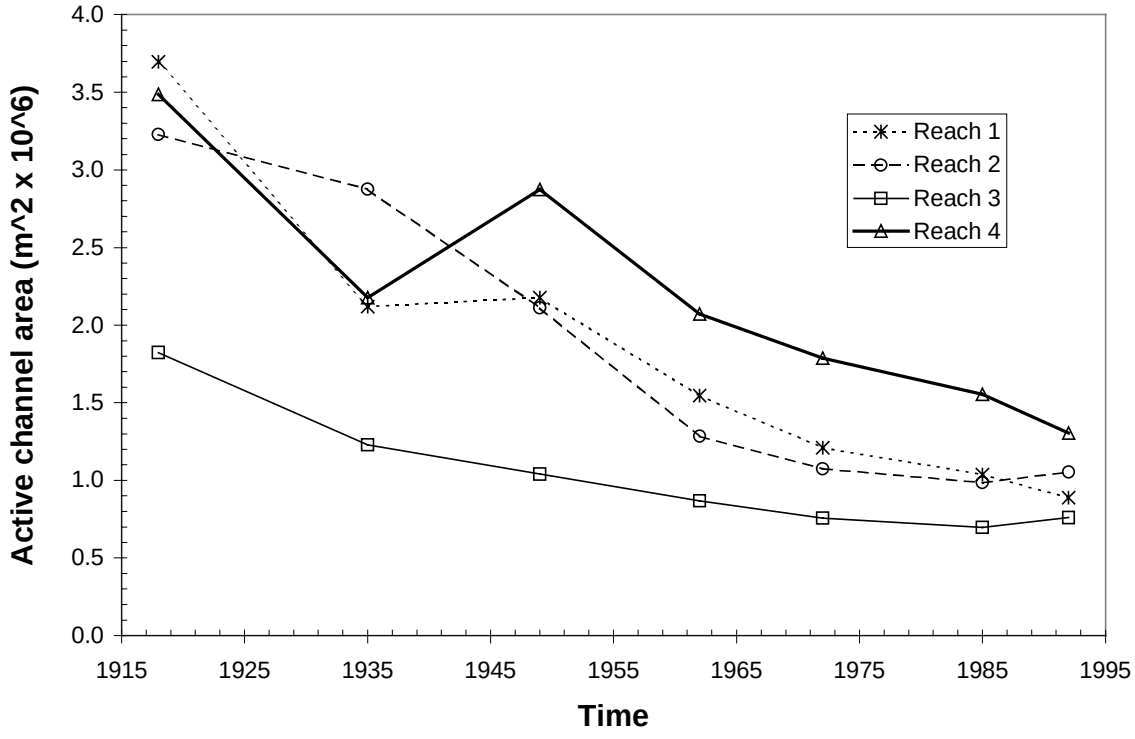

Figure 5-18 - Time series of active channel area, measured from digitized aerial photos as the non-vegetated channel area.

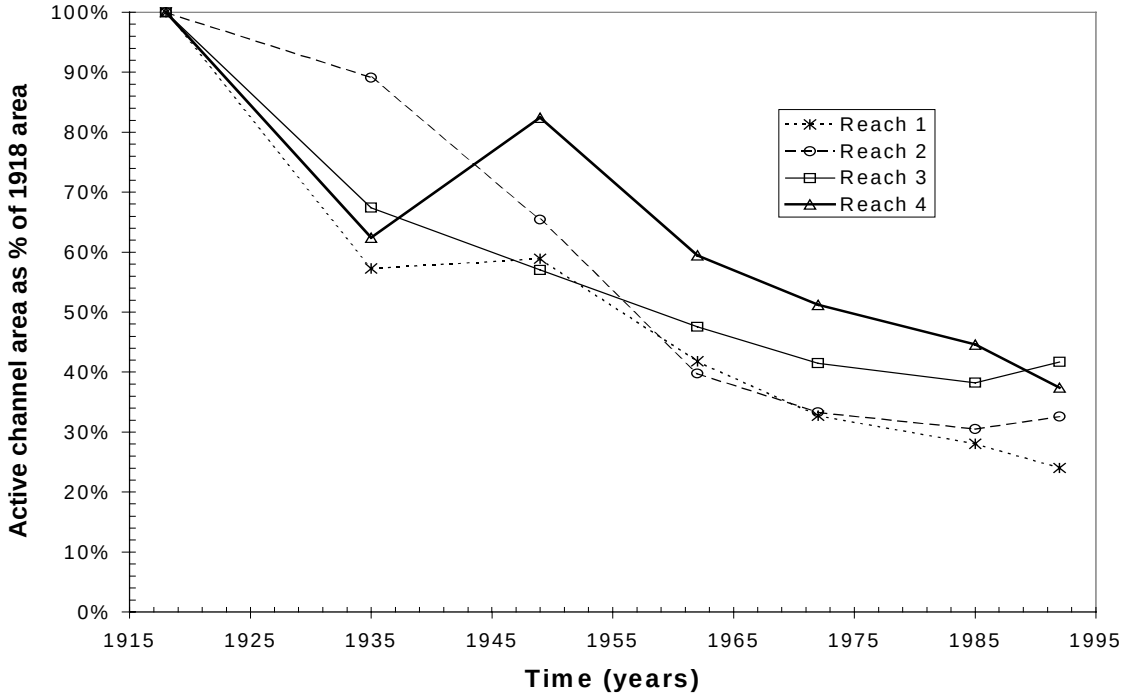

Figure 5-19 - Active channel area normalized by the active channel area in 1918.

Normalized active channel measurements were also made for the subreaches. The results are shown in Figure 5-20 and Figure 5-21. The subreaches identified as being more mobile (1.4, 1.8, 1.9, 2.2, 2.3, 2.6) all exhibit consistent decreases in active channel area to values that are less than or approximately 40% of the original channel area. These subreaches are all located more than 1 km downstream from a tributary and in unconfined portions of the valley. The subreaches that were less mobile (3.1, 3.2 and 3.5) achieve an area of about 60% of the original active channel area. The less mobile subreaches are either geologically confined or impacted by a manmade structure (Angostura diversion dam). Another pattern becomes evident from these plots. Subreaches 1.2, 2.1, 2.4 and 4.2 are all directly below the mouths of major tributaries and exhibit increases in channel area at some point in the study period.

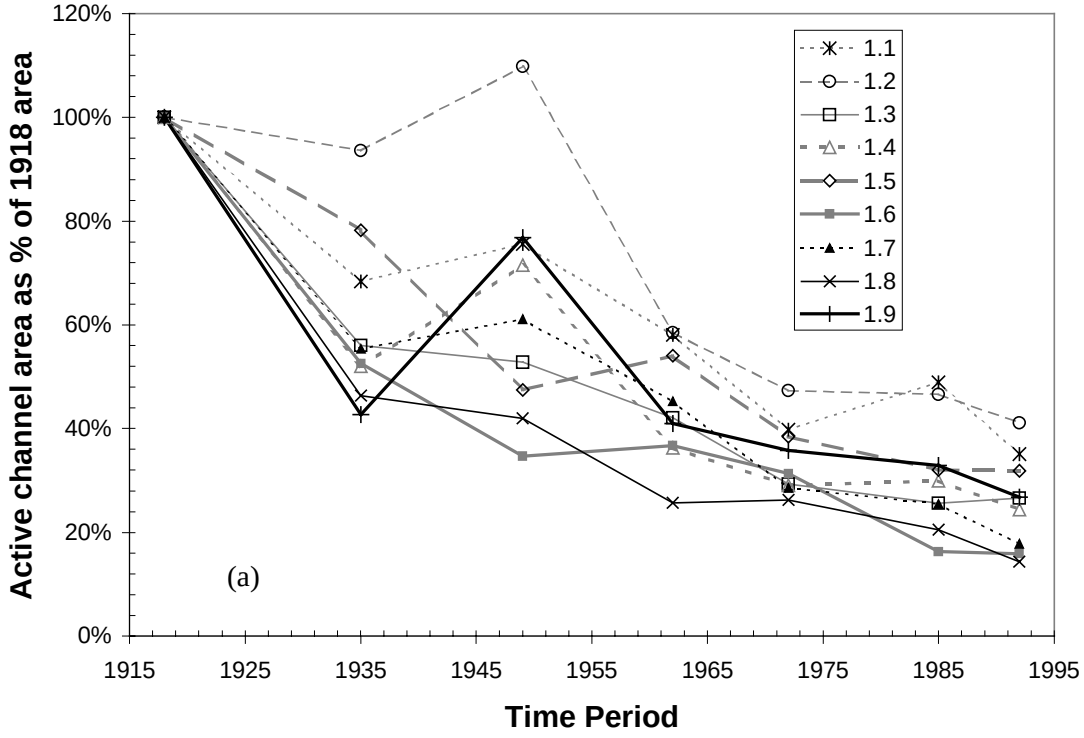

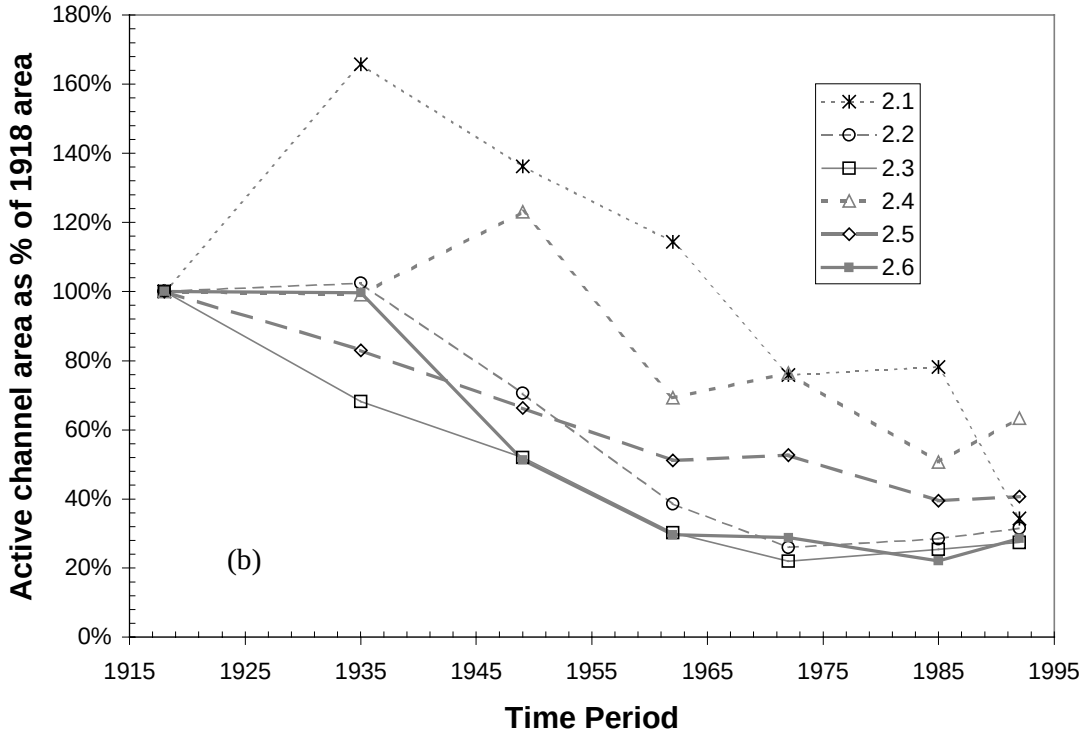

Figure 5-20 - Active channel area of subreaches normalized by the area in 1918 (a) Reach 1, (b) Reach 2.

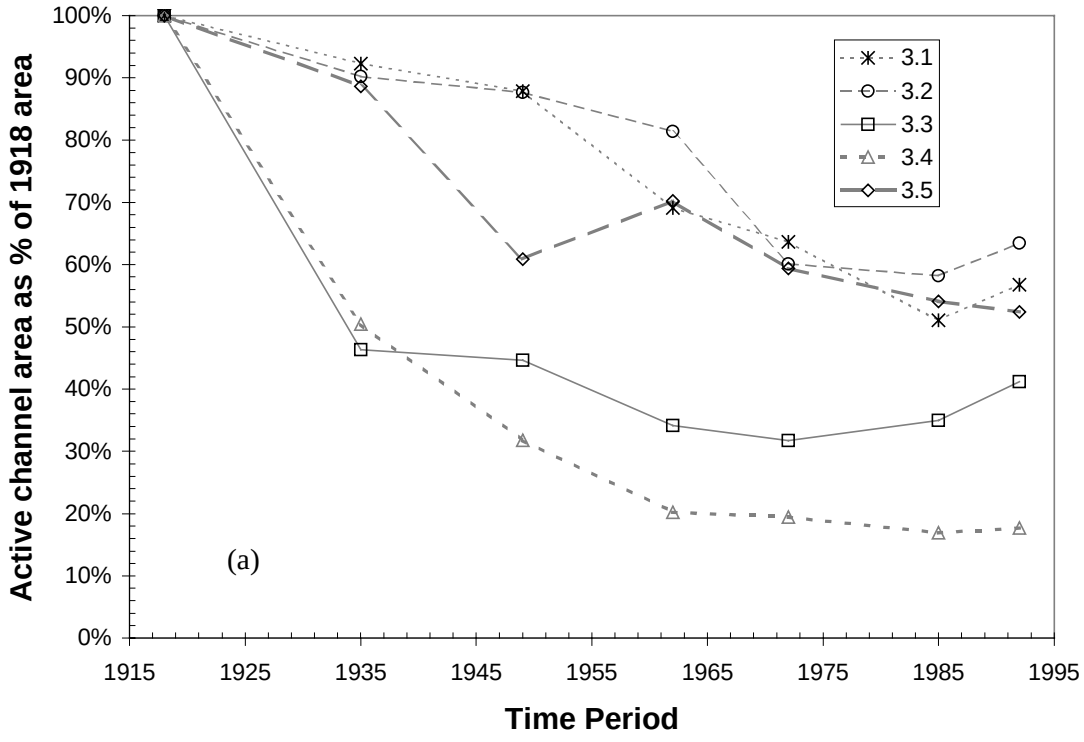

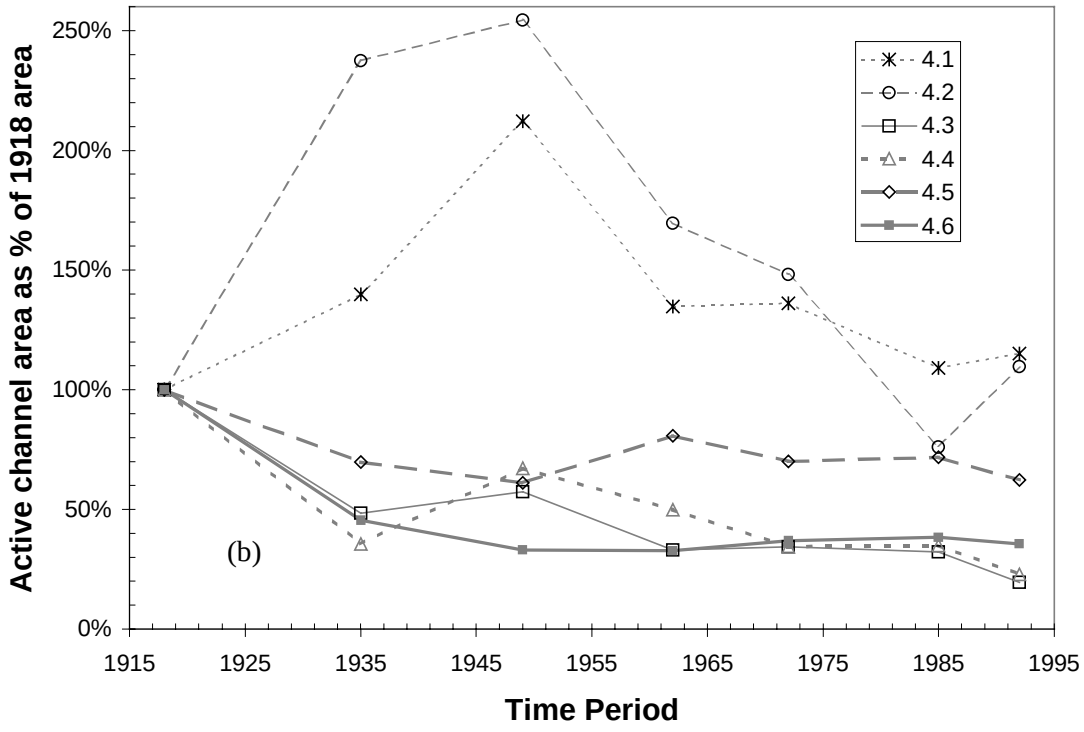

Figure 5-21 - Active channel area of subreaches normalized by the area in 1918 (a) Reach 3, (b) Reach 4.

Lateral Stability Index

Using the overlay coverages of different years, the percentage of the "active channel" that remained in the area of the old active channel was measured, as illustrated in Figure 5-22:

$$\text{Lateral Stability Index} = \frac{\text{Unchanged Active Channel Area}}{\text{Previous Active Channel Area}}.$$

A value close to one indicates that the channel has not moved and is relatively stable. Small values of the index indicate that the channel has moved from its location at the beginning of the time period.

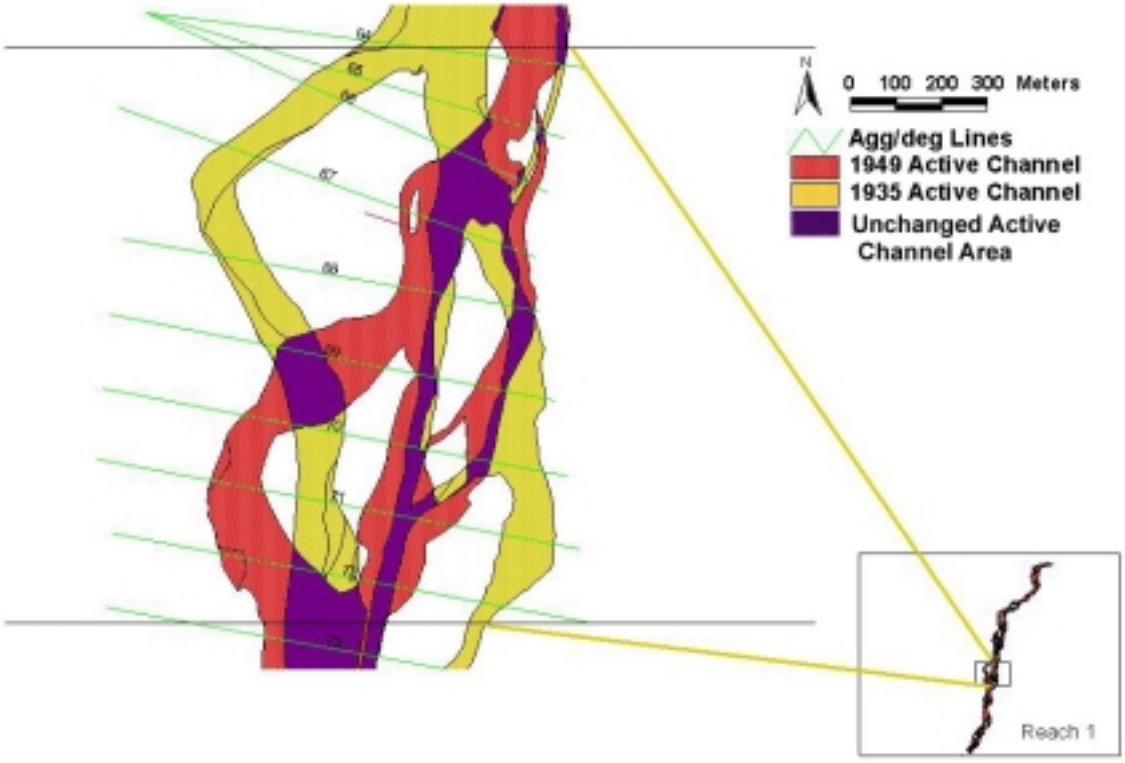

Figure 5-22 - Lateral stability index = Unchanged active channel area/previous active channel area.

Figure 5-23 shows the values of the lateral stability index for the entire time period for the four reaches. The increasing trend in this index shows the increasing level of lateral stability of the river. This could be considered a relative indication of the degree of lateral stability. A value of one indicates that the channel did not move at all.

The trend is toward increasing stability in all reaches through the entire study period, except for reach 4 from 1985 to 1992. Study of the 1985 and 1992 aerial photos reveals that simplification of the channel and a move from multi to single thread channel occurred during this period in reach 4. The result is an increase in vegetative growth on mid-channel bars and islands,

therefore abandonment of areas that were formerly part of the active channel. Incision of the channel bed makes it impossible for even the highest flows from Cochiti dam to flood these now abandoned areas.

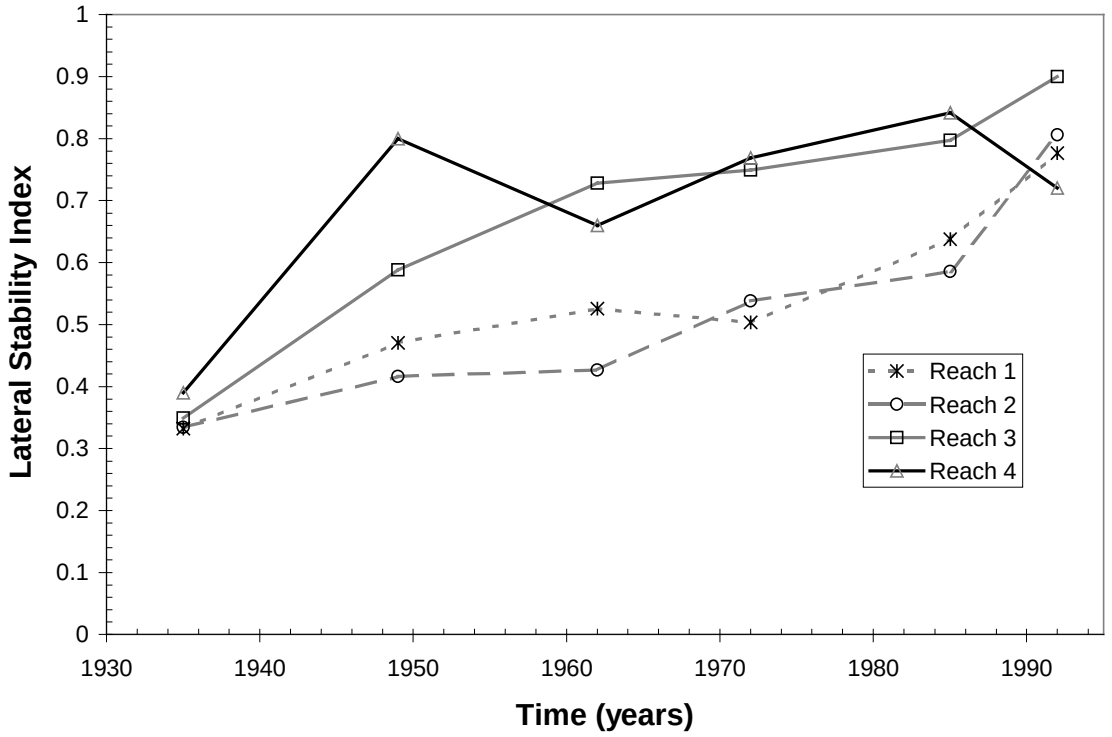

Figure 5-23 - Lateral stability index - Time series of the area of active channel that remained unchanged since the last aerial photo. It is expressed as a percentage of the previous total active channel area.

5.1.3 Summary and Discussion

The lateral stability and mobility indices utilized in this study provide important insights into where, when and how the channel moved laterally. Combined with the analysis in Chapters 3 and 4, a complete picture of the channel adjustments of the Rio Grande since 1918 begins to emerge.

The analysis of the spatial variability in the lateral mobility indices indicates that tributary inputs and geologic setting may have significant influence on how and where the channel moves laterally. High mobility measured by the total bankline change rate, *E*, and the normalized lateral movement rate, *N*, was always associated with high variability in width change and not necessarily with true migration. The least mobile reaches were either confined by geologic features or by manmade structures (Angostura diversion dam). Temporal trends in mobility demonstrate that the channel became less mobile with time since 1918.

The lateral stability indices computed from active channel areas suggest that the more mobile reaches underwent greater adjustment before attaining a "stable" configuration. The reaches that were initially less mobile did not have to adjust as much to attain a stable configuration. Also the subreaches directly downstream from tributaries exhibit wide fluctuations in channel area, including increases in channel area at some point in the study period. These changes are illustrated in Figure 5-24, which groups the subreach active channel area plot by degree of mobility and tributary influence. The tributaries that appear to influence the lateral response of these subreaches are the Santa Fe River (pre-Cochiti dam), Borrego Canyon, Galisteo Creek and the Jemez River. The subreach just downstream of Angostura diversion dam also exhibits similar behavior and is included in this grouping. Las Huertes Creek enters the main stem just downstream of Angostura, so it is difficult to determine if the measured response is associated with the dam or the tributary.

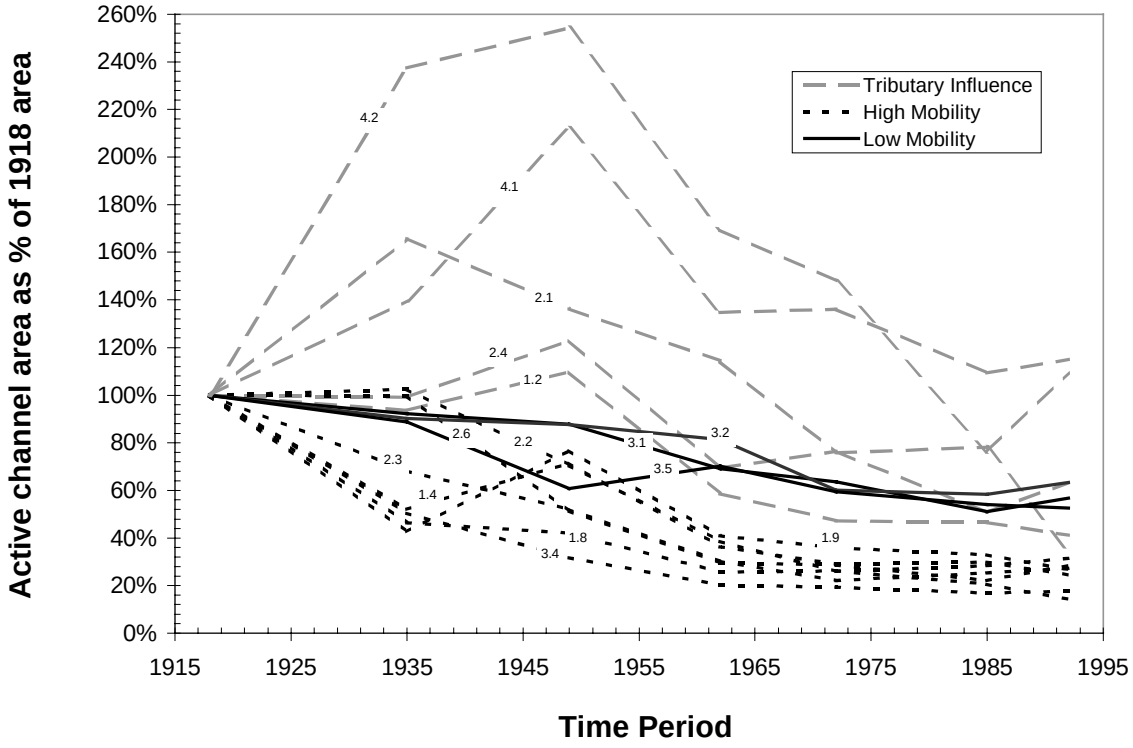

Figure 5-24 - Change in active channel area of the subreaches that exhibit either high or low mobility or tributary influence. The subreach number is given on the line.

The reaches associated with tributary mouths also exhibit large variability in width and not necessarily large migration rates, *M*. True migration rates seem to increase further downstream from tributaries where the channel is not confined.

Based on the indices presented in this chapter, it appears that the lateral mobility of the Cochiti reach has decreased with time since 1918 and that the lateral stability has increased. Also, the rate of change of the indices has decreased with time since 1918 indicating that there may be a relationship between how far away a river is from its dynamic equilibrium state and the rate of change of the channel. Using this underlying premise to model and predict lateral mobility is the focus of Chapter 6. With the measured lateral movement rates from this chapter and the other parameters from Chapters 3 and 4, the next step is to find associations between movement rates and other parameters in an attempt to model the historic changes in the channel with the intention of predicting future lateral mobility.

CHAPTER 6

LATERAL MOBILITY/STABILITY MODELS

As seen in Chapter 5, the Cochiti reach exhibits both spatial and temporal variability in lateral movement rates. This chapter presents three models to describe the variability in lateral movement rates of the Cochiti reach, measured by lateral migration (M) and width change (dW_{act}). All three models were calibrated using 1918 to 1985 data. The 1985 to 1992 data were reserved for validation as discussed in Chapter 7. The first model was a simple estimation of movement rates as a percentage of channel width. The second model was based on the premise proposed in Chapter 5 that the further a river is from a state of dynamic equilibrium, the more mobile it is. The third model explored associations of lateral mobility rates with discharge, slope, sediment supply, width, bed material, sinuosity, and other measures of channel form via multiple regression analysis.

Successful and sustainable management of the river corridor requires an understanding of which areas are more susceptible to adjustments resulting from changes in the input regime and which areas are not. This chapter is an attempt to understand the underlying differences along the reach that may contribute to variability in lateral response to altered inputs. Comprehending these differences is important to river managers from both ecological and engineering viewpoints. Habitat restoration efforts often require a laterally mobile channel whereas engineering management attempts to reduce risk to riverside structures and communities through a laterally stable channel. Knowledge of what makes a reach more or less mobile will help produce better management solutions for both objectives. The preceding two chapters have provided the basis from which to undertake an analysis of the relationships between lateral movement and channel form and processes. Understanding these relationships is important in understanding the river environment and may have value in predicting channel adjustment and lateral movement (Hooke 1986).

6.1 Simplified Model

Other studies have shown relationships between lateral movement and channel width (Hooke 1979; Brice 1982; MacDonald 1991). Brice (1982) proposed a line on a width vs. migration plot to separate stable from unstable rivers and suggested that the slope of 0.01 was appropriate. This line corresponds to migration rates that are 1% of channel width. It is interesting that his data points fall reasonably along this line, suggesting that a simple approximation of migration rate based on a flat percentage of channel width could provide a useful "first-order" model of lateral movement.

The methodology used is as follows:

1) Compute average rate of movement per unit width by dividing the movement rate (either M or dW_{act}) by the channel width at each cross-section then reach averaging.

2) Apply this percentage rate to the reach averaged width for each reach for each survey date to estimate the movement rate (M or dW_{act}).

3) Compare the estimated reach-averaged movement rate with the measured movement rate.

Using the 1918-85 Cochiti reach data, when the migration rate at each cross-section line is divided by the active channel width at that line and then reach averaged, the average migration rate is 1% of channel width per year. The migration rate computed from the average bankline change, M_{avg}, was used because it is more comparable to the method of measurement for migration rates on meandering rivers in other studies,

$$M_{avg} = \frac{M}{2} = \left(\frac{(\Delta r + \Delta l - dW_{act})/t}{2} \right) \quad \text{.....(6-1)}$$

Based on this average rate, the migration rates for the reaches were modeled using the following equation:

$$M_{pred} = 0.01 \cdot W_{act} \quad \text{.....(6-2)}$$

where W_{act} is the active channel width at the beginning of the time period.

The predicted rates for each reach produced an average error [$(M_{pred} - M_{avg})/M_{avg}$] of 122%. The results are plotted in Figure 6-1 and show the inaccuracies of using channel width as the sole predictor of lateral migration. The pre-dam migration rates are greater than 1% of channel width and the post-dam are less than 1%.

To illustrate the variability in migration rates of the Cochiti reach, the reach and subreach migration rate data (average migration rate = $M/2 = M_{avg}$) were plotted in relation to active channel width at the beginning of each time period (Figure 6-2, a and b). The average migration rate data from the Cochiti reach do not fall closely along the $M = 0.01W$ line (Figure 6-2a) and it is apparent that there is more variability in the migration rate data than can be predicted by channel width alone. Obviously, the relationship between width and lateral movement changes with the degree of stability of the channel, quantified by Brice in the form of stream type (Figure 2-1). The subreach data (Figure 6-2b) plot mostly between 0.1% and 5% of the width.

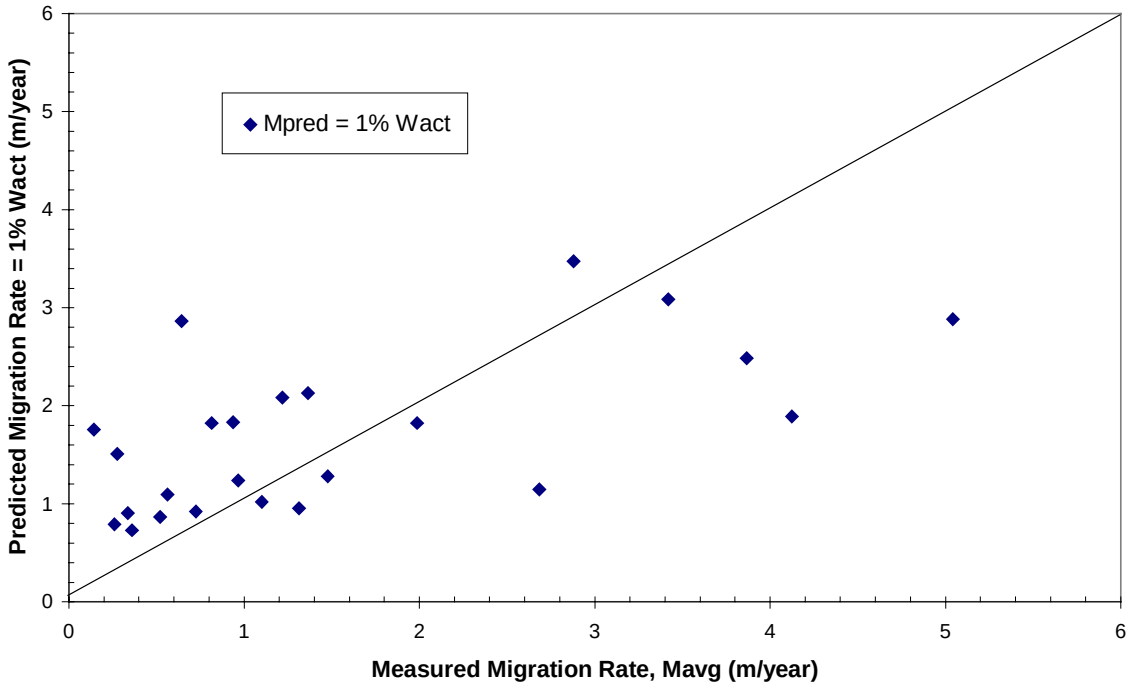

Figure 6-1 - Comparison of predicted migration rates vs. measured. The line represents perfect agreement.

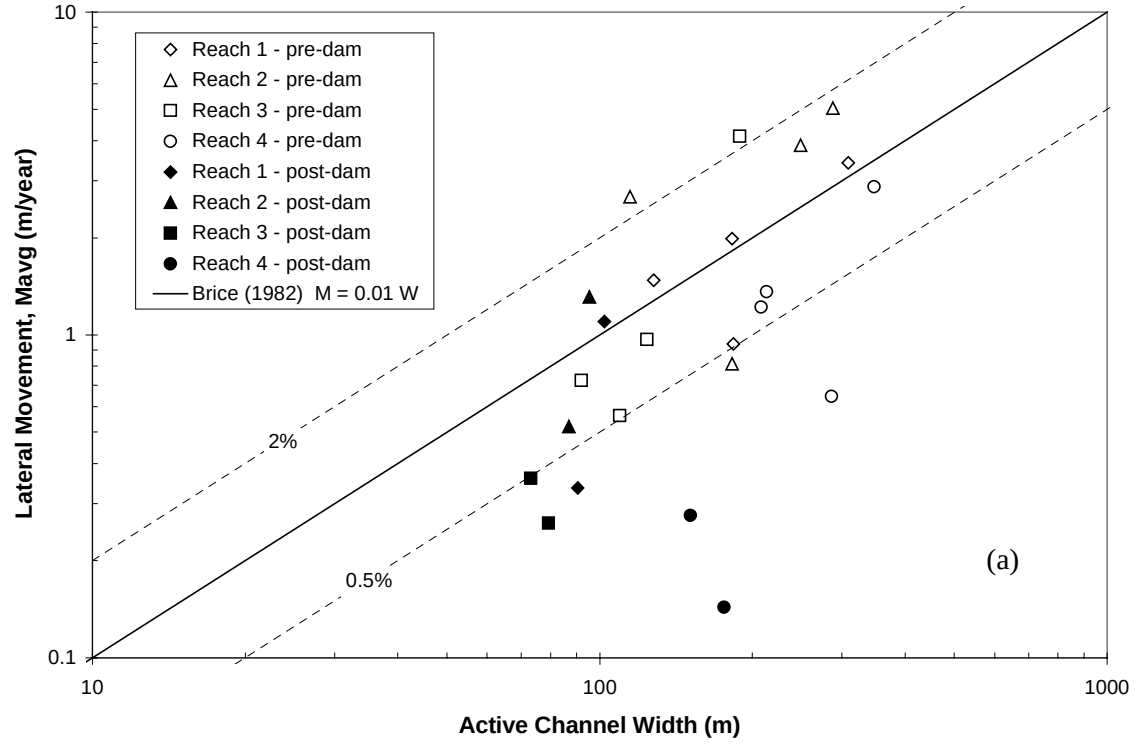

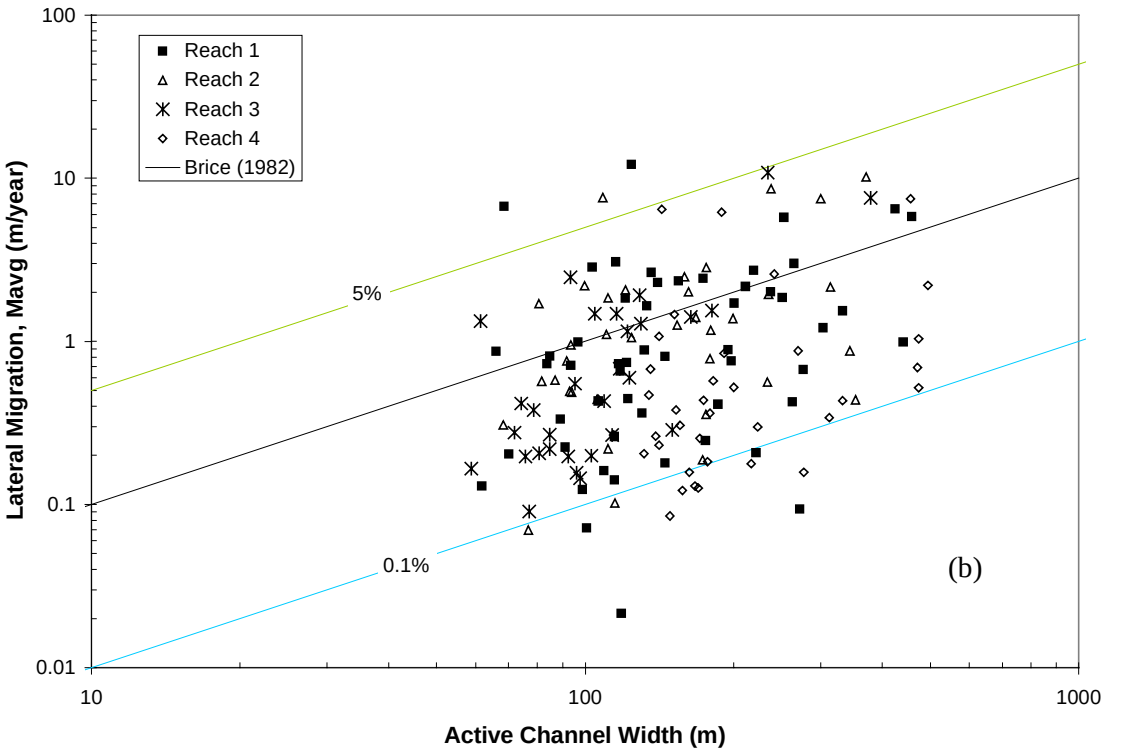

Figure 6-2 - Plots of active channel width vs. migration rate for (a) reach averaged data and (b) subreach averaged data.

The change in the active channel width was modeled in a similar manner. The weighted-reach-average of the change in active channel width (dW_{act}) divided by the active channel width resulting in an average width change rate of 2.1% of channel width per year for the 1918-85 period. This value was used to predict width change rates:

$$dW_{pred} = 0.021 \cdot W_{act} \quad \text{.....(6-3)}$$

where W_{act} is the active channel width at the beginning of the time period. The resulting comparison between predicted and measured width change rates is presented in Figure 6-3. The resulting fit was much better than for migration rate over the full range of measured rates. The lower rates (< 4 m/year) were over-predicted. The average error [$(dW_{pred} - dW_{meas})/dW_{meas}$] was 360%. Also, this model only predicted the absolute value of the channel width change and says nothing about whether the channel is widening or narrowing.

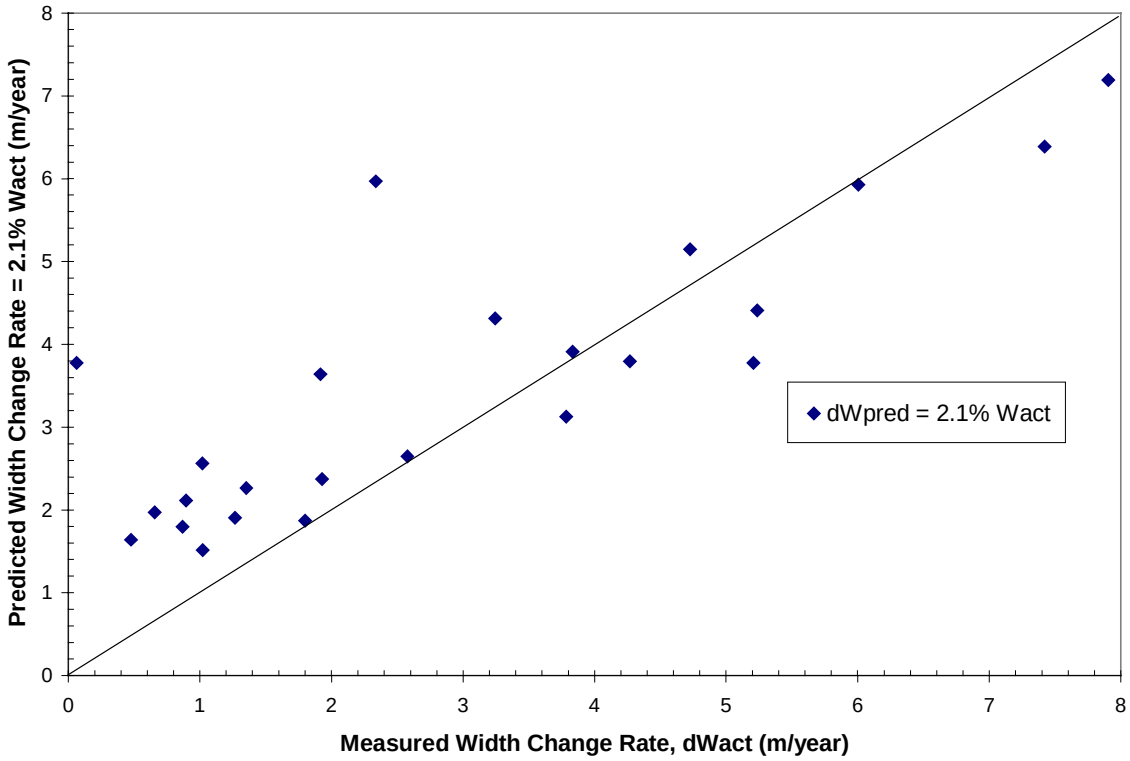

Figure 6-3 - Comparison of predicted vs. measured width change rates. The line indicates perfect agreement.

A simple estimation of width change based solely on width forces the rate of change to go to zero as the width goes to zero. This is contrary to equilibrium theory, which suggests that there is a stable or equilibrium width (non-zero) that the channel will maintain given constant input conditions. The imperfect fit of the Cochiti reach data to this simple model suggests that the rate

of change of channel width may be variable depending on how far the channel is from this stable configuration. The indices presented in Chapter 5 showed that the rate of lateral channel change decreased with time as the channel moved toward a more stable configuration. A model that employs this concept is presented in the following section.

6.2 Exponential Model

It was shown in Chapter 4 that the channel width appears to be moving toward a stable or equilibrium configuration as predicted by hydraulic geometry equations. Additionally, in Chapter 5, the rate of lateral channel change appeared to decrease with time as the channel stabilized. The following section describes models of width change and lateral migration rates based on how far away the channel form is from equilibrium rather than solely as a function of time, as in Williams and Wolman's (1984) hyperbolic model. The further the channel is from an equilibrium state, the more mobile it is and the more rapid the lateral changes. Equilibrium channel form is measured using the equilibrium width of the channel.

Width change

An exponential function (Figure 6-4) was selected to fit the width change and lateral migration rate data from the Cochiti reach. The hypothesis is that the magnitude of the slope of the width vs. time curve increases with deviation from the equilibrium width, W_e:

$$\frac{\Delta W}{\Delta t} = -k_1\left(W - W_e\right) \quad \text{.....(6-4)}$$

where:

ΔW = change in active channel width (m), during time period Δt; and

Δt = time period (years).

Differentializing equation (6-4) results in the following:

$$\frac{dW}{dt} = -k_1\left(W - W_e\right) \quad \text{.....(6-5)}$$

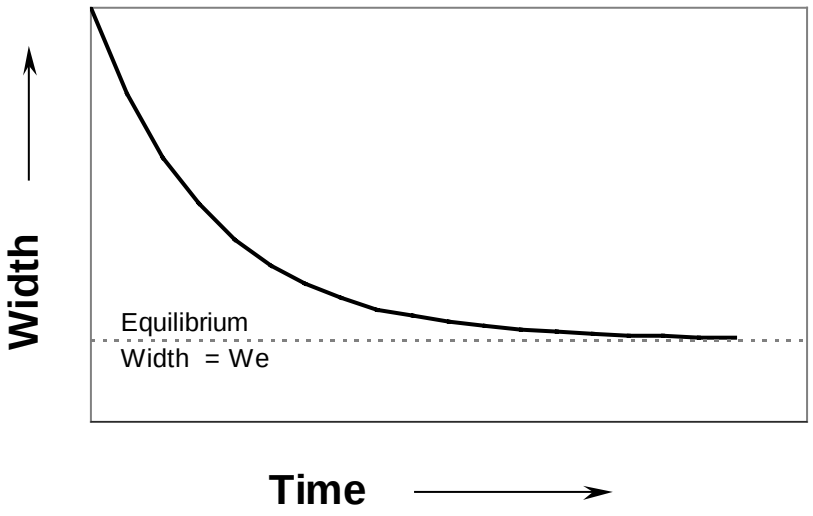

Figure 6-4 - Schematic of exponential channel width changes with time.

Rearranging and integrating equation 6-5:

$$\int_{W_o}^{W} \frac{dW}{(W - W_e)} = \int_{0}^{t} -k_1 dt$$

$$ln(W - W_e)\Big|_{W_0}^{W} = -k_1 t\Big|_0^t$$

$$\ln(W - W_e) - \ln(W_o - W_e) = -k_1 t + 0$$

$$\ln\left(\frac{W - W_e}{W_o - W_e}\right) = -k_1 t \qquad \text{.....(6-6)}$$

$$\left(\frac{W - W_e}{W_o - W_e}\right) = e^{-k_1 t}$$

$$W - W_e = (W_o - W_e) \cdot e^{-k_1 t}$$

The result is an exponential function (as shown in Figure 6-4):

$$W = W_e + (W_o - W_e) \cdot e^{-k_1 t} \qquad \text{.....(6-7)}$$

where:

k_1 = rate constant;

W_e = Equilibrium width toward which channel is moving;

W_o = Channel width at time, t_o; and

W = Channel width at time, t.

Plotting the width change rate vs. the width (Equation 6-5), the rate constant k_1 and the equilibrium width W_e can both be determined empirically from a regression line. The rate constant, k_1, is the slope of the regression line and the intercept is $k_1 W_e$.

Given the abundance of data on the Cochiti reach and the different possibilities for representing it, there were several options for estimating values for k_1 and *We*. Data at individual cross-sections, subreach averaged or reach-averaged width and width change values can be used. Also, the positive width change measurements indicating that the channel widened could be excluded. Three methods were selected for comparison:

1. subreach averaged data (Figure 6-5),
2. reach averaged data, and
3. reach averaged narrowing only data.

The results of the regressions are summarized in

Table 6-1. To determine which method best fit the historic data, the empirically determined k_1 and W_e were input into Equation 6-8 to model the width for each reach as a function of time from 1918 to 1985. The sum-squared error (SSE) between the predicted and observed reach-averaged active channel width was computed for each model.

The results from the equations producing the smallest SSE are plotted in Figure 6-6 and Figure 6-7. The regression results using the reach-averaged data (method 2) produced the best fit to the individual reach data (Figure 6-6) despite the higher r-square values for the regression with the reach-averaged, narrowing only data (method 3). Method 3 produced a negative value for the equilibrium width for reach 2. A similar selection method was used for the entire Cochiti reach. Method 3 produced the best fit for the entire Cochiti reach as shown in Figure 6-7.

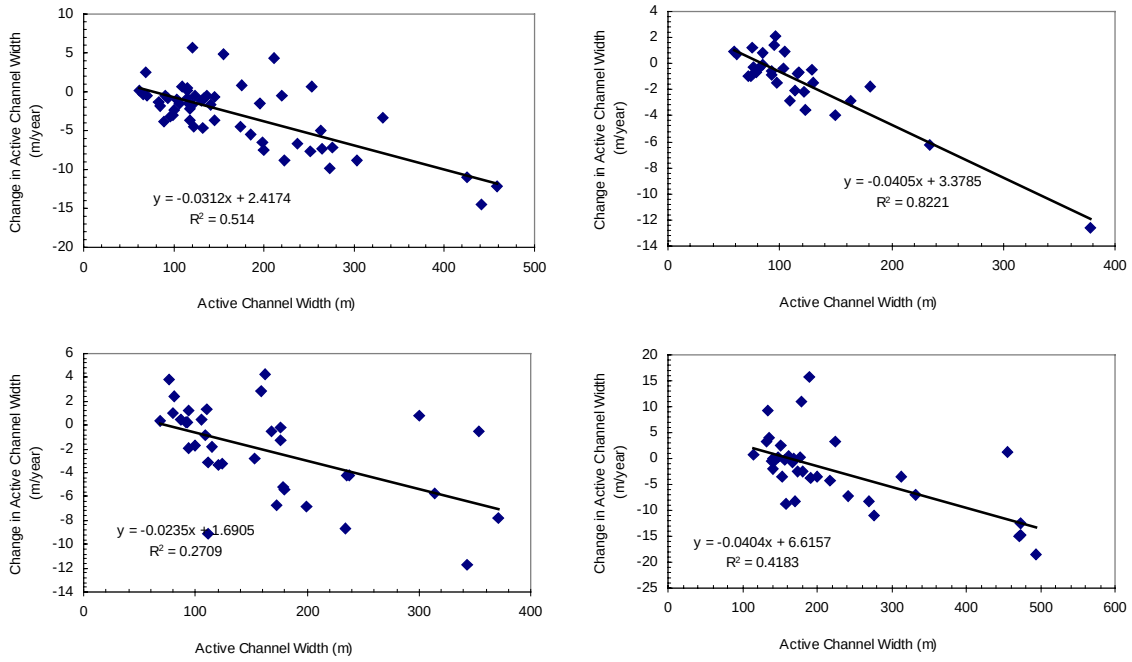

Figure 6-5 - Linear regression results of subreach-averaged data - observed width change (m/year) with observed active channel width (m).

Table 6-1 - Empirical estimation of k_1 and W_e from linear regressions of width vs. width change data.

Method 1 - Subreach averaged data				
Reach #	k_1	k_1W_e	W_e	**r-sq**
1	0.0312	2.4174	77	0.51
2	0.0235	1.6905	72	0.27
3	0.0405	3.3785	83	0.82
4	0.0404	6.6157	164	0.42
Method 2 - Reach Averaged Data				
Reach #	k_1	k_1W_e	W_e	**r-sq**
1	0.0262	1.5342	59	0.61
2	0.0178	0.6802	38	0.42
3	0.0341	2.6345	77	0.85
4	0.0326	4.5688	140	0.28
Method 3 - Reach Averaged Data - narrowing only				
Reach #	k_1	k_1W_e	W_e	**r-sq**
1	0.0283	1.2083	42.7	0.96
2	0.0116	-0.816	-70.3	0.25
3	0.0286	1.8086	63.2	0.89
4	0.0266	1.6564	62.3	0.83

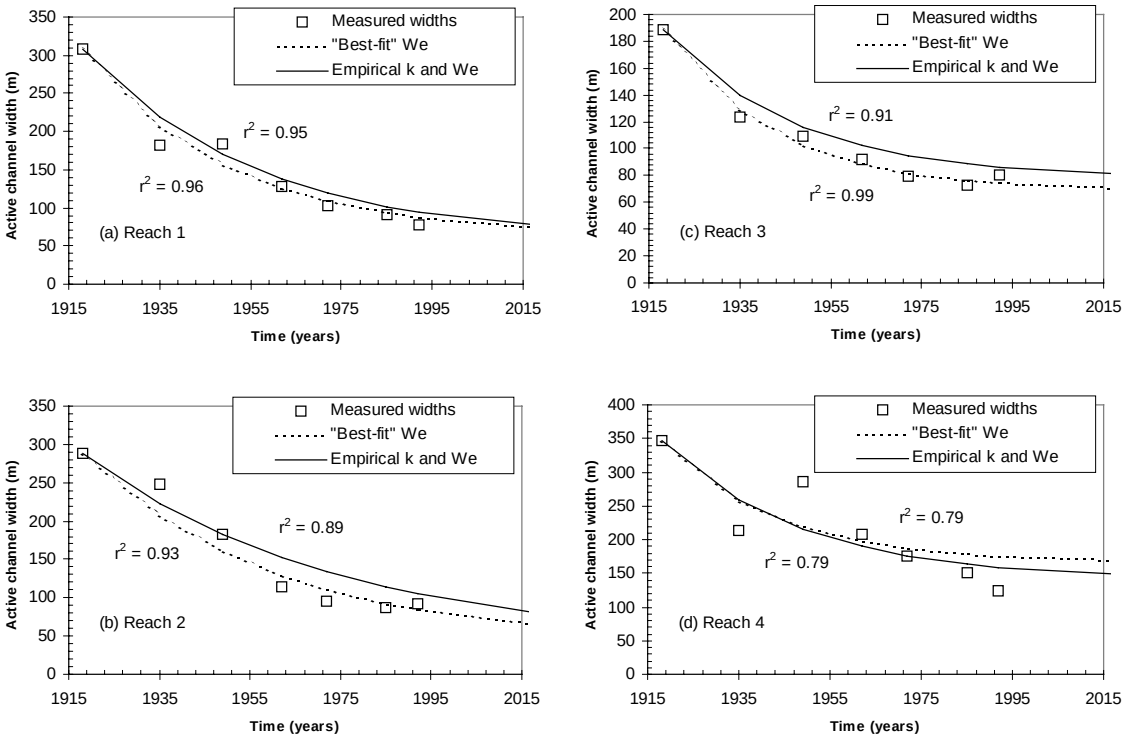

Figure 6-6 - Exponential models of width change applied to the reaches.

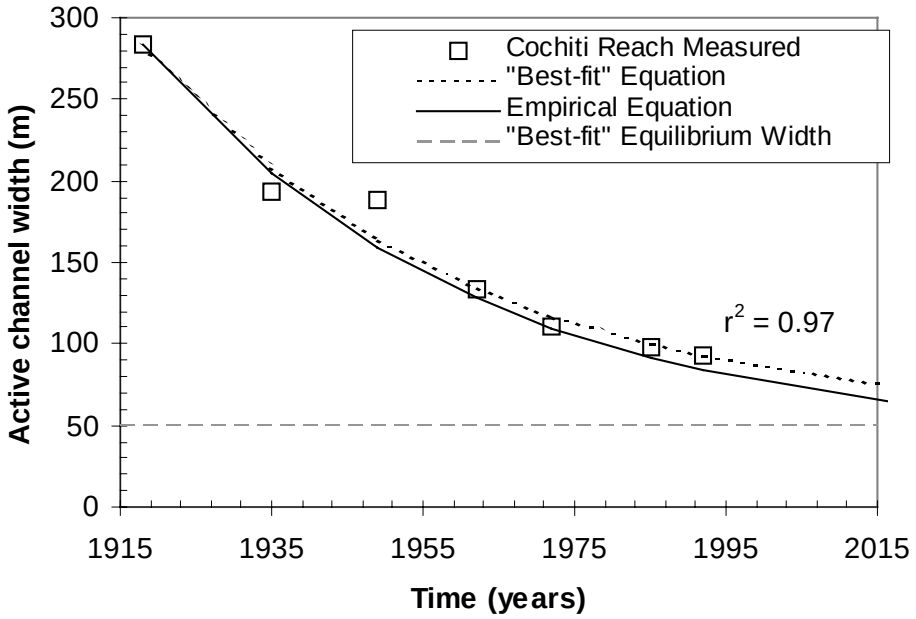

Figure 6-7 - Exponential model of width change applied to the entire Cochiti reach.

In an effort to better estimate the equilibrium width, the empirically determined k-values were used and the equilibrium width values were varied to produce a "best-fit" equation that minimized the SSE between the predicted and observed widths from 1918 to 1985. The results of these "best-fit" equations are also shown in Figure 6-6 and Figure 6-7.

One final method was attempted to model the width changes with Equation 6-7. The results of the Julien and Wargadalam (1995) hydraulic geometry equation for width for each reach were used as the equilibrium width, W_e (See Section 4.5.1). The k_1-value was determined by varying it until the SSE for each reach was minimized for 1918 to 1985. The results are plotted with their r-squared values in Figure 6-8. This model consistently over-predicted the 1992 width; but, the r-square values are comparable if not better than those resulting from the equations using empirically derived parameters.

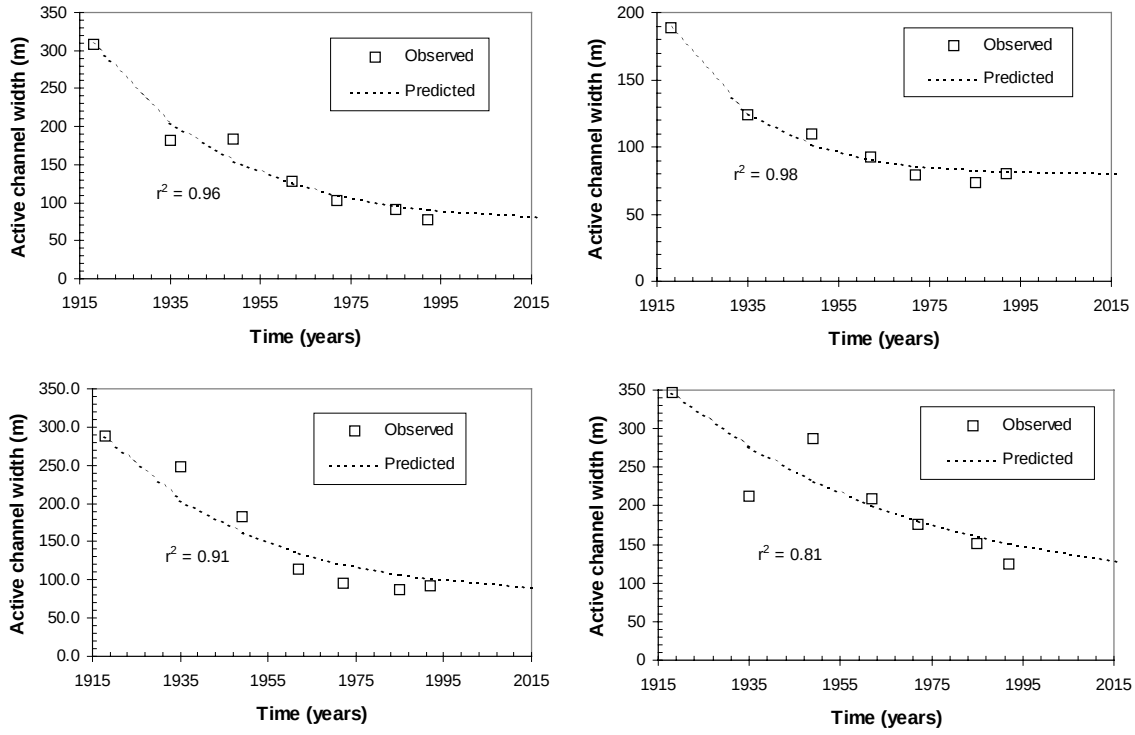

Figure 6-8 - Application of exponential model of width change using Julien and Wargalam's (1995) predicted equilibrium width and empirically derived *k*.

Migration Rate

Considering the theory that the lateral migration rate will also decrease as the channel width approaches the equilibrium width, the following equation was tested:

$$M = k_2(W - W_e) \quad \text{.....(6-8)}$$

where, M = lateral migration (total bankline change - width change) as defined in Chapter 5. The rate constant k_2 can be estimated from the slope of a linear regression between M and W. One problem with this equation is that as the channel width approaches the equilibrium width, the migration rate goes to zero. And, if the measured channel width is less than the predicted equilibrium width, then the resulting migration rate is less than zero.

The k_2-value was computed from the regressions shown in Figure 6-9 using only data from 1918-1985. The migration rates were computed for each time period (1918 - 1985) and each reach using Equation 6-9. The measured channel widths at the beginning of each survey period, and the equilibrium width computed from the "curve-fit" method described above, were also used as input. The results were very poor. Instead, using the “curve-fit” equilibrium width for each reach from the previous section, the k-value was varied to minimize the SSE between the measured values of M and the predicted (Table 6-2). The results are shown in Figure 6-10. The value of M is for the time period following the date shown, e.g., the 1918 value is for the 1918-35 time period. The prediction of M is extended to 1992 based on the 1992 measured width. So the 1992 value is the expected migration rate following 1992. The same method was applied again, but using the equilibrium width suggested by the Julien and Wargadalam (1995) hydraulic geometry equations. The results are plotted in Figure 6-11. Using the equilibrium width predicted by the hydraulic geometry equations does not increase the accuracy of the model.

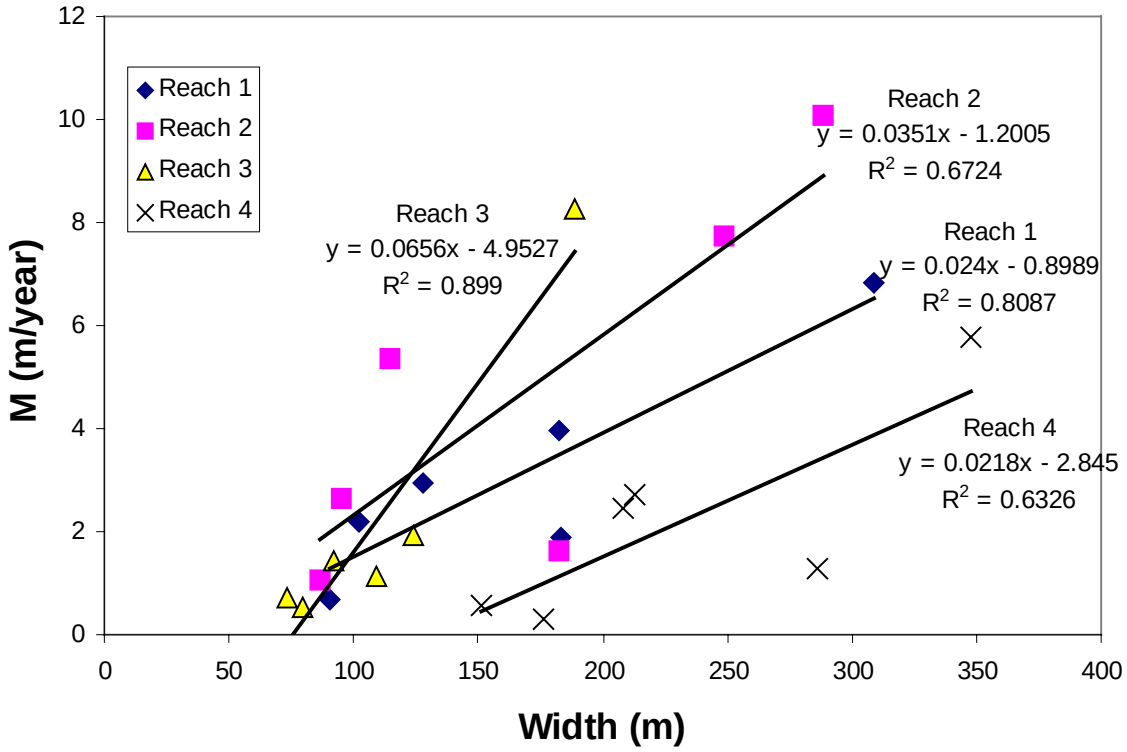

Figure 6-9 - Lateral migration, *M* (m/year) plotted against the active channel width (m) for estimation of the parameter *k*, the slope of the regression line.

Table 6-2 - Comparison of "best-fit" *k*-values and *k*-values resulting from the reach regressions in Figure 6-9.

	Regression results from Figure 6-9		Best-fit k-values and W_e from dW-W relationship	
Reach #	***k***	***W_e* (m)**	***k***	***W_e***
1	0.024	37	0.028	63
2	0.0351	34	0.036	41
3	0.0656	75	0.059	68
4	0.0218	131	0.021	124

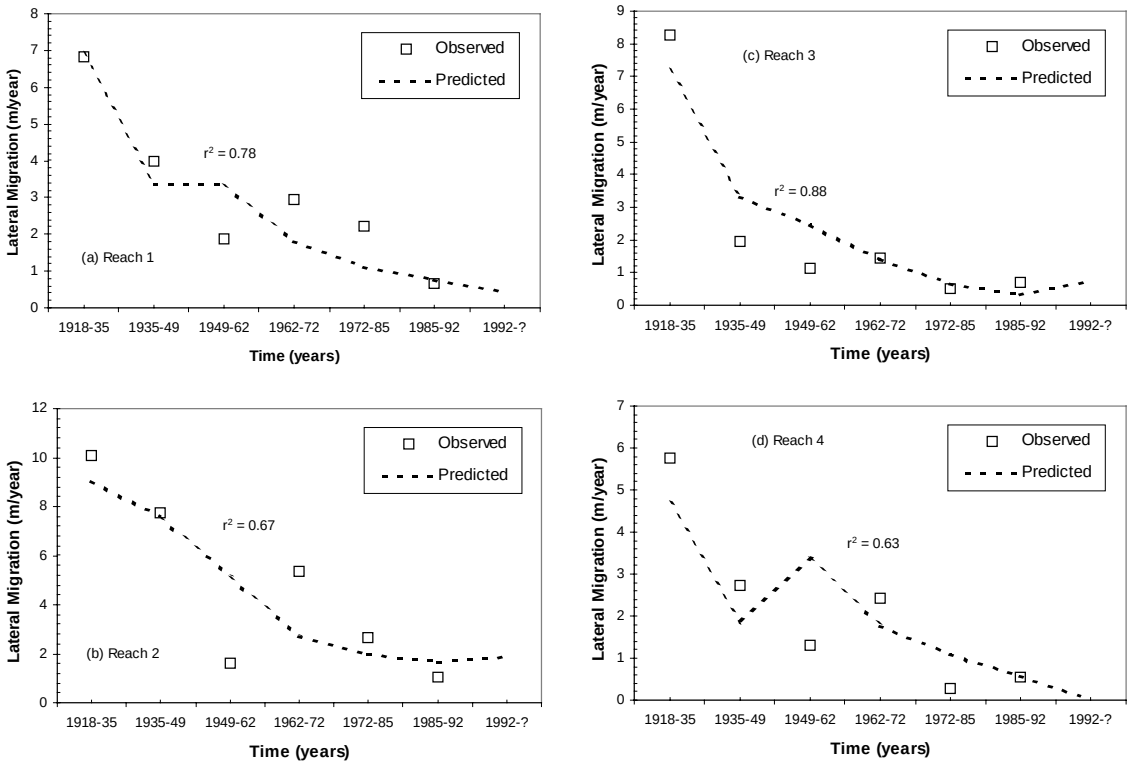

Figure 6-10 - Predicted *M* using W_e predicted from *dW-W* relationship and "best-fit" *k*-values.

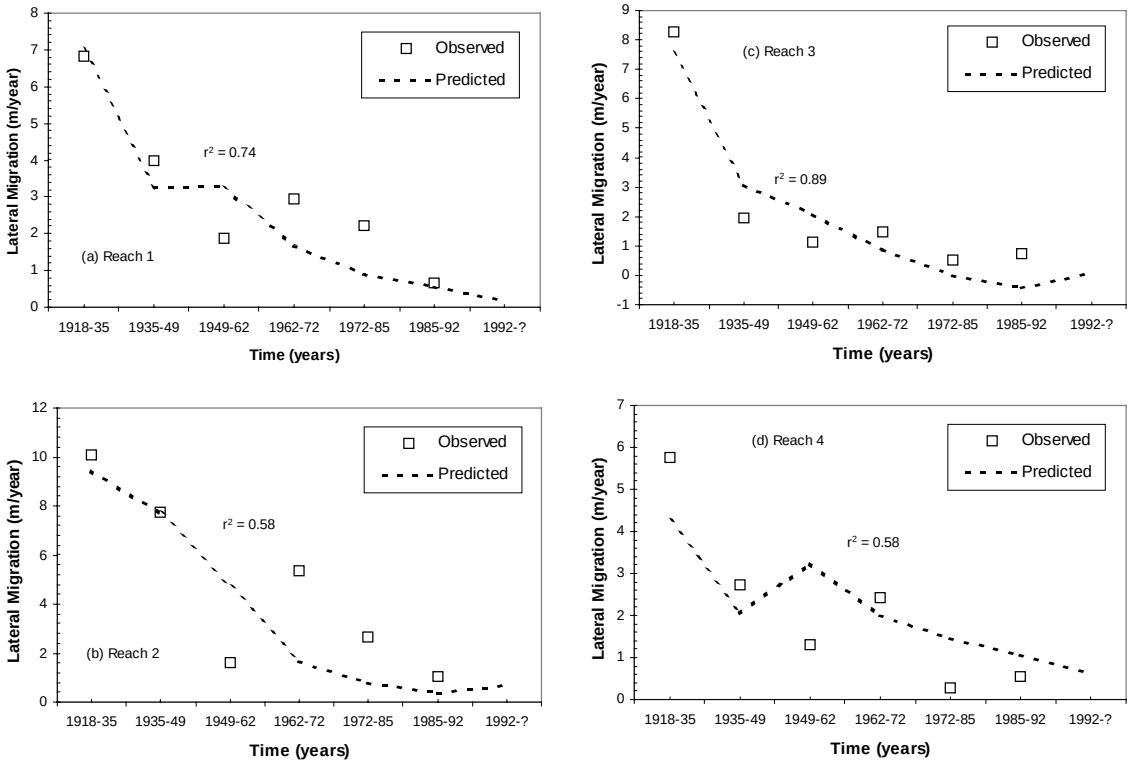

Figure 6-11 - Predicted *M* using W_e from hydraulic geometry equations.

Some problems encountered with this method are:

1) Potential to end up with a negative migration rate,
2) Potential to have a migration rate = 0, which is not realistic either,
3) Curve does not approach an asymptote, which in theory would provide the "dynamic equilibrium" value of migration rate,
4) Need for an estimate of the equilibrium width, and
5) Estimation of migration rate depends only on width and an estimated equilibrium width.

6.3 Statistical Analysis

The previous two sections analyzed the relationship between channel width, stream type and lateral movement. This section explores the associations between lateral migration rates and other hydraulic, sedimentologic and channel-form parameters via statistical analysis using a multiple regression model. Chorley (1966) provides justification for the use of multiple regression in geomorphic investigations because of the inherent multivariate nature of the systems…"one of the most significant characteristics of geological, geographical and geomorphic phenomena is that they are the result of a number of simultaneously operating variables which must be evaluated separately, relatively and in combination" (p.366). He notes that the natural high variability or noise (spatially and temporally) in geomorphic measurements often creates difficulty in sorting out the important factors, and that the noise can obscure significant relationships. Multiple regression analysis provides a useful tool for identification of significant relationships.

Additionally, Chorley (1966, p.367) recognized that "Statistical methods are an adjunct to hypothesis, experience and intuition--not a substitute for them". He continues to suggest that you first employ experience and intuition, and statistical methods help you test your hypotheses:

> Thus statistical methods, although providing a standardized, rigorous, conservative and objective framework for the extracting of the maximum amount of information from numerical data, are only an adjunct and not a substitute for the initial qualitative stage of any investigation. This qualitative stage is entirely a matter for the exercise of experience and controlled intuition, in which statistical methods are of no help--although they may subsequently be used to test the efficiency of this qualitative framework. Statistical methods are tools which assist and test imagination. Some of these tools, however, like Galileo's telescope, may prove to be vehicles which enable

> human imagination and intellectual grasp to operate on higher planes than ever before. For the geomorphologist, multivariate analysis may well be such a tool. (Chorley 1966, p. 377)

Recognizing the value of statistical analysis in identifying significant associations, it is esssential to note that association does not prove causation.

6.3.1 Expected relationships - Experience and Intuition

The Cochiti reach exhibits both spatial and temporal variability in both lateral migration and rate of change in channel width. Before blindly applying multiple regression analysis to a list of variables, expected relationships between independent and dependent variables need to be identified. Following Chorley's (1966) admonition to employ experience and intuition, this section identifies potential relationships between lateral movement and other parameters through other researchers' published **experience** and contributions from the author's **intuition**.

Other studies have employed statistical analyses to identify important associations between measured lateral movement rates and other hydraulic, sedimentary, and channel form parameters. Some of the significant relationships that emerged from these studies are summarized in Table 6-3. Parameters that have been identified to be important in describing and predicting lateral mobility are: channel form (Brice 1982), sinuosity and curvature of bends (Brice 1982; Hickin and Nanson 1975; Nanson and Hickin 1983; Hooke 1987; Thorne 1991; Biedenharn at al. 1989; Shields et al. 2000; MacDonald 1991), stream power (Nanson and Hickin 1986; Shields et al. 2000; Lawler et al. 1999), stream size measured by width or drainage area (Hooke 1980, Brice 1982,), sediment supply (Nanson and Hickin 1983; Carson 1984), and bank material, stability and vegetation (Hooke 1980; Thorne 1992; Millar 2000; Lawler et al. 1999).

Based on the results and observations of these other studies, it would be expected that the spatial and temporal variability of lateral migration of the Cochiti reach would be associated with the spatial and/or temporal variability in flow energy, bed material size, suspended sediment discharge, river size (channel width), and planform. Some of the relationships are straightforward, whereas others are more complex.

Based on observations on the Rio Grande and results of other studies, it seems that lateral migration rates increase with increasing flow energy. Flow energy includes the kinetic energy of the water discharge and the potential energy measured by either the valley or channel slope. Different measures of flow energy include total and specific stream power as described in chapter 2.3. Nanson and Hickin (1986), Lawler et al. (1999), Hooke (1979) and MacDonald (1991) all found that lateral migration increased as the energy of the flow increased in meandering rivers.

Table 6-3 - Summary of published relationships between lateral migration rates and other parameters.

Source	Significant Relationship	Notes
Hooke (1979)	$M \sim Q_{peak}$, *API*	*API* = Antecedent precipitation index
Hooke (1980)	$M \sim A$ (drainage area) $M \sim$ % silt-clay in bank	
Hickin and Nanson (1975) Nanson and Hickin (1983)	$M \sim R_c/W$	Also identified bank texture, planform and sediment supply rate as important
Hickin and Nanson (1984)	$M \sim R_c/W$	Also identified bank resistance as important
Nanson and Hickin (1983)	$M \sim Q$ and S $M \sim W$ and S $M \sim Q$, S and D_{50} $M \sim W$, S and D_{50}	
Biedenharn et al (1989)	$M \sim R_c/W$	
Thorne (1991)	$M \sim R_c/W$	Also identified bank material and geologic controls as important
Klaassen and Masselink (1992)	$M \sim W$, R_c/W	Assuming that bank resistance and sediment concentration do not vary. Bank vegetation was not important.
MacDonald (1991)	$M \sim h$ $M \sim Q$	
Lawler et al. (1999)	$M \sim L$	L = distance downstream. Also found stream power and bank material to be important
Shields et al. (2000)	$M \sim W$, R_c/W	Comparing pre and post dam rates
Begin (1981)	$M \sim R_c/W$	

Flow energy is also associated with planform shifts, and lateral migration is related to planform (Brice 1982). Bledsoe (1999) found that measures of stream power were significantly correlated with degree of lateral stability in river channels measured by the transition to braiding, and along those same lines Knighton and Nanson (1993) proposed that high flow energy was necessary for planform shifts from meandering to braided. Brice (1982) showed that both braided and meandering stream types exhibited either high or low lateral mobility depending on other factors. He suggested that the lateral mobility of meandering rivers is a function of downstream variability in width. For braided rivers, if the braidplain was sinuous and point bars were visible, the rivers tended to be highly mobile laterally, but if a braided river was straight and wide, it

tended to fall into the more stable region. These wide straight braided rivers were typically adjusted to a very large discharge, i.e., flow energy.

The associations between flow energy, planform and lateral migration can be combined to suggest that lateral migration may increase with increasing flow energy up to a threshold. Above the threshold, the river may either migrate laterally within a wide straight braidplain, or continue to wander, avulse and braid resulting in extremely high migration rates, such as on the Brahmaputra River (Coleman 1969). Several studies found that there was a maximum erosion rate for meandering rivers corresponding to a R_c/W somewhere between two and three (Hickin and Nanson 1975, 1984; Nanson and Hickin 1983; Biedenharn et al. 1989). The correlation between radius of curvature and migration rate suggests that there is an associated sinuosity that would correlate to maximum lateral migration rates.

The relationship between bed material size and migration rate is also not simple. A small bed material size (non-cohesive) is easier to transport and erode. As Nanson and Hickin (1986) showed, the bed material size at the toe of the slope can be a good indication of the resistance of the bank. However, at the other extreme, as the bed becomes armored, for instance downstream from a dam, the bed is no longer mobile and the flow often begins attacking the banks. Additionally, incision associated with armoring results in high, often unstable banks. The result is that high migration rates can be associated with both small and large bed material size. However, it would be expected that the highest rates would be associated with smaller sized material in a wandering/braided planform. Channel width has been noted to be important in associations with lateral migration (Brice 1982; Nanson and Hickin 1986). Channel width has also been used to scale for flow energy and for river size (Brice 1982; Nanson and Hickin 1986).

Sediment supply also impacts the rate of lateral migration. Carson (1984) suggested that high sediment supply is an important factor for development of braiding and that the banks are often a source of sediment. High rates of sediment transport can result in aggradation and avulsion, whereas extremely low sediment supply encourages bank erosion. Bledsoe (1999) suggests that sediment supply and bank resistance are the determining factors in whether instability in a channel is manifested laterally (braiding) or vertically (incision). It appears that it is really the sediment transport equilibrium state of a reach that would be the important factor here. If the reach is transport limited (that is, the supply exceeds the transport rate), then the channel will aggrade and possibly avulse. If the reach is supply limited, then incision and potential bank erosion could result. The most stable state would be that the sediment transport into the reach equals the transport out of the reach.

6.3.2 Parameter definition

Based on the discussion above, the following grouping of parameters were tested using the Cochiti reach data:

M = f {*Flow energy, Bed material, Sediment supply, Width, Planform*}

Ideally, a measure of bank resistance or stability should be included. Unfortunately, a consistent measure for the entire period of record was not available. It is expected that variation in bank material, stability and height could play a significant role in both the temporal and spatial variability of migration rates along the reach.

The dependent variables modeled using multiple regression analysis were lateral migration, M and change in active channel width, dW_{act}. The subreach and reach values were determined for each of these parameters in Chapter 5 for each time period from 1918 to 1985. The migration and width change data are shown in Appendix B, Tables B-1 and B-2.

This section describes quantification of the independent variables used as input to the multiple regression analysis to model M and dW_{act}. For variables sampled only at the beginning and end of each time period (e.g., active channel width), the value at the beginning of the time period was used as the input value to the regression. For variables measured over the time period, either an averaged value or maximum value for the time period was used (e.g., suspended sediment concentration and water discharge).

The independent variables selected for analysis are listed in Table 6-4.

Table 6-4 - Independent variables used in regression models

Model #	Independent Variable
1	Q - Channel-forming discharge (m^3/s)
2	S - Slope at the beginning of the time period
3	QS - total stream power (m^3/s)
4	$S(Q)^{0.5}$ - specific stream power $(m^3/s)^{0.5}$
5	$MI = S(Q/D_{50})^{0.5}$ – mobility index ($m/s^{0.5}$)
6	D_{50} - average median grain size of bed material (m)
7	W_{act} - active channel width at beginning of time period (m)
8	W_{tot} - total channel width at the beginning of the time period (m)
9	dW_{act} - rate of change of active channel width (m/year)
10	dW_{tot} - rate of change of total channel width (m/year)
11	W_r - width ratio Wact/Wtot
12	P - sinuosity at beginning of time period
13	P_{tot} - total sinuosity at beginning of time period
14	b - reach averaged number of channels at beginning of time period
15	C - average suspended sediment concentration (mg/L)

Flow Energy

Discharge - The peak mean-daily discharge value for the time period between aerial surveys was selected based on the results presented in Chapter 4 regarding channel-forming discharge. For example for the 1918 and 1935 surveys, the peak mean daily discharge between 1918 and 1934 was used. The gage data used for the corresponding reaches are shown in Table 6-5.

Table 6-5 - Daily mean discharge data

Reach #	Time Period	Gage Used for Peak Daily Mean Discharge Values
Reach 1	1918-35	Otowi
	1935-1992	Cochiti
Reach 2	1918-35	Otowi
	1935-1992	Cochiti
Reach 3	1918-35	Otowi
	1935-1992	San Felipe
Reach 4	1918-35	Otowi
	1935-1972	Bernalillo
	1972-1992	Albuquerque

Slope - Reach averaged slope measurements computed as described in Chapter 4 were used as input to the regression models. The value of the slope at the beginning (or the closest to the beginning) of each time period was used.

Stream Power and Unit Stream Power - Stream power, either total or specific (See discussion in Chapter 2.3) has been shown to be an important indicator of the erosive power and energy of a flow (Bledsoe 1999). The correlation of stream power with channel pattern and the importance of channel pattern on the lateral mobility of a channel support the use of these measures in the statistical analysis described in this section.

Both total and specific stream power were used in the model in the forms of QS and $S\sqrt{Q}$, respectively, in this analysis. These parameters were computed for each reach using the slope and discharge measurements described above. The slope and discharge were both estimated at a reach level. The representative values for each reach were applied to the corresponding subreaches. As a result, all of the subreaches within a particular reach have the same values for total and specific stream power for a given time period.

Mobility Index - The mobility index,

$$MI = S\sqrt{\frac{Q}{D_{50}}} \quad \text{.....(6-9)}$$

has dimensions of $L/T^{0.5}$, and is used in the multiple regressions in SI units, with discharge in m^3/s and D_{50} in meters, resulting in units of $m/s^{0.5}$. A mobility index was computed for each reach and subreach for each time period using the peak daily discharge for the time period, the time-average slope, and the time-averaged bed material size.

Sediment

Bed Material - The median bed material size estimates for the subreaches as presented in Chapter 4 were time averaged for each time period for the subreaches. A weighted average of the subreach data was performed to get the reach-averaged data, and was then time averaged.

Suspended Sediment Concentration – The average suspended sediment concentration was selected as a measure of sediment supply for each reach. It would be most appropriate to include a measure of bed material transport, but these data are not available for the entire period of record. Prior to construction of Cochiti Dam, the flows in the Rio Grande were very turbulent. As a result, Woodson and Martin (1962) suggested that suspended sediment samples from the Rio Grande are more nearly indicative of the total load than similar samples from other rivers.

Average suspended sediment concentrations measured from double mass curves of cumulative annual water discharge and suspended sediment yield as described in Chapter 4 were used. The reach averaged values were applied to the appropriate subreaches as the suspended sediment concentration probably does not change between subreaches.

Channel Width

Width and Width Change - The total channel width and active channel width were used as input to the regression models. The subreach-averaged and reach-averaged values computed by the methods described in Chapter 4 at the beginning of each time period were used. Additionally, the changes in active and total channel width were input into the regression. These measures would not be appropriate to use for predictive abilities because it would not be possible to estimate the future change of width during the time period of interest. However, it was considered to be important to determine if there was an association between channels that migrated and channels that also changed in width.

Planform

Channel Planform - The measures of channel pattern presented in Chapter 4 were used in the multiple regression analysis. These include:

- Sinuosity (P) - thalweg length/valley length
- Total Sinuosity (P_{tot}) - total centerline channel length/valley length
- Average number of channels (b)
- Width ratio (W_r) - active channel width/total channel width.

The subreach and reach values of these parameters at the beginning of each time period were used as input to the regression model.

6.3.3 Correlation and Scatter Plots

The first analysis performed was an application of a correlation model to all of the parameters described above. In the correlation model, no distinction is made between an independent and a dependent variable. Instead, the nature (i.e., positive or negative) and degree of relation between two variables is sought. The test is for *linear* correlation between variables and the resulting coefficient, r, is 1 or -1 for perfect correlation, and zero for no correlation. The correlation coefficient is **not** a measure of a linear correlation between two variables, but it does provide information about the covariance between the two variables (Pedhazur 1997). Additionally, the significance of the correlation can be tested using an F-statistic and a corresponding p-value indicating the confidence level.

Table 6-6 is the correlation matrix for the 1918-85 reach-averaged data. The correlation coefficient is listed first, and the significance or p-value is provided below. A p-value <0.05 indicates 95% confidence in the correlation. The correlation coefficients for any parameters that exhibit multicollinearity with another parameter are shaded in dark grey. These include the stream power parameters and their correlation with Q, S and D_{50}, the width measurements with each other, and the planform measures with each other. This was done to eliminate confusion when reviewing the table. The parameter, d, is a dummy variable indicating pre vs. post dam samples.

It should be noted that an underlying assumption of this model is that all of the samples are independent. It could be argued that sampling different points along a river at different time periods could violate the presumption of independence. This is particularly a problem with the subreach data, which are modeled as if they are 150 independent data points, when that is not the

reality. The result is that the p-value will not be accurate. It will artificially be smaller than it should be and as a result should be used with caution.

Keeping these cautions in mind, some interesting and significant correlations are apparent from this analysis. The bed material size, mobility index and suspended sediment concentration are all highly correlated with the presence of the dam. As shown in Chapters 4, the bed material coarsened and suspended sediment concentration decreased immediately following construction of the dam. Bed material size is in the denominator of the mobility index, so it decreases as bed material size increases.

Some of the hypotheses presented earlier in this chapter are supported by the correlations shown in Table 6-6. Lateral migration correlates well with discharge, stream power, mobility index and total channel width. When lateral movement is normalized by the width, the planform indices (P_{tot}, b, and W_r) become more significant. The only significant correlation with change in active channel width is with width itself. Total channel width correlates with total stream power, mobility index and discharge. This could indicate that, as Nanson and Hickin (1986) showed, the channel width may be useful as an estimator of flow energy.

Similar correlation matrices for subreach data and non-transformed reach data are presented in Appendix E, Tables E-1 through E-4. As expected, the p-values for the subreach data are much lower (indicating spurious high significance) and the correlation coefficients are also lower (indicating lower explained variance).

Continuing to explore relationships between individual parameters and the lateral movement rates, scatter plots were created of the significant parameters with the lateral movement rates. The plots presented here show the pre-dam and post-dam reach averaged data separately. Additionally, the subreach-averaged data are presented to illustrate the true variability within the reach.

The total channel width is plotted against lateral migration rate in Figure 6-12. The separation between pre and post dam data is evident as well as a trend toward increasing lateral migration with increasing total channel width. The trend in the subreach data is not so clear and the scatter is much greater.

Table 6-6 - Correlation matrix between reach-averaged parameters using 1918 - 1985 data. The p-value for the correlation coefficient is listed below the r-value. P-values <0.01 are highlighted as well as r-values > 0.65. The values highlighted in dark gray are auto-correlated. A subscript of 1 indicates the value of the variable at the beginning of the time period.

	Rch	d	Q	S_1	D_{50avg}	QS_1	$S_1Q^{0.5}$	MI	C	W_{act1}	W_{tot1}	dW_{tot}	dW_{act}	W_r	P_1	P_{tot1}	b_1	M	N
Reach	1.00	0.00	0.00	-0.73	-0.13	-0.27	-0.42	-0.18	0.38	0.19	-0.08	0.13	0.03	0.54	-0.39	-0.67	-0.72	-0.21	-0.40
		1	0.987	<.0001	0.541	0.208	0.043	0.412	0.070	0.365	0.721	0.558	0.880	0.007	0.058	0.000	<.0001	0.321	0.053
d		1.00	-0.61	-0.16	0.83	-0.54	-0.50	-0.75	-0.89	-0.56	-0.53	0.38	0.34	0.33	-0.18	-0.39	-0.33	-0.52	-0.40
			0.002	0.450	<.0001	0.007	0.014	<.0001	<.0001	0.004	0.007	0.066	0.104	0.114	0.404	0.060	0.112	0.009	0.051
Q			1.00	0.27	-0.56	0.91	0.82	0.88	0.49	0.68	0.71	-0.41	-0.20	-0.40	0.06	0.24	0.24	0.75	0.53
				0.194	0.005	<.0001	<.0001	<.0001	0.015	0.000	<.0001	0.046	0.345	0.055	0.776	0.267	0.262	<.0001	0.007
S_1				1.00	-0.08	0.61	0.76	0.52	-0.13	0.14	0.36	-0.28	-0.16	-0.62	0.12	0.66	0.71	0.37	0.42
					0.702	0.002	<.0001	0.010	0.557	0.511	0.087	0.182	0.467	0.001	0.590	0.001	0.000	0.071	0.040
D_{50avg}					1.00	-0.48	-0.44	-0.65	-0.79	-0.58	-0.51	0.34	0.38	0.25	-0.08	-0.30	-0.24	-0.45	-0.29
						0.018	0.034	0.001	<.0001	0.003	0.012	0.106	0.069	0.246	0.700	0.158	0.256	0.028	0.166
QS_1						1.00	0.98	0.94	0.33	0.60	0.72	-0.44	-0.23	-0.55	0.07	0.45	0.46	0.76	0.61
							<.0001	<.0001	0.119	0.002	<.0001	0.032	0.284	0.006	0.732	0.028	0.025	<.0001	0.002
$S_1Q^{0.5}$							1.00	0.91	0.25	0.53	0.68	-0.43	-0.24	-0.62	0.10	0.56	0.57	0.72	0.61
								<.0001	0.238	0.007	0.000	0.034	0.268	0.001	0.657	0.005	0.003	<.0001	0.002
MI								1.00	0.56	0.68	0.76	-0.50	-0.33	-0.52	0.09	0.45	0.42	0.76	0.61
									0.005	0.000	<.0001	0.012	0.110	0.009	0.668	0.028	0.039	<.0001	0.002
C									1.00	0.55	0.39	-0.25	-0.28	-0.04	-0.04	0.09	0.02	0.29	0.11
										0.005	0.063	0.232	0.190	0.836	0.852	0.683	0.934	0.172	0.616
W_{act1}										1.00	0.84	-0.56	-0.62	-0.27	0.21	0.15	0.12	0.62	0.35
											<.0001	0.004	0.001	0.199	0.337	0.473	0.561	0.001	0.090
W_{tot1}											1.00	-0.86	-0.51	-0.71	0.33	0.47	0.46	0.81	0.68
												<.0001	0.010	0.000	0.115	0.019	0.024	<.0001	0.000
dW_{tot}												1.00	0.57	0.81	-0.23	-0.53	-0.52	-0.65	-0.69
													0.004	<.0001	0.284	0.008	0.009	0.001	0.000
dW_{act}													1.00	0.27	-0.06	-0.23	-0.22	-0.35	-0.31
														0.20	0.77	0.27	0.30	0.10	0.13
W_r														1.00	-0.41	-0.84	-0.86	-0.63	-0.81
															0.047	<.0001	<.0001	0.001	<.0001
P_1															1.00	0.44	0.40	0.37	0.47
																0.032	0.055	0.078	0.020
P_{tot1}																1.00	0.98	0.35	0.58
																	<.0001	0.092	0.003
b_1																	1.00	0.35	0.58
																		0.091	0.003
M																		1.00	0.85
																			<.0001
N																			1

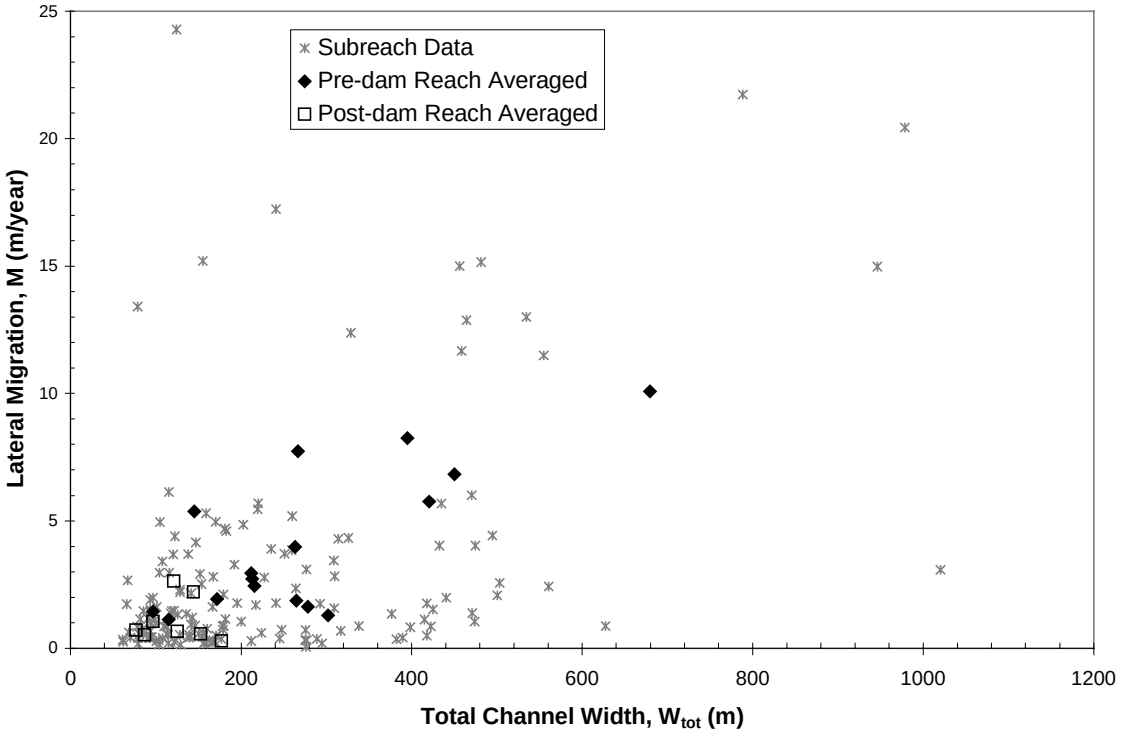

Figure 6-12 - Total channel width vs. lateral migration rate

The four different measures of flow energy are plotted against lateral migration Figure 6-13 through Figure 6-16. The first is discharge and no clear trend is evident. The highest migration rates occur at the highest discharges for the pre-dam reach-averaged data. Figure 6-14 shows the specific stream power. In this graph and the following plot (Figure 6-15) of total stream power, the pre-dam and post-dam reach averaged data are more clearly separated than in the discharge plot. Additionally, the reach averaged migration rates appear to increase with increasing stream power and attain a peak value then decline. It is possible that this peak corresponds to the transition to a straighter and wider braided channel configuration as discussed in Section 6.3.1.

The mobility index (Figure 6-16) shows a more clear demarcation between the pre and post dam periods. The bed material size is in the denominator of the mobility index. Following construction of Cochiti Dam, the bed material size increased significantly, producing a similar decline in the mobility index. Migration rates greater than 3 meters per year do not occur at *MI* below 0.8. This corresponds to Chang's (1988) 0.76 threshold from meandering to braided transition.

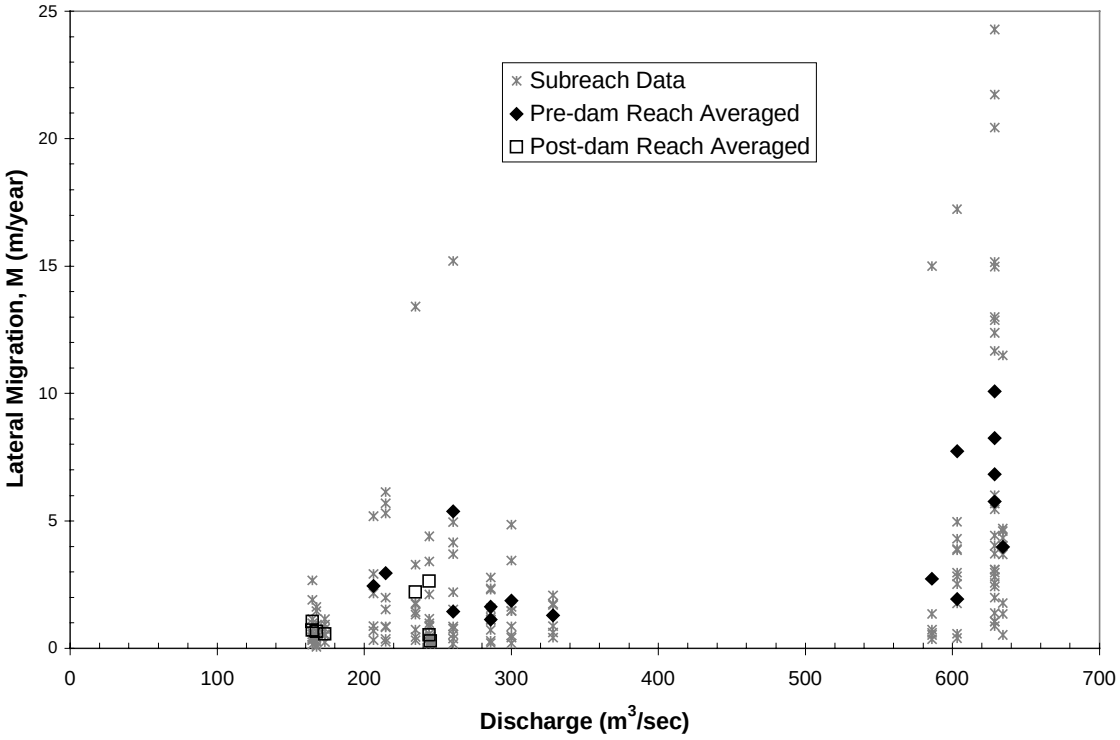

Figure 6-13 - Discharge vs. lateral migration rate.

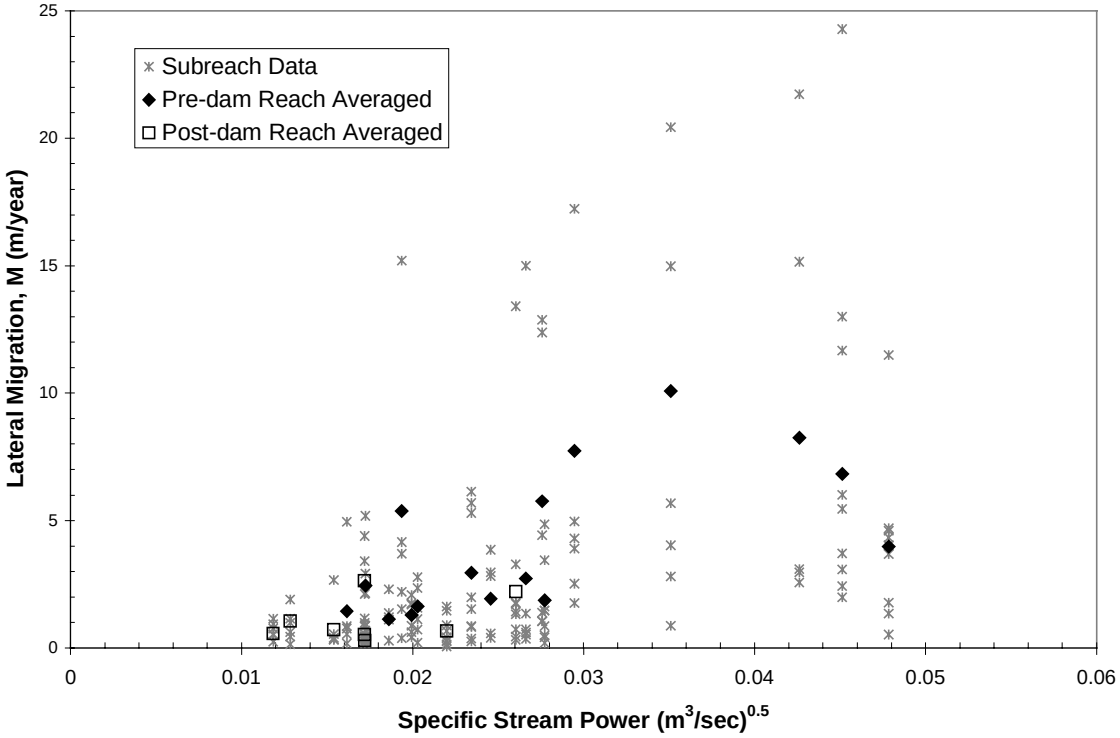

Figure 6-14 - Specific stream power vs. lateral migration rate.

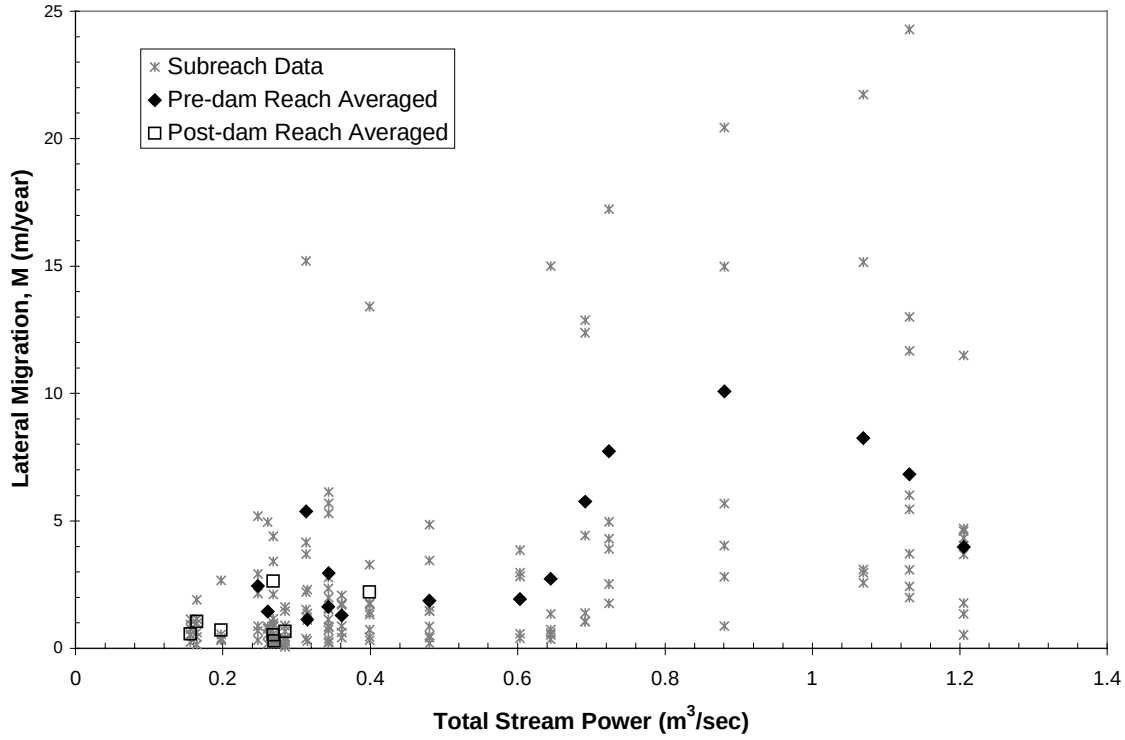

Figure 6-15 - Total stream power vs. lateral migration rate

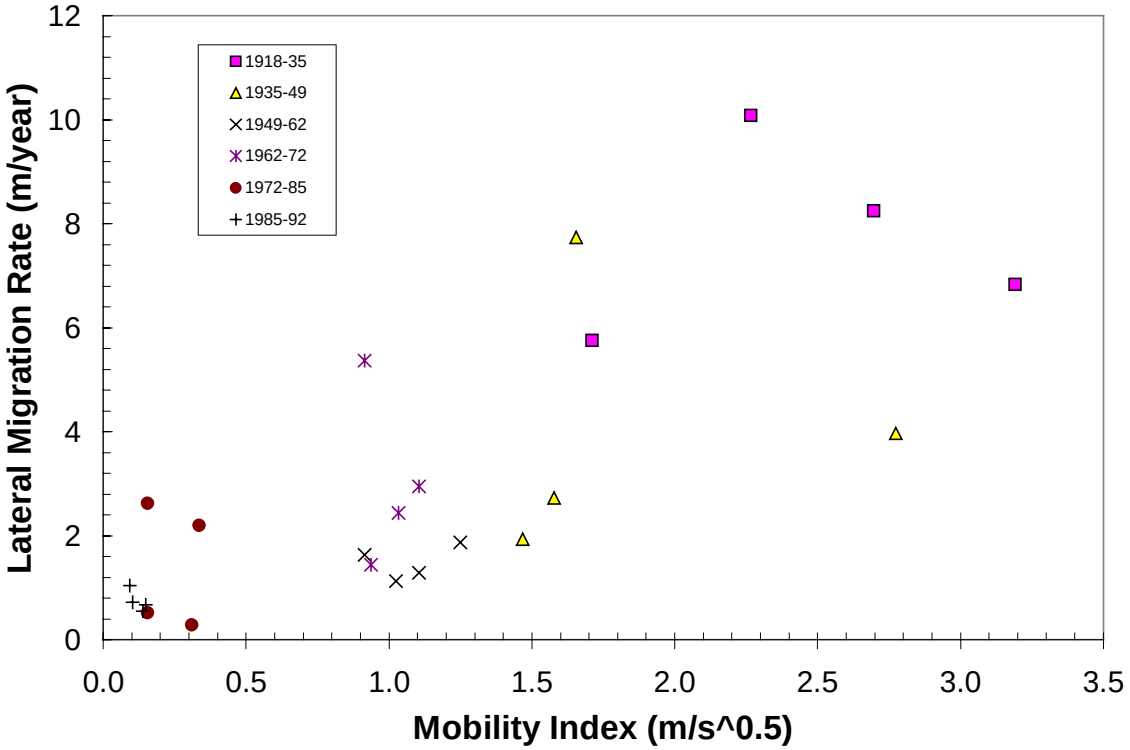

Figure 6-16 - Mobility index vs. lateral migration rate

The measure of planform that produced the highest correlation with migration rate was the width ratio. This is the ratio of active channel to total channel width. It approaches a value of one as the channel moves toward being single thread. In Figure 6-17, there is a trend toward declining migration rate as the width ratio approaches one.

Rate of change of active channel width only produced significant correlations with measures of width. The change in active channel width is plotted against both active and total channel widths in Figure 6-18. There is a clear association between wider channel widths and greater rates of narrowing.

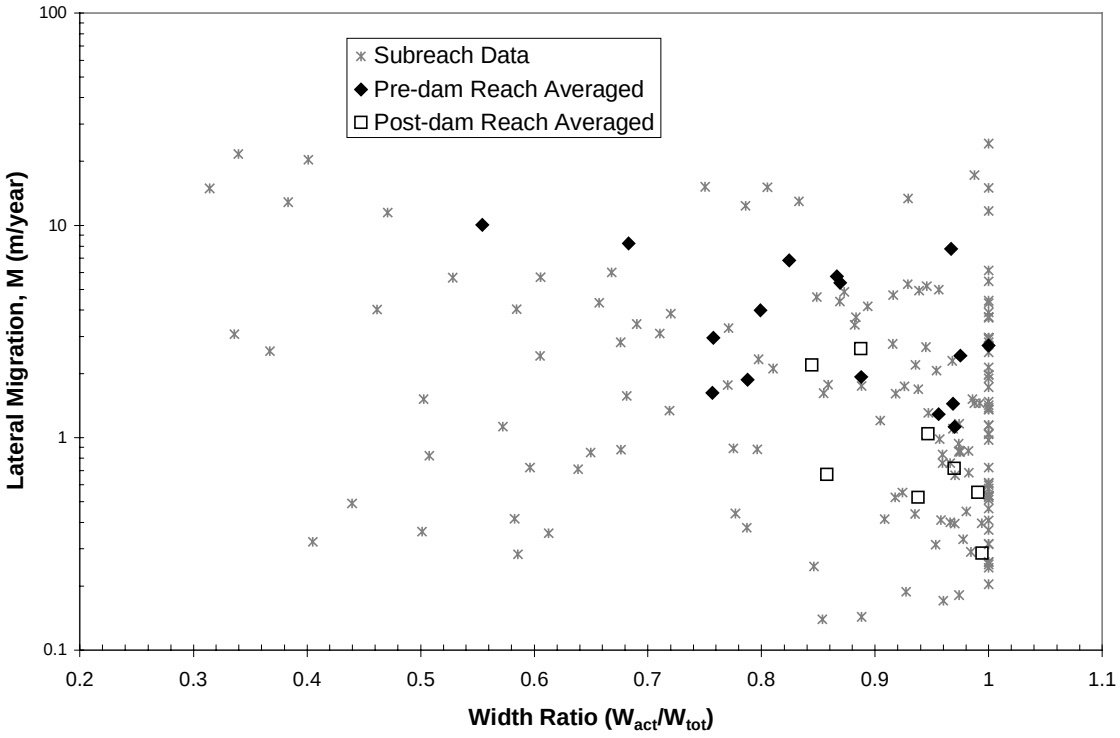

Figure 6-17 - Width ratio vs. lateral migration rate.

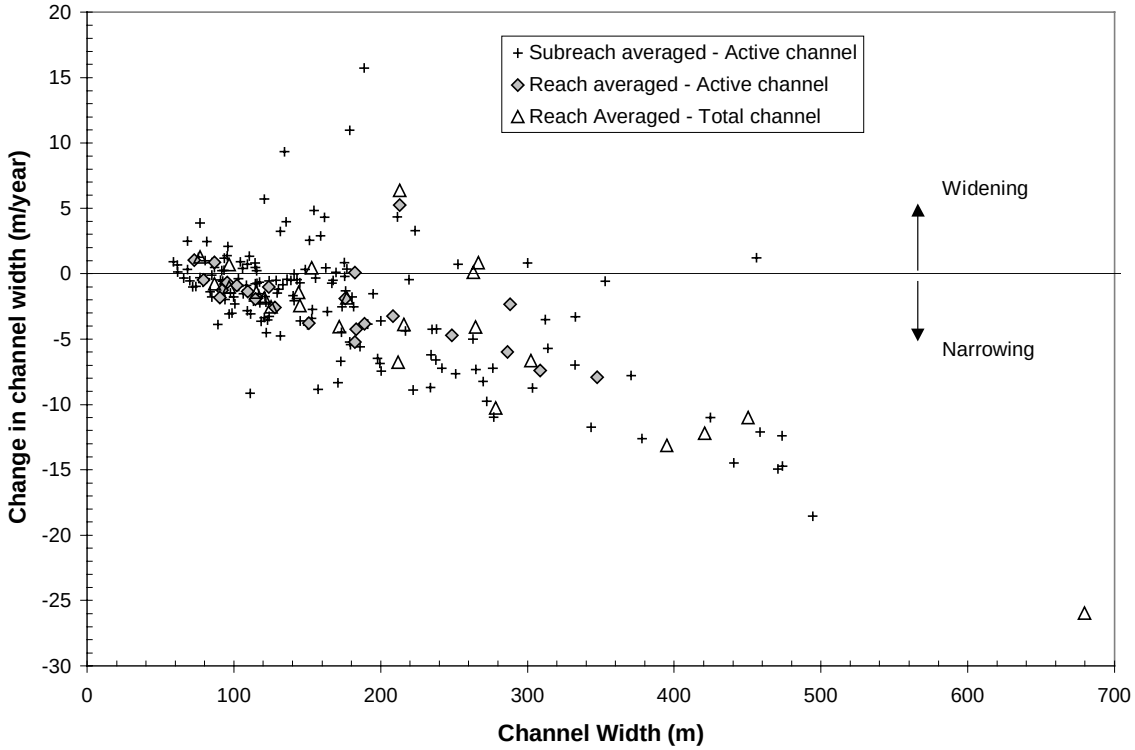

Figure 6-18 - Channel width vs. change in active channel width

6.3.4 Regression models

Linear and $\log_{10}$-transformed regressions were performed using the variables described above. First each variable individually (as shown in Table 6-4) was regressed against M and dW_{act} (Models 1-15). Mutiple regression analyses with stepwise selection techniques were then applied to different combinations of the measures of flow energy, width change and planform. The regression models were structured to compare the different measures of flow energy, width change and planform. Table 6-7 illustrates the structure of the regression models by indicating which input variables were used for each regression model (Models 16-63). Each measure of flow energy (Q, S, and D_{50} individually, $S\sqrt{Q}$, QS, and MI) was used in combination with measures of width or width change (dW_{act}, dW_{tot}, and W_{tot}) and of planform (P, P_{tot}, b, and W_r). Suspended sediment concentration was included in each model as an estimator of sediment supply. Preliminary results showed that the active channel width was not significant and as a result it was not included. A total of 63 models was applied to each data set: the reach averaged data, the $\log_{10}$-transformed reach averaged data, the subreach averaged data and the $\log_{10}$-transformed subreach averaged data. The models utilized data from each time period from 1918-1985 using migration rate (M) as the dependent variable.

Table 6-7 - Structure of independent variables used as input to multiple regression models with stepwise selection for M as dependent variable.

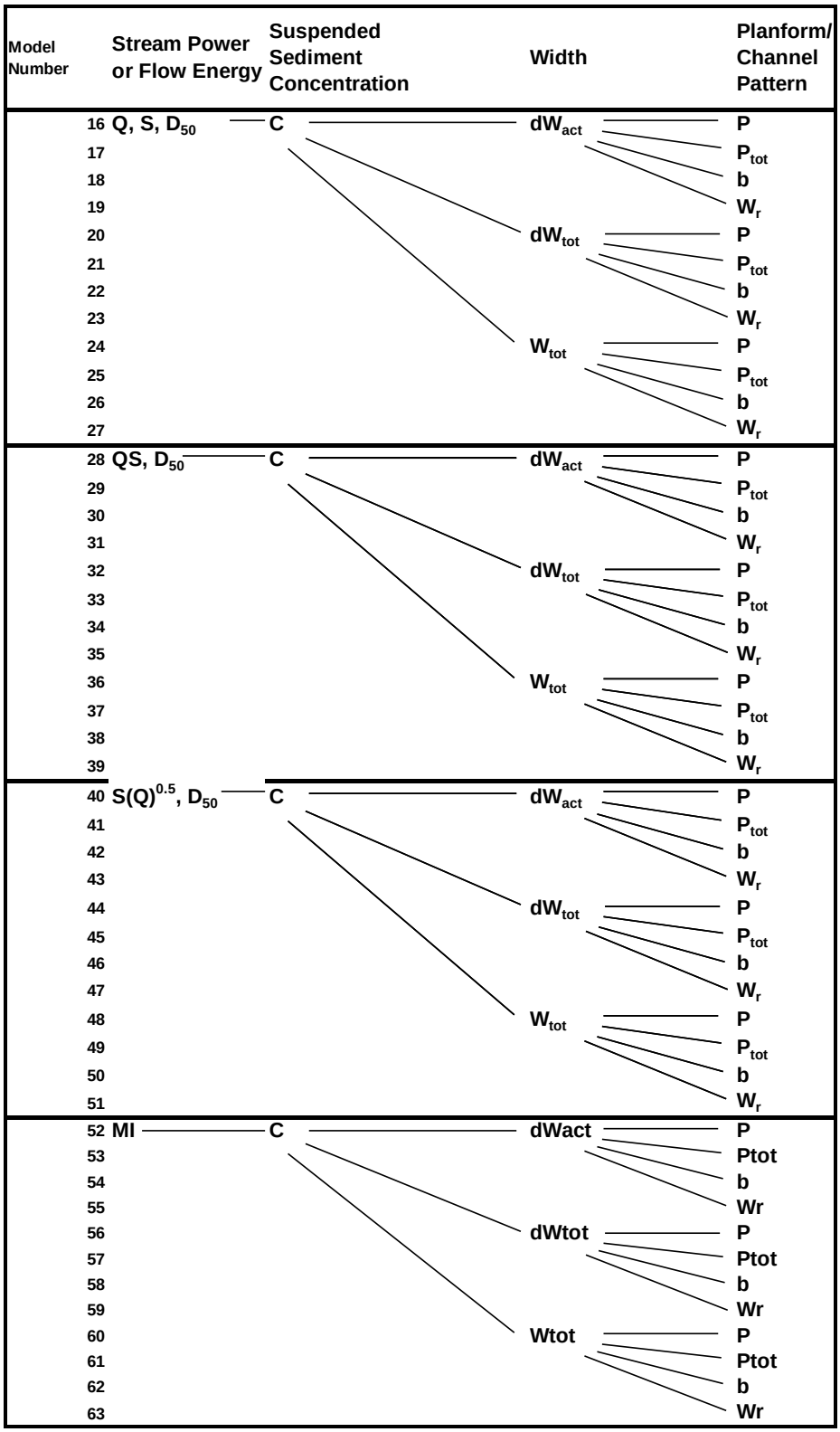

For the width change rate (dW_{act}), a similar input variable structure was used, but the active channel width and total channel width were both included as independent variables, and the width change variables (dW_{act} and dW_{tot}) were not included as independent variables. The result was a total of 46 models that were applied to the four different data sets from 1918-1985. The 1985 to 1992 data were reserved for validation of the resulting equations.

Migration rate regression

The results of all of the regression analyses for lateral migration rates (M) are presented in Appendix E, Tables E-5 through E-8. The arithmetic regression results are described below followed by the results using the $\log_{10}$-transformed data. In general, the reach-averaged data produced higher explained variance (R-squared) values than the subreach-averaged data. For the reach-averaged data, $\log_{10}$ transformation did not increase the accuracy of the models. However, the $\log_{10}$-transformation did produce better results for the subreach-averaged data. The decreased accuracy using the subreach data is likely a result of the natural variability in the system that is not accounted for by the chosen parameters, for instance bank material and stability, bank vegetation, variations in water slope with stage, and other details of cross-section and planform geometry.

Arithmetic regressions - A measure of stream power or flow energy was present in all of the significant ($R^2 > 0.5$ and $p < 0.005$) relationships. The highest description of variance was from models combining a stream power measure with either total channel width or a planform measure.

Using the subreach-averaged data, the highest R-squared value is 0.34 and the residual plots reveal that the residuals are far from normally distributed. The level of significance determined by the p-values is very high as a result of the higher number of observations. However, this p-value is not accurate and may be unrealistically low because of the lack of independence between the samples. The low R-square values reduce the predictive capabilities of the equations.

Sinuosity was important in several of the relationships. However, the exponent or coefficient for sinuosity was generally so high that it was considered to be unrealistic for predictive possibilities. The sinuosity of the Cochiti reach between 1918 and 1985 based on the reach-averaged data is less than 1.2. If a higher value of sinuosity were input, the resulting variation in M could be extreme and unrealistic. As a result, the usefulness of these equations is limited. The results do, however, reveal that there is a significant relationship between migration rate and sinuosity.

The following model combines discharge with width ratio:

$$M = 8.88 + 0.009\,Q - 10.19\,W_r \qquad (6.13)$$

64.9	48.9	15.9	(% explained variance)
0.0001	0.0006	0.0129	(p-value - significance of r^2; F-test)
	0.0018	0.0129	(p-value - significance that exponent ≠ 0; F-test)

The stepwise selection method using the subreach-averaged data resulted in inclusion of a planform parameter in 20 of the 28 models. The resulting R-square values are < 50% as with all of the subreach results, but, the inclusion of planform indicates the significance of its association with the variability in lateral migration rates.

The total channel width, or the width of the channel from outer-bankline to outer-bankline including vegetated islands and mid-channel bars, explained 61% of the variance in the lateral migration rate:

$$M = -0.240 + 0.015\,W_{tot} \qquad (6.14)$$

60.9	60.9	(% explained variance)
<0.0001	<0.0001	(p-value - significance of r^2; F-test)
	<0.0001	(p-value - significance that exponent ≠ 0; F-test)

Each of the measures of flow energy separately described between 46 and 51% of the variance. Total stream power produced the best results, followed by mobility index, discharge, and specific stream power:

$$M = 0.086 + 6.408\,QS \qquad (6.15)$$

51.2	51.2	(% explained variance)
0.0004	0.0004	(p-value - significance of r^2; F-test)
	0.0004	(p-value - significance that exponent ≠ 0; F-test)

$$M = 0.459 + 2.328\,MI \qquad (6.16)$$

51.1	51.1	(% explained variance)
0.0004	0.0004	(p-value - significance of r^2; F-test)
	0.0004	(p-value - significance that exponent ≠ 0; F-test)

$$M = -0.795 + 0.011\,Q \qquad (6.17)$$

48.9	48.9	(% explained variance)
0.0006	0.0006	(p-value - significance of r^2; F-test)
	0.0006	(p-value - significance that exponent ≠ 0; F-test)

$$M = -1.523 + 195.5\ S\sqrt{Q} \qquad (6.18)$$

45.8	45.8	(% explained variance)
0.0011	0.0011	(p-value - significance of r^2; F-test)
	0.0011	(p-value - significance that exponent ≠ 0; F-test)

Inclusion of bed material and suspended sediment concentration did not increase the accuracy or significance of the equations. Based on the regression results using subreach-averaged data (Appendix E, Table E-6), the total channel width and change in total channel width both contribute significantly to the variability in *M*.

Log$_{10}$-transformed regressions - The R-squared values from the log$_{10}$-transformed reach-averaged data are lower than the arithmetic results, but higher than the arithmetic for the subreach-averaged data. The Q-Q plots of the residuals are much closer to a straight line, indicating that the log$_{10}$-transformation creates a more normal distribution, which is an underlying assumption of the multiple regression model. Again, some measure of flow energy shows up in all of the significant relationships ($p < 0.005$). Discharge combined with width ratio produced the highest explained variance using the reach-averaged data:

$$M = 0.004\ Q^{1.010}\ W_r^{-2.436} \qquad (6.19)$$

53.0	39.2	13.8	(% explained variance)
0.0016	0.0031	0.0395	(p-value - significance of r^2; F-test)
	0.0115	0.0395	(p-value - significance that exponent ≠ 0; F-test)

The negative exponent for W_r indicates that as the number of channels or island width increased, the migration rate increased.

Using subreach-averaged data, the log$_{10}$-transformation produced better results than the arithmetic regressions. As with the reach-averaged data, all of the significant regressions included some measure of flow energy and/or total channel width.

The rate of change of total channel width (dW_{tot}) showed up as significant in the eight best models. For the log$_{10}$-transformed data, the absolute value ($|dW_{tot}|$) of this measure was used, so in this analysis it is really the magnitude of the width change and not whether it narrowed or widened that was important. There are several ways that this could be addressed in future studies. Cross-section lines that narrowed could be averaged separately from those that widened, resulting in an average value for narrowing and widening separately for each reach. The exponent for $|dW_{tot}|$ is positive, indicating that the higher width change rates are associated with higher lateral migration rates.

Sinuosity also showed up as a significant variable. This time the exponents are not as large and perhaps more reasonable, but it should still be kept in mind that the maximum value of sinuosity for the subreaches is 1.34, so these equations are not applicable to sinuosities > 1.34. The models that include mobility index with suspended sediment concentration are not presented because of near collinearity between *MI, C* and D_{50} as demonstrated by the high correlation between these variables.

$$M = 3.15 \quad Q^{1.102} \quad S^{1.118} \quad P^{3.269} \qquad (6.20)$$

30.9	21.1	3.9	6.0	(% explained variance)
<0.0001	<0.0001	0.010	0.002	(p-value - significance of r^2; F-test)
	<0.0001	0.010	0.007	(p-value - significance that exponent ≠ 0; F-test)

$$M = 2.82 \quad (QS)^{1.106} \quad P^{3.275} \qquad (6.21)$$

30.9	26.4	4.5	(% explained variance)
<0.0001	<0.0001	0.006	(p-value - significance of r^2; F-test)
	<0.0001	0.006	(p-value - significance that exponent ≠ 0; F-test)

The measures of flow energy individually contribute more (20% to 26%) to the explained variance than any of the other parameters.

Width Change

The results of all of the regression models applied to the change in active channel width are presented in Appendix E, Tables E-9 through E-12.

Arithmetic regressions - In the arithmetic regressions the active channel and total channel width were the only variables that contributed significantly to the variability in the active channel width change. The results using the reach-averaged data are as follows:

$$dW_{act} = 1.391 - 0.022\ W_{act} \qquad (6.22)$$

34.4	34.4	(% explained variance)
0.0066	0.0066	(p-value - significance of r^2; F-test)
	0.0066	(p-value - significance that exponent ≠ 0; t-test)

The coefficients indicate that the rate of change of width will scale to approximately 1% of the total width and 2% of the active channel width. The measures of rate of change of width do include a sign indicating whether the channel on average was narrowing (-) or widening (+). The resulting negative coefficient for active or total channel width in the regressions will produce a negative rate of change if the initial channel width is above a certain threshold. The values of the

coefficients are such that if the active channel width is > 64 m, then the rate of change of width would be negative (narrowing). Obviously, this is not the case, as some sections of the Cochiti reach with widths greater than 64 m actually widen. A threshold width, below which a channel would widen rather than narrow, is a realistic concept, but the data do not support the values predicted by this model. The 1985-92 data were not included in this regression. Two of the reaches widen during that time period. It appears that total channel width is not a good predictor of active channel width change, as the resulting equation would indicate channel narrowing for any total channel width.

The subreach averaged data produced better results than the reach averaged. Similar equations result from the arithmetic regressions of the subreach averaged data, except that the change in active channel width scales to about 3% of the active channel width:

$$dW_{act} = 3.28 - 0.032\ W_{act} \qquad (6.23)$$

42.9	42.9	(% explained variance)
<0.0001	<0.0001	(p-value - significance of r^2; F-test)
	<0.0001	(p-value - significance that exponent ≠ 0; F-test)

Again, these equations result in threshold widths of 102.5 m and 10.8 m for active and total channel, respectively, below which the channel would widen rather than narrow. Again, the active channel width produces better results than the total channel width. The increased accuracy using subreach data is likely a result of the better representation of what is really going on in the channel by the way the data are averaged. Averaging narrowing and widening over a long reach of channel can result in a width change value that may not be very representative of the changes occurring in the channel.

<u>Log_{10}-transformed regressions</u> – The absolute value of the width change was used as the dependent variable in the following models. The log_{10}-transformed regression models produced better results than the arithmetic for modeling variability in width change using reach-averaged data. Either active or total channel width appears as significant in all of the models. The highest description of variability is 50%:

$$dW_{act} = 9.23 \times 10^{-8} \quad (S\sqrt{Q})^{-1.550} \quad W_{act}^{2.182} \qquad (6.24)$$

49.5	14.8	34.8	(% explained variance)
0.0030	0.0396	0.0008	(p-value - significance of r^2; F-test)
	0.0396	0.0062	(p-value - significance that exponent ≠ 0; F-test)

$$dW_{act} = 7.70\text{x}10^{-6} \quad (QS)^{-1.026} \quad W_{act}^{2.288} \tag{6.25}$$

49.3	14.5	34.8	(% explained variance)
0.0031	0.0412	0.0062	(p-value - significance of r^2; F-test)
	0.0412	0.0008	(p-value - significance that exponent ≠ 0; F-test)

$$dW_{act} = 7.87\text{x}10^{-4} \quad W_{act}^{1.536} \tag{6.26}$$

34.8	34.8	(% explained variance)
0.0062	0.0062	(p-value - significance of r^2; F-test)
	0.0062	(p-value - significance that exponent ≠ 0; F-test)

The subreach averaged $\log_{10}$-transformed results for active channel width:

$$dW_{\text{act}} = 6.32\text{x}10^{-4} \quad W_{act}^{1.579} \tag{6.27}$$

34.9	34.9	(% explained variance)
<0.0001	<0.0001	(p-value - significance of r^2; F-test)
	<0.0001	(p-value - significance that exponent ≠ 0; F-test)

Summary – The highest percentage of explained variance results from models containing measures of both flow energy and planform. A comparison of the predicted migration rate with the measured migration rates for the models producing the smallest error are presented in Figure 6-19 and Figure 6-20. The solid line on the plot indicates perfect agreement between predicted and observed whereas the dashed lines indicate +/- 50% error. The models generally underpredict the higher values of lateral migration rates.

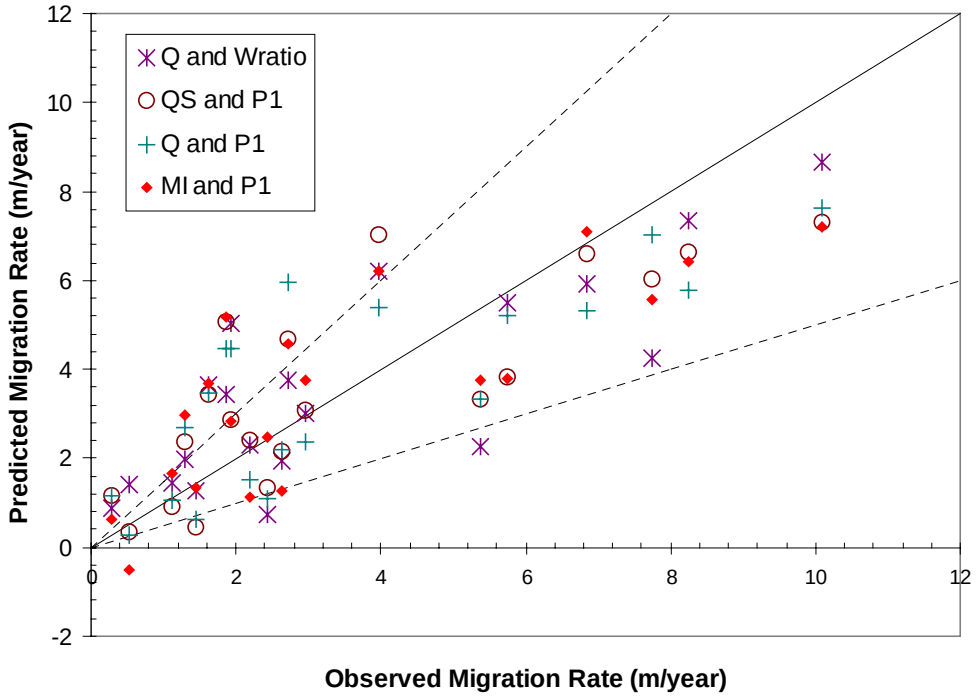

Figure 6-19 - Results of arithmetic regression models using reach-averaged data from 1918 to 1985.

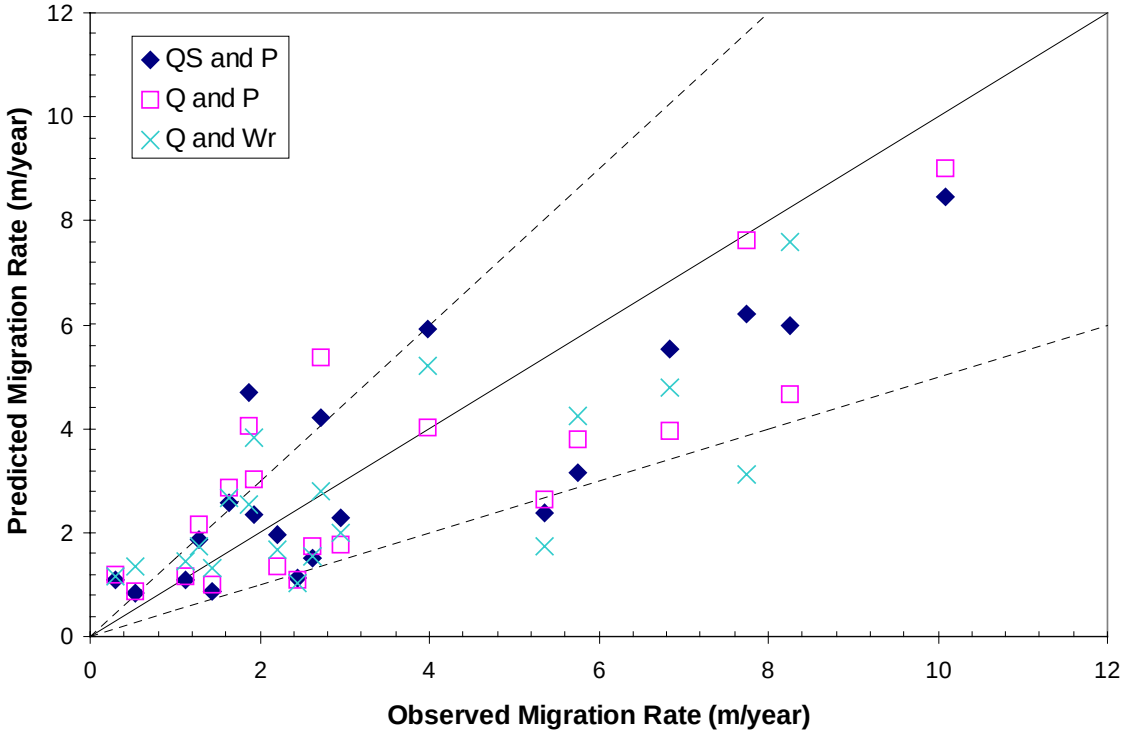

Figure 6-20 - Results of $\log_{10}$-transformed equations using reach averaged data from 1918 to 1985.

6.4 Summary

Three different methods of modeling lateral movement rates measured by width change and lateral migration were presented. The first was a simple estimation of migration rate and width change based on a percentage of channel width. A flat percentage of width did not model the migration rate well, but it did highlight the differences between the pre and post dam migration rates. The pre-dam rates generally were greater than 1% of the channel width. The post-dam migration rates were generally less than 1% of the channel width. This 1% differentiation corresponds to Brice's (1982) delineation between stable and unstable channels.

The second method was based on the premise that the rate of lateral movement decreased as the river moved toward an equilibrium condition. This was accomplished via an exponential model with empirically derived parameters applied to each of the reaches. The results fit the historic data well, with up to 98% of the variance in width change rate explained and 89% for lateral migration rate.

The final method was an application of multiple regression models to the reach-averaged and subreach-averaged data sets. The resulting equations do not explain more than 65% of the variance, but they do identify potentially important associations. The variables that contribute most to the variability in migration rate are flow energy and planform. Total stream power was the best measure of flow energy, and width ratio and sinuosity were both significant measures of planform. The active channel width was the most significant parameter in explaining the variance in the rate of change of active channel width. In general, the results using the reach-averaged data were better, indicating that there is more variability at the subreach level that is not accounted for in the parameters used in these models. The potential for application of these models in a predictive capacity is explored in the following chapter.

CHAPTER 7

DISCUSSION AND APPLICATIONS

This chapter assembles the analyses presented in Chapters 4, 5 and 6 into one big picture and discusses the results in the context of other rivers and other studies. The sections are outlined as follows:

7.1 - Summarizes the historic geomorphic analysis of the Cochiti reach, including the temporal trends of hydraulic, sedimentary and morphologic variables observed in the study reach from 1918 to 1992 are described. Compares these data and trends with those reported in other published studies from other rivers. Summarizes the spatial variability in the reach and provides a "snapshot" of the river for each of the survey dates from 1918 to 1992.

7.2 - Summarizes the results that provide evidence of a trend toward an equilibrium state exhibited by the Cochiti reach.

7.3 - Provides validation of the lateral movement models presented in Chapter 6 by predicting the lateral movement of the Cochiti reach between 1985 and 1992.

7.4 - Additionally, the models are tested with lateral movement data and compared with models from published studies of other rivers.

7.5 - Finally, the ecological implications and potential applications of the methods presented in this study to other rivers are explored.

7.1 Channel Adjustment

Chapters 4 and 5 quantified the inputs to the Cochiti reach and the resulting response. Each variable (e.g., slope, bed material) was analyzed separately. The next two sections combine the results from those chapters into a single "big picture". First the temporal changes are summarized and discussed. Then the spatial variability is illustrated through presentation of a "snapshot" of the river at each survey date from 1918 to 1992.

7.1.1 Temporal variability

Figure 7-1 presents a summarization of the temporal changes in the inputs to the Cochiti reach and the corresponding response of the channel.

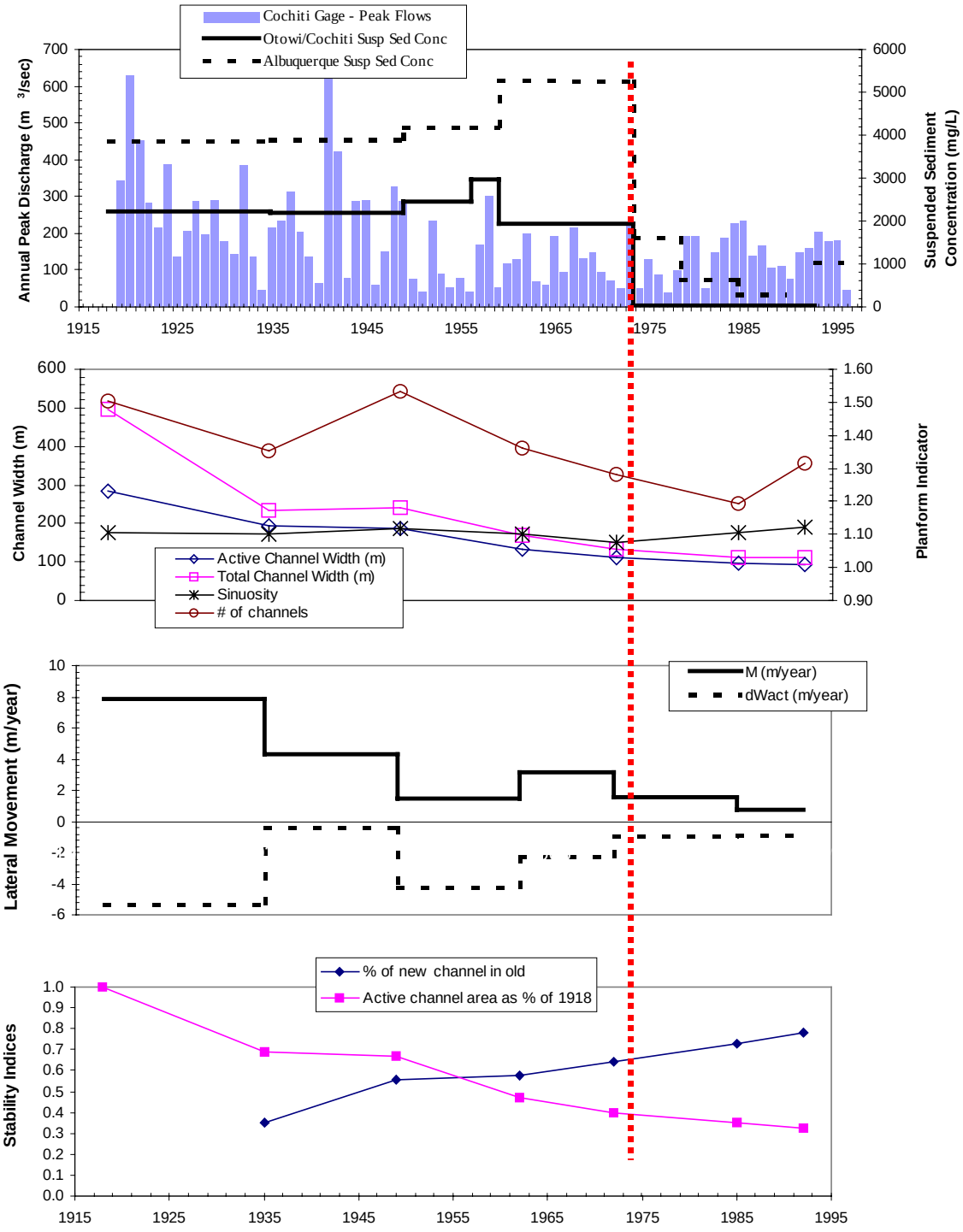

Figure 7-1 - Changes in Cochiti reach from 1918 to 1992.

The high energy and high sediment supply of the late 1800's and early 1900's created a wide, braided, multi-channel configuration that was laterally mobile. The sandy bed of the channel responded to the temporal variability in the sediment inputs by alternating aggradation and degradation with the net sum being gradual aggradation of the bed. As the peak discharges began to decrease (ca. 1930's) due to natural and anthropogenic factors the channel responded by narrowing, simplifying and reducing its rate of lateral migration.

Analysis of inputs to the Cochiti reach reveal that prior to construction of Cochiti dam, the peak flows were decreasing. Uncovering the reasons for the decline are beyond the scope of this study, however, changes in upstream agricultural diversion, land use and construction of upstream dams occurred during this time period (ca. 1920-1970) (Scurlock 1998). Also, climatic variations have been documented between the late 1800's and mid-1900's (Scurlock 1998; Crawford et al. 1993; Graf 1994). As a result, the variation in water discharge prior to construction of Cochiti dam are likely a result of combined natural and anthropogenic factors. The time period from the 1850's through the 1920's was characterized occurrences of rainfalls greater than 1.25 cm (0.5 inches) becoming more and more frequent with the trend peaking in the 1920's followed by a decline in frequency (Crawford et al. 1993; Graf 1994).

There is little evidence of sediment supply changes prior to construction of Cochiti dam, other than the obvious fact that if the water discharge decreased, the transport capacity of the flow probably decreased. Also, changes in bed material (Figure 4-14) and bed elevation (Figure 4-15) were minor during this time period. However, lateral changes in the channel were significant. The width declined in all sections of the study reach from 1918 to 1972 (Figure 4-18). Simplification of the channel also occurred during this time period as evidenced by increases in the width ratio (W_r = *Active channel width/Total channel width*. See Figure 4-28).

The temporal changes in the characteristics of the Cochiti reach can be summarized using Schumm's (1969) qualitative model of channel metamorphoses (See Section 2.3). The pre-dam period was characterized by decreasing water discharge, which according the Equation 2-3 should lead the following changes:

$$Q^- \rightarrow W^-, d^-, (W/d)^-, \lambda^-, S^+$$

Based on the discussion above, and the results in Chapters 4 and 5, all of the changes described by Equation 2-3 were seen in the Cochiti reach except for increasing slope. Slope is one of the least adjustable parameters and the time period for adjustment can be very long (Knighton 1998).

Following construction of Cochiti dam, the largest peak flows (>5,000 cfs or 142 m^3/sec) were attenuated (Figure 4-5), however, no significant decrease in peak flow was identified between the 1942-72 and 1973-96 time periods (Table 4-2). The sediment supply decreased dramatically following dam construction (Figure 4-9). The corresponding response of the channel was immediate coarsening of the bed material size (Figure 4-14) and bed degradation (Figure 4-16). Laterally, the study reach as a whole continued to narrow and stabilize. The planform shifted from a braided configuration as meandering became more pronounced with increasing sinuosity (Figure 4-27). Following construction of the dam, the lower peak flows combined with depleted sediment supply resulted in degradation and coarsening of the bed and continued narrowing and decreased lateral mobility. Post-dam lateral adjustments were not as pronounced as the vertical changes.

The post-dam period (1973 to 1992) was characterized by decreased water discharge and bed material load corresponding to Equation 2-7:

$$Q^-, Q_{sb}^- \rightarrow W^-, d^{\pm}, (W/d)^-, \lambda^-, P^+, S^{\pm}$$

Based on the findings of Chapters 4 and 5 as discussed above and presented in Figure 7-1, the reach narrowed and sinuosity increased following construction of the dam. According to Lagasse (1980) and Mosely and Boelman (1998, Draft) the width-depth ratio decreased for the Cochiti reach since construction of the dam. As seen in Figure 4-13, there is no evidence of a significant trend in the slope, though the increased bed degradation at the downstream end of the reach suggest an increase in channel slope. The increasing trend in sinuosity suggests that the meander wavelength is decreasing. These changes during both the pre and post dam periods suggest that dimension, shape, gradient, and pattern of the Rio Grande are responding to changes in water and sediment discharge as proposed by Schumm (1969).

The changes observed in the discharge regime and responding channel width suggest that the peak discharges play a significant role in determining the resulting shape of the channel. In this semi-arid climate, it does not appear that the channel is adjusted and formed by discharges that are relatively frequent, such as bankfull discharge as suggested by Wolman and Miller (1960) and supported by Surian (1999). Large, infrequent floods appeared to have a greater impact on the lateral adjustment and mobility of the Rio Grande.

7.1.2 Spatial Variability

Figures 7-1 through 7-7 provide snapshots in time of the entire Cochiti reach at the survey dates utilized in this study (1918, 1935, 1949, 1962, 1972, 1985, and 1992). These figures are an attempt to summarize the spatial variability in the channel that was explored in detail in Chapters 4 and 5. Several important features are emphasized by these plots. Tributary influences on lateral migration rates are evident. The most pronounced impacts are by Galisteo Creek and the Jemez River between 1918 and 1949 (Figure 7-2 and Figure 7-3) with migration rates as high as 80 m/year. Both of these tributaries were dammed, the Jemez in 1953 and Galisteo in 1970. It is likely that their diminished influence on migration rates is in apart a result of lfow and sediment regulation following dam construction. Impacts of other tributaries become more pronounced as the average migration rate decreases with time. Similar response to tributary inputs have been found in other studies as discussed by Gilvear and Winterbottom (1992). Zones of instability often exist downstream of tributaries and are characterized by larger bed material particle sizes with wider, shallower and steeper channels. Lagasse (1980) also noted the importance of tributary influence on the response of the Cochiti reach during the 1970's.

Reach 3 is the most stable through the entire time period studied. It is also geologically confined by a mesa on the right bank, as can be seen in the aerial photo in Figure 7-9. Between 1985 and 1992, the number of channels in Reach 4 increased. Inspection of the aerial photos and field observations show that the channel is becoming more stable and entrenched into narrower channels. The mid-channel bars transitions into vegetated islands as the combined effects of bed degradation and reduced peak flows eliminated inundation of the bar surfaces. The photo in Figure 7-9 illustrates this process. Other changes between 19185 and 1992 included widening of Reaches 2 and 3 over significant portions.

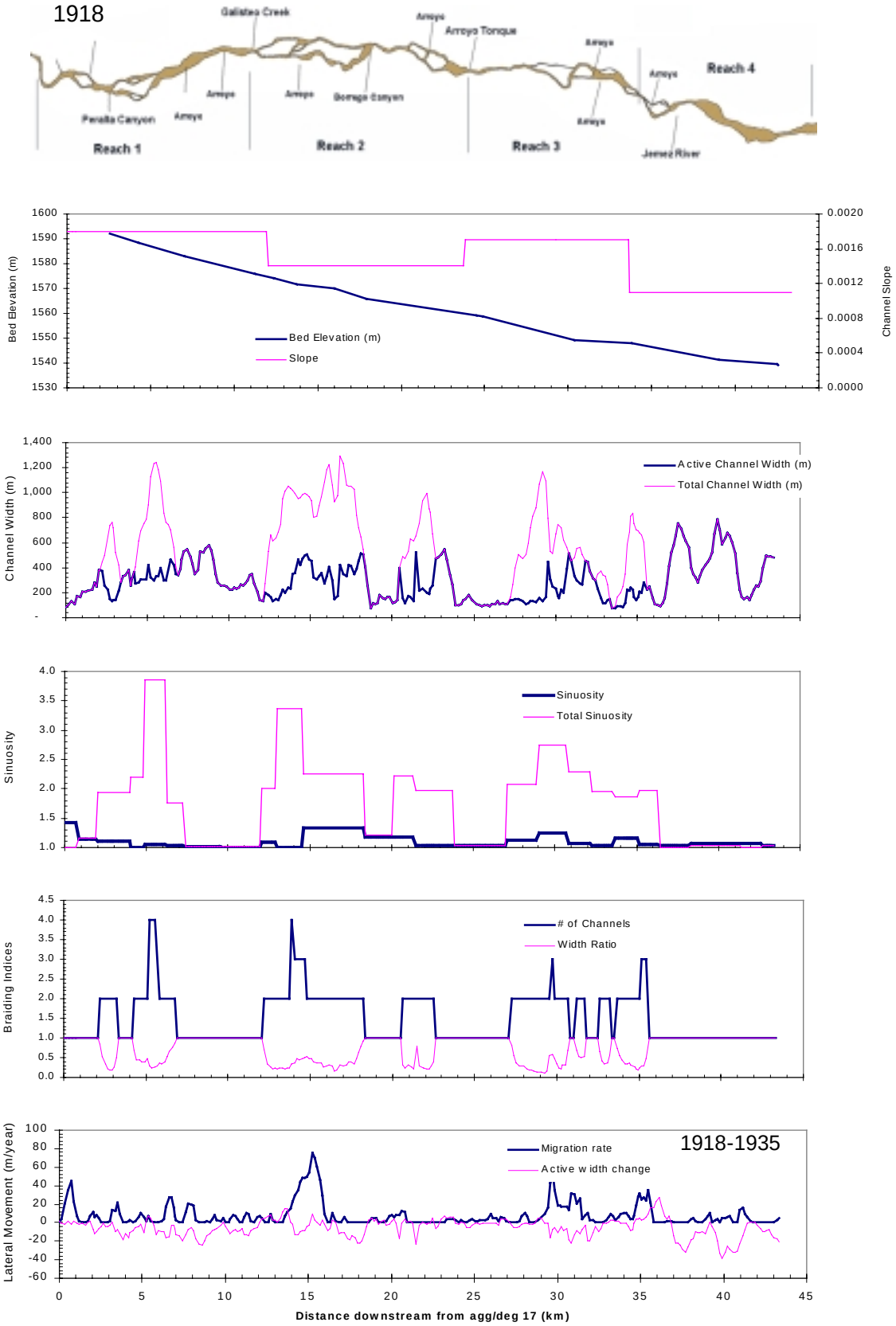

Figure 7-2 - Cochiti reach 1918

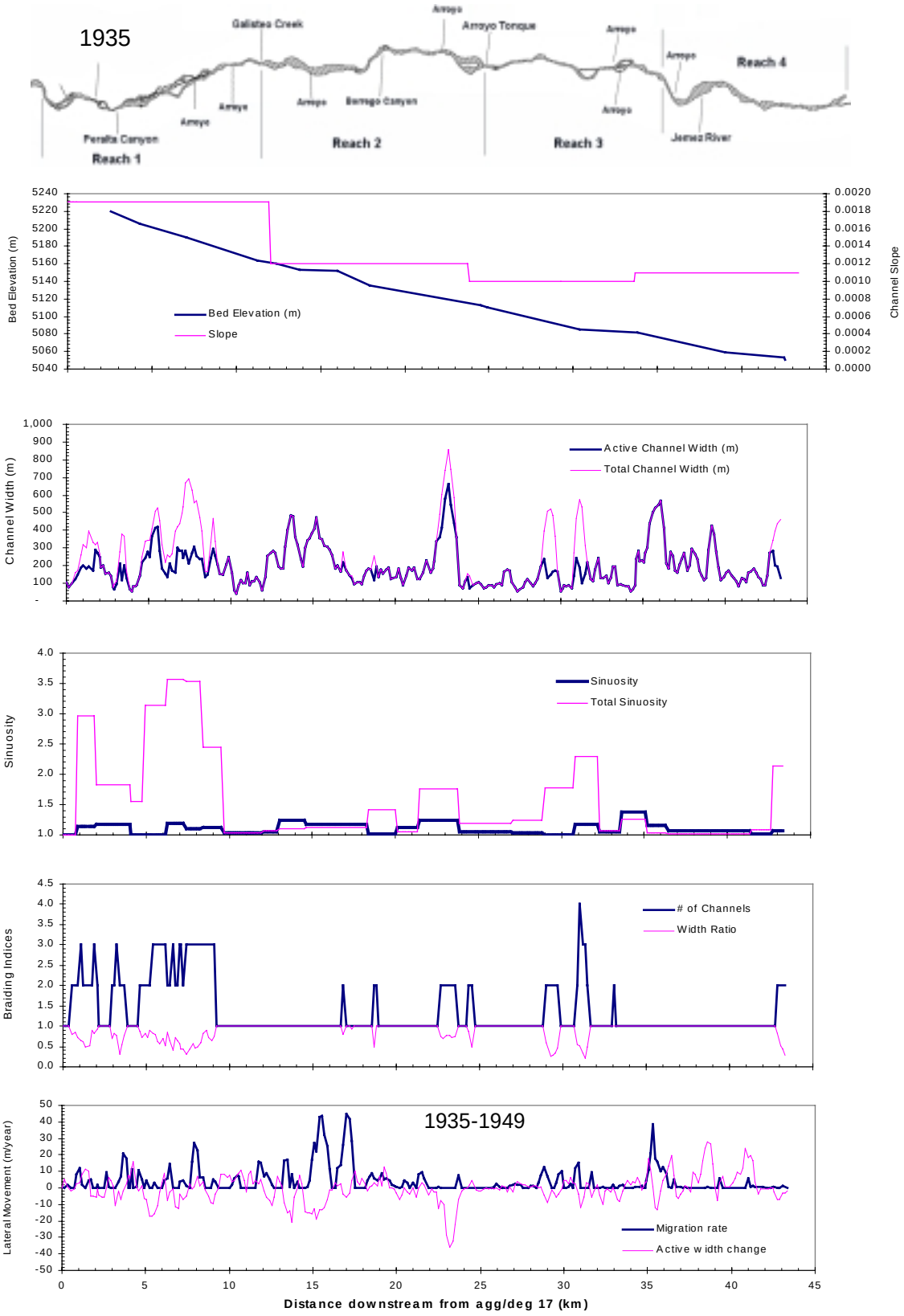

Figure 7-3 - 1935 Cochiti reach

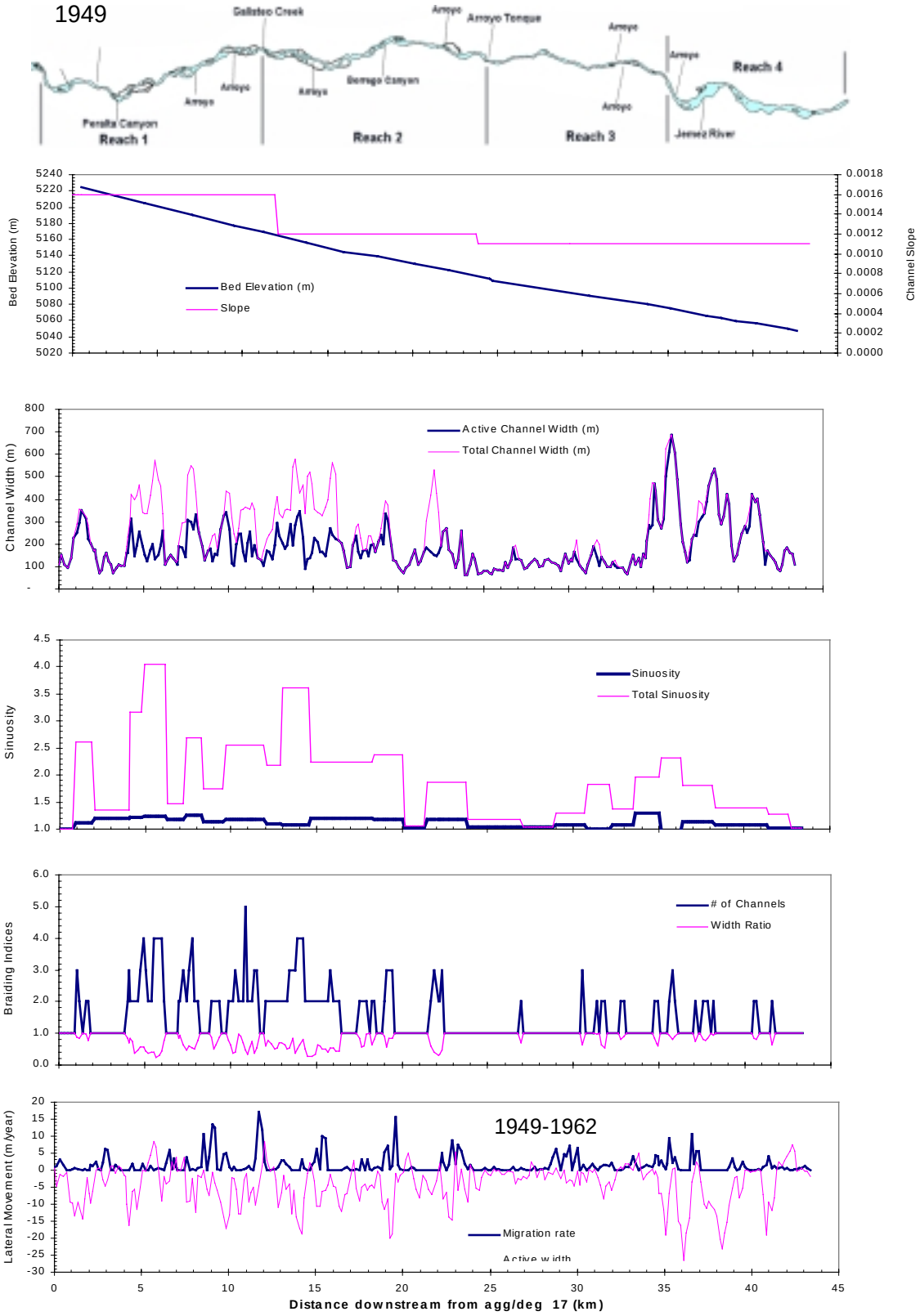

Figure 7-4 - 1949 Cochiti reach

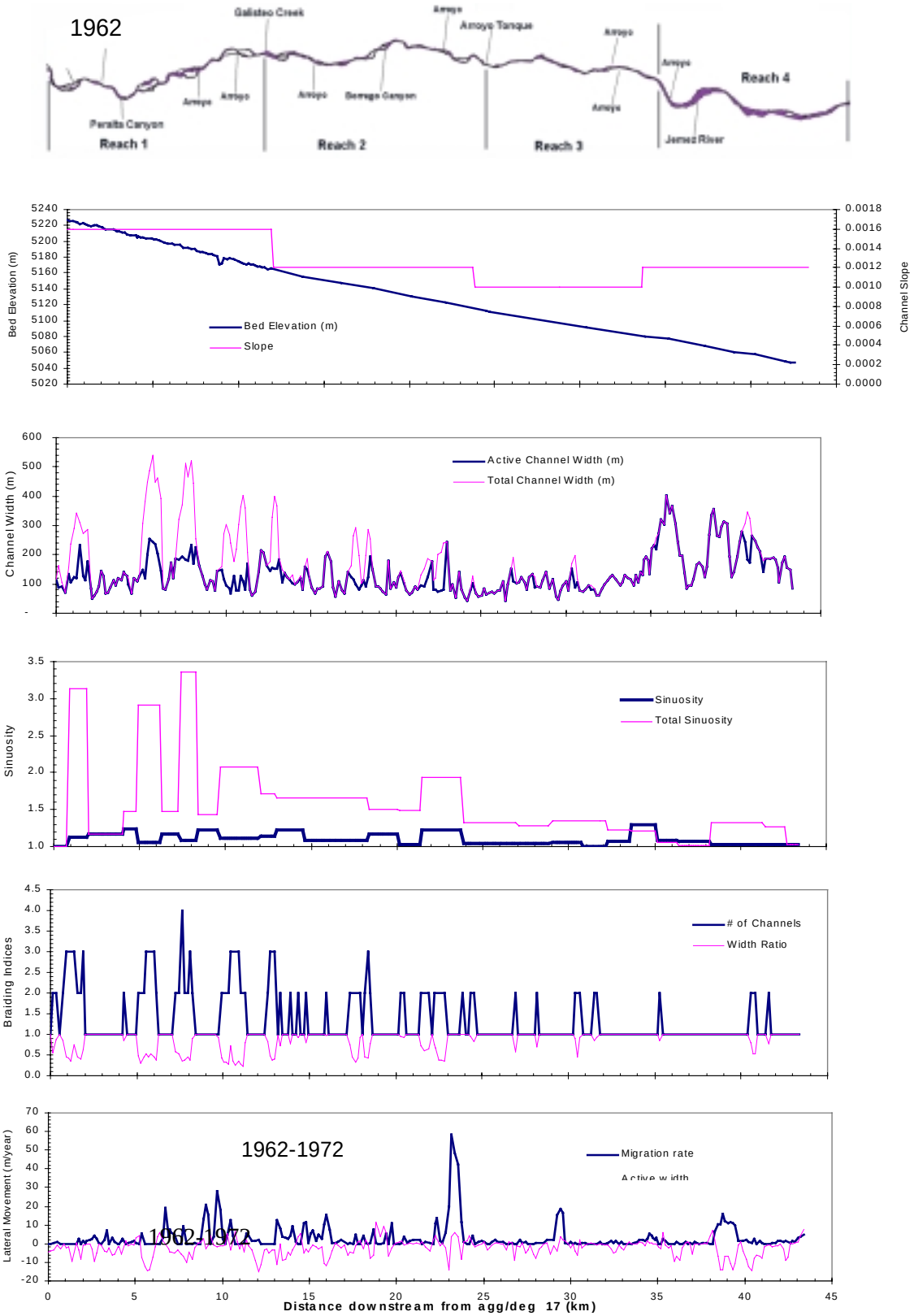

Figure 7-5 - 1962 Cochiti reach

Figure 7-6 - 1972 Cochiti reach

Figure 7-7 - 1985 Cochiti reach

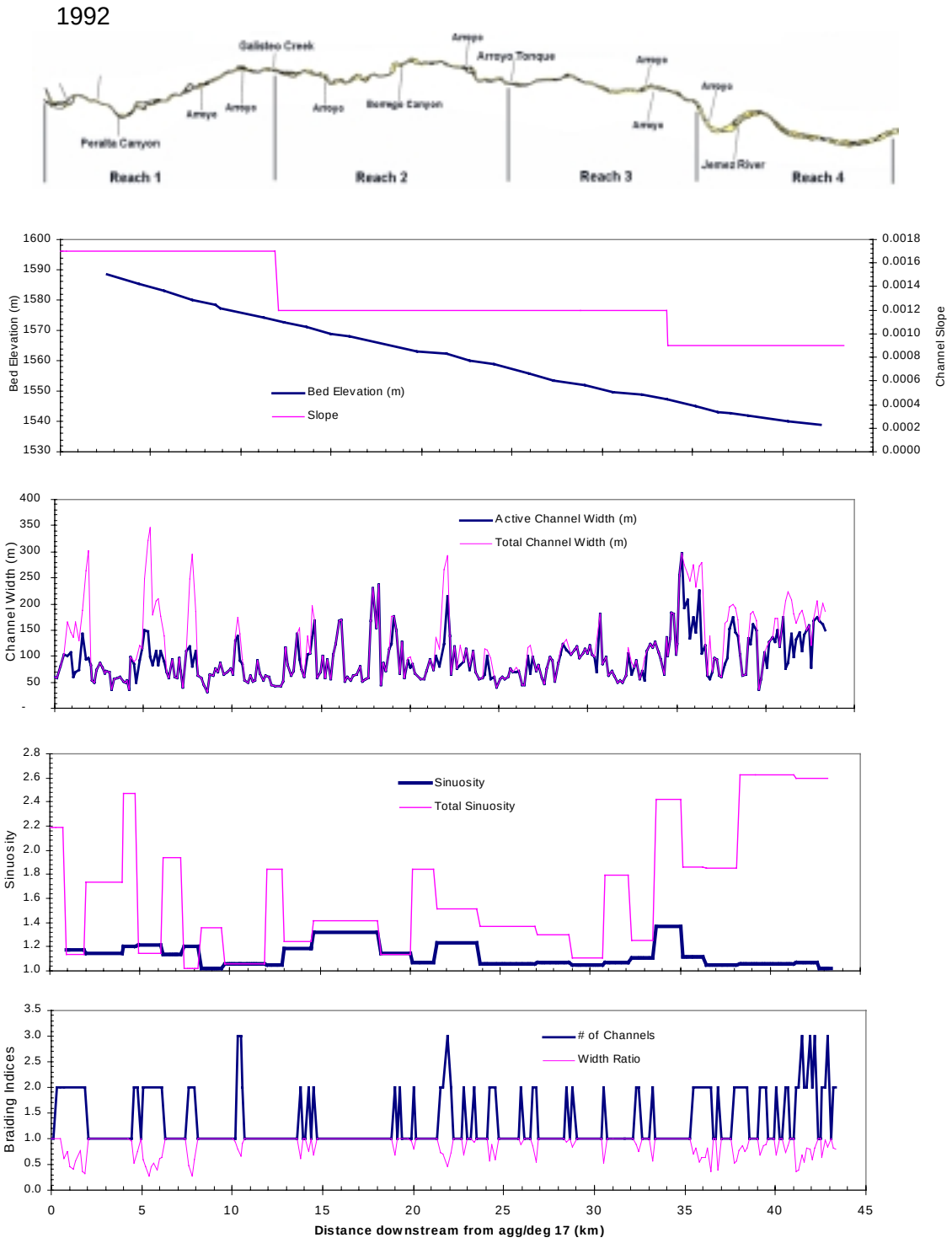

Figure 7-8 - Cochiti reach 1992

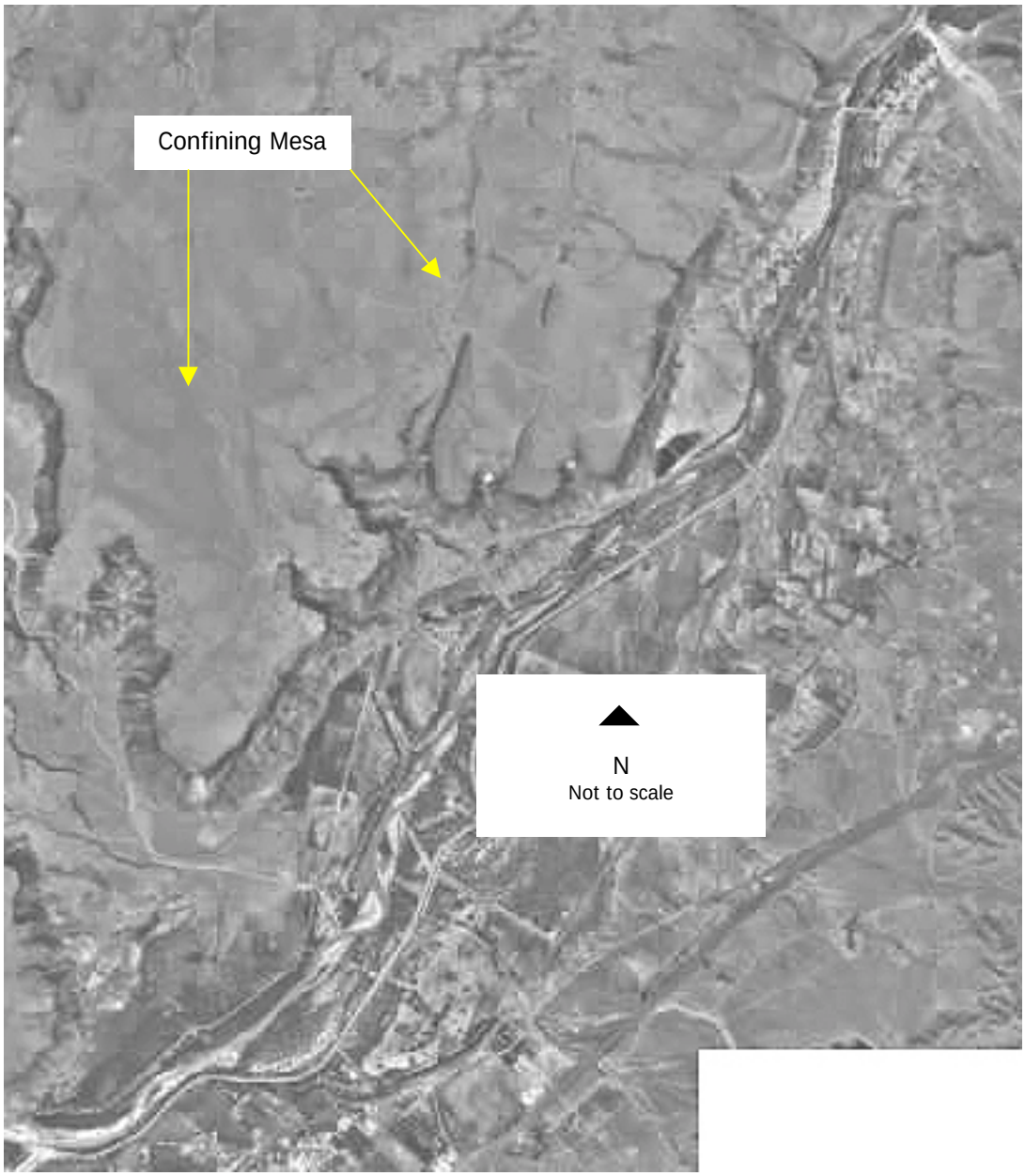

Figure 7-9 - Aerial photo of Reach 3 - Arroyo Tonque to Angostura Diversion dam.

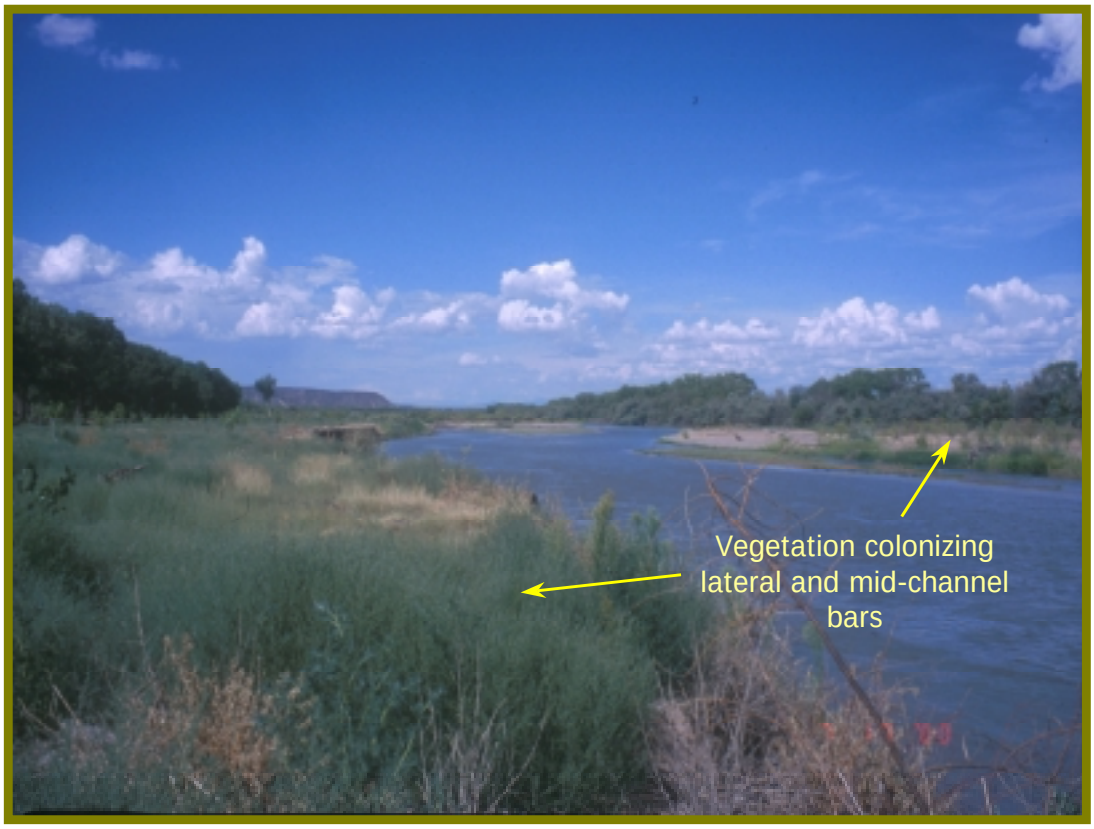

Figure 7-10 - Stabilization of mid-channel and lateral bars in Reach 4. Photo is looking upstream from the right bank near CO-27 (July 2000).

7.2 Comparison of adjustment with other studies

The simplification of the Rio Grande as measured by active channel area are comparable to those seen on the Platte River between 1938 and 1995 (Johnson 1997, 1998). Following a significant decline in active channel area and subsequent stabilization in area, some sections of the Platte River increased in active channel area between 1988 and 1995. Johnson (1997) suggests that the Platte may have reached a new equilibrium after adjusting to past effects of channel narrowing and woodland expansion. The largest dams on the Platte were constructed over 50 years ago suggesting that adjustment to a state of dynamic equilibrium took about 20 years. Johnson (1997) also found that the greatest adjustments in channel area occurred in areas closer to the source of water and sediment reduction, i.e., diversions and dam.

In order to compare the movement rates computed in this study with published rates, an average of the bankline changes were used rather than the sum of the bankline changes. This was accomplished by dividing the true migration rate, *M*, by two. Additionally, the reach averaged

rates were averaged over the pre (1918 – 1972) and post-dam (1972 – 1992) time periods. A weighted average was performed using the length of the time period as a weight.

The average pre and post dam migration rates are presented in Table 7-1 along with migration rate data from other rivers impacted by dams. The channel mobility on the Cochiti reach as a whole was 3.6 times greater prior to impoundment than after, which is comparable to the findings of others studying the effects of similar flow regulation. The other data presented in this table are for meandering alluvial rivers, except for the Hanjiang River in China, which was wandering-braided prior to regulation (Xu 1997b).

Reaches 3 and 4 of the Cochiti reach exhibit the greatest changes between pre and post dam rates. Some differences are expected from the variability in methods of measurement. It is possible that averaging the right and left bank movement results in a lower rate, but this does not effect the pre/post ratio, which would be high even if the sums of bankline movements were used.

Table 7-1 - Pre and post dam migration rate data.

River	*Location*	*Pre-dam migration rate (m/yr)*	*Post-dam migration rate (m/yr)*	*Pre/Post*	*Reference*
Hanjiang	China	7.6	2.1	3.6	Xu (1997b)
Milk	D/s from Fresno Dam, MT	1.7	0.5	3.4	Bradley & Smith (1984)
Missouri	D/s from Garrison Dam, ND	5.6	1.3	4.3	Johnson (1992)
Missouri	Ft. Peck to Brockton, MT	6.6	1.8	3.7	Shields et al (2000)
Rio Grande	D/s from Cochiti Dam, NM				This study
	Reach 1	2.1	0.8	2.5	
	Reach 2	3.3	1.0	3.2	
	Reach 3	1.8	0.3	6.1	
	Reach 4	1.6	0.2	8.6	
	Entire Cochiti reach	2.3	0.6	3.6	

The pre and post dam Cochiti reach data can be compared to the published data from Table 2-3; these are plotted in Figure 7-11. Most of the published data are for meandering streams and rivers, but the Brice data set and others contain a few measurements for braided rivers. Data from the Brahmaputra and the Mississippi rivers were removed from the analysis due to the uniqueness of those systems. The weighted averages of M, using average bankline change (M_{avg}) were used and were also normalized by the channel width for comparison with other studies. It can be seen that the rates from the Cochiti reach (Figure 7-11) fall well within the general distribution with perhaps higher widths and lower migration rates than some of the other studies. The pre-dam rates and widths are higher than post-dam.

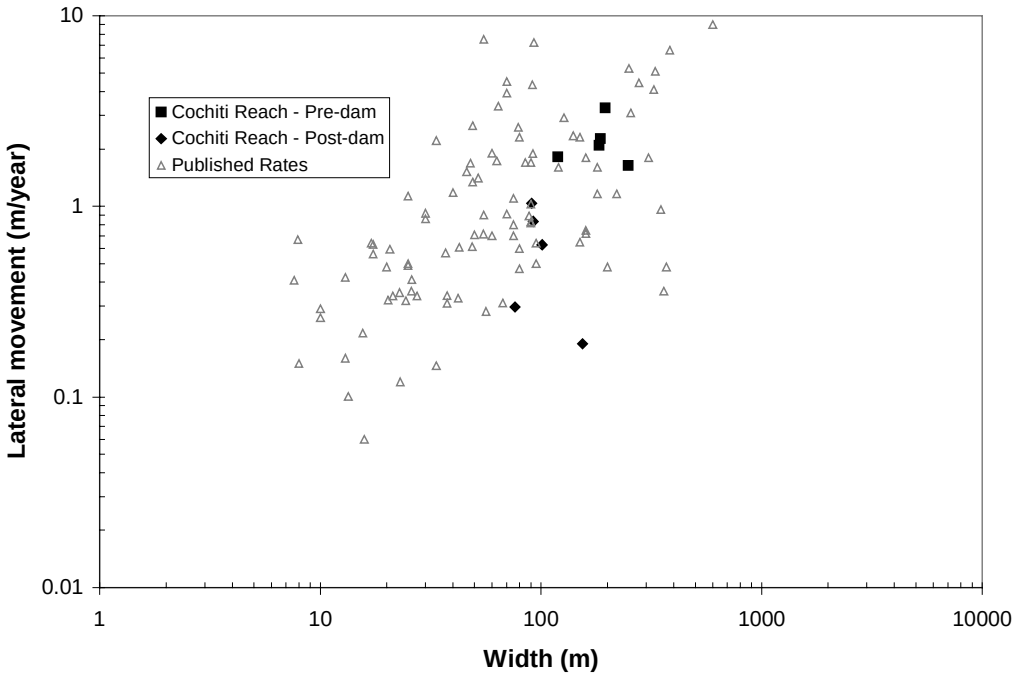

Figure 7-11 - Cochiti reach pre and post dam width and lateral movement data plotted with other published results.

Comparison between published rates and those measured on the Cochiti reach is complicated by the differing methods of calculation and use of the terms "mean" and "maximum" in reporting the rates. The mean value, minimum, maximum and 25th, 50th, and 75th, quartiles were calculated for the Cochiti reach data and the other published data (as shown in Table 2-1). The results of this comparison (Figure 7-12) show that the pre-dam values of M_{avg} are greater than the other published data. The post-dam Rio Grande data fall below the median value.

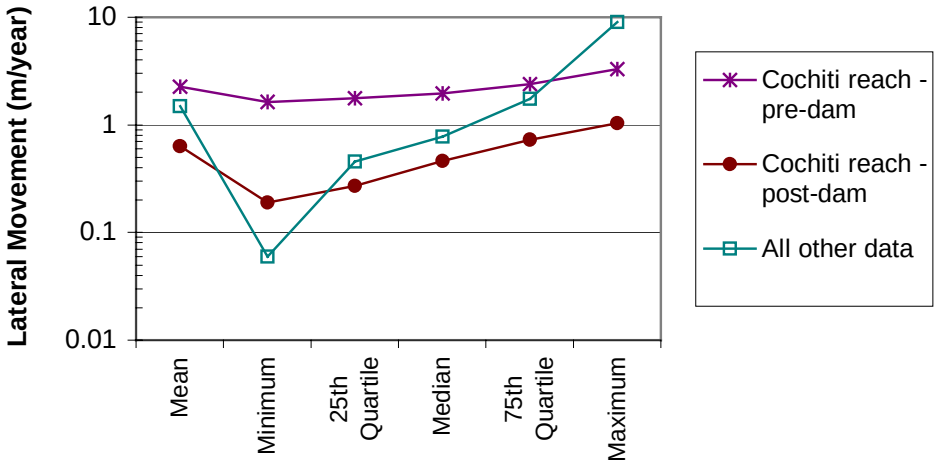

Figure 7-12 - Comparison of Rio Grande lateral movement rates with other published rates.

When the lateral movement rates are expressed as percent of the channel width (Figure 7-13), the Rio Grande movement rates are lower relative to the rest of the data because the pre-dam channel widths of the Cochiti reach are large. All of the Cochiti reach both pre and post dam fall below the median except for the pre-dam reach 2.

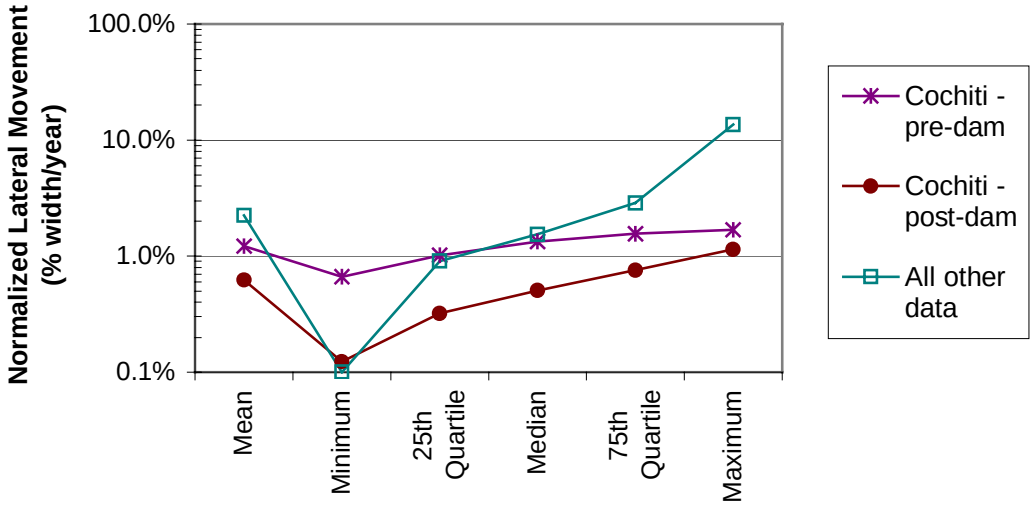

Figure 7-13 - Comparison of Rio Grande normalized lateral movement rates with other published rates.

7.3 Equilibrium?

Measurements performed in this study clearly show that during the early, pre-dam period, rates of lateral movement were high, the channel bed underwent cycles of aggradation and degradation with a net aggradational trend, and the width of the channel was significantly larger than equilibrium widths predicted by hydraulic geometry equations (Figure 4-24). Defining an equilibrium state by consistent "mean measurable behavior" would suggest that the pre-dam channel was not in a state of dynamic equilibrium and was undergoing true channel change (Hooke 1977). Schumm's (1969) hypothesis described above is for "stable" alluvial channels, i.e., ones that have shown no progressive channel adjustments during the last 10 years of record. The channel changes proposed in Schumm's model are responses to alterations in hydrologic or sediment regime. The time period required for a channel to complete its adjustment to a hydrologic change may be long, resulting in an extended period of "instability" characterized by considerable bank erosion and lateral shifting (Schumm 1969). The changes in the characteristics of the Cochiti reach support the concept that the river was undergoing a metamorphosis from one stable state to another in a manner that is consistent with the changes in the hydrologic regime. The variability in lateral movement and the measured changes in input

conditions, prior to construction of Cochiti Dam suggest that the channel was undergoing adjustment to a changing hydrologic regime.

Construction of Cochiti dam was the zenith of man's attempts to stabilize the Rio Grande and succeeded in decreasing the mobility of the channel. Prior to dam construction, the Corps channelized the river and attempted to stabilize the banks with jetty-jacks and levee construction with limited success. Since construction of Cochiti dam, localized bank protection measured have been employed, such as rip-rap on the outer banklines of bends (in the Santo Domingo reach during the late-1980's), but other than that the channel has been left to migrate across the floodplain within its levees since the 1960's. Determining exactly which impacts, either human induced or natural have resulted in decreased lateral mobility of the channel may be left to speculation. However, construction of Cochiti dam and the resulting incision of the channel downstream was clearly the final straw that pushed the channel into its current narrow, deeper, and faster configuration.

Regardless of how or why the channel has become stable, it is clear that its degree of stability has increased and that its rate of lateral change decreased. This evidence validates the Simons-Albertson (1963) and Julien-Wargadalam (1995) estimates of equilibrium width and shows that an exponential model of width change may be a useful tool for some channels experiencing regular declines in width (Williams and Wolman 1984). Additionally, this conclusion is corroborated by Lagasse (1980) who concluded that the section of the Rio Grande between Cochiti dam and Angostura diversion dam were approaching a stable state, while the reach downstream from the Jemez River was still in a period of adjustment.

The post-dam "stable" state is not necessarily a natural state. Flow regulation by the dam created a discharge regime that is not truly a bankfull discharge, resulting in indeterminacy regarding the true dominant discharge. Bank erosion is primarily caused by erosion at the toe of the slopes and mass wasting of the bank material. Flows released by the dam are not large enough to inundate the flood plain or even reach the top of the bank in many areas.

7.4 Lateral Mobility Models

Three models were developed (Chapter 6) to describe the historic changes in lateral migration and width change rates. These models were calibrated using the 1918 to 1985 Cochiti reach data. The 1985-1992 data were reserved for validation of the models. The results of the validation are presented and discussed in this section. The modeling approach consisted of three levels of models for each measure of lateral movement: migration and width change.

The first model is a very crude, back-of-the envelope calculation assuming that the movement rate is a percentage of the active channel width. The second model is based on the assumption that the rate of change of width increases with deviation from equilibrium width. An exponential model was empirically fit to the 1918-85 width data and used to predict the 1985-92 width change. Using a similar concept for migration rate based on deviation from equilibrium width, the migration rates were also predicted. Different means of empirically estimating the rate constants and equilibrium width were employed.

The third model employed multiple regression analysis with stepwise selection to identify significant associates between either migration rate or active channel width change and different measures of flow energy, sediment supply, bed material and planform. Using the 1918 to 1985 data, the models with the highest R^2-value were selected for validation with the 1985 to 1992 data.

The validation results for migration rate are presented in Table 7-2 and Figure 7-14. The best estimation of the 1985-92 migration rate was using the multiple regression equations. The model combining discharge and width ratio and the model using only the mobility index produced the smallest error in predicting the 1985-92 rates. Predictions of migration rates for each of the four reaches using four of the multiple regression models are presented in Figure 7-15 and Figure 7-16.

The results for prediction of the 1992 width are presented in Table 7-3 and Figure 7-17. All of the computations for width change presumed that the width change was negative, therefore the channel narrowed. As a result, for all but two of the models, the widths of reaches 2 and 3 are underpredicted because those reaches widened between 1985 and 1992. On average, the best models (minimum error) were the simple estimation of width change as percentage of previous width, and the regression result including unit stream power and active channel width.

The regression equations were used to predict the rate of change of active channel width (dW_{act}). The best results were achieved using a $\log_{10}$- transformation, which required that only the absolute value of the width change be predicted. The regression equation that produced the least error combining unit stream power and active channel width, as mentioned above, is:

$$dW_{act} = 9.23x10^{-8}\left[S\sqrt{Q}\right]^{-1.550} W_{act1}^{\ 2.182} \quad \text{..... (7-1)}$$

where: dW_{act} = rate of change of active channel width (m/year);

$S\sqrt{Q}$ = unit stream power; and

W_{act1} = active channel width at beginning of time period.

Equation 7-1 can then be used to estimate the active channel width at the end of the time period (W_{act2}):

$$W_{act2} = W_{act1} - \left(\Delta t \cdot dW_{act}\right)$$

$$W_{act2} = W_{act1} - \left(\Delta t \cdot 9.23 \times 10^{-8} \cdot \left[S\sqrt{Q}\right]^{1.550} \cdot W_{act1}^{\,2.182} \right) \quad \text{.....(7-2)}$$

where: Δt = length of time period (years).

Similarly, the regression equation resulting from using only the active channel width is:

$$dW_{act} = 7.87 \times 10^{-4} \cdot W_{act1}^{\,1.536} \quad \text{..... (7-3)}$$

Equation 7-3 can also be used to estimate the active channel width at the end of the time period (W_{act2}):

$$W_{act2} = W_{act1} - \left(\Delta t \cdot 7.87 \times 10^{-4} \cdot W_{act1}^{\,1.536}\right) \quad \text{.....(7-4)}$$

The results of application of Equations 7-2 and 7-4 to reaches 1 through 4 of the Cochiti reach from 1918 to 1992 to estimate the active channel width are presented in Figure 7-18.

Measurement of lateral channel variables at the subreach level did not increase the accuracy of the lateral movement predictions. In fact, the high variability in these measurement highlight that there are other, more localized factors, such as bank stability and vegetation that impact channel adjustment at a smaller spatial scale.

Table 7-2 - Validation of migration rate models using the 1985-92 lateral migration rate results.

Equation	Reach #	Observed M (m/year)	Predicted M (m/year)	Error (pred - obs)/obs	Average Absolute Error
Simple Model		$M_{avg\text{-}obs}$	$M_{avg\text{-}pred}$		
$M_{avg} = 0.01\ W_{act}$	1	0.34	0.90	169%	
	2	0.52	0.87	67%	
	3	0.36	0.73	103%	
	4	0.28	1.51	446%	196%
Exponential Models: $M_{pred} = k_2\ (W\text{-}W_e)$					
Best-fit k_2, W_e from dW_{act} model		M_{obs}	M_{pred}		
k_2=0.028, W_e=63	1	0.67	0.42	-38%	
k_2=0.036, W_e=41	2	1.04	1.89	82%	
k_2=0.059, W_e=68	3	0.72	0.72	1%	
k_2=0.021, W_e=124	4	0.55	0.01	-98%	55%
Best-fit k_2, W_e from Hydraulic Geom Eqn					
k_2=0.030, W_e=72	1	0.67	0.17	-74%	
k_2=0.045, W_e=78	2	1.04	0.66	-37%	
k_2=0.069, W_e=79	3	0.72	0.07	-90%	
k_2=0.016, W_e=85	4	0.55	0.63	15%	54%
Log_{10}-transformed regression Models:					
		M_{obs}	M_{pred}		
$M = 2.518\ MI^{0.708}$	1	0.67	0.65	-3%	
	2	1.04	0.47	-55%	
	3	0.72	0.51	-30%	
	4	0.55	0.62	12%	25%
$M = 0.004\ Q^{1.010}\ W_r^{-2.436}$	1	0.67	1.14	70%	
	2	1.04	0.89	-15%	
	3	0.72	0.84	16%	
	4	0.55	0.83	51%	38%
$M = 0.001\ Q^{1.270}$	1	0.67	0.94	40%	
	2	1.04	0.92	-12%	
	3	0.72	0.92	28%	
	4	0.55	0.98	78%	39%
$M = 6.268\ (QS)^{1.195}$	1	0.67	1.40	108%	
	2	1.04	0.73	-30%	
	3	0.72	0.90	26%	
	4	0.55	0.68	23%	47%
$M = 2.52\ (QS)^{1.064}\ P^{8.762}$	1	0.67	1.35	102%	
	2	1.04	1.61	54%	
	3	0.72	0.70	-3%	
	4	0.55	0.73	32%	48%

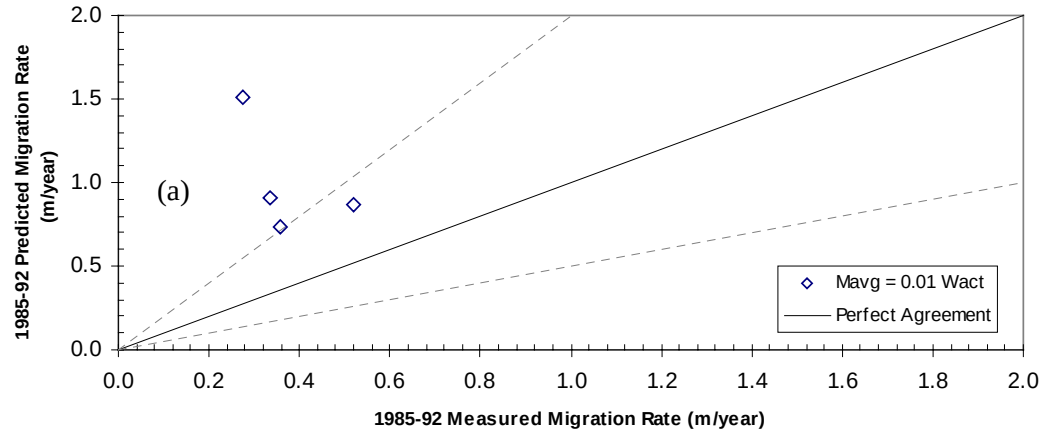

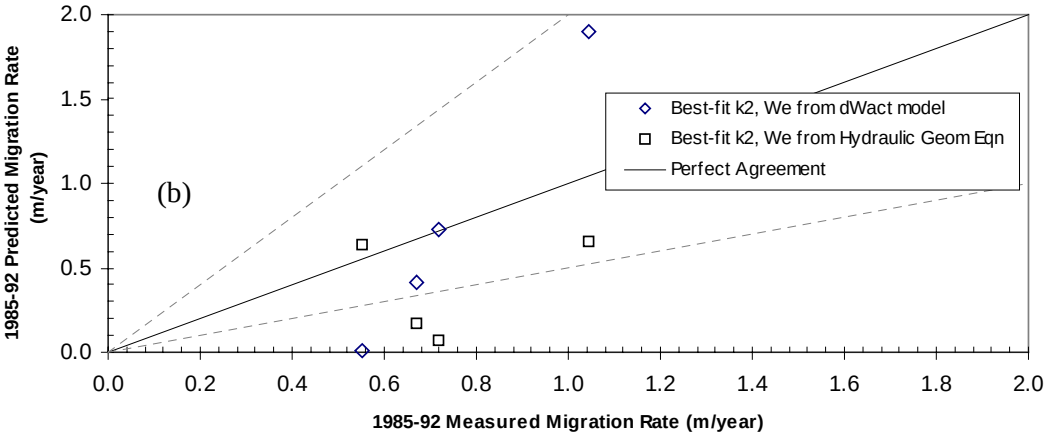

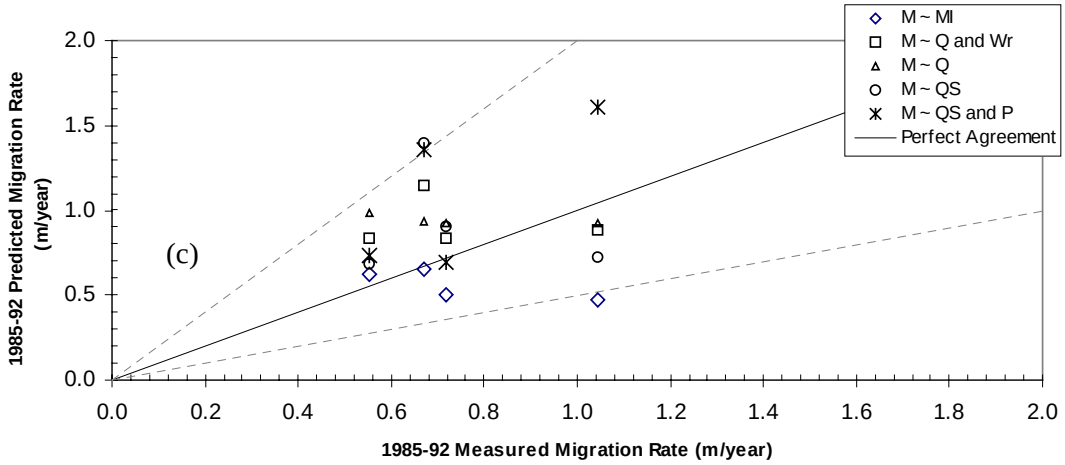

Figure 7-14 - Validation results for 1985-92 lateral migration rate of reaches 1-4 of the Cochiti reach, Rio Grande, NM. (a) Simplified model, (b) Exponential models, (c) Regression models.

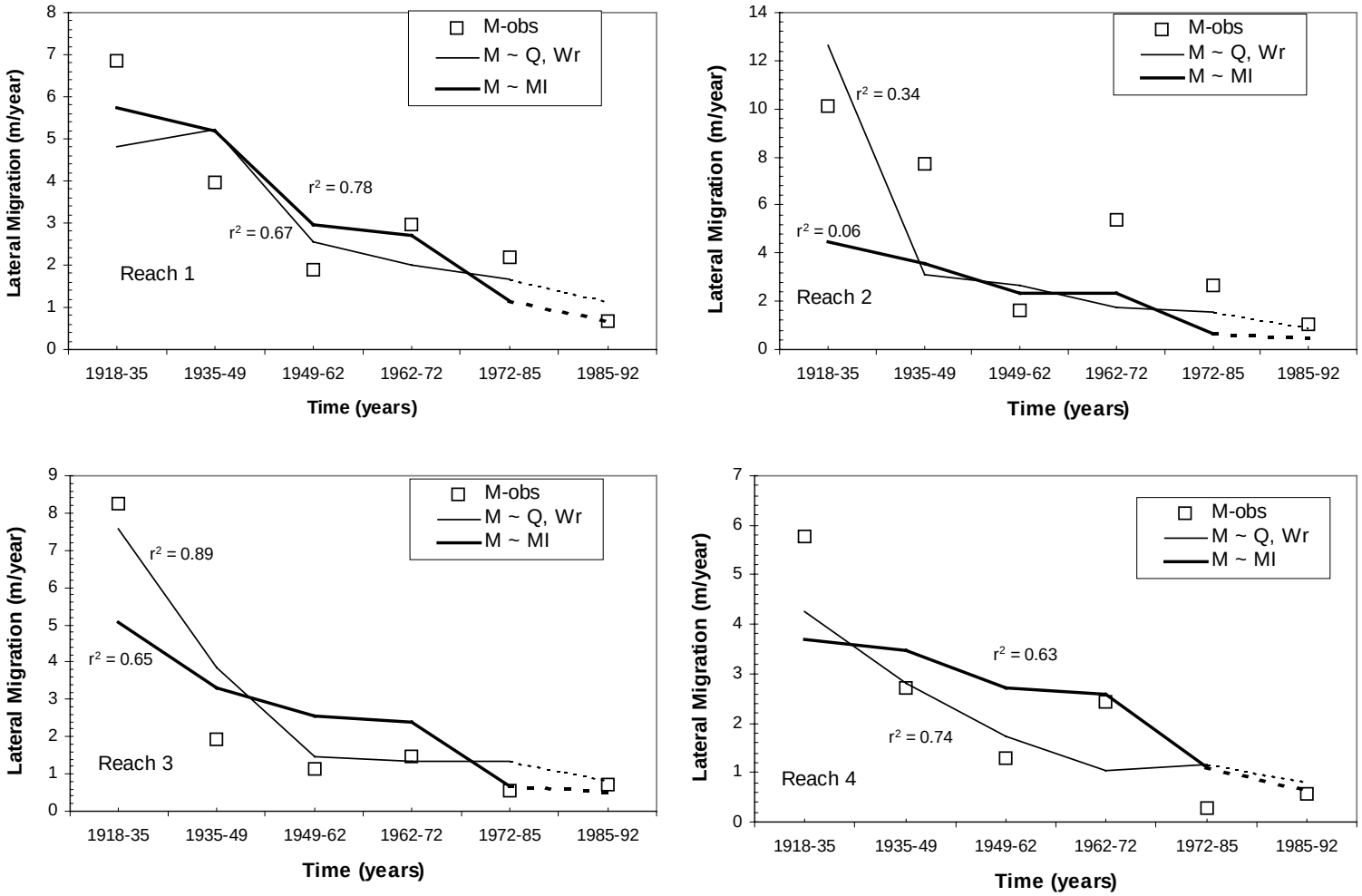

Figure 7-15 - Regression equations applied to the reaches 1 through 4 of the Cochiti reach. The solid line represents calibration with 1918-1985 data, and the dashed line represents the validation with 1985-1992 data. The r^2-values are computed for the entire time period.

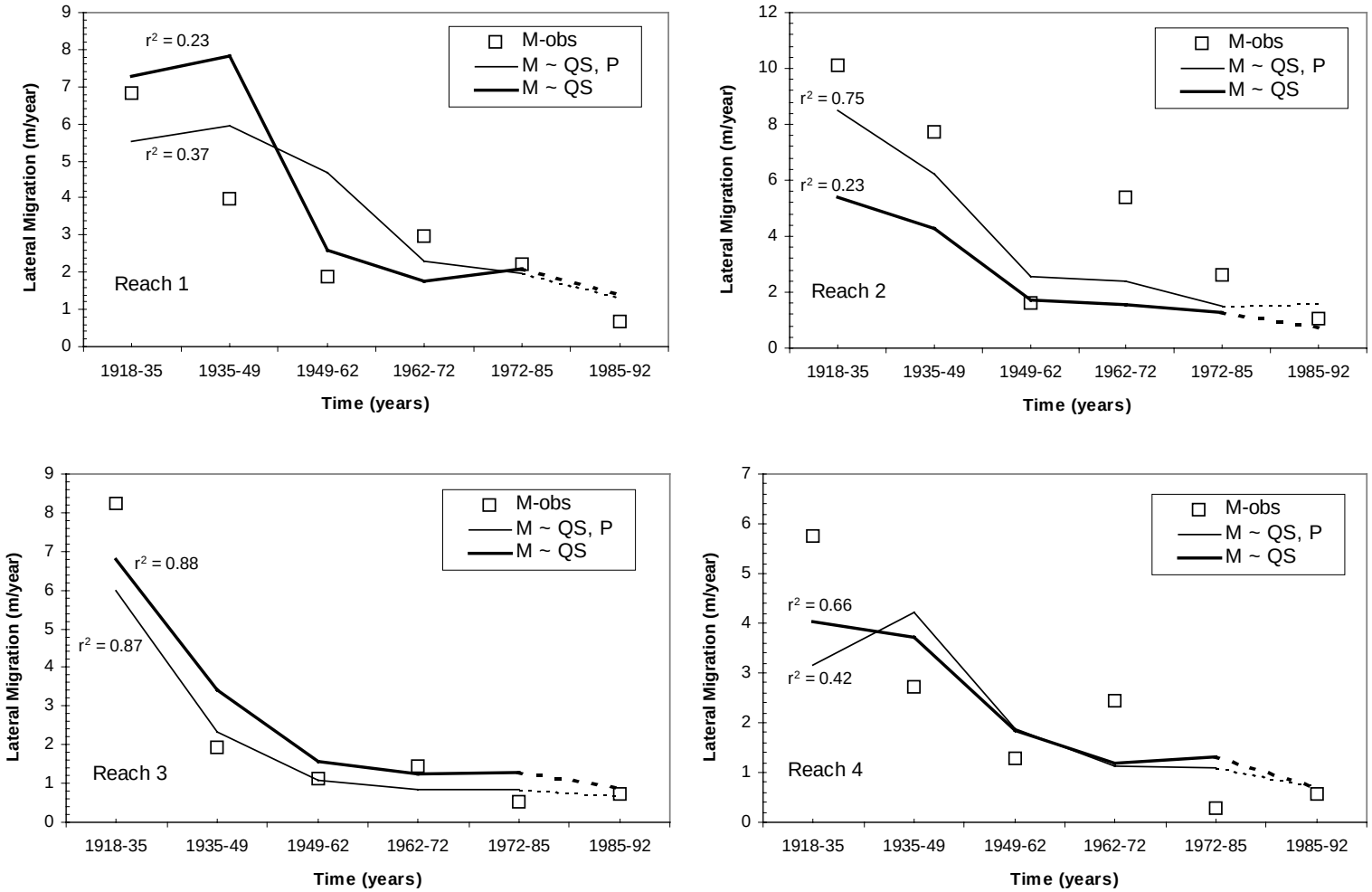

Figure 7-16 - Regression equations applied to the reaches 1 through 4 of the Cochiti reach. The solid line represents calibration with 1918-1985 data, and the dashed line represents the validation with 1985-1992 data. The r^2-values are computed for the entire time period.

Table 7-3 - Validation of width change models using the 1992 reach-averaged active channel width.

Equation	Reach #	1992 Active Channel Width (m)	Estimated 1992 Channel Width (m)	Error (pred - obs)/obs	Average Absolute Error
Simple Model		$W_{act\text{-}obs}$	$W_{act\text{-}pred}$		
$dW_{act} = 0.021\ W_{act\text{-}1}$	1	78	79	2%	
$W_{act\text{-}2} = W_{act\text{-}1} + dW_{act}$	2	93	76	-18%	
	3	80	64	-20%	
	4	124	132	6%	12%
Exponential Model (Equation 6-8):					
Empirical k_1 (from subreach data), best-fit W_e		$W_{act\text{-}obs}$	$W_{act\text{-}pred}$		
k_1=0.031, W_e=63	1	78	88	12%	
k_1=0.024, W_e=41	2	93	85	-9%	
k_1=0.041, W_e=68	3	80	74	-7%	
k_1=0.040, W_e=167	4	124	176	41%	17%
Empirical k_1 and W_e from reach-avg data					
k_1=0.026, W_e=59	1	78	95	21%	
k_1=0.018, W_e=38	2	93	105	13%	
k_1=0.034, W_e=77	3	80	86	7%	
k_1=0.033, W_e=140	4	124	159	28%	17%
Empirical k_1, W_e from Hydraulic Geom Eqn					
k_1=0.034, W_e=72	1	78	91	17%	
k_1=0.030, W_e=78	2	93	102	9%	
k_1=0.051, W_e=79	3	80	82	2%	
k_1=0.019, W_e=85	4	124	151	22%	13%
Log_{10}-transformed regression Models:					
		$W_{act\text{-}obs}$	$W_{act\text{-}pred}$		
$dW_{act} = 9.23 \times 10^{-8}\ (S(Q)^{0.5})^{-1.550}\ W_{act}^{2.182}$	1	78	86	10%	
	2	93	77	-17%	
	3	80	68	-15%	
	4	124	115	-7%	12%
$dW_{act} = 7.70 \times 10^{-6}\ (QS)^{-1.026}\ W_{act}^{2.288}$	1	78	82	5%	
	2	93	68	-27%	
	3	80	63	-21%	
	4	124	80	-36%	22%
$dW_{act} = 7.87 \times 10^{-4}\ W_{act}^{1.536}$	1	78	77	-1%	
	2	93	59	-37%	
	3	80	59	-27%	
	4	124	44	-64%	32%

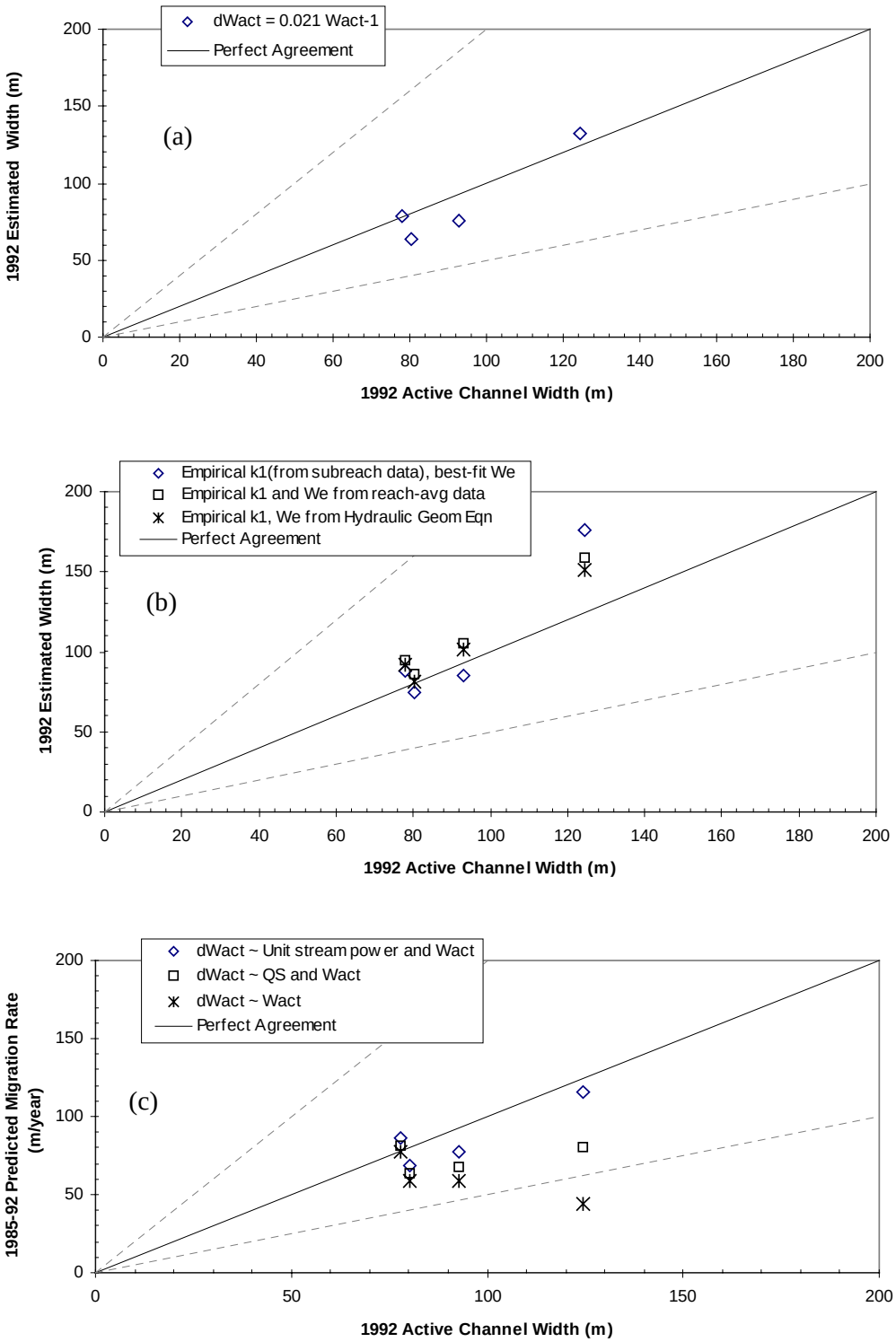

Figure 7-17 - Validation results for 1992 active channel width of reaches 1-4 of the Cochiti reach, Rio Grande, NM. (a) Simplified model, (b) Exponential models, (c) Regression models.

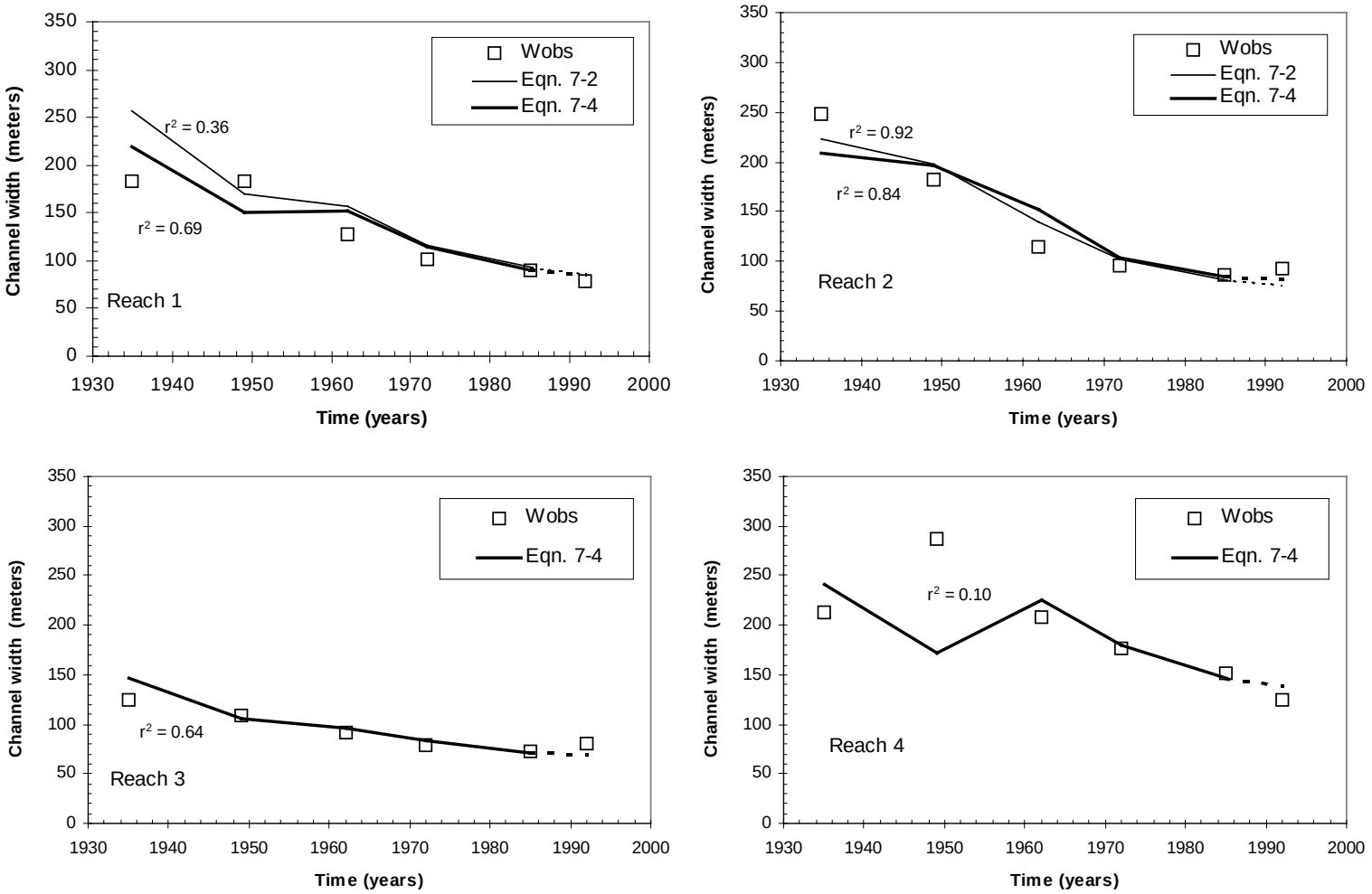

Figure 7-18 - Regression equations 7-2 and 7-4 applied to the reaches 1 through 4 of the Cochiti reach for active channel width estimation. The solid line represents calibration with 1918-1985 data, and the dashed line represents the validation with 1985-1992 data. The r^2-values are computed for the entire time period.

7.5 Comparison with other Rivers

Simple Model

Brice (1982) showed that different stream types (as defined in Figure 2-1) exhibit varying rates of lateral migration. Equiwidth channels generally exhibited smaller migration rates and were more stable laterally. Wide-bend channels, or meandering channels whose width varies downstream by at least a factor of two between bends and the straight sections between bends, and braided point-bar channels were the least laterally stable. Brice (1982) showed that a line could be drawn on a plot of channel width versus lateral movement (bank erosion) that divided most equiwidth channels from most wide-bend and braided point-bar channels (Figure 2-6). This line represents migration rates that equal 1% of the channel width ($M = 0.01\ W$).

Published lateral movement data (Table 2-1) are plotted against channel width, along with the Cochiti reach pre and post dam data in Figure 7-19. This is the same data plotted in Figure 7-11, but it is now grouped by channel pattern in an attempt to see where the Cochiti reach data and other published data fall within Brice's channel type classification and with respect to the 1% line. Brice's data are included and grouped using the braided, wide-bend and equiwidth stream types. Most of the other data are from meandering rivers, and there are a few other braided-river data points in addition to Brice's.

Most of the meandering rivers fall above the line, in the region that Brice suggested to be less laterally stable. It is expected that the rivers that scientists and engineers choose to study when they are concerned with lateral migration rates will be rivers that are active laterally. As a result, much of the data from other studies plot in the less stable region.

The pre-dam Cochiti reach data mostly plot above the line in the region of more mobile rivers. However, pre-dam reach 4 plots below the line because of its large width and lower migration rate. During this time period, it was more of a straight braided configuration, which Brice points out often fall below the curve because their channels are wide relative to their discharges. The post-dam data plot below the line in the zone of less mobile equiwidth rivers, except for reach 2, which is more mobile and plots just above the line.

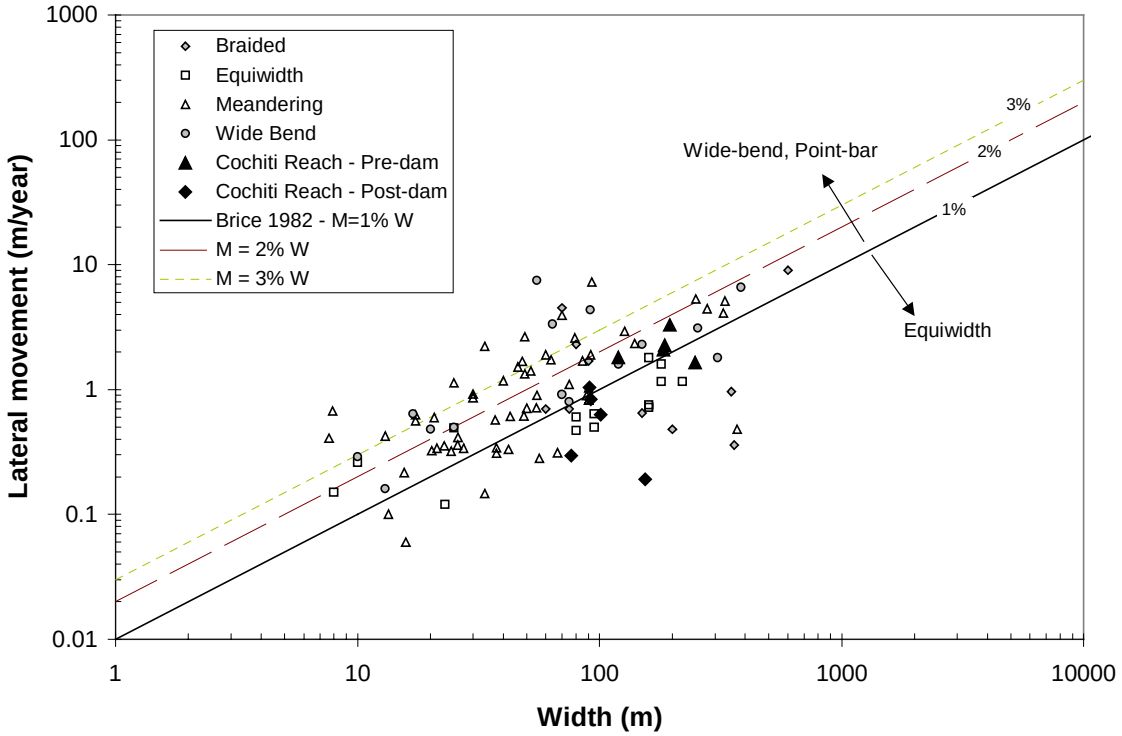

Figure 7-19 - Lateral movement rate in relation to channel width for different types of streams.

Exponential Model

To explore the possibilities of using the exponential method presented in section 6.2 to model width changes on other rivers that exhibited regular narrowing trends, the Williams and Wolman (1984) data for the Jemez River, Wolf Creek, the Arkansas River and the North Canadian River, Oklahoma were plotted. Figure 7-20 shows how the relationship between width change and width on the rivers described above compared with that observed on the Cochiti reach. The Williams and Wolman (1984) data are presented at individual cross-sections for different years following dam construction.

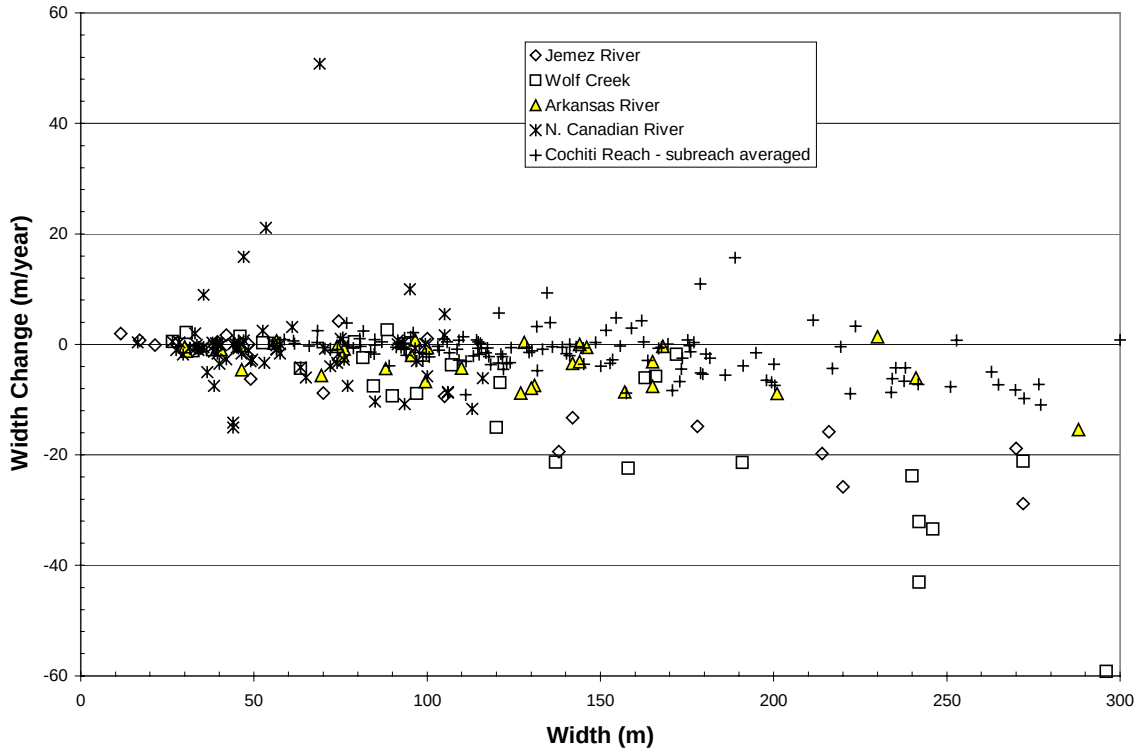

Figure 7-20 - Comparison of width vs. width change rate relationship between Cochiti reach and other published data. Non-Rio Grande river data are from Williams and Wolman (1984) and represent narrowing associated with dam closure.

In order to apply the exponential model to this other data, the values of k_1 and W_e need to be determined empirically, as it is clear the same values used in Cochiti would not apply. To estimate the values of k_1 and W_e, the data were reach-averaged for each year that the narrowing trend continued (Figure 7-21). The reach-averaged narrowing data from the Cochiti reach are plotted for comparison. The k_1-values from the different rivers vary considerably. The resulting models of width change are presented in Figure 7-22. For comparison, the r-square values from Williams and Wolman's (1984) hyperbolic model are presented in Table 7-4. Williams and Wolman (1984) model the width change at each cross-section, which is why there is a range of r-squared values. The exponential model was applied to the reach-averaged widths for each river. The r-square values are comparable to Williams and Wolman's (1984) results from their hyperbolic model, except for the Arkansas River, which resulted in a very poor fit using the exponential model.

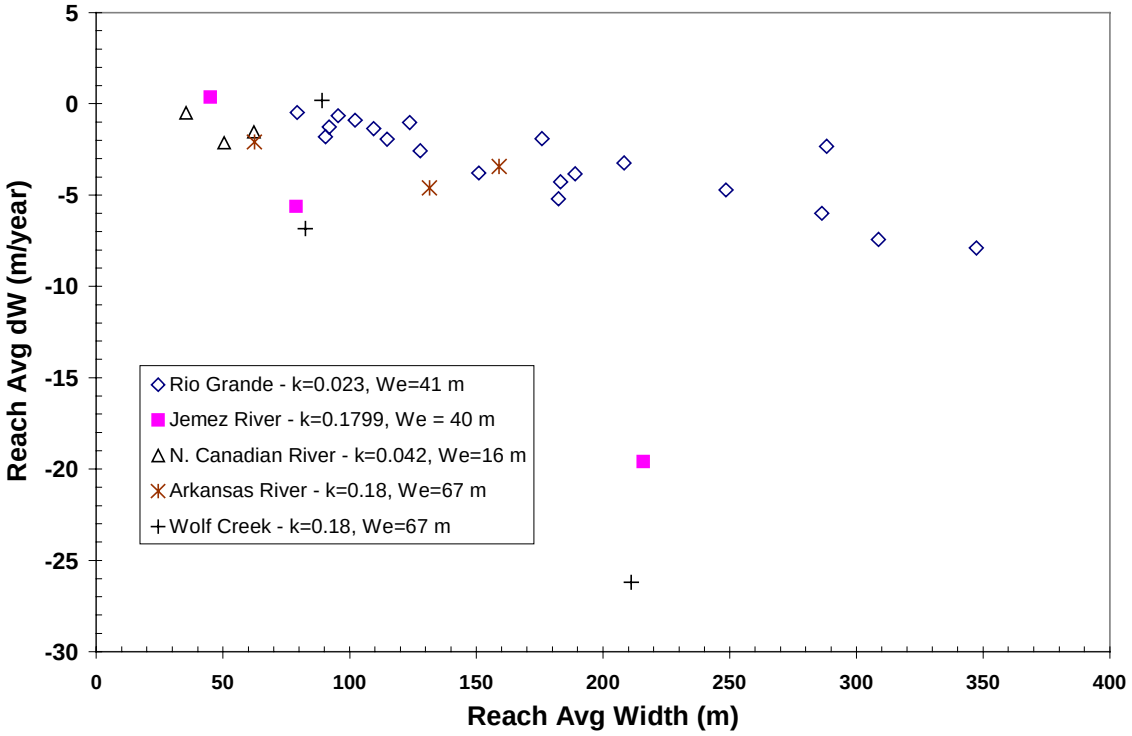

Figure 7-21 - Reach averaged channel width versus reach averaged annual change in width (m/year) for time periods where narrowing occurred (dW<0) except for last time period for the Jemez River, which widened 0.4 m/year. Non-Rio Grande data are from Williams and Wolman (1984) and represent narrowing associated with dam closure.

Table 7-4 - Comparison of width models between the exponential model and the hyperbolic model from Williams and Wolman (1984).

	r^2 Values	
River	**Exponential Model (Figure 7-3)**	**Hyperbolic Model from Williams and Wolman (1984)**
Jemez River, New Mexico, Jemez Canyon Dam	0.78	0.37 – 0.83
Arkansas River, Colorado, John Martin Dam	0.0	0.79 – 0.99
Wolf Creek, Oklahoma, Fort Supply Dam	0.84	0.34 – 0.99
North Canadian River, Oklahoma, Canton Dam	0.94	0.30 – 0.99

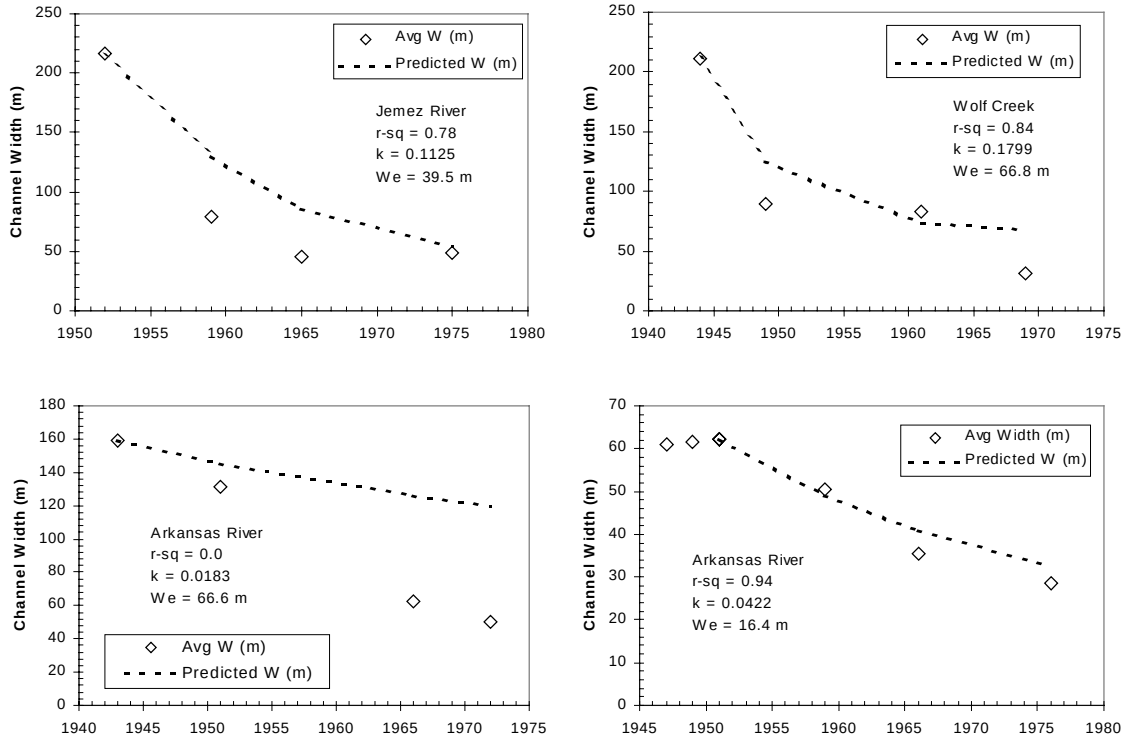

Figure 7-22 - Application of exponential model to width change data from Williams and Wolman (1984).

Regression Models

It is possible to compare the equations resulting from the multiple regression analysis presented in section 6.3 with those from other published studies. However, some of the differences in data and methods should be noted. A comparison is made between this study and a few selected other studies in Table 7-6.

Table 7-5. Based on this comparison, it appears that Shields et al. (2000) is the most comparable to this study. Unfortunately, the only significant association found was with R_c/W, which was not included in the analysis presented in section 6.3. Nanson and Hickin (1986) and MacDonald (1991) provide the best equations for comparison with this study.

The percent of explained variance (R^2-value) found in the models in section 6.3 are comparable to those found by Nanson and Hickin (1986). The highest values are less than 70%. Nanson and Hickin (1986) found that the highest explained variance (69.1%) was produced by a combination of Q, S, and D_{50} to model the variation in volume of migration measured by $M*h$ where h = bank height. Difficulties arise in comparing the results of the equations from section

6.3 with those of others when parameters are used in different forms. For instance, Nanson and Hickin (1986) used unit stream power, $\omega = \gamma \frac{QS}{W}$, while a surrogate for ω was used in this study, $S\sqrt{Q}$. A comparison of published equations with the results from Section 6.3 are presented in Table 7-6.

Table 7-5 - Comparison of selected studies utilizing regression analysis to model lateral migration rates.

	This Study	**Hooke (1980)**	**Nanson and Hickin (1986)**	**Shields et al. (2000)**	**Lawler (1999)**	**MacDonald (1991)**
Planform	Planform transition	Meandering	Meandering	Sinuous braided	Meandering	Meandering
Special Impacts	Dam Impacts			Dam Impacts		
# study periods	6 study periods	3 study periods	1 study period	3 study periods	2 study periods	1 study period
Time period	1918-1992	1974-76 and 1842-1975	21-33 yrs	1890's to 1991	1996-97	~20 years
# of rivers	Single river	16 sites on 7 rivers	18 reaches	Single river	Single river	16 sites
Type of variability analyzed	Spatial and temporal variability with in reach	Regional variability	Regional variability	Spatial and temporal variability with in reach	Spatial variability in one river	Regional variability
Method of measure-ment	Aerial photos/ maps	Field msrmts and aerial photos/maps	Aerial photos/ maps	Aerial photos/ maps	Field msmnts	Aerial photos/ Maps
Signifi-cance level used in regressions	95%	Not given	90%	90%	Not given	Not given
Significant associations identified With migration rates	Flow energy Planform	Drainage area	Flow energy Bed material	R_c/W	Distance downstream	Discharge, width, bank height

Table 7-6 - Comparison of regression results with those from other studies

This Study	Nanson and Hickin (1986)	MacDonald (1991)
$M = 54.3Q^{1.1203}S^{1.4531}$ $R^2 = 0.50$	$M = 1.663Q^{0.482}S^{0.368}$ $R^2 = 0.53$	
$M = 1778W_{act}^{0.8278}S^{1.6205}$ $R^2 = 0.36$ $M = 6.155W_{tot}^{0.9392}S^{0.8928}$ $R^2 = 0.45$	$M = 0.301W^{0.895}S^{0.271}$ $R^2 = 0.54$	
$M = 2611(S\sqrt{Q})^{1.871}$ $R^2 = 0.48$	$M \cdot h = 0.45\omega^{0.401}$ $R^2 = 0.20$	
$M = 194.3(S\sqrt{Q})^{1.545}D_{50}^{-0.1871}$ $R^2 = 0.54$	$M \cdot h = 0.607\omega^{0.823}D_{50}^{-0.207}$ $R^2 = 0.29$	
$M = 0.007W_{tot}^{1.096}$ $R^2 = 0.42$		$M = 0.28W^{0.0.34}$ $R^2 = 0.34$
$M = 0.001Q^{1.270}$ $R^2 = 0.39$		$M = 0.022Q^{0.52}$ $R^2 = 0.75$

The regression results from this study support Brice's (1982) conclusion that planform is an important factor in lateral migration. The inclusion of planform measures in this study reveals that migration rates increase with increasing sinuosity (P < 1.2-1.3). Also, the migration rates increase with decreasing width ratio, signifying that the reaches with more or larger mid-channel vegetated bars were more laterally mobile. Also reaches with higher total channel width (including bars) also exhibited higher mobility.

It was anticipated that decreasing the spatial scale of measurement would increase the accuracy of the regressions, however this was not the case. This illustrates that there are other factors not accounted for in this study that contribute to the spatial variability in M in the Cochiti reach. Such factors may include bank stability, vegetation, detailed cross-section geometry, meander geometry and randomness.

7.6 Ecological Implications

Predicting the effects of human modification of streamflow on natural ecosystems is complex. Complex relationships exist between the biota and hydrogeomorphic processes (Johnson 1994). The movement of the Cochiti reach towards a more stable configuration with decreased lateral mobility and encompassing reduced channel area may have negative ecological implications. The dynamic nature of a natural river system increases the biodiversity of the river's aquatic and riparian habitats (Ward et al. 1999; Winterbottom 2000). Human attempts to "stabilize" the middle Rio Grande in New Mexico have succeeded in reducing the dynamism in both the inputs to the reach and in the responding form of the channel. Decreased frequency and intensity of flooding has been documented to have major effects on riparian ecosystems (Busch and Smith 1995). Ward et al. (1999) states that floodplain rivers with ecological integrity are by definition non-equilibrium systems. A natural and diverse disturbance regime (e.g., discharge events in excess of bankfull) combined with some freedom of lateral migration are necessary elements of non-equilibrium systems Ward et al. (1999) defines.

Additionally, connection of the river with its floodplain is a key element in maintaining ecological integrity and diversity of river systems (Ward et al. 1999). On the Cochiti reach, incision of the channel bed following construction of the dam disconnected the channel from the floodplain. The resulting narrow and deep configuration of the channel and reduced peak flows creates a situation in which even the highest flows no longer achieve bankfull conditions. Bravard et al. (1997) found that incision and narrowing of channels at a watershed scale decreased habitat heterogeneity, and, thus decreased biodiversity.

Given the unliklihood of the removal of Cochiti Dam, this study provides insights into the response of the Cochiti reach that may be useful for creation of sustainable habitat restoration under the current regulated conditions. For instance, increased lateral mobility is observed in some sections downstream from tributaries. Identification of more mobile subreaches lends itself to implementation of innovative river management practices, such as the "streamway" concept employed in France (Piegay et al. 1997).

Along the Galaure River, actively meandering sections of the river were identified and all bank protection measures are prohibited in those sections where ecological conservation or risk management are of interest. Within the non-protection areas or defined "streamway", the community agreed to allow the river to freely move laterally. The management plan created a contract between riverside property owners and the managing agency that restricts construction of

protective measures and financially encourages natural vegetative rehabilitation of the floodplain. The use of GIS-based maps of risk of lateral movement proved to be an extremely useful tool in the development of the management plan (Piegay et al. 1997).

CHAPTER 8

CONCLUSIONS AND RECOMMENDATIONS

8.1 Conclusions

The 45-kilometer long Cochiti reach of the Rio Grande, NM provided an excellent case study in lateral response of an alluvial river to natural and anthropogenic alterations in water and sediment inflows. An extensive database that documents the changing water and sediment regimes and the corresponding lateral and vertical adjustments of the channel from 1918 to 1992 (Leon et al. 1999h) was utilized to quantify historic trends, measure indices of lateral mobility and stability, and model lateral movement rates. The primary conclusions are as follows:

1) The historic analysis revealed significant differences (>50%) between pre and post dam inputs and responses. During the pre-dam period (1918-72) the peak flows decreased and the channel exhibited a corresponding decrease in width and lateral movement rates. Following construction of Cochiti dam in 1973, the sediment supply was virtually eliminated and the channel bed coarsened from sand to gravel and degraded up to two meters. The pre-dam trends toward narrowing and stability continued following construction of the dam.

2) Between 1918 and 1992, the channel moved toward a more stable/equilibrium configuration as evidenced by agreement with hydraulic geometry equations and decreased rates of lateral movement. Comparisons with existing hydraulic geometry equations indicate that the 1992 width is close to an equilibrium width. The 1918 channel width was on average 2.3 times greater than the estimated equilibrium width from the Julien-Wargadalam (1995) hydraulic geometry equations.

3) Four indices of lateral movement and two indices of lateral stability were computed from bankline movement and channel changes measured from digitized coverages of the active channel. The lateral movement indices provide two different measures of gross bankline change (*E*, total bankline change and *N*, bankline movement normalized by channel width) and two that separate the lateral movement into migration (*M*) and width change

(dW_{act}). The degree of lateral stability was quantified using two indices computed from changes in active channel area. The following temporal and spatial trends were identified:

a) Between 1918 and 1992 the rates of lateral movement decreased and the degree of stability increased.

b) Increased rates of lateral migration were noticed downstream of tributary confluences. The most stable reaches were single thread and in areas with geologic control of lateral movement.

4) Three models of lateral migration and width change rate were developed utilizing the Cochiti reach data from 1918 to 1985 as measured by the indices described above:

a) A simple model predicting lateral movement rates based solely on the active channel width provided a rough approximation of movement rates. The measured rates of migration as percentage of width were comparable to those measured in other rivers.

b) The assumption that lateral channel changes were proportional to the deviation from equilibrium allowed for the fit of an exponential function to changes in active channel width and migration rates. The exponential model explained up to 98% of the temporal variance in width and up to 88% of the temporal variation in migration rates.

c) Multiple regression models showed that lateral migration rates were significantly associated with measures of flow energy and the ratio of active channel width to total channel width. Rates of change in active channel width were associated with the active channel widths at the beginning of the time period. The models explained up to 65% of the variability in migration rates and 50% of the variability in width change for the 1918 to 1985 time period.

5) The models were validated using the 1985 to 1992 lateral movement measurements from the Cochiti reach. The regression equations using the mobility index or water discharge combined with width ratio predicted the 1985-92 migration rate with 25 to 38% average error. The 1992 width was predicted equally well (12% average error) by the simple estimation of width change rate as percent of width and by the regression results using unit stream power and active channel width. The exponential model was also applied to the Williams and Wolman (1984) width change data for channels that narrowed

following dam completion. The exponential model accurately modeled the width changes ($r^2 > 0.75$) for three out of the four rivers modeled.

8.2 Recommendations

The database utilized in this study (Leon et al. 1999h) is one of the most comprehensive sets of data available for an alluvial river in the western United States. Daily water discharge records on the middle Rio Grande began in 1895 and sediment sampling commenced in the 1940's, creating one of the longest hydraulic and sediment records available in the US. Documentation of channel response began in 1918 with a topographic survey followed by aerial photos from 1935 to 1992 and commencement of cross-section surveys in the 1930's. Further documentation of the channel continued with regular surveys of established cross sections by the U.S. Bureau of Reclamation. Continued data collection and further use and validation of the models presented in this dissertation could enhance their future predictive capabilities on the Cochiti reach. More specifically, incorporation of digitized aerial photos of the active channel taken after 1992, quantification of changes in bank vegetation both historic and current, and measurement and prediction of bed load transport would all be useful in increasing the predictive capabilities of the regression analysis.

Incorporation of the planform data into a Geographic Information System (GIS) allowed for automation of measuring the characteristics of the channel planform and the lateral movement of the channel. Use of the GIS made it possible to measure lateral movements every 150 meters along the channel for 45 km and six different time periods quickly and accurately. The increased spatial resolution possible with a GIS will be useful for future mapping and identification of stable or unstable sections of the river. Measurements of lateral migration rates and width changes rates using the bankline delineated in the GIS coverages of the non-vegetated active channel were comparable to those found in other studies that utilized field measurement and/or measurements from aerial photos.

The methods of compilation, manipulation, and analysis of the historic data employed in this study can be applied to similar rivers and other reaches of the middle Rio Grande. Already, database similar to that used in this dissertation has been compiled by CSU on the Bernalillo to San Acacia reach of the Rio Grande, just downstream from the Cochiti reach (Bauer 1999). A qualitative geomorphic analysis of the Rio Grande between Bernalillo and San Acacia was conducted by Bauer (1999) and a quantitative analysis of channel adjustments of the Rio Grande between the Rio Puerco and San Acacia diversion dam were conducted by Richard et al. (2000, draft). Future applications of the models presented in this dissertation to the database compiled

on the Bernalillo to San Acacia reach of the Rio Grande (Bauer et al. 1999) and possibly to other rivers would improve river management while increasing the validity and robustness of the methodologies presented herein.

The longer-term (74 years) view of channel adjustments taken in this study, as compared to earlier short-term (< 25 year) studies of the Cochiti reach (Lagasse 1980, 1981, 1994; Leon 1998), provides more information regarding the historical character of the river that will be useful in restoration planning. Implementation of environmental legislation, such as the Endangered Species Act of 1973 can result in the creation of Habitat Conservation Plans and require the determination of restoration goals. This dissertation presents an historic study of changing processes acting on the channel and the resulting response of the Cochiti reach that can give river managers, engineers, geomorphologists, and ecologists a picture of how the river behaved historically. The predictive capabilities of the models presented herein can aid managers in design of management strategies once specific restoration goals have been identified.

Lastly, the author concludes that empirical methods and simplifying concepts such as stability or equilibrium are useful tools for understanding the inherent dynamic nature of fluvial systems. The results of the analyses in this dissertation indicate that combined human-induced and natural changes in water and sediment inputs produced a more stable, less active channel. Just as the dams and diversions attempt to force rivers into manageable and stable conditions, empirical models and equilibrium concepts are human constructs that endeavor to describe rivers in a more controllable and convenient manner. Fortunately, the chaotic nature of fluvial systems does not easily permit human management or simple description, for it is the chaotic and often unmanageable nature of rivers that sustains diverse ecosystems, as well as human fascination.

> *Landscape is often seen as static; but it never is static. From its first rock in the sky to its last embrace by the estuary at the sea, the river has been surrounded by forces and elements constantly moving and dynamic, interacting to produce its life and character.* (Horgan 1954, p.7)

REFERENCES

Abam, T. K. S. and Omuso, W. O. 2000. Technical note on river cross-sectional change in the Niger Delta. *Geomorphology*, 34:111-26.

Abernethy, B. and Rutherfurd, I. D. 1998. Where along a river's length will vegetation most effectively stabilize stream banks? *Geomorphology*, 23:55-75.

Ainsworth, C. M. 1932. Effect of the Operation of Elephant Butte Reservoir on the River, through the Palomas, Rincon, Mesilla, and El Paso valleys. Consulting Engineers Report, International Boundary and Water Commission File, El Paso, TX.

Alekseevskii, N. I. and Berkovich, K. M. 1992. Stability of braided river stretches and its relation to sediment transport. Plenum Publishing Corporation, pp. 380-384.

Andrews, E. D. 1980. Effective and bankfull discharges of streams in the Yampa river basin, Colorado and Wyoming. *Journal of Hydrology*, 46:311-30.

Bagnold, R. A. 1980. An empirical correlation of bedload transport rates in flumes and natural rivers. *Proceedings of the Royal Society*, 372A:453-473.

Bauer, T., Leon, C., Richard, G., and Julien, P. 1999. Middle Rio Grande, Bernalillo Bridge to San Acacia - Hydraulic Geometry, Discharge and Sediment Data Base and Report. Colorado State University, Fort Collins, CO.

Bauer, T. R. 1999 Morphology of the Middle Rio Grande from Bernalillo Bridge to the San Acacia Diversion Dam, New Mexico. M.S. Thesis. Colorado State University, Fort Collins, CO.

Begin, Z. B. 1981. Stream curvature and bank erosion: A model based on the momentum equation. *Journal of Geology*, 89:497-804.

Beschta, R. L. 1998. Long-term changes in channel morphology of gravel-bed rivers: three case studies. In: Klingeman, P. C., Beschta, R. L., Komar, P. D., and Bradley, J. B. (eds), Gravel-Bed Rivers in the Environment. Water Resources Pulications, LLC., Colorado, pp. 229-56.

Biedenharn, D. S., Combs, P. G., Hill, G. J., Pinkard, C. F. Jr., and Pinkston, C. B. 1989. Relationship between channel migration and radius of curvature on the Red River. In: Wang, S. S. Y. (ed), Sediment Transport Modeling. ASCE, NY, NY, pp. 536-541.

Biedenharn, D. S., Thorne, C. R., and Watson, C. C. 2000. Recent morphological evolution of the Lower Mississippi River. *Geomorphology*, 34:227-249.

Bledsoe, B. P. 1999. Specific stream power as an indicator of channel pattern, stability, and response to urbanization. Ph.D. Dissertation. Colorado State University, Fort Collins, CO.

Blench, T. 1957. Regime behaviour of canals and rivers. Butterworths Scientifice Publications, London.

Bradley, C. and Smith, D. G. 1984. Meandering channel Response to Altered Flow Regime: Milk River, Alberta and Montana. *Water Resources Research*, 20:1913-1920.

Bravard, J-P., Amoros, C., Pautou, G., Bornette, G., Bournaud, M., Creuze des Chatelliers, M., Gibert, J., Piery, J-L., Perrin, J-F., and Tachet, H. 1997. River incision in south-east France: Morphological phenomena and ecological effects. *Regulated Rivers: Research and Management*, 13:75-90.

Brewer, P. A. and Lewin, J. 1998. Planform cyclicity in an unstable reach: Complex fluvial response to environmental change. *Earth Surface Processes and Landforms*, 93:989-1008.

Brice, J. C. 1982. Stream Channel Stability Assessment, January 1982, Final Report. U.S. Department of Transportation, FHA, Washington, D.C.

Bridge, J. S. 1993. The interaction between channel geometry, water flow, sediment transport and deposition in braided rivers. In: Best, J. L. and Bristow, C. S. (eds), Braided Rivers. Geological Society, London, UK, pp. 13-71.

Brookes, A. 1992. River channel change. In: Calow, P. and Petts, G. E. (eds), The Rivers Handbook, Hydrological and Ecological Principles. Blackwell Scientific Publications, Oxford, pp. 55-75.

Bullard, K. L. and Lane, W. L. 1993. Middle Rio Grande Peak Flow Frequency Study. U.S. Department of Interior, Bureau of Reclamation.

Burnett, A. W. and Schumm, S. A. 1983. Alluvial river response to neotectonic deformation in Louisiana and Mississippi. *Science*, 222:49-50.

Busch, D. E. and Smith, S. D. 1995. Mechanisms associated with decline of woody species in riparian ecosystems of the southwestern U.S. *Ecological Monographs*, 65:347-370.

Callander, R. A. 1969. Instability and river channels. *Journal of Fluid Mechanics*, 36:pp. 465-480.

Carson, M. A. 1984. The Meandering-Braided River Threshold: A Reappraisal. *Journal of Hydrology*, 73:315-334.

Chang, H. H. 1979. Minimum Stream Power and River Channel Patterns. *Journal of Hydrology*, 41:303-27.

Chang, H. H. 1984. Analysis of River Meanders. *Journal of Hydraulic Engineering*, 110:37-49.

Chang, H. H. 1988. On the cause of river meandering. In: White, W. R. (ed), International Conference on River Regime, 18-20 May, 1988. Hydraulics Research Limited, Wallingford, UK, pp. 83-93.

Chorley, R. J. 1966. The application of statistical methods to geomorphology. In: Dury, G. H. (ed), Essays in Geomorphology. American Elsevier Publishing Company, Inc., NY, NY, pp. 275-387.

Church, M. 1995. Geomorphic response to river flow regulation: Case studies and time-scales. *Regulated Rivers: Research and Management*, 11:3-22.

Coleman, J. M. 1969. Brahmaputra River: Channel Processes and Sedimentation. *Sedimentary Geology*, 3:129-239.

Crawford, C. S., Cully, A. C., Leutheuser, R, Sifuentes, M. S., White, L. H., and Wilber, J. P. 1993. Middle Rio Grande Ecosystem: Bosque Biological Management Plan. U.S. Fish and Wildlife Service, Albuquerque, NM.

Culbertson, J. K. and Dawdy, D. R. 1964. A Study of Fluvial Characteristics and Hydraulic Variables Middle Rio Grande, New Mexico. U.S. Geological Survey Water Supply Paper 1498-F. U.S. Geological Survey, Washington, D.C.

Dade, W. B. 2000. Grain size, sediment transport and alluvial channel pattern. *Geomorphology*, 35:119-126.

Dade, W. B. and Friend, P. F. 1998. Grain-Size, Sediment-Transport Regime, and Channel Slope in Alluvial Rivers. *Journal of Geology*, 106:661-675.

Dewey, J. D., Roybal, F. E., and Funderburg, D. E. 1979. Hydrologic Data on Channel Adjustments 1970 to 1975, on the Rio Grande Downstream from Cochiti Dam, New Mexico Before and After Closure. U.S. Geological Survey Water Resources Investigations 79-70. U.S. Geological Survey, Albuquerque, NM.

Dubler, D. R. 1997. Effective Discharge Determination in the Yazoo River Basin, Mississippi. M.S. Thesis. Colorado State University, Fort Collins, CO.

Elliott, C. M. 1984. River Meandering. American Society of Civil Engineers, NY, NY.

Everitt, B. L. 1968. Use of the cottonwood in an investigation of the recent history of a flood plain. *American Journal of Science*, 266:417-439.

Ferguson, R. 1987. Hydraulic and Sedimentary Controls of Channel Pattern. In: Richards, K. (ed), River Channels. Environment and Process. Basil Blackwell, Oxford, UK, pp. 129-158.

Fiock, L. R. 1931. Effect of the Operation of Elephant Butte Reservoir on the River through Rio Grande Project. International Boundary and Water Commission File, El Paso, Texas.

Friedman, J. M., Osterkamp, W. R., Scott, M. L., and Auble, G. T. 1998. Downstream effects of dams on channel geometry and bottomland vegetation: Regional patterns in the Great Plains. *Wetlands*, 18:619-633.

Friend, P. F. and Sinha, R. 1993. Braiding and meandering parameters. In: Best, J. L. and Bristow C. S. (eds), Braided Rivers. Geological Society Special Publication No. 75. Geological Society, London, UK, pp. 105-111.

Gilvear, D. J. 1993. River management and conservation issues on formerly braided river systems; the case of the River Tay, Scotland. In: Best, J.L. and Bristow, C.S. (eds), Braided Rivers. pp. 231-240.

Gilvear, D. J. and Winterbottom, S. J. 1992. Channel change and flood events since 1783 on the regulated River Tay, Scotland: Implications for flood hazard management. *Regulated Rivers: Research and Management*, 7:247-260.

Gilvear, D., Winterbottom, S., and Sichingabula, H. 2000. Character of channel planform change and meander development: Luangwa River, Zambia. *Earth Surface Processes and Landforms*, 25:421-436.

Graf, W. L. 1994. Plutonium and the Rio Grande - Environmental Change and Contamination in the Nuclear Age. Oxford University Press, New York.

Gray, D. H. and MacDonald, A. 1989. The Role of Vegetation in River Bank Erosion. In: Ports, M. A. (ed), Proceedings of the 1989 national conference on hydraulic engineering. ASCE. Hydraulics Division, NY, NY, pp. 218-223.

Gurnell, A. and Petts, G. 1995. Changing River Channels. John Wiley & Sons, Ltd., Chichester, UK.

Gurnell, A. M. 1997. Channel change on the River Dee meanders, 1946-1992, from the analysis of aerial photos. *Regulated Rivers: Research and Management*, 13:13-26.

Gurnell, A. M., Downward, S. R., and Jones, R. 1994. Channel planform change on the River Dee meanders, 1876-1992. *Regulated Rivers: Research and Management*, 9:187-204.

Hasegawa, K. 1989. Studies on Qualitative and Quantitatie Prediction of Meander Channel Shift. In: Parker, G. and Ikeda, S. (eds), River Meandering, Water Resources Monograph 12. American Geophysical Union, Washington, D.C., pp. 215-235.

Henderson, F. M. 1961. Stability of Alluvial Channels. *Journal of the Hydraulics Division*, 87:109-138.

Hey, R. D. 1988. Mathematical models of channel morphology. In: Anderson, M. G. (ed), Modelling Geomorphological Systems. John Wiley & Sons, Ltd., Chichester, pp. 99-125.

Hey, R. D. and Thorne, C. R. 1986. Stable channels with mobile gravel beds. *Journal of Hydraulic Engineering*, 112:671-689.

Hickin, E. J. 1974. The development of meanders in natural river-channels. *American Journal of Science*, 274:414-42.

Hickin, E. J. and Nanson, G. C. 1975. The character of channel migration of the Beatton River, Northeast British Columbia, Canada. *Bulletin of the Geological Society of America*, 86:487-494.

Hickin, E. J. and Nanson, G. C. 1984. Lateral Migration Rates of River Bends. *Journal of Hydraulic Engineering*, 110:1557-1567.

Hong, L. B. and Davies, T. R. H. 1979. A study of stream braiding. *Geological Society of America Bulletin, Part II*, 90:1839-1859.

Hooke, J. M. 1977. The distribution and nature of changes in river channel patterns: The example of Devon. In: Gregory, K. J.(ed), River Channel Changes. John Wiley & Sons, Ltd., Chichester, pp. 265-280.

Hooke, J. M. 1979. An analysis of the processes of river bank erosion. *Journal of Hydrology*, 42:39-62.

Hooke, J. M. 1980. Magnitude and distribution of rates of river bank erosion. *Earth Surface Processes*, 5:143-157.

Hooke, J. M. 1987. Changes in meander morphology. In: Gardiner, V. (ed), International Geomorphology, 1986, Part 1. John Wiley and Sons, Ltd., Chichester, UK, pp. 591-609.

Hooke, J. M. 1995. Processes of channel planform change on meandering channels in the UK. In: Gurnell, A. and Petts, G. (eds), Changing River Channels. John Wiley & Sons, Ltd., Chichester, pp. 87-115.

Hooke, J. M. and Redmond, C. E. 1989. Use of Cartographic Sources for Analyzing River Channel Change with Examples from Britain. In: Petts, G. E. (ed), Historical Change of Large Alluvial Rivers: Western Europe. John Wiley & Sons, Ltd., pp. 79-93.

Hooke, J. M. and Redmond, C. E. 1992. Causes and nature of river planform change. In: Billi, P., Hey, R. D., Thorne, C. R., and Tacconi, P. (eds), Dynamics of Gravel-bed Rivers. John Wiley & Sons, Ltd., Chichester, pp. 557-571.

Horgan, P. 1954. Great River. The Rio Grande in North American History. v. 1 and v. 2. Rinehart & Company, Inc., New York, NY.

Huang, H. Q. and Nanson, G. C. 1997. Vegetation and channel variation; a case study of four small streams in southeastern Australia. *Geomorphology*, 18:237-249.

Huang, H. Q. and Nanson, G. C. 1998. The influence of bank strength on channel geometry: An integrated analysis of some observations. *Earth Surface Processes and Landforms*, 23:865-876.

Ikeda, H. 1989. Sedimentary Controls on Channel Migration and Origin of Point Bars in Sand-Bedded Meandering Rivers. In: G. Parker and S. Ikeda (eds), River Meandering, Water Resources Monograph 12. American Geophysical Union, Washington, D.C., pp. 51-68.

International Boundary and Water Commission, United States and Mexico. 1933. Report on the Changes in Regimen of the Rio Grande in the Valleys Below Since the Construction of Elephant Butte Dam, 1917-1932. El Paso, Texas.

Johnson, W. C 1992. Dams and Riparian Forests: Case Study from the Upper Missouri River. *Rivers*, 3:229-242.

Johnson, W. C. 1994. Woodland expansion in the Platte River, Nebraska: Patterns and causes. *Ecological Monographs*, 64:45-84.

Johnson, W. C. 1997. Equilibrium response of riparian vegetation to flow regulation in the Platte River, Nebraska. *Regulated Rivers: Research and Management*, 13:403-415.

Johnson, W. C. 1998. Adjustment of riparian vegetation to river regulation in the Great Plains, USA. *Wetlands*, 18:608-618.

Johnson, W. C., Burgess, R. L., and Keammerer, W. R. 1976. Forest overstory vegetation and evironment on the Missouri River floodplain in North Dakota. *Ecological Monographs*, 46:59-84.

Julien, P. Y. 1988. Downstream Hydraulic Geometry of Noncohesive Alluvial Channels. In: White, W.R. (ed), International Conference on River Regime, 18-20 May, 1988, Hydraulics Research Limited, Wallingford, UK, pp. 9-16.

Julien, P. Y. and Wargadalam, J. 1995. Alluvial Channel Geometry: Theory and Applications. *Journal of Hydraulic Engineering*, 121:312-25.

Kellerhals, R and Church, M. 1989. The morphology of large rivers: characterization and management. In: Dodge, D. P. (ed), Proceedings of the International Large Rivers Symposium 1986. Ministry of Supply and Service Canada, Canada, pp. 31-48.

Klaassen, G. J. and Masselink, G. 1992. Planform Changes of a Braided River with Fine Sand as Bed and Bank Material. In: Larsen, P. and Eisenhauer, N. (ed), Sediment Management: 5th International Symposium on River Sedimentation. Karlsruhe, Germany, pp. 459-471.

Klaassen, G. J. and Vermeer, K. 1988. Channel Characteristics of the Braiding Jamuna River, Bangladesh. In: White, W. R. (ed), International Conference on River Regime, 18-20 May, 1988. Hydraulics Research Limited, Wallingford, UK, pp. 173-89.

Klimek, K. and Trafas, K. 1972. Young-Holocene changes in the course of the Dunajec River in the Beskid Sadecki Mts. (Western Carpathians). *Studia Geomorphologica Carpatho-Balcanica*, VI:85-91.

Knighton, A. D. and Nanson, G. C. 1993. Anastamosis and the continuum of channel pattern. *Earth Surface Processes and Landforms*, 18:613-25.

Knighton, D. 1998. Fluvial Forms and Processes - A New Perspective. John Wiley & Sons, Inc., New York, NY.

Kolb, C. R. 1963. Sediments forming the bed and banks of the lower Mississippi River and their effect on river migration. *Sedimentology*, 2:227-34.

Komura, S. and Simons, D. B. 1967. River-Bed Degradation below Dams. *Journal of the Hydraulics Division*, 93:1-14.

Laczay, I. A. 1977. Channel pattern changes of Hungarian rivers: The example of the Hernad River. In: Gregory, K. J. (ed), River Channel Changes. John Wiley & Sons, Ltd., Chichester, pp. 185-192.

Lagasse, P. F. 1980. An Assessment of the Response of the Rio Grande to Dam Construction - Cochiti to Isleta Reach. U.S. Army Corps of Engineers, Albuquerque, NM.

Lagasse, P. F. 1981. Environmental Geology and Hydrology in New Mexico. New Mexico Geological Society Special Publication No. 10. New Mexico Geological Society, Albuquerque, NM.

Lagasse, P. F. 1994. Variable Response of the Rio Grande to Dam Construction. In: The Variability of Large Alluvial Rivers. ASCE Press, New York, New York, pp.

Lane, S. N., Richards, K. S., and Chandler, J. H. 1996. Discharge and sediment supply controls on erosion and deposition in a dynamic alluvial channel. *Geomorphology*, 15:15-Jan.

Lawler, D. M. 1992. Process Dominance in Bank Erosion Systems. In: Carling, P. A. and Petts G. E. (eds), Lowland Floodplain Rivers: Geomorphological Perspectives. John Wiley & Sons Ltd., 117-143.

Lawler, D. M. 1993. The measurement of river bank erosion and lateral channel change: a review. *Earth Surface Processes and Landforms*, 18:777-821.

Lawler, D. M., Grove, J. R., Couperthwaite, J. S., and Leeks, G. J. L. 1999. Downstream change in river bank erosion rates in Swale-Ouse system, northern England. *Hydrological Processes*, 13:977-992.

Leon, C. 1998. Morphology of the Middle Rio Grande from Cochiti Dam to Bernalillo Bridge New Mexico. M.S. Thesis, Colorado State University, Fort Collins, CO.

Leon, C., Richard, G., Bauer, T., and Julien, P. 1999a. Middle Rio Grande, Cochiti to Bernalillo Bridge, Hydraulic Geometry, Discharge and Sediment Data Base and Report., Volume I - Cross section geometry data and plots. Prepared for U.S. Bureau of Reclamation, Albuquerque Office, by Colorado State University, Fort Collins, CO, 242 pp.

Leon, C., Richard, G., Bauer, T., and Julien, P. 1999b. Middle Rio Grande, Cochiti to Bernalillo Bridge, Hydraulic Geometry, Discharge and Sediment Data Base and Report., Volume IA-Cross section geometry data and plots - Agg/deg and SCS Lines. Prepared for U.S. Bureau of Reclamation, Albuquerque Office, by Colorado State University, Fort Collins, CO, 17 pp.

Leon, C., Richard, G., Bauer, T., and Julien, P. 1999c. Middle Rio Grande, Cochiti to Bernalillo Bridge, Hydraulic Geometry, Discharge and Sediment Data Base and Report., Volume II - Daily mean discharge plots. Prepared for U.S. Bureau of Reclamation, Albuquerque Office, by Colorado State University, Fort Collins, CO, 39 pp.

Leon, C., Richard, G., Bauer, T., and Julien, P. 1999d. Middle Rio Grande, Cochiti to Bernalillo Bridge, Hydraulic Geometry, Discharge and Sediment Data Base and Report., Volume IIIA - Bed Material Data. Prepared for U.S. Bureau of Reclamation, Albuquerque Office, by Colorado State University, Fort Collins, CO, 120 pp.

Leon, C., Richard, G., Bauer, T., and Julien, P. 1999e. Middle Rio Grande, Cochiti to Bernalillo Bridge, Hydraulic Geometry, Discharge and Sediment Data Base and Report., Volume IIIB - Suspended sediment concentration data and plots. Prepared for U.S. Bureau of Reclamation, Albuquerque Office, by Colorado State University, Fort Collins, CO, 206 pp.

Leon, C., Richard, G., Bauer, T., and Julien, P. 1999f. Middle Rio Grande, Cochiti to Bernalillo Bridge, Hydraulic Geometry, Discharge and Sediment Data Base and Report., Volume IIIC - Suspended sediment discharge data and plots. Prepared for U.S. Bureau of Reclamation, Albuquerque Office, by Colorado State University, Fort Collins, CO, 193 pp.

Leon, C., Richard, G., Bauer, T., and Julien, P. 1999g. Middle Rio Grande, Cochiti to Bernalillo Bridge, Hydraulic Geometry, Discharge and Sediment Data Base and Report., Volume IIID - Suspended sediment particle size data and plots. Prepared for U.S. Bureau of Reclamation, Albuquerque Office, by Colorado State University, Fort Collins, CO, 124 pp.

Leon, C., Richard, G., Bauer, T., and Julien, P. 1999h. Middle Rio Grande, Cochiti to Bernalillo Bridge, Hydraulic Geometry, Discharge and Sediment Data Base CD-Rom, Prepared for U.S. Bureau of Reclamation, Albuquerque Office, by Colorado State University, Fort Collins, CO, 124 pp.

Leopold, L. B. 1994. A view of the river. Harvard University Press, Cambridge, MA.

Leopold, L. B. and Maddock, T. Jr. 1953. The Hydraulic Geometry of Stream Channels and Some Physiographic Implications. *USGS Professional Paper 252*, 57 pp.

Leopold, L. B. and Wolman, G. M. 1957. River Channel Patterns: Braided, Meandering and Straight, USGS Professional Paper 282-B. U.S. Government Prining Office, Washington, D.C.

Lewin, J. 1977. Channel pattern changes. In: Gregory, K. J. (ed), River Channel Changes. John Wiley & Sons, Ltd., Chichester, pp. 167-184.

Lewin, J., Macklin, M. G., and Newson, M. D. 1988. Regime theory and environmental change - irreconcilable concepts? In: White, W. R. (ed), International Conference on River Regime. Hydraulics Research Limited, Wallingford, UK, pp. 431-445.

Ligeng, L. and Schiara, M. 1992. Expansion Rate of Meandering River Bends. In: Larsen, P. and Eisenhauer, N. (ed), Sediment management: 5th International Symposium on River Sedimentation. Karlsruhe, Germany, pp. 49-54.

MacDonald, T. E. 1991. Inventory and analysis of stream meander problems in Minnesota. M.S. Thesis, University of Minnesota.

Mackin, J. H. 1948. Concept of the Graded River. *Bulletin of the Geological Society of America*, 59:463-512.

Macklin, M. G., Passmore, D., and Newson, M. D. 1998. Controls of short- and long-term river instability: Processes and patterns in gravel-bed rivers, Tyne Basin, England. In: Klingeman, P. C., Beschta, R. L., Komar, P. D., and Bradley, J. B. (eds), Gravel-Bed Rivers in the Environment. Water Resources Pulications, LLC., Colorado, pp. 257-78.

Marston, R. A., Girel, J., Pautou, G., Piegay, H., Bravard, Jean-Paul, and Arneson, C. 1995. Channel metamorphosis, floodplain disturbance, and vegetation development: Ain River, France. *Geomorphology*, 13:121-31.

Millar, R. G. 2000. Influence of bank vegetation on alluvial channel patterns. *Water Resources Research*, 36:1109-1118.

Mosley, H. and Boelman, S. 1998. Santa Ana Reach. Geomorphic Report. - DRAFT. U.S. Bureau of Reclamation, Albuquerque, NM.

Mosley, M. P. 1975. Channel Changes on the River Bollin, Cheshire, 1872-1973. *East Midland Geographer*, 6:185-199.

Mosselman, E. 1995. A review of mathematical models of river planform changes. *Earth Surface Processes and Landforms*, 20:661-670.

Nanson, G. C. and Croke, J. C. 1992. A genetic classification of floodplains. *Geomorphology*, 4:459-86.

Nanson, G. C. and Hickin, E. J. 1983. Channel Migration and Incision on the Beatton River. *Journal of Hydraulic Engineering*, 109:327-337.

Nanson, G. C. and Hickin, E. J. 1986. A statistical analysis of bank erosion and channel migration in western Canada. *Geological Society of America Bulletin*, 97:497-504.

Nash, D. B. 1994. Effective sediment-transporting discharge from a magnitude-frequency analysis. *Journal of Geology*, 102:79-95.

Nicholas, A. P., Woodward, J. C., Christopoulos, G., and Macklin, M. G. 1999. Modelling and monitoring river response to environmental change: The impact of dam construction and alluvial gravel extraction on bank erosion rates in the Lower Alfios Basin, Greece. In: Brown, A. G. and Quine, T. A. (eds), Fluvial Processes and Environmental Change. John Wiley & Sons, Ltd., Chichester, England, pp. 118-137.

Nordin, C. F. 1964. Aspects of Flow Resistance and Sediment Transport Rio Grande Near Bernalillo New Mexico, U.S. Geological Survey Water-Supply Paper 1498-H. U.S. Geological Survey, Washington, D.C.

Nordin, C. F. and Beverage, J. P. 1964. Temporary Storage of Fine Sediment in Islands and Point Bars of Alluvial Channels of the Rio Grande, New Mexico and Texas, U.S. Geological Survey Professional Paper 475-D, U.S. Government Printing Office, Washington, D.C.

Nordin, C. F. and Beverage, J. P. 1965. Sediment Transport in the Rio Grande, New Mexico, U.S. Geological Survey Professional Paper 462-F. U.S. Government Printing Office, Washington, D.C.

Nordin, C. F. and Culbertson, J. K. 1961. Particle-size distribution of stream-bed material in the middle Rio Grande basin, New Mexico, U.S. Geological Survey Professional Paper 424-C, Article 265. U.S. Geological Survey, Washington, D.C.

Norman, V. W. 1968. Trends of Suspended Sediments in the Upper Rio Grande Basin in New Mexico, University of New Mexico, Albuquerque, NM.

Nouh, M. 1988. Regime channels of an extremely arid zone. In: White, W. R. (ed) International Conference on River Regime, 18-20 May, 1988. Hydraulics Research Limited, Wallingford, UK, pp. 55-66.

Osman, A. M. and Thorne, C. R. 1988a. Riverbank Stability Analysis. I: Theory. *Journal of Hydraulic Engineering*, 114:134-150.

Osman, A. M. and Thorne, C. R. 1988b. Riverbank Stability Analysis. II: Applications. *Journal of Hydraulic Engineering*, 114:151-172.

Osterkamp, W. R. 1978. Gradient, discharge, and particle-size relations of alluvial channels in Kansas, with observations on braiding. *American Journal of Science*, 278:1253-1268.

Parker, G. 1976. On the cause and characteristic scales of meandering and braiding in rivers. *Journal of Fluid Mechanics*, 76:457-480.

Parker, G. 1979. Hydraulic geometry of active gravel rivers. *Journal of the Hydraulics Division*, 105:1185-1201.

Parker, G. 1984. Theory of meander bend deformation. In: Elliott, C. M. (ed), River Meandering, Proceedings of the Conference Rivers '83. ASCE, NY, pp. 722-732.

Parker, G. and Ikeda, S. 1989. River Meandering, Water Resources Monograph 12. American Geophysical Union, Washington, D.C.

Pemberton, E. L. 1964. Sediment Investigations - Middle Rio Grande. *Journal of the Hydraulics Division - ASCE*, HY2:163-185.

Pemberton, E. L. 1976. Channel Changes in the Colorado River Below Grand Canyon Dam. In: Proceedings of the Federal Interagency Sedimentation Conference (3rd) at Denver, Colorado. pp. 5-61 - 5-73.

Piegay, H., Cuaz, M., Javelle, E., and Mandier, P. 1997. Bank Erosion Management Based on Geomorphological, Ecological and Economic Criteria on the Galaure River, France. *Regulated Rivers-Research & Management*, 13:433-448.

Pizzuto, J. E. 1994. Channel adjustments to changing discharges, Powder River, Montana. *Geological Society of America Bulletin*, 106:1494-1501.

Poff, N. L., Allan, J. D., Bain, M. B., Karr, J. R., Prestegaard, K. L., Richter, B. D., Sparks, R. E., and Stromberg, J. C. 1997. The Natural Flow Regime. *BioScience*, 47:769-784.

Renwick, W. H. 1992. Equilibrium, disequilibrium, and nonequilibrium landforms in the landscape. *Geomorphology*, 5:265-276.

Richard, G., Leon, C., and Julien, P. 2000. Rio Puerco Reach Geomorphic Analysis, Middle Rio Grande, New Mexico - Draft. Colorado State University, Fort Collins, CO.

Richards, K. 1982. Rivers - Form and process in alluvial channels. Methuen, London.

Richter, B. D., Baumgartner, J. V., Powell, J., and Braun, D. P. 1996. A method for assessing hydrologic alteration within ecosystems. *Conservation Biology*, 10:1163-1174.

Rinaldi, M. and Simon, A. 1998. Bed-level adjustments in the Arno River, central Italy. *Geomorphology*, 22:57-71.

Rittenhouse, G. 1944. Sources of Modern Sands in the Middle Rio Grande Valley, New Mexico. *Journal of Geology*, 52:145-183.

Robertson-Rintoul, M. S. E. and Richards, K. S. 1993. Braided-channel pattern and paleohydrology using an index of total sinuosity. In: Best, J.L. and Bristow, C.S. (eds), Braided Rivers. Geological Society Special Publication No. 75. Geological Society, London, UK, pp. 113-118.

Rosgen, D. 1996. Applied River Morphology. Wildland Hydrology, Pagosa Springs, CO.

Salas, J. D., Smith, R. A., Tabios, G. Q. III, and Jeo, J-H. 1998. Statistical computer techniques in water resources and environmental engineering. Colorado State University, Fort Collins, CO.

Sanchez, V. and Baird, D. 1997. River Channel Changes Downstream of Cochiti Dam. Middle Rio Grande, New Mexico. In: Proceedings of the conference of Management of Landscapes Disturbed by Channel Incision. University of Mississippi, Oxford, MS.

Schumm, S. A. 1969. River Metamorphosis. *Journal of the Hydraulics Division*, 95:255-273.

Schumm, S. A. 1973. Goemorphic thresholds and complex response of drainage systems. In: Morisawa, M. (ed), Fluvial geomorphology. New York State University Publications in Geomorphology, Binghamton, NY, pp. 299-309.

Schumm, S. A., Harvey, M., and Watson, C. 1984. Incised Channels, Morphology, Dynamics and Control. Water Resources Publications, Littleton, CO.

Schumm, S. A. and Khan, H. R. 1972. Experimental Study of Channel Patterns. *Geological Society of America Bulletin*, 83:1755-1770.

Scott, M. L, Auble, G. T., and Friedman, J. M. 1997. Flood dependency of cottonwood establishment along the Missouri River, Montana, USA. *Ecological Applications*, 7:677-690.

Scurlock, D. 1998. From the Rio to the Sierra: An Environmental History of the Middle Rio Grande Basin. U.S. Department of Agriculture, Fort Collins, CO.

Shields, F. D. Jr., Simon, A., and Steffen, L. J. 2000. Reservoir effects on downstream river channel migration. *Environmental Conservation*, 27:54-66.

Simons, D. B. and Albertson, M. L. 1963. Uniform water conveyance channels in alluvial material. *Transactions of the American Society of Civil Engineers, Paper 3399*, 128:65-167.

Surian, Nicola 1999. Channel changes due to river regulation: The case of the Piave River, Italy. *Earth Surface Processes and Landforms*, 24:1135-1151.

The Nature Conservancy 1997. Indicators of Hydrologic Alteration - User's Manual. Smythe Scientific Software.

Thorne, C. R. 1991. Bank erosion and meander migration of the Red and Mississippi Rivers, USA. In: Van-de-Ven, F.H.M., Gutknecht, D., Loucks, D. P., and Salewicz K. A. (eds), Hydrology for the Water Management of Large River Basins (Proceedings of the Vienna Symposium, August 1991). International Association of Hydrological Sciences, pp. 301-313.

Thorne, C. 1992. Bend Scour and Bank Erosion on the Meandering Red River, Louisiana. In: Carling, P. A. and Petts, G. E. (eds), Lowland Floodplain Rivers: Geomorphological Perspectives. John Wiley & Sons Ltd., pp. 96-115.

Thorne, C. R. and Osman, A. M. 1988. The influence of bank stability on regime geometry of natural channels. In: White, W. R. (ed), International Conference on River Regime, 18-20 May, 1988. Hydraulics Research Limited, Wallingford, UK, pp. 135-147.

Thorne, C. R., Russell, A. P. G., and Alam, M. K. 1993. Planform pattern and channel evolution of the Brahmaputra River, Bangladesh. In: Best, J. L. and Bristow C. S. (eds) Braided Rivers, Geological Society Special Publication No. 75. Geological Society, London, UK, pp. 257-276.

Thorne, C. R. and Tovey, N. K. 1981. Stability of composite river banks. *Earth Surface Processes and Landforms*, 6:469-484.

U.S. Army Corps of Engineers. 1978. Cochiti Lake. Rio Grande Basin, New Mexico. Water Control Manual. Appendix C to Rio Grande Basin Master Water Control Manual. U.S. Army Corps of Engineers, Albuquerque, NM.

U.S. Bureau of Reclamation, U. S. Engineer Office. 1951. Profiles of the Rio Grande, San Marcial - Cochiti, Middle Rio Grande Project - NM, May 16, 1951. Drawing No. 163-518-122, Albuquerque, NM.

U.S. Bureau of Reclamation, Hydraulics Division. 1967. Summary Report Rio Grande Aggradation or Degradation 1936 - 1962 Middle Rio Grande Project. Albuquerque, NM.

U.S. Bureau of Reclamation, Hydraulics Division. 1972 Summary Report Rio Grande Aggradation or Degradation 1936 - 1962 Middle Rio Grande Project. U.S. Bureau of Reclamation, Albuquerque, NM.

U.S. Bureau of Reclamation. 1998. Rio Grande Geomorphology Study (1918-1992). USBR, Remote Sensing and Geographic Information Group, Denver, CO.

van den Berg, J. H. 1995. Prediction of alluvial channel pattern of perennial rivers. *Geomorphology*, 12:259-279.

Van Steeter, M. M. and Pitlick J. 1998. Geomorphology and endangered fish habitats of the upper Colorado River, 1. Historic changes in streamflow, sediment load, and channel morphology. *Water Resources Research*, 34:287-302.

Warburton, J., Davies, T. R. H., and Mandl, M. G. 1993. A meso-scale field investigation of channel change and floodplain characteristics in an upland braided gravel-bed river, New Zealand. In: Best, J. L. & Bristow C. S. (eds), Braided Rivers, Geological Society Special Publication No. 75. Geological Society, London, UK, pp. 241-255.

Ward, J. V., Tockner, K., and Schiemer, F. 1999. Biodiversity of floodplain river ecosystems: Ecotones and connectivity. *Regulated Rivers: Research and Management*, 15:125-139.

Wargadalam, J. 1993. Hydraulic Geometry Equations of Alluvial Channels, Ph.D. Dissertation. Colorado State University, Fort Collins, CO.

Williams, G. P. 1978. Bank-Full Discharge of Rivers. *Water Resources Research*, 14:1141-1154.

Williams, G. P. and Wolman, M. G. 1984. Downstream Effects of Dams on Alluvial Rivers, USGS Professional Paper 1286. U.S. Government Printing Office, Washington, D.C.

Winterbottom, S. J. 2000. Medium and short-term channel planform changes on the Rivers Tay and Tummel, Scotland. *Geomorphology*, 34:195-208.

Wolman, M. G. and Miller, J. P 1960. Magnitude and frequency of forces in geomorphic processes. *Journal of Geology*, 68:54-74.

Woodson, R. C. and Martin, J. T. 1962. The Rio Grande comprehensive plan in New Mexico and its effects on the river regime through the middle valley. In: Carlson, E. J. and Dodge, E. A. (eds), Control of Alluvial Rivers by Steel Jetties, American Society of Civil Engineers Proceedings,Waterways and Harbors Division Journal 88. American Society of Civil Engineers, NY, NY, pp. 53-81.

Xu, J. 1996a. Channel pattern change downstream from a reservoir: An example of wandering braided rivers. *Geomorphology*, 15:147-158.

Xu, J. 1996b. Underlying gravel layers in a large sand bed river and their influence on downstream-dam channel adjustment. *Geomorphology*, 17:351-359.

Xu, J. 1996c. Wandering braided river channel pattern developed under quasi-equilibrium: an example from the Hanjiang River, China. *Journal of Hydrology*, 181:85-103.

Xu, J. 1997a. Evolution of mid-channel bars in a braided river and complex response to reservoir construction: an example from the Middle Hanjiang River, China. *Earth Surface Processes and Landforms*, 22:953-965.

Xu, J. 1997b. Study of sedimentation zones in a large sand-bed braided river: and example from the Hanjiang River of China. *Geomorphology*, 21:153-165.